skb.se

SKB R-24-01

ISSN 1402-3091

ID 2074465

December 2025

Baseline conditions of Forsmark prior to start of underground constructions

Baseline Forsmark

Lino Mercier
Svensk Kärnbränslehantering AB

Keywords: Baseline Forsmark, Forsmark, Site characterisation, Site descriptive modelling

Preface

Baseline Forsmark is a multidisciplinary description of prevailing geological, geomechanical, hydrogeological, hydrogeochemical, hydrological, and ecological conditions prior to the start of construction of the extension of the final repository for short-lived radioactive waste (SFR) and the spent fuel repository (SFK). The description represents a standard (reference or baseline) against which future geoscientific and ecological conditions can be compared. Baseline Forsmark is documented in this main report and a series of underlying discipline specific reports. These include geology, rock mechanics, depth and stratigraphy of regolith, digital elevation model, hydrogeochemistry, as well as hydrology and hydrogeology. In addition, appendix 1 of this report gives a description of the bedrock thermal properties. The aim of this report is to present an overview of the Forsmark area, available boreholes and surface monitoring locations and of key questions at the completion of the site descriptive models for SFR and SFK (SDM-Site and SDM-PSU respectively). Moreover, a summary of the updated knowledge, new data and methodologies at the Baseline stage is given for the different disciplines. Most of the prevailing conditions are previously described in the site-descriptive models SDM-Site (SKB 2008a) and SDM-PSU (SKB 2013), which were established at the completion of the surface-based site investigations conducted between 2002 and 2008 and between 2009 and 2010, respectively. A series of methodology reports were developed by SKB between 2002 and 2007 to support the development of discipline-specific models for SDM-Site and SDM-PSU. A new series of methodology reports have been developed by SKB between 2020 and 2024 to support the continuing development of qualified discipline-specific models. The following site experts have been part of the Baseline team:

Catchment topography and regolith geology
Juri Palmtag, SKB, Gustav Sohlenius, SGU

Bedrock geology
Peter Hultgren, SKB, Jesper Petersson, Geos AB

Bedrock thermal properties and rock mechanics
Abel Sánchez Juncal, SKB, Eva Hakami, Hakami konsult AB

Discrete fracture networks (DFN)
Sven Follin, SKB

Bedrock hydrogeology
Sven Follin, SKB

Bedrock hydrogeochemistry
Lino Mercier, SKB

Bedrock transport properties
Sten Berglund, HydroResearch AB

Climate, hydrology, and near-surface hydrogeology and hydrogeochemistry
Kent Werner, SKB, Hedi Rasul, SKB.

Ecology and land use
Jörg Stephan, SKB

The document has been subjected to internal factual review by Georg Lindgren, Allan Hedin, Susanne Grigull, Jean-Marc Mayotte, Sari Peura, Peter Saetre, Jan-Olof Selroos, Martin Stigsson, Rémi Vachon, Johan Liakka, Assen Simeonov, Anna-Maria Jakobsson, Henrik Widestrand, Diego Mas Ivars, Frederic Wagner, Albin Nordström, Birgitta Kalinowski, Teresita Morales and Lindsay Krall.

Stockholm, December 2025.

Lino Mercier, Sven Follin, Mats Tröjbom

Editors

Summary

This document constitutes the main report of Baseline Forsmark that is a multidisciplinary description of prevailing geological, geomechanical, hydrogeological, hydrogeochemical, hydrological, and ecological conditions prior to the start of construction of the extension of the final repository for short-lived radioactive waste (SFR) and the spent fuel repository (SFK). The aim of this report is to present an overview of the updated knowledge, new data and new or updated methodologies at the Baseline stage for the different disciplines. Moreover, a description is given of the Forsmark area, available boreholes and surface monitoring locations, and key questions at the completion of the development of the site descriptive models for SFR and SFK (SDM-Site and SDM-PSU respectively). The Baseline stage includes data acquired from surface-based investigations performed up to 2022-10-31 that are used to improve the knowledge related to the previous SDM. Some of the new modelling methodologies, or parts therein, have been tested in Baseline Forsmark to gain experience and provide feedback for improvements. The Baseline description represents a standard (reference or baseline) against which future geoscientific and ecological conditions can be compared. This gives a basis for assessing if future changes can be linked to the repository construction or natural or other anthropogenic causes.

Sammanfattning

Detta dokument utgör huvudrapporten för Baseline Forsmark, som är en tvärvetenskaplig beskrivning av geologiska, geomekaniska, hydrogeologiska, hydrogeokemiska, hydrologiska och ekologiska förhållanden före utbyggnaden av slutförvaret för kortlivat radioaktivt avfall (SFR) och slutförvaret för använt kärnbränsle (SFK). Syftet med rapporten är att ge en översikt över uppdaterad kunskap, nya data samt nya eller uppdaterade metoder för de olika ämnesområdena. Dessutom ges en beskrivning av Forsmarksområdet, tillgängliga borrhål och platser för ytövervakning samt nyckelfrågor vid färdigställandet av de platsbeskrivande modellerna för SFR och SFK (SDM-Site respektive SDM-PSU).

Baseline omfattar data som samlats in från ytbaserade undersökningar fram till 2022-10-31 och används för att förbättra kunskapen i förhållande till tidigare platsbeskrivande modeller. Vissa av de nya modelleringsmetodikerna, eller delar av dem, har testats i Baseline Forsmark för att få erfarenhet och ge återkoppling för förbättringar.

Baseline-beskrivningen representerar en standard eller referens mot vilken framtida geovetenskapliga och ekologiska förhållanden kan jämföras. Detta ger möjlighet att bedöma om framtida förändringar kan kopplas till byggnationen av förvaret eller till naturliga eller andra antropogena orsaker.

Innehåll

1 Introduction

1.1 Definition and objectives of Baseline Forsmark

SKB has started to construct the extension of the existing final repository for short-lived radioactive waste (SFR) located in Forsmark in the municipality of Östhammar. Furthermore, SKB plans to construct a final repository for spent nuclear fuel (SFK) nearby. Figure 1-1 and Figure 1-2 show the locations and names of these repositories.

Baseline Forsmark is a multidisciplinary description of prevailing geological, geomechanical, hydrogeological, hydrogeochemical, hydrological, and ecological conditions prior to the start of constructions and hence represents a standard (reference or baseline) against which future geoscientific and ecological conditions can be compared. This gives a basis for assessing if future changes can be linked to the repository construction or natural or other anthropogenic causes. Baseline Forsmark does not present an integrated site descriptive model. Most of the prevailing conditions are previously described in the site-descriptive models SDM-Site (SKB 2008a) and SDM-PSU (SKB 2013), which were established at the completion of the surface-based site investigations conducted between 2002 and 2008 and between 2009 and 2010, respectively. Besides revisiting SDM-Site and SDM-PSU, Baseline Forsmark describes complementary data and interpretations acquired from surface-based investigations performed up to 2022-10-31. The descriptions in SDM-Site, SDM-PSU, and Baseline Forsmark are input to future site descriptive models for the Forsmark site.

Figure 1-3 illustrates the relation between past and future site-descriptive models and safety assessments for SFK and SFR. When data from the underground investigations at SFR and SFK are available these can be included in forthcoming site descriptive models.

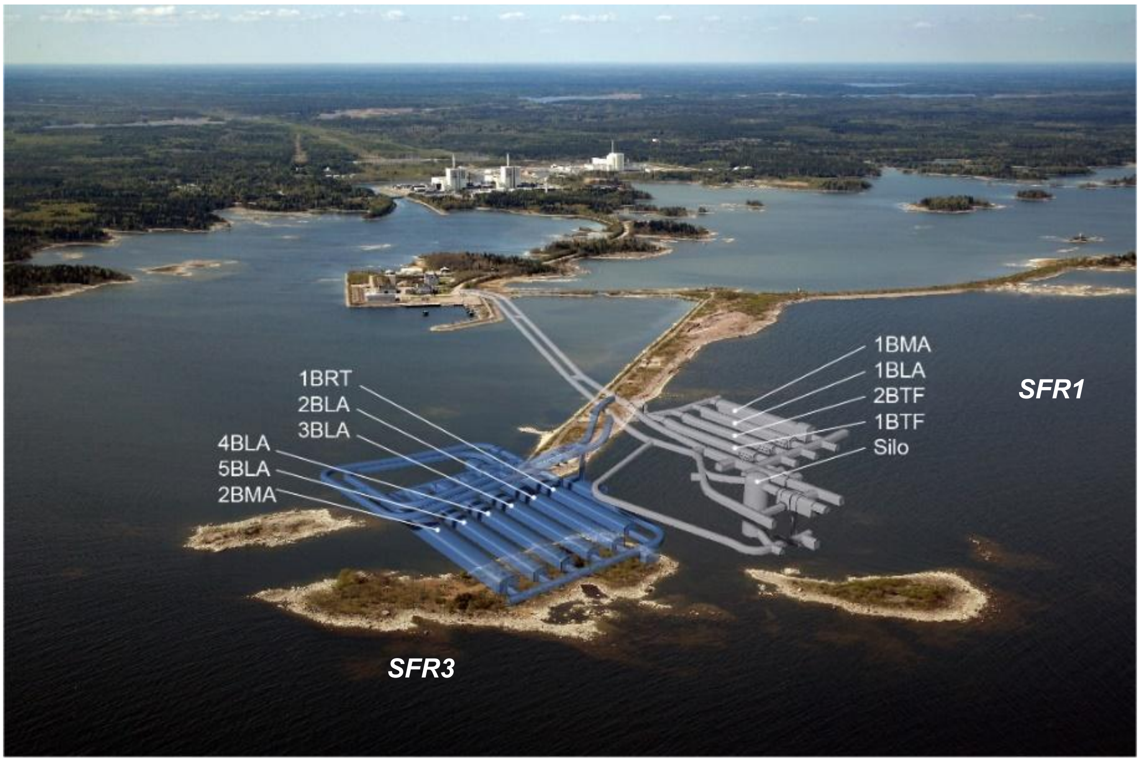

Figure 1-1. *Illustration of the proposed layout for the extension, SFR3 (shown in blue), of the existing repository, SFR1 (shown in grey), for short-lived low- and intermediate-level radioactive waste. SFR1 is situated about 1.5 km northeast of the Forsmark Power Plant at about 65 m depth below the Baltic Sea. SFR3 will be constructed at about 130 m depth below the Baltic Sea.*

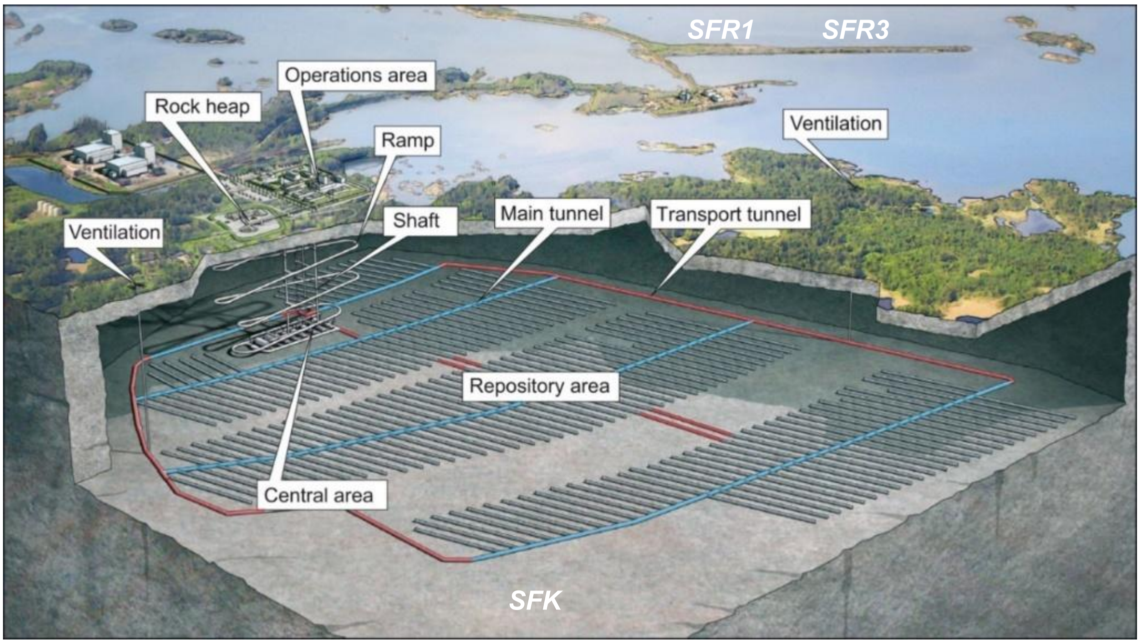

Figure 1-2. Illustration of the proposed layout of the different facility parts of the final repository for spent nuclear fuel, SFK. SFK will be situated about 1 km southeast of the Forsmark Power Plant at about 500 m depth below the ground surface.

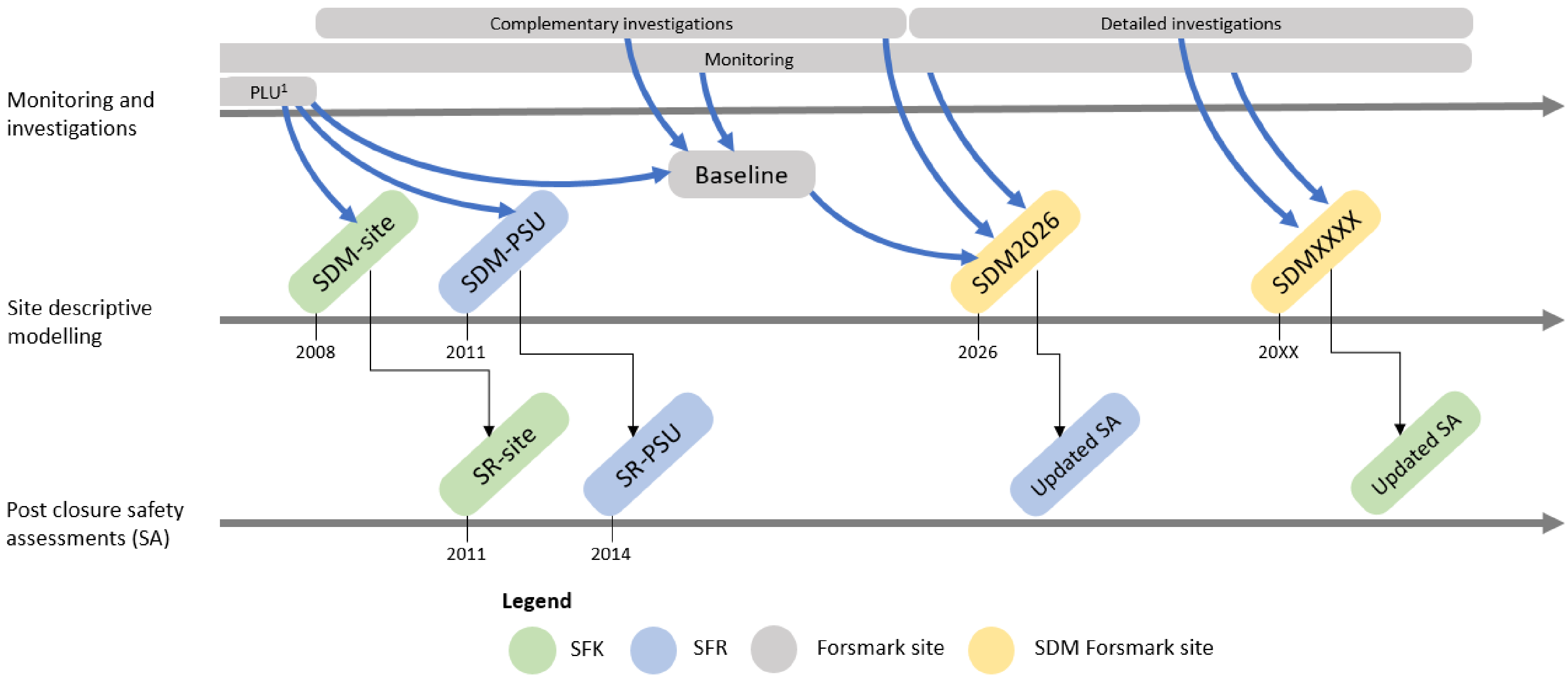

Figure 1-3. *Illustration showing the relation between past and future site-descriptive models and safety assessments for SFK and SFR.*
[1] *PLU refers to the Site investigations.*

1.2 Forsmark catchment and previous model domains

SKB uses models on different spatial scales for different purposes, e.g., for site descriptions, predictions or quantitative assessments, or for a combination of these. The spatial scale considered in Baseline Forsmark is named the Forsmark catchment. Figure 1-4 shows the border of the Forsmark catchment along with the footprints of the principal model domains used for regional and local (or facility) scale site-descriptive modelling in SDM-Site and SDM-PSU. The border of a catchment is a water divide, i.e., a hydraulic boundary. The border of the Forsmark catchment is based on topographic and bathymetric data, see SKBdoc 1940271 for details. The area of the Forsmark catchment area is c. 216 km2 and the elevation ranges between c. +25 m and c. –57 m (RH 2000 elevation system).

1.2.1 Model domains for hydrological-hydrogeological applications

The model domains used for groundwater flow and solute transport modelling in SDM-Site and SDM-PSU were somewhat larger than the principal regional domains shown in Figure 1-4, but not as large as the Forsmark catchment in Baseline Forsmark. In brief, the border of the catchment is assumed to be a no-flow boundary also for groundwater flow. A flux or a mixed boundary condition is assumed for all terrestrial parts with hydrologic interactions between surface water and groundwater, and a specified pressure boundary condition is assumed in all submerged parts. Finally, a no-flow boundary is assumed at –1,100 m elevation, which was also the case in the groundwater flow modelling for SDM-Site and SDM-PSU (Follin et al. 2007, Öhman et al. 2013).

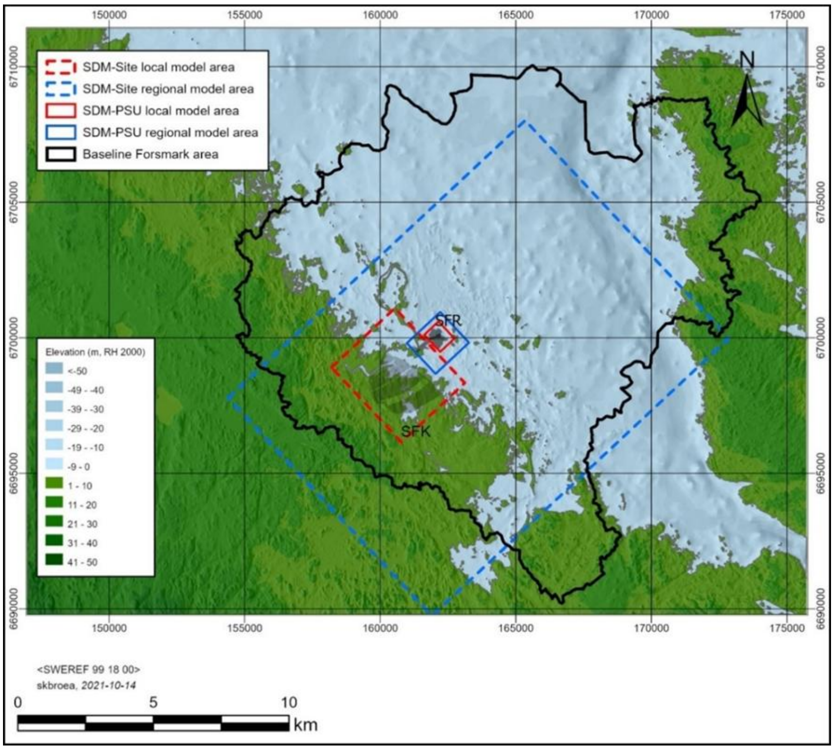

Figure 1-4. *Forsmark catchment and model areas in SDM-Site and SDM-PSU.*

1.3 Geological setting of SFK, SFR1 and SFR3

Figure 1-5 illustrates that SFK will be situated inside a tectonic lens and that SFR1 is situated within a high-strain belt that forms the north-eastern margin to the tectonic lens. SFR3 will be adjacent to SFR1. Details of the structural concepts relative to the tectonic evolution of the Forsmark site in a regional perspective are provided in Section 4.4, and the relevance of the structural concept for hydrogeological modelling is described in Chapter 7.

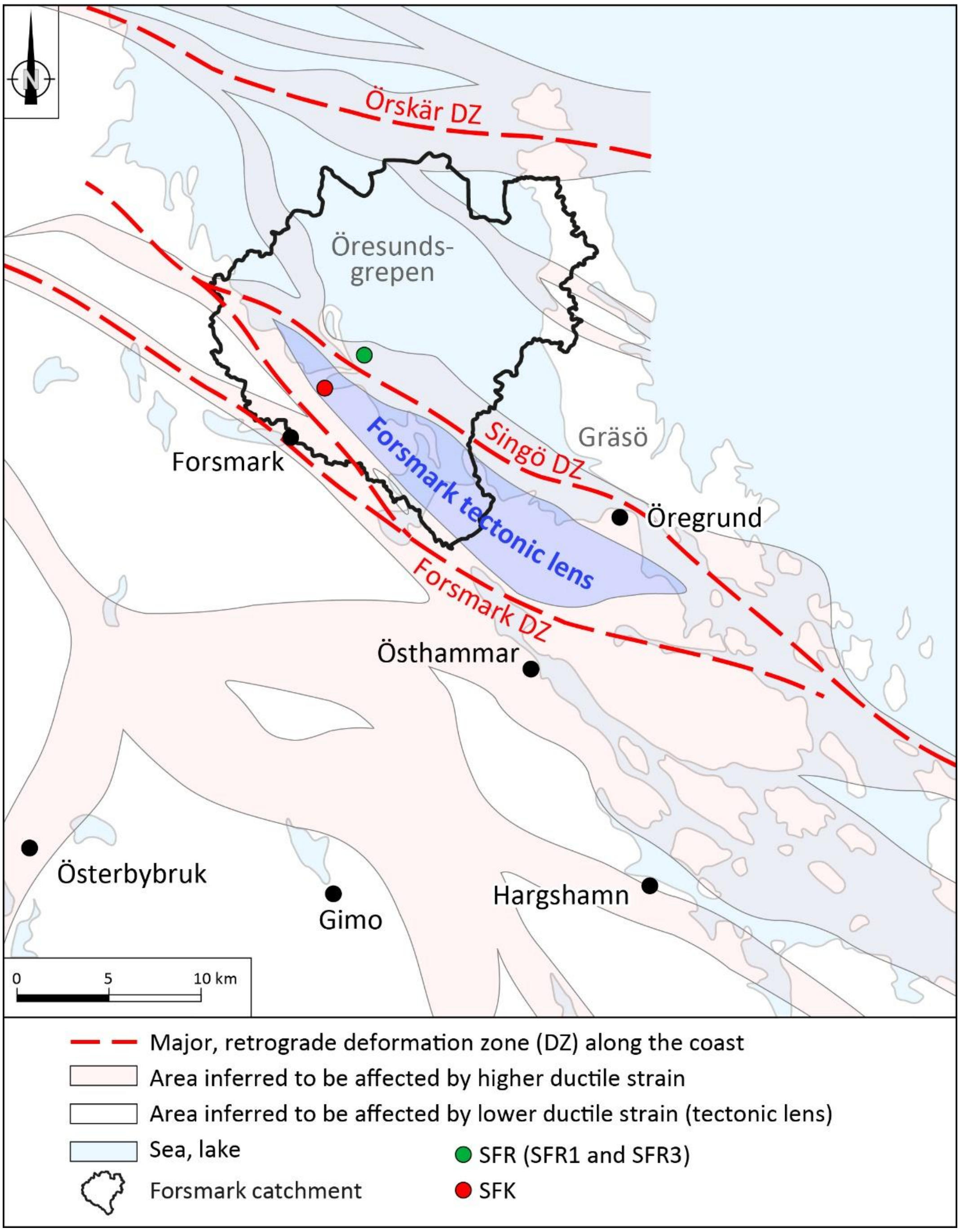

Figure 1-5. *Tectonic lens at Forsmark and areas affected by strong ductile deformation. The Forsmark catchment is inserted for reference. Modified after Petersson et al. (2024).*

1.4 Hydraulic influence of the existing SFR1 repository

The existing repository for short-lived radioactive waste, SFR1, was constructed in 1988 and has been in operation with atmospheric conditions in all its underground openings for about 35 years. The groundwater inflow to SFR1 is measured with two drainage pits, named UB and NDB. The measurements are shown in Figure 1-6. UB measures the inflow to the tunnel leading to SFR1 where the tunnel crosses the Singö deformation zone (labelled Singö DZ in Figure 1-5). NDB is located at the bottom of SFR1 and measures the inflow to the remaining repository openings. Between 1988 and 2023, the total inflow rate (UB + NDB) decreased significantly, from c. 700 L/min to c. 163 L/min. This trend is predominantly due to a decreasing inflow to NDB whereas the decrease in inflow to UB is much smaller (Figure 1-6).

The changes in hydraulic head (groundwater level) following the drainage of SFR1 have been recorded in several boreholes drilled near SFR1, first manually for several years, but following the site investigations SDM-Site and SDM-PSU automatically on a diurnal basis since 2007. Each borehole has several monitoring sections. The total recorded changes in head (drawdown) in the monitoring sections are evident (several metres) after 35 years of drainage of SFR1 but decrease radially away from SFR1, although the influences vary heterogeneously between monitoring sections. The state of the present hydraulic influence of SFR1 reflects the decrease in inflow shown in Figure 1-6 and is regarded almost pseudo-stationary. Potential changes in hydraulic influence after start of SFR3 construction work will be possible to identify using the monitoring sections.

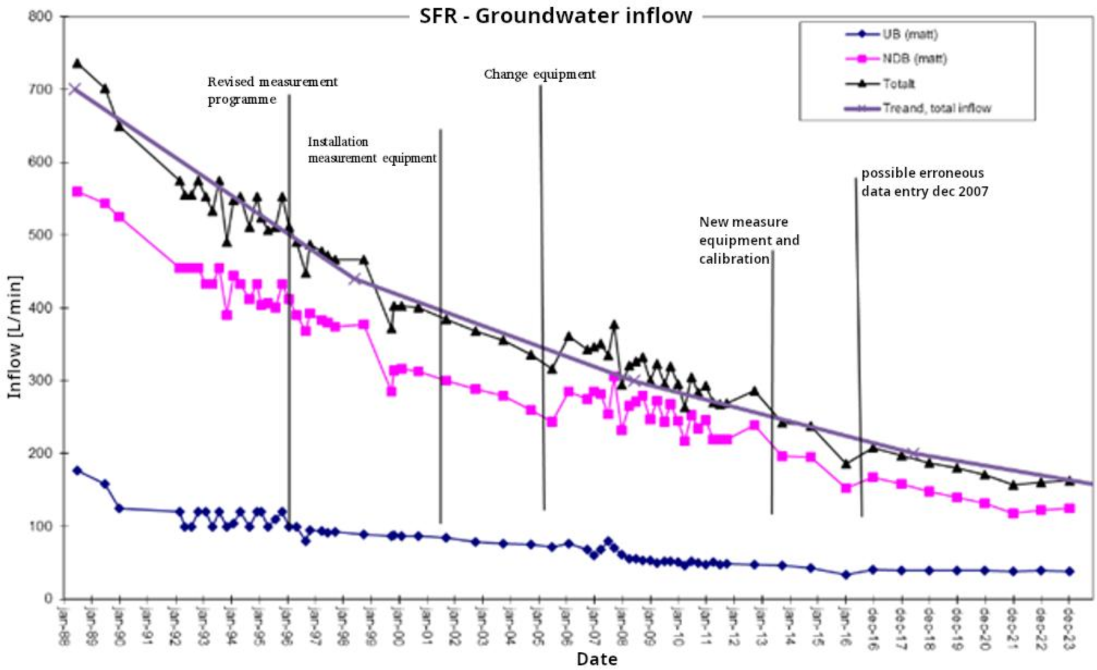

Figure 1-6. *Measured total inflow to SFR1 has fallen from c. 700 L/min in January 1988 to c.163 L/min in December 2023. UB and NDB refer to two pumping pits, see SKB (2013) for details.*

1.5 Updated methodology reports

A series of methodology reports were produced by SKB between 2002 and 2007 to support the development of discipline-specific models for SDM-Site and SDM-PSU. A new series of methodology reports have been established by SKB between 2020 and 2024 to support the development of discipline-specific models for SDM 2026 and onwards, see Table 1-1. Some of the new modelling methodologies, or parts therein, have been tested in Baseline Forsmark to gain experience and provide feedback for improvements prior to SDM 2026. The observations made are commented in the subsequent discipline-specific chapters.

Table 1-1. Modelling methodology reports developed within Baseline Forsmark.

Report	Title
R-20-10	Methodology for deterministic geological modelling of the Forsmark site. Application to the development of the final repository for spent nuclear fuel
R-20-11	Methodology for discrete fracture network modelling of the Forsmark site. Part 1 - concepts, data, and interpretation methods
R-20-13	Methodology for rock mechanics modelling of the Forsmark site
R-20-14	Methodology for hydrological-hydrogeological modelling of the Forsmark site
R-20-15	Methodology for hydrogeochemical modelling of the Forsmark site
R-20-16	Methodology for elevation and regolith modelling of the Forsmark site
R-20-17	Methodology for site descriptive and safety assessment transport modelling of the Forsmark site.
R-20-18	Methodology for modelling of thermal properties of the Forsmark site. Part 1 - Recommended data and interpretation methods
R-20-19	Methodology for modelling of thermal properties of the Forsmark site. Part 2 - Background and methodology development

1.6 This report

Chapter 2 presents an overview of boreholes and surface monitoring installations.

Chapters 3 through 11 present discipline-specific baseline conditions. Of particular interest are new data acquired by each discipline after the completion of SDM-Site and SDM-PSU. Notably, the quantity of newly acquired data varies considerably across disciplines. Moreover, in the light of updated acquisition methods and/or longer monitoring time series some disciplines have had reasons to revisit old data acquired prior to the completion of SDM-Site and SDM-PSU, and, where applicable, address the quality and limitations of using old data for modelling in SDM 2026 and onwards. Finally, where applicable, the experiences gained from testing the new modelling methodologies are assessed.

Figure 1-7 shows an overview figure for the report hierarchy of different reports and how they relate to the main Baseline Forsmark report.

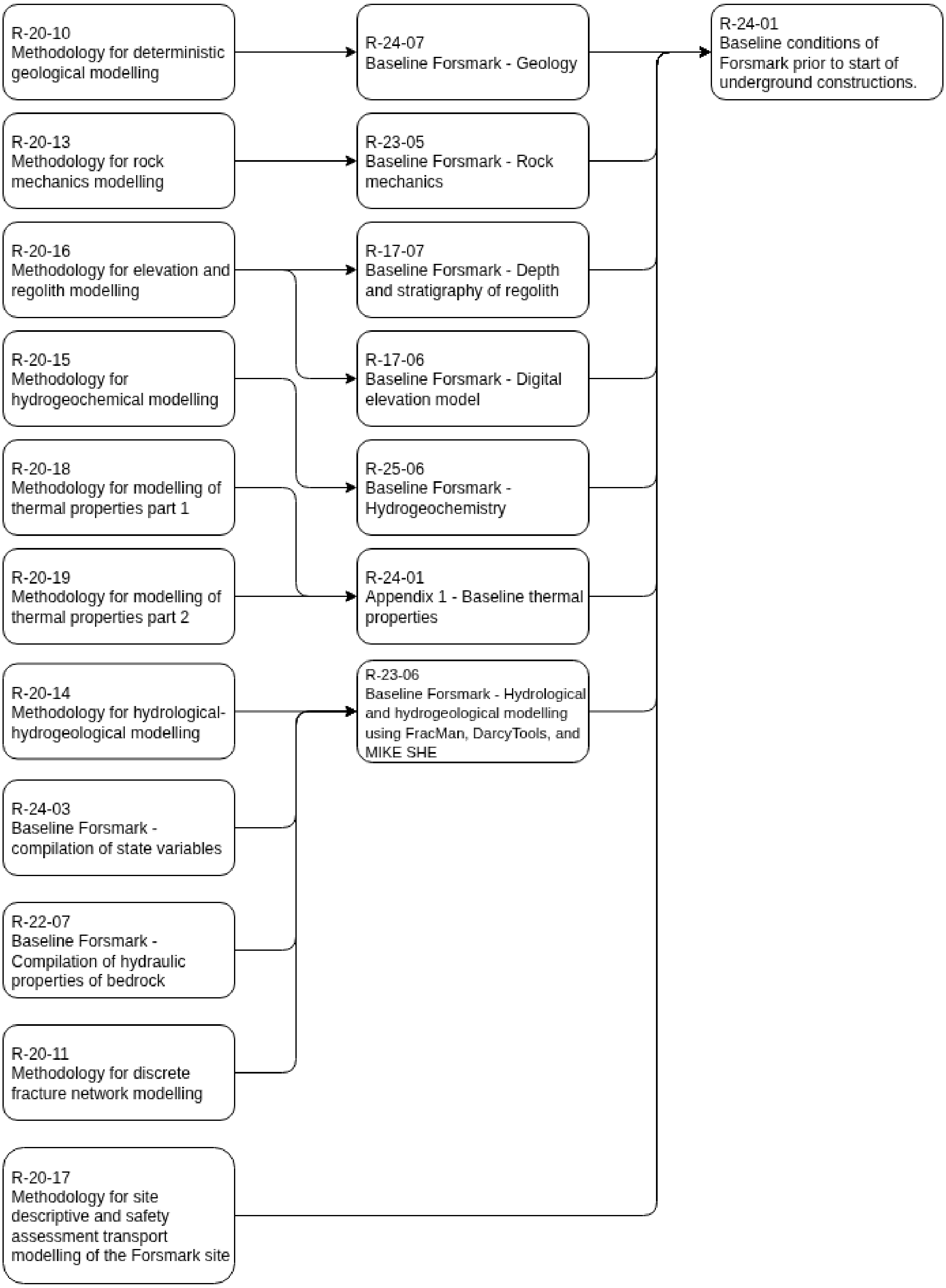

Figure 1-7. *Report hierarchy for reports related to Baseline Forsmark.*

Table 1-2. Discipline-specific background reports for Baseline Forsmark.

Report	Title
R-24-07	Baseline Forsmark – Geology. Updating of existing site descriptive models.
R-23-05	Baseline Forsmark – Rock mechanics
R-17-07	Baseline Forsmark – Depth and stratigraphy of regolith
R-17-06	Baseline Forsmark – Digital elevation model
R-25-06	Baseline Forsmark – Hydrogeochemistry
R-23-06	Baseline Forsmark – Hydrological and hydrogeological modelling using FracMan, DarcyTools, and MIKE SHE

1.7 Nomenclature

Deformation zone	Deformation zone is a general term that refers to an essentially 3D structure along which there is a concentration of brittle, ductile or combined brittle and ductile deformation. Brittle deformation zones generally consist of one or several zones of crushed and/or intensely fractured material (core zones) surrounded by zones of fractured and/or hydrothermally altered rock (damage zones). Confidence in their existence is assigned to three classes: high, medium and low.
Fracture (broken, unbroken, sealed, open and partly open)	A natural break in the rock. In drill cores, there are broken and unbroken fractures, depending on whether the core is split or not. Broken fractures include both open fractures and originally sealed fractures which were broken during the drilling or the following treatment of the drill core. To decide if a fracture was open, partly open or sealed in situ, SKB has developed a classification system. A broken fracture is classified as open if it fulfils one of the following criteria: (1) distinguishable aperture in the borehole image, (2) weathered or altered fracture surfaces or (3) a poor fit of the fracture planes. Otherwise, it is mapped as sealed. Unbroken fractures are generally classified as sealed, except in those cases where they display macroscopically distinguishable apertures and consequently are classified as partly open. Sealed fractures are typically fully filled with minerals having normally some tensile strength. These fractures are considered to have zero aperture.
Fracture domain (SDM-Site)	A fracture domain is a rock volume in 3D outside deterministically modelled deformation zones in which the rock units identified in boreholes show similar fracture frequency characteristics.
Fracture zone	Fracture zone is a term used to denote a brittle deformation zone without any specification whether there has or has not been a shear sense of movement along the zone.
Possible deformation zone (SDM-Site)	In the single-hole interpretation work, possible deformation zones are identified on the basis of fracture frequency, rock alteration and focused resistivity along a borehole. Other data that have assisted in their identification include the occurrence of low radar amplitude anomalies in the borehole radar data, low magnetic susceptibility and caliper anomalies. Confidence in their existence is assigned to three classes: high, medium and low

Properties data	Properties data relate to static characteristics which may be described using models that compile the information available for the system before start of construction. It can result in a best estimate from the information available.
Rock domain	A rock domain refers to a rock volume in 3D in which the rock units identified in boreholes show specifically similar composition, grain size, degree of bedrock homogeneity, and degree and style of ductile deformation have been combined and distinguished from each other.
Sheet joint	Sheet joints are tensional fractures commonly found at shallow depths in the bedrock, particularly in the area investigated in SDM-Site. The proposed mechanism for sheet joint formation in the uppermost bedrock involves compression parallel to a convex bedrock surface; a situation that can occur due to elastic bending of the lithosphere during phases of isostatic rebound, e.g., uplift following the retreat of thick ice sheets
State variable	State variables are used to describe the current state of a transient system.

1.8 Abbreviations

SDM-Site	Short for "Site description of Forsmark at completion of the site investigation phase, SDM-Site Forsmark", SKB TR-08-05.
SDM-PSU	Short for "Site description of the SFR area at Forsmark at completion of the site investigation phase, SDM-PSU Forsmark", SKB TR-11-04.
SR-Site	Short for "Long-term safety for the final repository for spent nuclear fuel at Forsmark. Main report of the SR-Site project", SKB-TR-01
SR-PSU	Short for "Safety analysis for SFR Long-term safety. Main report for the safety assessment SR-PSU", SKB TR-14-01
RFM	Rock domains in SDM-Site are denoted RFM followed by two digits, RFMxx.
RFR	Rock domains in SDM-PSU are denoted RFR followed by two digits, RFRxx.
ZFM	Deformation zones in both SDM-Site and SFM-PSU are denoted ZFM followed by two to eight letters or digits, ZFMxx. An indication of the strike of a steeply dipping zone is included in the identification code (e.g. ZFMNNW1209).
FFM	Fracture domains in SDM-Site are denoted FFM followed by two to digits, FFMxx.
PDZ	Possible deformations zones in both SDM-Site and SDM-PSU are denoted PDZ.
SBA	Shallow bedrock aquifer structures are denoted SBA in SDM-PSU. Eight SBA structures are modelled in the upper 200 m bedrock, SBA1 to SBA8.
CCC	Complete chemical characterisation
COF	Connected open and partly open fractures
DEM	Digital elevation model. SKB used RHB 70 in SDM-Site and SDM-PSU. SKB has been using RH 2000 since 2021.

DFN	Discrete fracture network. The concept used in SDM-Site and SDM-PSU is denoted DFN-2008 (Follin 2008). A recent concept is DFN-2020 (Selroos et al. 2022).
ECPM	Equivalent continuous porous medium
HFM	Percussion borehole drilled in SDM-Site
HFR	Percussion borehole drilled in SDM-PSU
JFM	Deterministically modelled sheet joints are denoted JFM followed by two digits, JFMxx.
KFM	Cored borehole drilled in SDM-Site
KFR	Cored borehole drilled in SDM-PSU
NDB	Lower measurement pit in SFR1
UB	Upper measurement pit in SFR1
PFL	Posiva flow log
RVS	Rock visualization system
SFR1	The existing, shallow repository for short-lived radioactive waste
SFR3	The planned extension to SFR1
SFK	The planned, deep repository for long-lived spent nuclear fuel
NT	IUCN Red List of Threatened Species: Near Threatened
VU	IUCN Red List of Threatened Species: Vulnerable

2 Overview of boreholes and surface monitoring locations

This chapter gives an overview of boreholes for investigations and monitoring in the bedrock and regolith, as well as installations for monitoring in the surface system. The chapter is divided into chronological sub-sections that summarise installations from SFR1, SDM-site, SDM-PSU, and supplementary installations after the site investigations.

2.1 Boreholes drilled and investigated for SFR1

Figure 2-1 shows 45 cored boreholes drilled and investigated between 1980-1986 in support of discipline-specific descriptions of the bedrock conditions where the existing repository for short-lived radioactive waste, SFR1, is situated. Table 2-1 shows an overview of the borehole length, the bottom elevation, data availability by discipline, number of monitoring sections and state variables measured in the borehole.

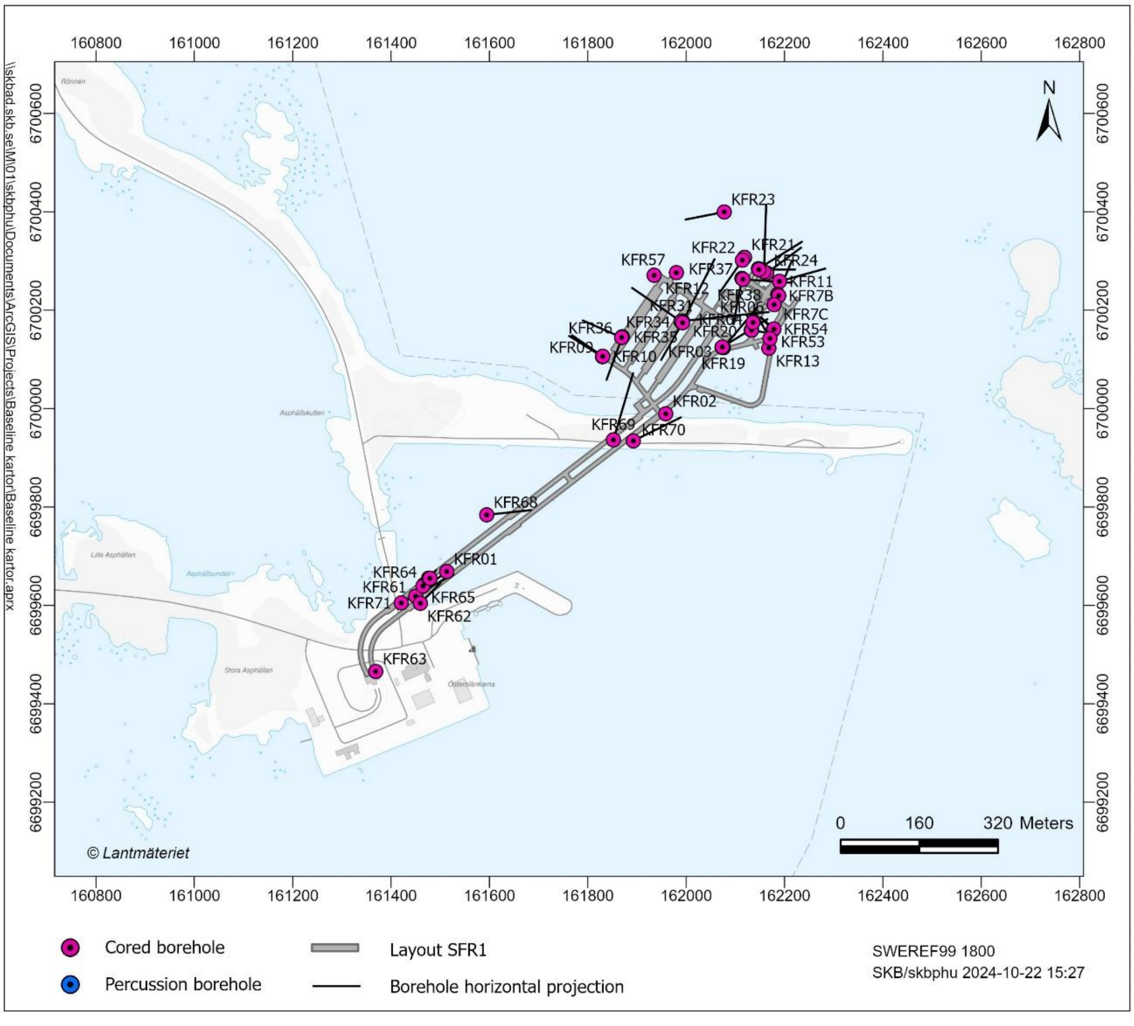

Figure 2-1. *Plane view showing 45 boreholes drilled and investigated in support of the description of the bedrock conditions where the existing repository for short-lived radioactive waste, SFR1, is constructed.*

Table 2-1. Overview of interest by discipline of the data acquired in the boreholes shown in Figure 2-1. R = regolith geology, G = bedrock geology, M = rock mechanics, T = thermal properties, S = near-surface hydrogeology, H = bedrock hydrogeology, C = hydrogeochemistry, Tr = transport properties.

Borehole	Borehole length (m from TOC)	End of borehole (m RH2000)	Discipline interest R, G, M, T, S, H, C, Tr	Number of monitoring sections	Monitored parameters P = pressure C = chemistry
KFR01	62.3	-101.75	G, H, C, Tr	2	P,C
KFR02	170.33	-255.57	G, H, C, Tr	4	P,C
KFR03	101.6	-183.78	G, H, C, Tr	4	P,C
KFR04	100.5	-174.08	G, H, C, Tr	4	P,C
KFR05	131.4	-200.45	G, H, C, Tr	4	P,C
KFR06	39	-110.85	G, H	0	_
KFR08	104.4	-94.93	G, H, C, Tr	3	P,C
KFR09	80.24	-84.25	G, H, C, Tr	1	P,C
KFR10	107.28	-153.98	G, H	0	_
KFR11	98.07	-103.34	G, H	0	_
KFR12	50.26	-137.2	G, H	0	_
KFR13	76.6	-199.76	G, H, C, Tr	3	P,C
KFR19	110.17	-54.36	G, H, C, Tr	4	P,C
KFR20	109.7	-61.11	G, H	0	_
KFR21	250.8	-250.62	G, H	0	_
KFR22	160.1	-138.47	G, H	0	_
KFR23	160.2	-138.55	G, H	0	_
KFR23	160.2	-138.55	G, H	0	_
KFR24	159.2	-133.33	G, H	0	_
KFR25	196.5	-141.17	G, H	0	_
KFR27	501.64	-496.9			
KFR31	242.1	-160.54	G, H	0	_
KFR32	209.7	-146.93	G, H	0	_
KFR33	167	-110.3	G, H	0	_
KFR34	142	-101.98	G, H	0	_
KFR35	140.2	-104.44	G, H	0	_
KFR36	123.9	-83.94	G, H	0	_
KFR37	204.9	-177.16	G, H	0	_
KFR38	185.4	-151.85	G, H	0	_
KFR53	40.6	-99.8	G, H	0	_
KFR54	53.3	-120.89	G, H	0	_
KFR55	61.89	-137.2	G, H, C, Tr	4	P,C
KFR56	81.73	-48.53	G, H, C, Tr	1	P,C
KFR57	25.38	-112.8	G, H	0	_
KFR61	70.9	-47.67	G, H	0	_
KFR62	82.8	-57.76	G, H	0	_
KFR63	15.08	-14.09	G, H	0	_
KFR64	54.17	-46.43	G, H	0	_
KFR65	39.68	-39.5	G, H	0	_
KFR66	29.17	-28.99	G, H	0	_
KFR67	48.95	-44.18	G, H	0	_
KFR68	128.03	-90.35	G, H	0	_
KFR69	201.2	-140.67	G, H	0	_
KFR70	172.5	-131.94	G, H	0	_
KFR71	120.9	-28.9	G, H	0	_
KFR7A	74.7	-134.71	G, H, C, Tr	3	P,C
KFR7B	21.1	-153.44	G, H, C, Tr	2	P,C
KFR7C	34	-165.16	G, H	0	_

***Rock matrix porewater**

2.2 Boreholes and installations investigated for SDM-Site

Figure 2-2 shows 25 cored boreholes and 38 percussion boreholes drilled and investigated between 2002 and 2007 in support of SDM-Site (SKB R-08-05 appendix 3) and the discipline-specific descriptions of the bedrock conditions where the planned repository for spent fuel, SFK, will be constructed. Table 2-2 shows an overview of the borehole length, the bottom elevation, data availability by discipline, number of monitoring sections and state variables measured in the borehole.

Borehole data in support of the description of the regolith (mainly Quaternary deposits) in SDM-Site come from investigations in almost 100 groundwater monitoring wells, see Figure 2-3. Table 2-3 shows an overview of the borehole length, the bottom elevation, data availability by discipline, number of monitoring sections and state variables measured in the borehole.

The site investigation for SDM-Site performed many surface investigations. The installations installed for monitoring of water levels in lakes and sea, discharge in streams and meteorological monitoring are shown in Figure 2-9 and 2-10.

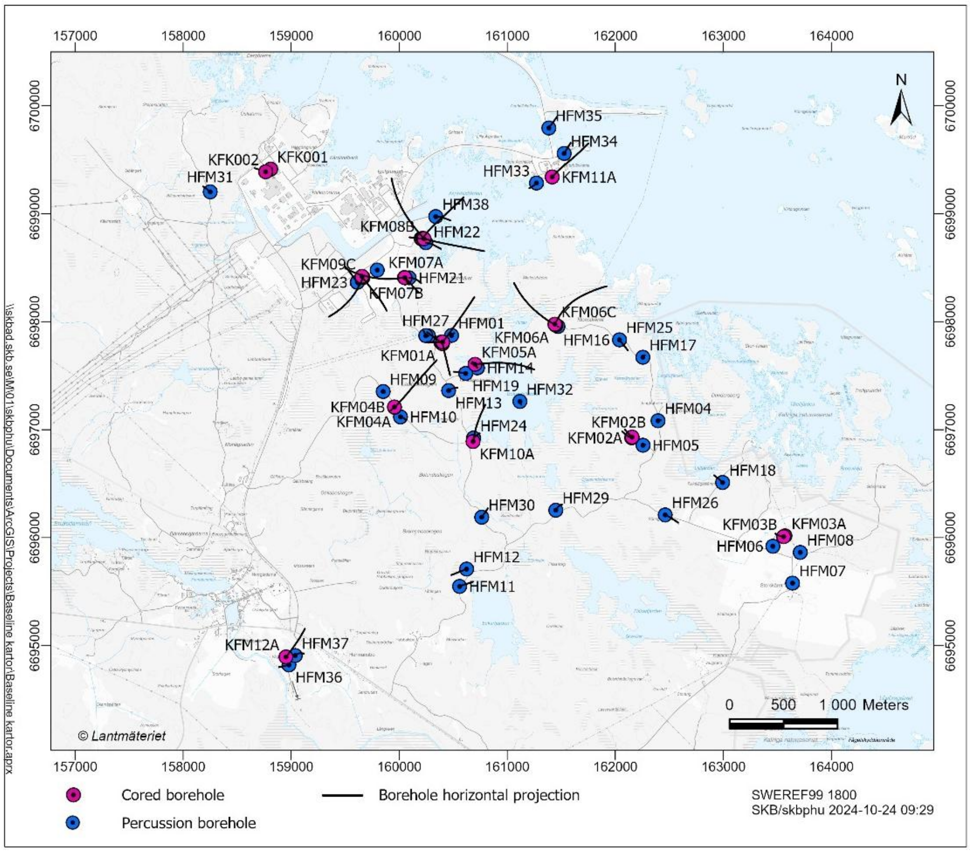

Figure 2-2. *Plane view showing 25 cored boreholes, and 38 percussion boreholes drilled in support of SDM-Site and the discipline-specific descriptions of the bedrock conditions where the planned repository for spent fuel, SFK, will be constructed.*

Table 2-2. Overview of interest by discipline of the data acquired in the boreholes shown Figure 2-2. R = regolith geology, G = bedrock geology, M = rock mechanics, T = thermal properties, S = near-surface hydrogeology, H = bedrock hydrogeology, C = hydrogeochemistry, Tr = transport properties.

Borehole	Borehole length (m from TOC)	End of borehole (m RH2000)	Discipline interest R, G, M, T, S, H, C, Tr	Number of monitoring sections	Monitored parameters P = pressure C = chemistry
KFK001	502.94	-500.55	R, G, M	0	-
KFK002	213.52	-184.71	R, G, M	0	-
KFM90A	24.18	-23.43	R, G, T	0	-
KFM90B	18.20	-18.38	R, G, T	0	-
KFM90C	20.00	-20.39	R, G, T	0	-
KFM90D	20.40	-20.36	R, G, T	0	-
KFM90E	20.30	-20.32	R, G, T	0	-
KFM90F	20.10	-20.32	R, G, T	0	-
KFM01A	1001.49	-982.08	R, G, M, T, H, Tr	6	p
KFM01B	500.52	-479.16	R, G, M, T, H, Tr	3	p
KFM01C	452.1	-334.01	R, G, M, T, H	3	p
KFM01D	800.24	-612.29	R, G, M, T, H, Tr	7	p
KFM02A	1002.44	-988.67	R, G, M, T, H, Tr	8	p
KFM02B	573.87	-557.7	R, G, M, T, H	7	p
KFM03A	1001.19	-988.01	R, G, M, T, H, Tr	9	p
KFM03B	101.54	-92.49	R, G, H, Tr	2	p
KFM04A	1001.42	-796.22	R, G, M, T, H, Tr	7	p
KFM05A	1002.71	-826.91	R, G, M, T, H, Tr	6	p
KFM06A	1000.64	-827.28	R, G, M, T, H, Tr	8	p
KFM06B	100.33	-95.38	R, G, M, T, H, Tr	3	p
KFM06C	1000.91	-781.23	R, G, M, T, H	10	p
KFM07A	1002.1	-820.75	R,G, M, T, H, C, Tr	6	P, C
KFM07B	298.93	-237.73	R, G, M, H	3	P
KFM07C	500.34	-494.17	R, G, M, H	4	P
KFM08A	1001.19	-759.21	R,G, M, T, H, C, T, Tr	9	P, C
KFM08B	200.54	-166.68	R,G, M, T, H	3	P
KFM08C	951.08	-780.62	R,G, M, T, H, C, T, Tr	5	P, C
KFM08D	942.3	-748.1	R,G, M, T, H, C	7	P, C
KFM09A	799.67	-621.02	R, G M, T, M, H, C, Tr	3	P
KFM09B	616.45	-471.82	R, G, M, T, M, H, C	3	P
KFM10A	500.16	-337.89	R, G, M, T, H, Tr	5	P
KFM11A	851.21	-713.05	R, G, M, T, H	7	P
KFM12A	601.04	-501.01	R, G, M, T, H	5	P
KFM13	150.21	-127.44	R, G, S, H	1	P
KFM14	60.18	-57.85	R, G, S, H	1	P
KFM15	62.3	-58.3	R, G, S, H	1	P
KFM16	60.35	-50.32	R, G, S, H	1	P
KFM17	60.45	-56.47	R, G, S, H	1	P
KFM18	60.46	-56.71	R, G, S, H	1	P
KFM19	102.37	-89.94	R, G, S, H	1	P
KFM20	60.5	-57.31	R, G, S, H	1	P
KFM21	101.06	-92.4	R, G, S, H	3	P
KFM22	60.26	-57.18	R, G, S, H	1	P
KFM23	100.64	-93.74	R, G, S, H	3	P
KFM24	550.17	-544.91	R, G, M, T, S, H	1	P
HFM01	200.2	-195.17	R, G, H	3	P
HFM02	100	-96.68	R, G, H	3	P
HFM03	26	-22.63	R, G, H	2	P
HFM04	221.7	-213.97	R, G, H	3	P
HFM05	200.1	-189.72	R, G, H	2	P
HFM06	110.7	-103.12	R, G, H	1	P
HFM07	122.5	-115.69	R, G, H	1	P
HFM08	143.5	-135.11	R, G, H	2	P
HFM09	50.25	-41.2	R, G, H	1	P
HFM10	150	-133.92	R, G, H	2	P
HFM11	182.35	-117.72	R, G, H	2	P
HFM12	209.55	-136.53	R, G, H	2	P
HFM13	175.6	-146.62	R, G, H	3	P
HFM14	150.5	-127.14	R, G, H	1	P
HFM15	99.5	-65.33	R, G, H	2	P
HFM16	132.5	-128.34	R, G, H	3	P
HFM17	210.65	-203.71	R, G, H	1	P
HFM18	180.65	-142.53	R, G, H	3	P
HFM19	185.2	-143.75	R, G, H	3	P

Table 2-2. (continued) Overview of interest by discipline of the data acquired in the boreholes shown Figure 2-2. R = regolith geology, G = bedrock geology, M = rock mechanics, T = thermal properties, S = near-surface hydrogeology, H = bedrock hydrogeology, C = hydrogeochemistry, Tr = transport properties.

HFM20	301	-297.4	R, G, H	4	P
HFM21	202	-153.18	R, G, H	4	P
HFM22	222	-155.41	R, G, H	3	P
HFM23	211.5	-72.6	R, G, H	1	P
HFM24	151.35	-129.09	R, G, H	3	P
HFM25	187.5	-133.91	R, G, H	1	P
HFM26	202.7	-143.88	R, G, H	1	P
HFM27	127.5	-114.81	R, G, H	4	P
HFM28	151.2	-143.59	R, G, H	1	P
HFM29	199.7	-177.72	R, G, H	1	P
HFM30	200.75	-170.39	R, G, H	4	P
HFM31	200.75	-176.7	R, G, H	1	P
HFM32	202.65	-198.23	R, G, H	4	P
HFM33	140.2	-110.17	R, G, H	4	P
HFM34	200.75	-161.1	R, G, H	3	P
HFM35	200.75	-150.23	R, G, H	4	P
HFM36	152.55	-110.1	R, G, H	3	P
HFM37	191.75	-158.99	R, G, H	1	P
HFM38	200.75	-140.5	R, G, H	3	P

***Rock matrix porewater**

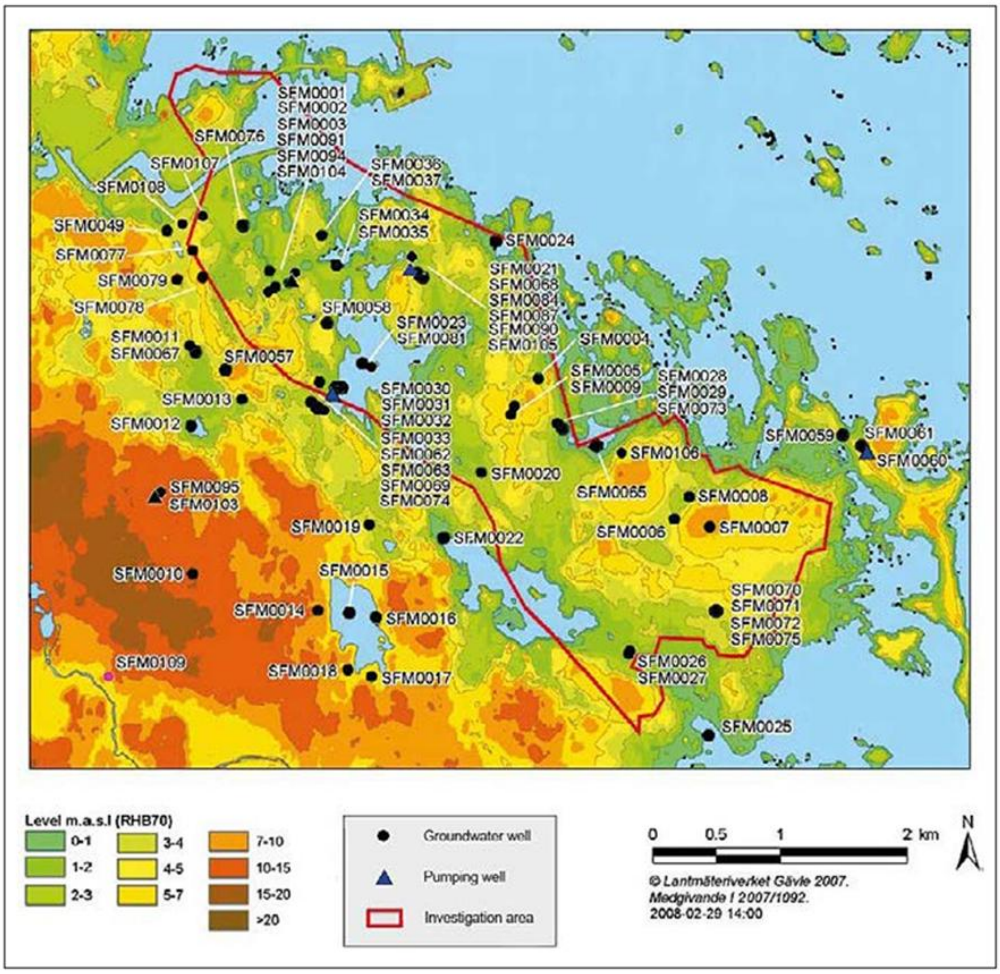

Figure 2-3. Plane view showing almost 100 groundwater monitoring wells drilled and investigated in support of SDM-Site and the discipline-specific descriptions of the regolith and surface waters conditions where the repository for spent fuel, SFK, will be constructed.

Table 2-3. Overview of interest by discipline of the data acquired in the boreholes shown Figure 2-3. R = regolith geology, G = bedrock geology, M = rock mechanics, T = thermal properties, S = near-surface hydrogeology, H = bedrock hydrogeology, C = hydrogeochemistry, Tr = transport properties.

Borehole	Borehole length (m from TOC)	End of borehole (m RH2000)	Discipline interest R, G, M, T, S, H, C, Tr	Number of monitoring sections	Monitored parameters P = pressure C = chemistry
SFM0001	5.65	-3.66	R, S, H	1	P
SFM000110	3.05	-0.47	R, S, H	1	P
SFM000112	3	0.16	R, S, H	1	P
SFM000114	3	0.53	R, S, H	1	P
SFM000116	3.75	-0.18	R, S, H	1	P
SFM000118	2.25	-0.37	R, S, H	1	P
SFM000121	6.5	-3.63	R, S	1	P
SFM000122	7.5	-4.47	R, S	1	P
SFM000123	3.5	-1.82	R, S	1	P
SFM000124	3.5	-1.13	R, S	1	P
SFM000125	4.5	-0.78	R, S	1	P
SFM000126	7.17	-0.71	R, S, H	1	P
SFM000132	3.1	1.09	R, S, H	1	P
SFM000133	3.1	0.75	R, S, H	1	P
SFM000134	2.1	2.08	R, S, H	1	P
SFM000135	2.1	1.7	R, S, H	1	P
SFM000138	2	0.74	R, S, H	1	P
SFM000139	3	0.85	R, S	1	P
SFM000140	2	1.58	R, S, H	1	P
SFM000141	2	0.42	R, S, H	1	P
SFM000142	1	0.57	R, S, H	1	P
SFM000143	3	-0.73	R, S	1	P
SFM000144	2.5	-0.04	R, S	1	P
SFM000145	2	-0.54	R, S	1	P
SFM000146	3.1	0	R, S	1	P
SFM000147	2.4	0.38	R, S	1	P, C?
SFM000149	2.25	-0.96	R, S	1	P
SFM000153	3.2	0.97	R, S	1	P
SFM000154	2.4	1.63	R, S	1	P
SFM000160	2.5	1.75	R, S, H	1	P
SFM000161	2	1.19	R, S, H	1	P
SFM000162	1.5	0.51	R, S, H	1	P
SFM000163	6.88	-0.21	R, S, H	1	P
SFM000167	10.91	-2.83	R, S, H	1	P
SFM000168	5.17	0.64	R, S, H	1	P
SFM000169	4	-0.67	R, S, H	1	P
SFM000171	3.5	-1.76	R, S, H	1	P
SFM000173	5.1	-3.12	R, S, H	1	P
SFM000174	3	1.57	R, S, H	1	P
SFM000175	6	-0.67	R, S, H	1	P
SFM000176	7	-0.72	R, S, H	1	P
SFM000177	6	-0.18	R, S, H	1	P
SFM000179	5	1.89	R, S, H	1	P
SFM000180	6	1.95	R, S, H	1	P
SFM000181	5	5.56	R, S, H	1	P
SFM000182	5	-1.34	R, S, H	1	P
SFM000183	7.1	-3.6	R, S, H	1	P
SFM000187	4	0.14	R, S, H	1	P
SFM000188	4	-1.71	R, S, H	1	P
SFM000190	7	-0.38	R, S, H	1	P
SFM000191	9.2	-3.71	R, S, H	1	P
SFM000192	9	-4.56	R, S, H	1	P
SFM000193	5.1	1.95	R, S, H	1	P
SFM000194	4	1.3	R, S, H	1	P
SFM000195	7	-2.23	R, S, H	1	P
SFM000196	11	-6.75	R, S, H	1	P
SFM000197	8	-4.3	R, S, H	1	P
SFM000198	7	-2.84	R, S, H	1	P
SFM0002	6.11	-3.8	R, S, H	1	P
SFM0003	11.48	-8.86	R, S, H	1	P
SFM0004	6.02	-1.69	R, S, H	1	P
SFM0005	3.21	3.78	R, S, H	1	P
SFM0006	4.21	2.26	R, S, H	1	P
SFM0008	6.14	-2.19	R, S, H	1	P
SFM0009	4	1.82	R, S, H	1	P

Table 2-3. (continued). Overview of interest by discipline of the data acquired in the boreholes shown Figure 2-3. R = regolith geology, G = bedrock geology, M = rock mechanics, T = thermal properties, S = near-surface hydrogeology, H = bedrock hydrogeology, C = hydrogeochemistry, Tr = transport properties.

	Borehole length (m from TOC)	End of borehole (m RH2000)	Discipline interest	Number of	Monitored parameters
Borehole			R, G, M, T, S, H, C, Tr	monitoring sections	P = pressure
					C = chemistry
SFM0010	3	11.72	R, S, H	1	P
SFM0011	5.95	-1.67	R, S, H	1	P
SFM0012	6.42	-3.22	R, S, H	1	P
SFM0013	6.5	-3.32	R, S, H	1	P
SFM0014	4.27	3.8	R, S, H	1	P
SFM0015	7.34	-1.5	R, S, H	1	P
SFM0016	9.57	-2.13	R, S, H	1	P
SFM0017	6.64	1.87	R, S, H	1	P
SFM0018	6.5	1.36	R, S, H	1	P
SFM0019	7.1	-0.54	R, S, H	1	P
SFM0020	5	-1.57	R, S, H	1	P
SFM0021	4.14	-0.85	R, S, H	1	P
SFM0022	5.8	-3.84	R, S, H	1	P
SFM0023	5.7	-3.98	R, S, H	1	P
SFM0024	3.21	-2.56	R, S, H	1	P
SFM0025	7.06	-6.02	R, S, H	1	P
SFM0026	18.49	-15.23	R, S, H	1	P
SFM0028	9.05	-6.75	R, S, H	1	P
SFM0030	6.02	-2.03	R, S, H	1	P
SFM0033	5.16	-2.12	R, S, H	1	P
SFM0034	4.11	-1.24	R, S, H	1	P
SFM0036	4.09	-1.3	R, S, H	1	P
SFM0049	6	-1.97	R, S, C	1	P, C
SFM0057	4.55	0.45	R, S, C	1	P
SFM0058	4.75	-0.11	R, S, H	1	P
SFM0059	6.15	-1.16	R, S, H	1	P
SFM0061	8.07	-2.47	R, S, H	1	P
SFM0062	3.95	-2.11	R, S, H	1	P
SFM0065	4.98	-3.69	R, S, H	1	P
SFM0076	3.16	0.66	R, S	1	P
SFM0077	8	-2.98	R, S, C	1	P, C
SFM0078	5.6	-0.36	R, S, C	1	P, C
SFM0079	6.7	-2.5	R, S, C	1	P, C
SFM0080	9.62	-5.07	R, S, H	1	P
SFM0081	5.25	-3.77	R, S, H	1	P
SFM0084	4.1	-2.68	R, S, H	1	P
SFM0087	2.35	-0.71	R, S, H	1	P
SFM0091	2.3	-0.7	R, S, H	1	P
SFM0095	7.1	6.28	R, S, H	1	P
SFM0104	7.2	-1.27	R, S, H	1	P
SFM0105	4.2	0.8	R, S, H	1	P
SFM0106	5.3	0.88	R, S, H	1	P
SFM0107	7.05	-3.9	R, S, C	1	P

2.3 Boreholes drilled and investigated for SDM-PSU

Figure 2-4 shows seven cored boreholes and four percussion boreholes drilled and investigated between 2008 and 2009 in support of SDM-PSU and the discipline-specific descriptions of the bedrock conditions where SFR3 will be constructed. Table 2-4 shows an overview of the borehole length, the bottom elevation, data availability by discipline, number of monitoring sections and state variables measured in the borehole.

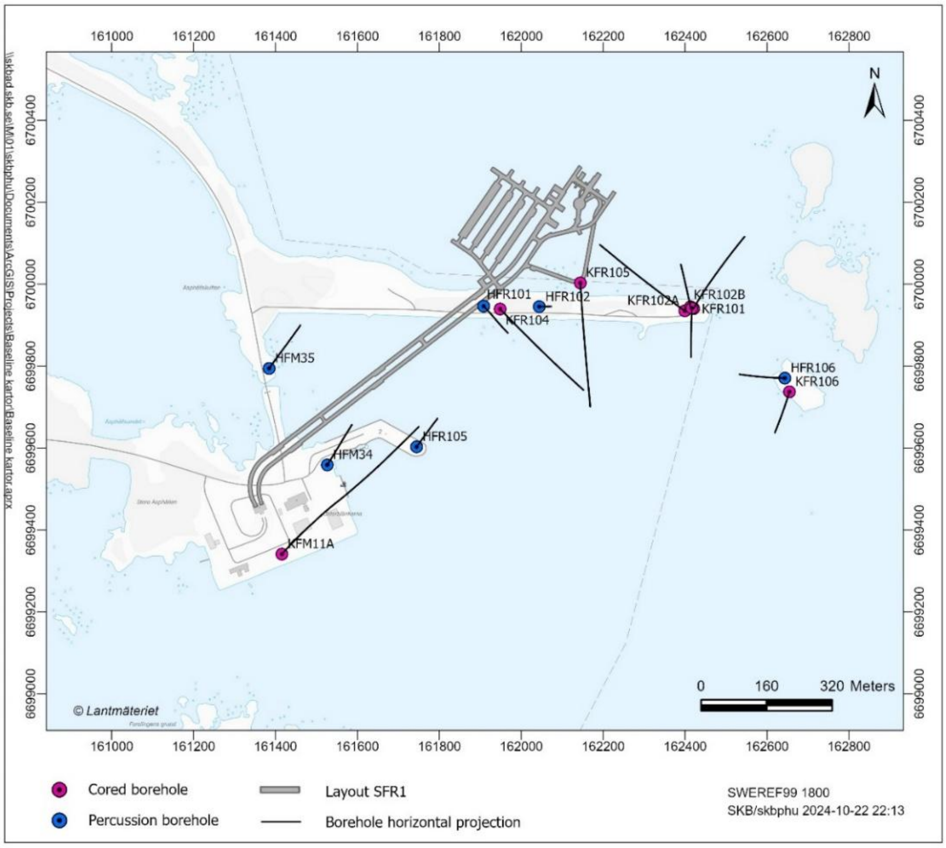

Figure 2-4. *Plane view showing seven cored boreholes, and four percussion boreholes drilled and investigated in support of SDM-PSU and the discipline-specific descriptions of the bedrock conditions where the planned extension SFR3 will be constructed. Note that three boreholes in this figure, KFM11A, HFM34, and HFM35, were drilled already in 2007 in support of SDM-Site, cf. Figure 2-2 and Table 2-2.*

Table 2-4. Overview of interest by discipline of the data acquired in the boreholes shown Figure 2-4. R = regolith geology, G = bedrock geology, M = rock mechanics, T = thermal properties, S = near-surface hydrogeology, H = bedrock hydrogeology, C = hydrogeochemistry, Tr = transport properties.

	Borehole length (m from TOC)	End of borehole (m RH2000)	Discipline interest	Number of	Monitored parameters
Borehole			R, G, M, T, S, H, C, Tr	monitoring sections	P = pressure
					C = chemistry
KFR101	341.76	-261.85	R, S, H	3	p
KFR102A	600.83	-537.14	R, S, H	8	p
KFR102B	180.08	-142.69	R, S, H Tr	3	p
KFR103	200.5	-158.71	R, S, H	3	p
KFR104	454.57	-351.53	R, S, H	3	p
KFR105	306.81	-156.45	R, S, H Tr	5	p
KFR102B	180.08	-142.69	R, S, H	3	p
KFR103	200.5	-158.71	R, S, H	3	p
KFR104	454.57	-351.53	R, S, H	3	p
KFR105	306.81	-156.45	R, S, H	5	p
KFR106	300.13	-279.63	R, S, H	3	p
HFR101	209.3	-186.66	R, S, H	1	P
HFR102	55.04	-43.9	R, S, H	2	p
HFR106	190.4	-152.91	R, S, H	4	p

2.4 Supplementary boreholes and investigations in the SFK area

Figure 2-5 shows 15 cored boreholes and five percussion boreholes drilled and investigated between 2011 and 2018, i.e., after SDM-Site. All boreholes in bedrock were drilled to support a detailed characterization of the superficial bedrock close to the access area of the spent fuel repository, SFK. One of the cored boreholes was drilled next to the planned skip shaft and reached "repository depth". Monitoring wells were installed in the regolith to characterise the overburden prior to start of construction works and environmental impact assessments.

Table 2-5 shows an overview of the borehole length, the bottom elevation, data availability by discipline, number of monitoring sections and state variables measured in the borehole.

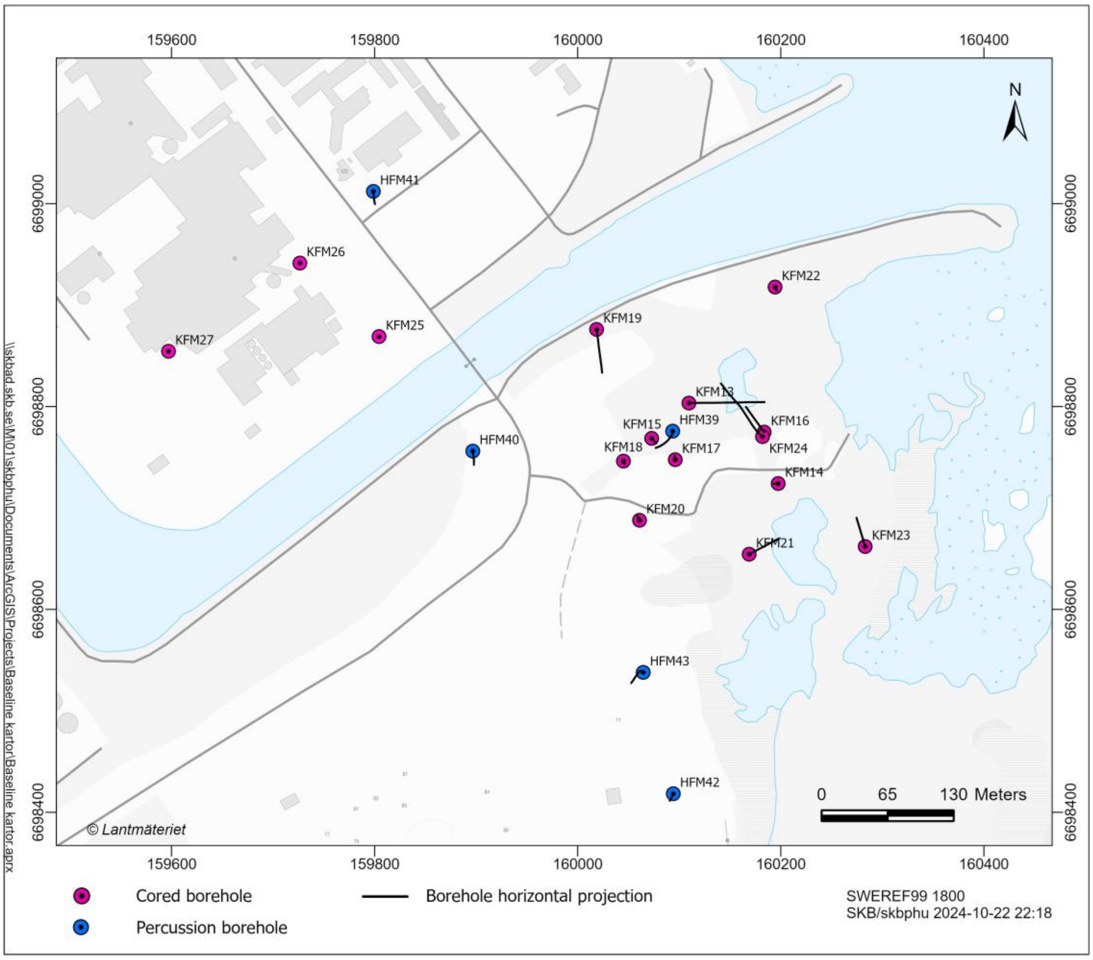

***Figure 2-5.** Plane view showing 15 cored boreholes, and five percussion boreholes drilled and investigated between 2011 and 2018, i.e., after SDM-Site. The boreholes support a detailed characterization of the superficial bedrock close to the access area of the spent fuel repository, SFK.*

Table 2-5. Overview of interest by discipline of data acquired in the boreholes shown Figure 2-5. R = regolith geology, G = bedrock geology, M = rock mechanics, T = thermal properties, S = near-surface hydrogeology, H = bedrock hydrogeology, C = hydrogeochemistry, Tr = transport properties.

Borehole	Borehole length (m from TOC)	End of borehole (m RH2000)	Discipline interest R, G, M, T, S, H, C, Tr	Number of monitoring sections	Monitored parameters P = pressure C = chemistry
KFM13	150.21	-127.44	R, G, S, H	1	P
KFM14	60.18	-57.85	R, G, S, H	1	P
KFM15	62.3	-58.3	R, G, S, H	1	P
KFM16	60.35	-50.32	R, G, S, H	1	P
KFM17	60.45	-56.47	R, G, S, H	1	P
KFM18	60.46	-56.71	R, G, S, H	1	P
KFM19	102.37	-89.94	R, G, S, H	1	P
KFM20	60.5	-57.31	R, G, S, H	1	P
KFM21	101.06	-92.4	R, G, S, H	3	P
KFM22	60.26	-57.18	R, G, S, H	1	P
KFM23	100.64	-93.74	R, G, S, H	3	P
KFM24	550.17	-544.91	R, G, S, H	1	P
KFM25	100.72	-99.64	R, G, S, H	1	p
KFM26	100.72	-99.64	R, G, S, H	1	p
KFM27	100.74	-97.44	R, G, S, H	1	p
HFM39	100.64	-94.37	R, G, S, H	2	p
HFM40	151.2	-144.62	R, G, S, H	1	p
HFM41	101.7	-98.16	R, G, S, H	1	p
HFM42	101.5	-97.04	R, G, H	1	_
HFM43	195.3	-190.89	R, G, H	2	p

2.5 Supplementary boreholes and investigations in the SFR area

Figure 2-6 shows five cored boreholes and four percussion boreholes drilled and investigated between 2018 and 2021, i.e., after SDM-PSU. The cored boreholes support a more detailed characterization of the bedrock where the extension to SFR1, SFR3, will be constructed, whereas the percussion boreholes support the hydrogeological properties transverse the strike of the Singö deformation zone. Table **2-5** shows an overview of the borehole length, the bottom elevation, data availability by discipline, number of monitoring sections and state variables measured in the borehole.

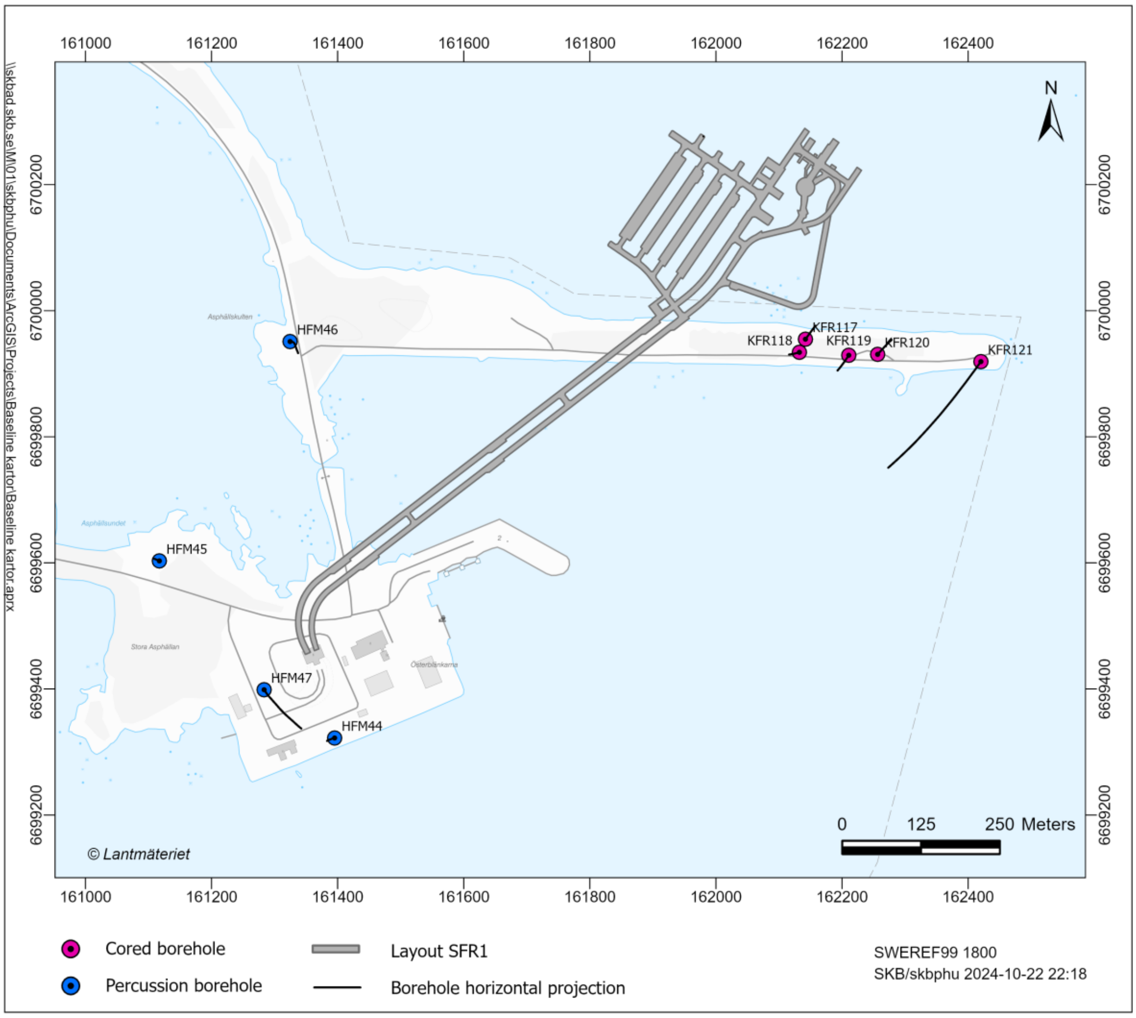

Figure 2-6. *Plane view showing five cored boreholes and four percussion boreholes drilled and investigated between 2018 and 2021, i.e., after SDM-PSU. The cored boreholes support a more detailed characterization of the bedrock where the extension to SFR1, SFR3, will be constructed. The percussion boreholes support the hydrogeological properties transverse the strike of the Singö deformation zones.*

Table 2-6. Overview of interest by discipline of data acquired in the boreholes shown Figure 2-6. R = regolith geology, G = bedrock geology, M = rock mechanics, T = thermal properties, S = near-surface hydrogeology, H = bedrock hydrogeology, C = hydrogeo-chemistry, Tr = transport properties.

Borehole	Borehole length (m from TOC)	End of borehole (m RH2000)	Discipline interest R, G, M, T, S, H, C, Tr	Number of monitoring sections	Monitored parameters P = pressure C = chemistry
KFR117	176.01	-171.51	G, M, H,	_	P
KFR118	175.48	-171.5	G, M, H,	1	P
KFR119	176.47	-170.77	G, M, H,	1	P
KFR120	176.91	-170.8	G, M, H,	_	P
KFR121	362.53	-282.11	G, M, H,	1	P
HFM44	199.6	-196.16	G, H,	1	P
HFM45	200.30	-196.09			
HFM46	200	-196.6	G, H,	1	P
HFM47	200.4	-173.45	G, H,	2	P

2.6 Surface-system monitoring installations

Figure 2-7 to Figure 2-10 show surface system investigations and monitoring locations. Table 2-7 shows an overview of the borehole length, the bottom elevation, data availability by discipline, number of monitoring sections and state variables measured in the borehole.

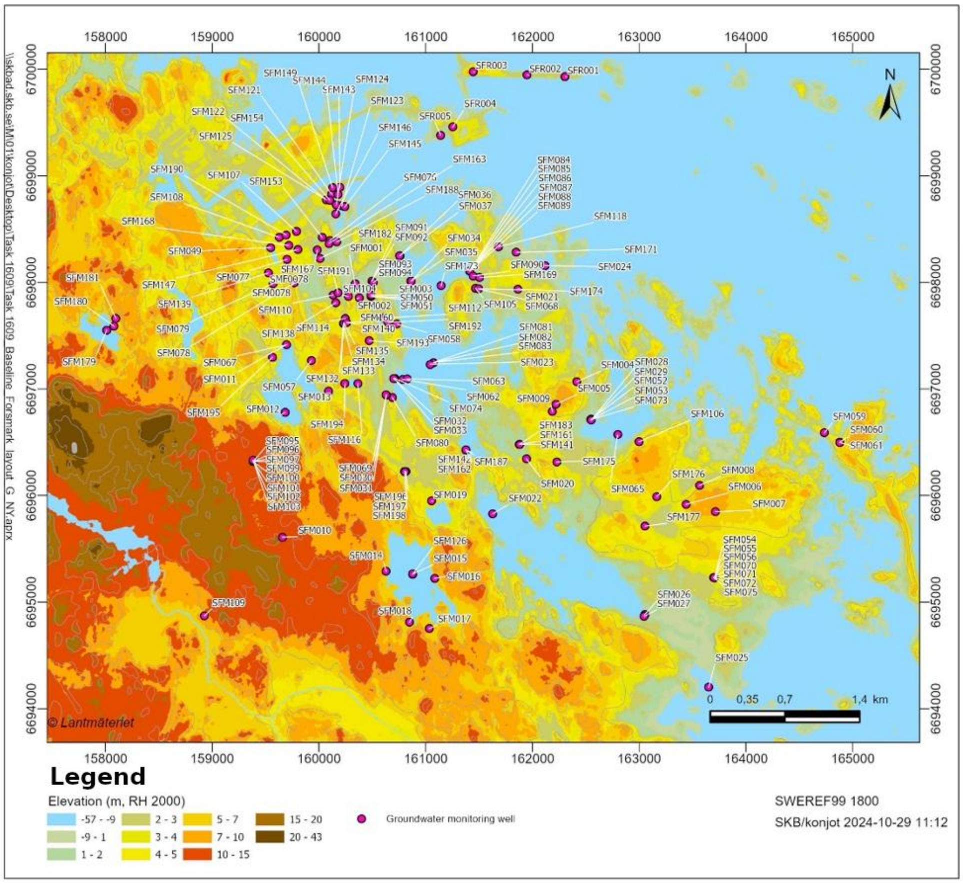

Figure 2-7. Plane view showing groundwater monitoring wells drilled and investigated in support of Baseline Forsmark.

Table 2-7. Overview of interest by discipline of data acquired in the boreholes shown Figure 2-7. R = regolith geology, G = bedrock geology, M = rock mechanics, T = thermal properties, S = near-surface hydrogeology, H = bedrock hydrogeology, C = hydrogeochemistry, Tr = transport properties.

Borehole	Borehole length (m from TOC)	End of borehole (m RH2000)	Discipline interest R, G, M, T, S, H, C, Tr	Number of monitoring sections	Monitored parameters P = pressure C = chemistry
SFM000121	6.5	-3.63	R, S	1	P,
SFM000122	7.5	-4.47	R, S	1	P,
SFM000123	3.5	-1.82	R, S	1	P,
SFM000124	3.5	-1.13	R, S	1	P,
SFM000125	4.5	-0.78	R, S	1	P,
SFM000126	7.17	-0.71	R, S	1	P,
SFM000132	3.1	1.09	R, S	1	P,
SFM000133	3.1	0.75	R, S	1	P,
SFM000134	2.1	2.08	R, S	1	P,
SFM000135	2.1	1.7	R, S	1	P,
SFM000138	2	0.74	R, S	1	P,
SFM000139	3	0.85	R, S	1	P,
SFM000140	2	1.58	R, S	1	P,
SFM000141	2	0.42	R, S	1	P,
SFM000142	1	0.57	R, S	1	P,
SFM000143	3	-0.55	R, S	1	P,
SFM000144	4	-1.35	R, S	1	P,
SFM000145	3	-1.35	R, S	1	P,
SFM000146	4	-0.71	R, S	1	P,
SFM000147	3	-0.04	R, S	1	P,
SFM000149	3	-1.53	R, S	1	P,
SFM000153	5	-0.65	R, S	1	P,
SFM000160	2.5	1.75	R, S	1	P,
SFM000161	2	1.19	R, S	1	P,
SFM000162	1.5	0.51	R, S	1	P,
SFM000163	6.88	-0.21	R, S	1	P,
SFM000167	10.91	-2.83	R, S	1	P,
SFM000168	5.17	0.64	R, S	1	P,
SFM000169	0	-0.67	R, S	1	P,
SFM000171	0	-1.76	R, S	1	P,
SFM000173	0	-3.12	R, S	1	P,
SFM000174	0	1.57	R, S	1	P,
SFM000175	0	-0.67	R, S	1	P,
SFM000176	0	-0.72	R, S	1	P,
SFM000177	0	-0.18	R, S	1	P,
SFM000179	0	1.89	R, S	1	P,
SFM000180	0	1.95	R, S	1	P,
SFM000181	0	5.56	R, S	1	P,
SFM000182	0	-1.34	R, S	1	P,
SFM000183	0	-3.6	R, S	1	P,
SFM000187	0	0.14	R, S	1	P,
SFM000188	0	-1.71	R, S	1	P,
SFM000190	0	-0.38	R, S	1	P,
SFM000191	0	-3.71	R, S	1	P,
SFM000192	0	-4.56	R, S	1	P,
SFM000193	0	1.95	R, S	1	P,
SFM000194	0	1.3	R, S	1	P,
SFM000195	0	-2.23	R, S	1	P,
SFM000196	0	-6.75	R, S	1	P,
SFM000197	0	-4.3	R, S	1	P,
SFM000198	0	-2.84	R, S	1	P,

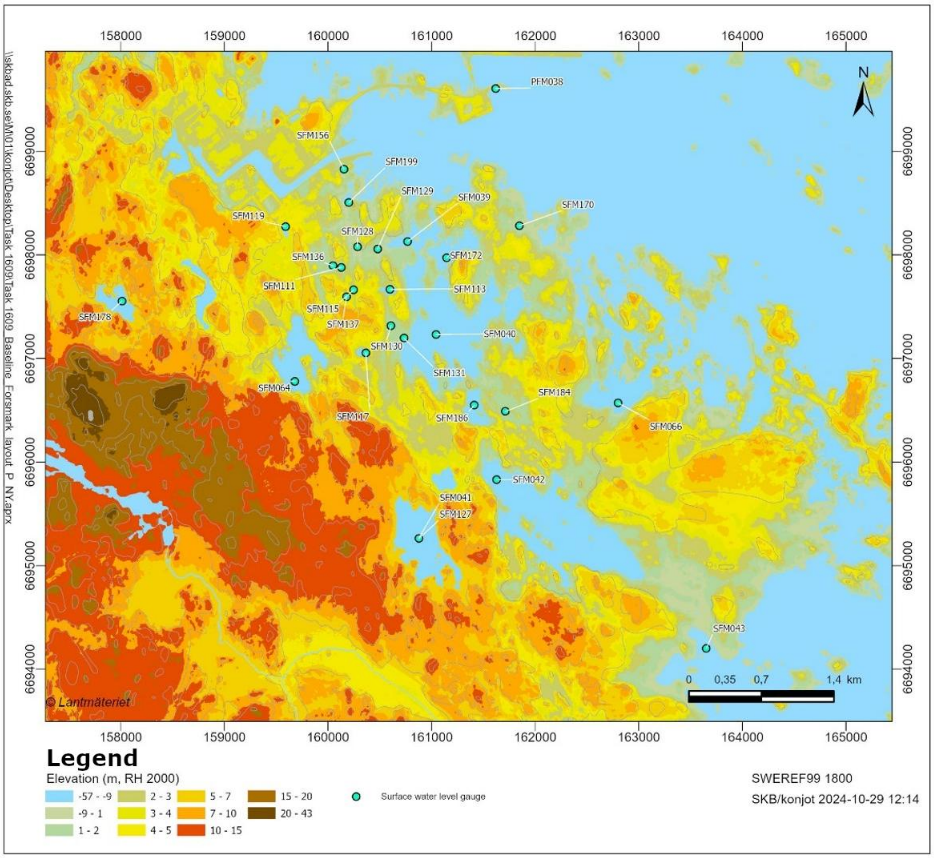

Figure 2-8. Topographic map showing surface-water level gauges in the sea, lakes and ponds for which monitoring data are available in support of Baseline Forsmark.

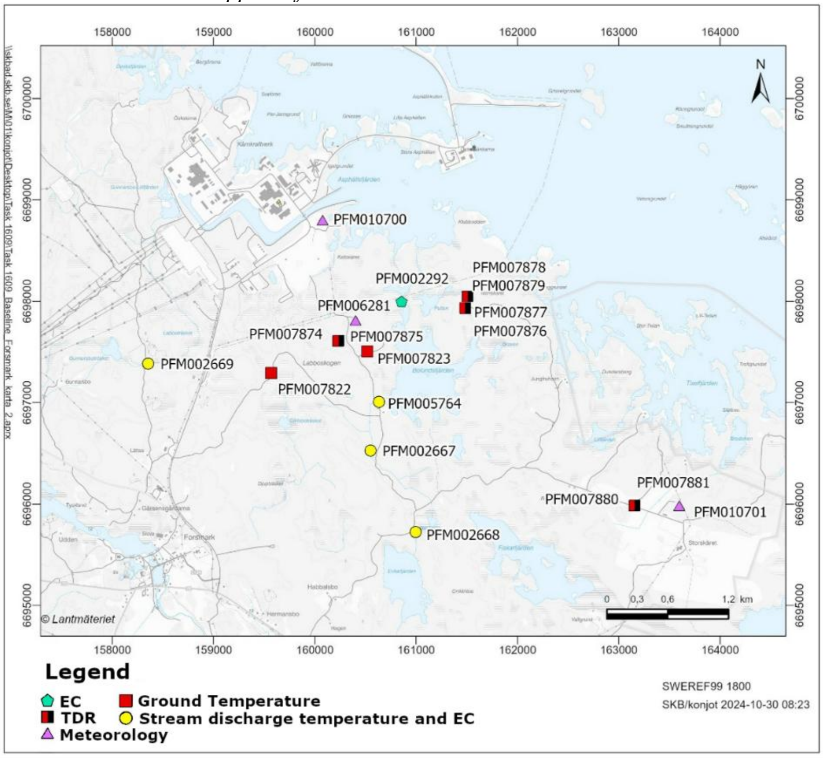

Figure 2-9. Plane view showing locations of sampling points used for monitoring of surface water electrical conductivity (EC), ground temperature (TDR; at these stations also water content and EC are measured), meteorology, and stream discharge (at these stations also temperature and EC are measured), and for which data are available in support of Baseline Forsmark.

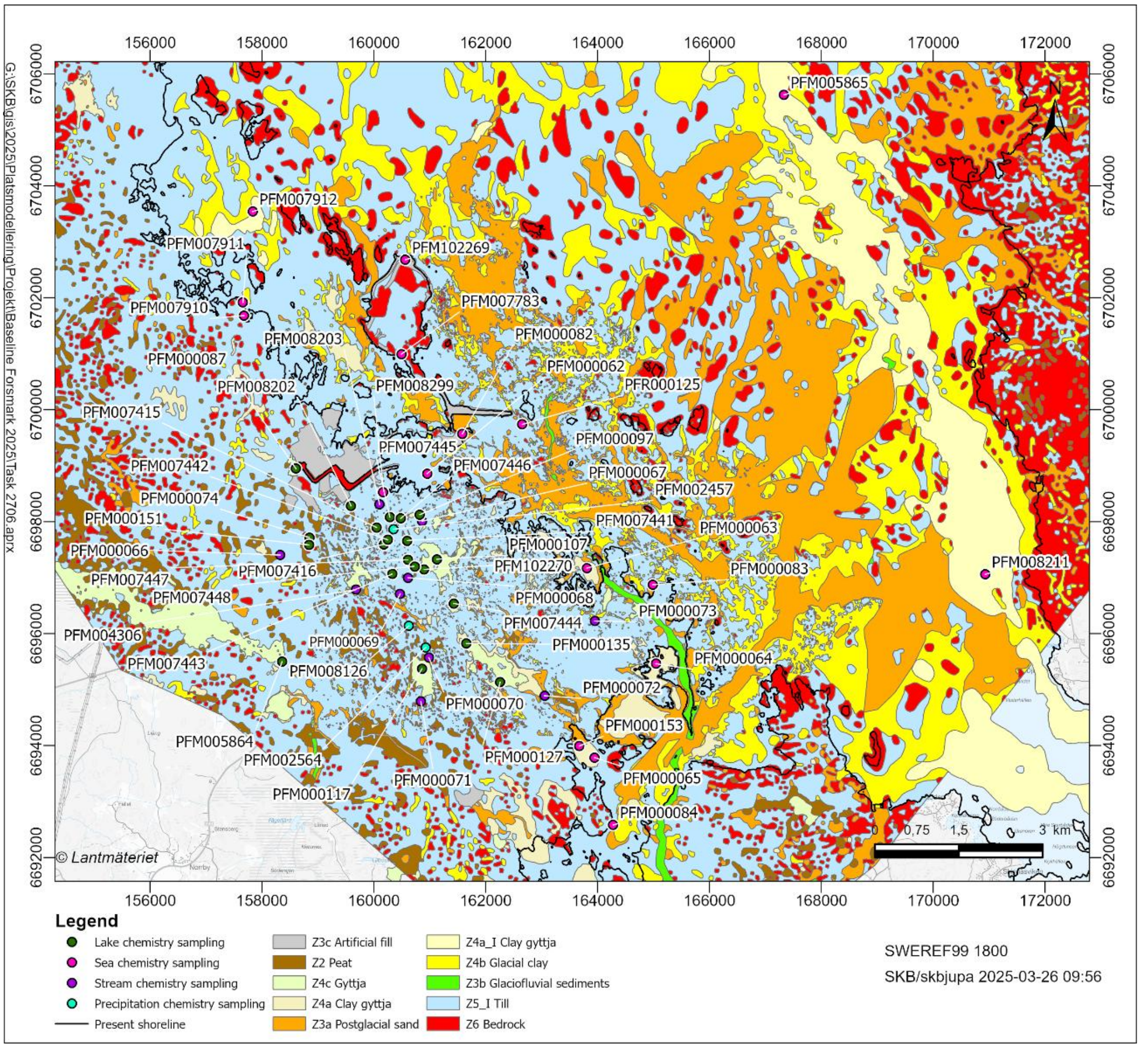

Figure 2-10. *Regolith map showing locations of surface water sampling points used for monitoring as well as sampling points used for hydrochemical investigations or monitoring of sea water, lakes, streams and precipitation.*

3 Topography and regolith geology

This chapter describes the present-day surface system conditions at the Forsmark site in terms of topography and regolith. Regolith refers to all loose, unconsolidated deposits overlying the bedrock. The regolith models covers an area of 500 km2 which is larger and includes than the Forsmark catchment (Figure 1-4). Two major models covering the same 500 km2 area comprise following information:

- The Digital Elevation Model (DEM) shows the height of the topographic surface for the ground and the seafloor in relation to the sea level.
- The Regolith Depth Model (RDM) shows the total depth, thickness and the stratigraphical distribution of the most commonly occurring regolith types.

These two models are coupled and useful for understanding and modelling the hydrological and geochemical processes affecting the system. They are used as input for transport models regarding both existing and future terrestrial and bathymetric features used in SKB's safety assessments and for evaluating the environmental impact of the repositories.

3.1 State of knowledge

The Forsmark area is a coastal site on the shoreline of the Baltic Sea in northern Uppland. The initial area of Forsmark surfaced from the sea approximately 3000 years ago. The swift post-glacial land uplift, coupled with the flat topographic relief of less than 25 m, induces rapid shoreline displacement and leading to the development of a relatively young terrestrial ecosystem characterized by several newly established shallow lakes and wetlands which currently are filled with sediments and peat.

The general distribution and properties of regolith in the Forsmark area correspond to most other Swedish coastal areas below the highest coastline (e.g. Persson 1997) the highest topographical areas are dominated by till and outcrops whereas lower laying areas are dominated by fine grained water laid deposit, mostly different types of clay. In the Forsmark area most large areas with water laid sand and clay are situated at the seafloor, whereas the terrestrial areas are dominated by till and outcrops. The average regolith thickness is c. 4.2 m with outcrops included (Petrone et al. 2020).

Another feature that can be observed is that the inland areas have a higher proportion of peat compared to more recently uplifted coastal areas, which is an effect of the successive infilling of peat in wetlands. That is illustrated by the lower proportion of peat in coastal areas shown on SGU:s maps of Quaternary deposits (e.g. Persson 1985). One thing that is special for the Forsmark area compared to most other Swedish coastal areas is the occurrence of clayey till with a low boulder frequency. The till is typical for this region and is probably formed because of glacial erosions of soft sedimentary rocks and clays at the floor of the Bothnian Bay (Strömberg 1989).

The regolith has mainly been deposited during the last phase of the latest glaciation or during the time after the deglaciation. There are, however, findings of a locally occurring highly consolidated clayey till that might have been deposited during an older phase of the latest glaciation (Sundh et al. 2004). Where observed this till is lying directly on the bedrock (e. g. Albrecht 2005) but geographical distribution of this till is not known.

Physical and chemical regolith properties do not differ significantly from other areas in the region (cf. SGU´s databases). One feature typical for Forsmark and other coastal areas in the county of Uppsala is, however, the high content of calcite in till, glacial clay and some of the gyttja sediments. The calcite and the occurrence of young wetlands give rise to the many sites with higher nature values in the Forsmark and neighbouring areas. After the site investigations studies of deposits from wetlands with high nature values have shown that certain deposits might become acidic if exposed to oxygen (Sohlenius et al. 2020), and it cannot be excluded that a lower groundwater table caused by the construction of the repository can cause that.

Most of SKB's studies on digital elevation data (Brydsten and Strömgren, 2004; Strömgren and Brydsten, 2008, 2013) and regolith from the site investigations are summarised in (Hedenström et al. 2008, SKB 2013; Nyberg et al 2011) but data has also been obtained after SDM-site (e.g. Sohlenius et al. 2019, 2020). Data from the regolith surveys has been used for a model showing the thickness and distribution for the most common regolith types (RDM, Petrone et al. 2020).

3.1.1 Key remaining issues after completion of SDM-Site and SDM-PSU

- In some shallow coastal areas the DEM and RDM was based on a lower density of data implying increased uncertainty compared to other areas.
- The uncertainties in the RDM were not quantified but it can be assumed that these uncertainties varied due to varying density and quality of input data.
- The description of some regolith properties used as input to the radionuclide models could be improved by comparison with additional data.

3.1.2 Summary of updated knowledge at Baseline stage

New high-resolution data have been collected and have subsequently been used to update the DEM (Petrone and Strömgren 2020) to a much higher resolution than used in previous SDM.

The new DEM and updated modelling methodologies have resulted in a more detailed RDM with additional regolith types (Petrone et al. 2020). A few new areas were detailed mapped in connection to construction work around the Söderviken area. These results are included in the baseline models.

3.2 Description of Baseline data

3.2.1 Elevation and bathymetry data

The baseline Digital Elevation Model (Petrone and Strömgren, 2020), integrates a variety of data sets utilized in earlier modelling efforts (Brydsten and Strömgren, 2004; Strömgren and Brydsten, 2008, 2013) along with new data acquired post SDM-site. This model incorporates new LiDAR data for the terrestrial Forsmark baseline area, containing over 150 million elevation data points, which was provided to the SKB by the National Land Survey of Sweden. Additionally, Lidar data was also used to create a new shoreline together with aerial photographs, point measurements using differential GPS and data base maps from the National Land Survey of Sweden.

The lake bathymetry is based on depth measurements which were acquired from lakes, as documented by Brunberg and Blomqvist, (2004) and Brunberg and Blomqvist (1998). This included lakes such as Bruksdammen and upstream bodies of water, for which depth measurements were digitized by Petrone and Strömgren (2020). After SDM-site additional depth data was obtained through echo sounding in Lake Eckarfjärden which was used for the Baseline DEM (Petrone and Strömgren 2020). No other lakes were included in the site investigations for SDM-site and in the Baseline models these lakes were assigned with a generic depth value of 0, 0.59 and 0.96 depth for lakes smaller than 2.9 Ha, 2.9 to 5 Ha, and larger than 5 Ha respectively.

Marine bathymetry data was primarily collected during the SDM-Site investigations with variability in data quality observed across different datasets (Figure 3-1). A significant portion of this data was gathered along specific lines utilizing a single-beam echo sounder (Elhammer and Sandkvist 2005), resulting in a high density of data along these lines, while the data density diminishes considerably in areas exceeding 1 km between the lines.

In a detailed study of the marine bathymetry around the SFR area conducted in 2011, depth data was acquired using a Swath sonar (Nyberg et al. 2011). This technology provides comprehensive bathymetric coverage along the surveyed lines, with the width of coverage varying based on water depth and instrument settings. The resolution in this area is 5 × 5 m, with depth measurements taken at intervals of 5 m.

For the shallow bays, data originated from measurements conducted by Brydsten and Strömgren (2004), and in some locations, depth values were estimated due to the absence of direct measurements. A detailed description of the data which was used to produce the baseline DEM are shown in Table 2-1 and Table 2-2 in Petrone and Strömgren (2020).

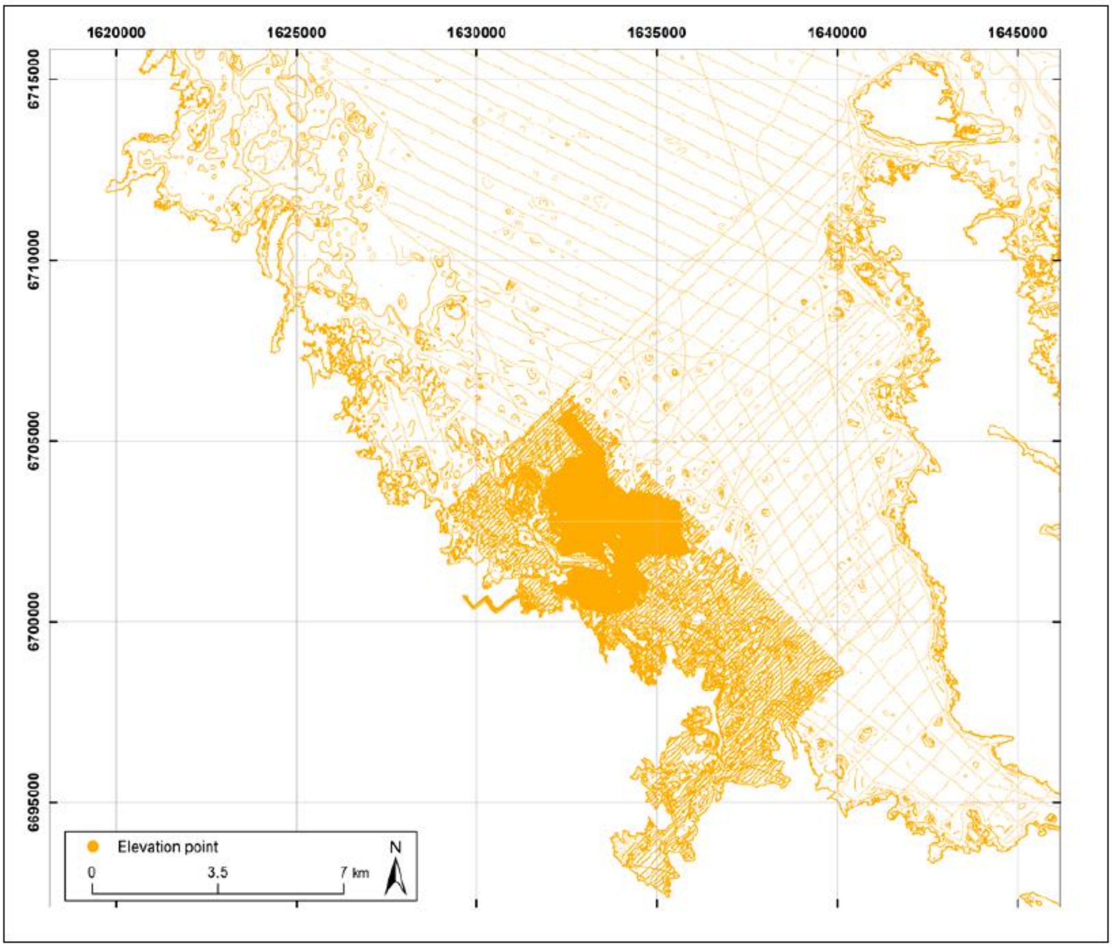

Figure 3-1. Visualisation of data points used in the interpolation of the marine bathymetry model (from Petrone and Strömgren, 2020).

3.2.2 Regolith properties data

SKB´s methods for investigating and modelling regolith during and after the site investigations in Forsmark are summarised in (Sohlenius and Svensson 2022) which also describes the methods used for regolith investigations carried out by other actors. In both areas covered by water and terrestrial area the surficial and stratigraphical distribution of different types of regolith have been mapped using several methods (Figure 3-2). The central part of the area was mapped during SKB´s site investigations whereas data from SGU´s regular mapping program was used in the peripheral parts. The most recently mapped area is the Gunnarsboträskets drainage area (Sohlenius et al. 2019; Area 1b) which can act as a hydrological reference site that will be used for determining natural hydrological conditions, which can be compared with the conditions around the SFK area during construction. That area was mapped with slightly different methods than other terrestrial areas mainly because of the access to high resolution topographical data (LiDAR data) that was used to delineate different types of regolith with a high accuracy. The different regolith maps have been combined in to a common map which consequently forms a mosaic with varying degree of accuracy (Figure 3-2). In terrestrial areas (Area 1 and 2) the map is based om direct observations in the field as well as interpretations of aerial photographs. In marine areas hydroacoustics and geophysics were used supported by physical samples.

Stratigraphy and total depth of regolith has been investigated both using geophysical measurements and direct observations from drillings and excavations. Many of these studies were conducted in connection with the mapping of areas 1, 4, 6 and 7 which are the most thoroughly investigated areas, whereas areas 2 and 8 almost lacks stratigraphical observations. In the marine area the stratigraphical results are mostly based om geophysical investigations whereas drillings and other direct observations were used in terrestrial area (Area 1) as well as in lakes and shallow marine areas (Area 7). The interpretations in marine area 6 were partly validated in in a study by Borgiel et al. (2022).

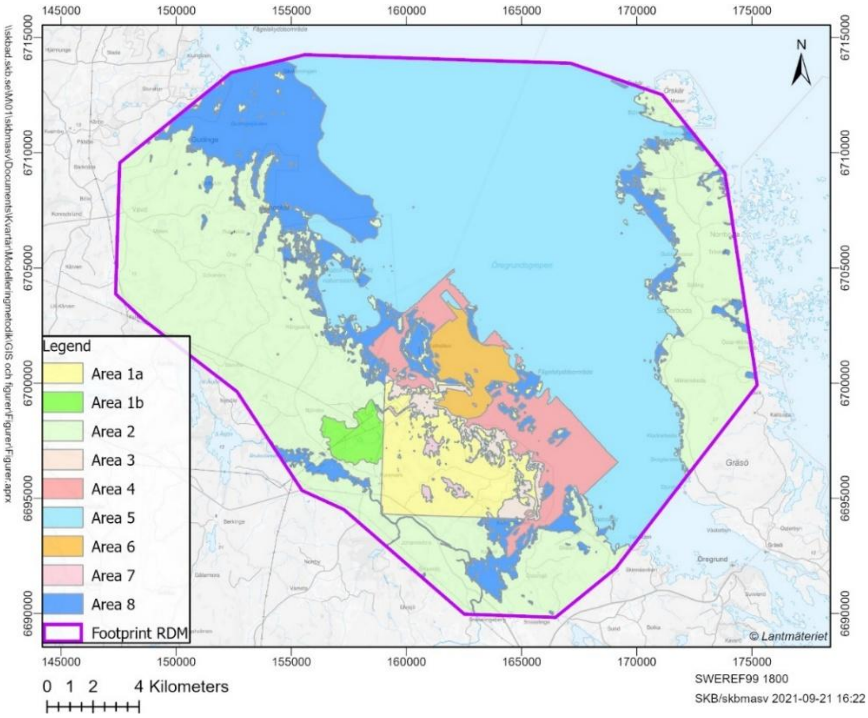

***Figure 3-2.** Several methods used to produce a map showing the surficial distribution of regolith in the area representing the RDM (from Sohlenius and Svensson 2022). The different methods are shortly described in Table 3-2.*

Table 3-2. Short description and references to the methods used to produce the regolith map (Figure 3-5). The geographical distribution of the different areas is shown in Figure 3-2 (From Sohlenius and Svensson 2022).

Area	Type of data	Reference
1a (Terrestrial)	Detailed regolith map for presentation in 1:10 000	Sohlenius et al. (2004)
1b (Terrestrial)	Detailed regolith map for presentation in 1:10 000	Sohlenius et al. (2019)
2 (Terrestrial)	SGU map of regolith for presentation in 1:50 000	SGU database
3 (Marine)	Distribution of regolith in shallow coastal areas	Ising (2005)
4 (Marine)	Detailed distribution of regolith in coastal areas with water depths between 3 and 6 m.	Elhammer and Sandkvist (2005)
5 (Marine)	Distribution of regolith at the sea floor in areas with water depths > 6 m.	The central part of the area was interpreted by Elhammer and Sandkvist (2005) and reinterpreted by Nyberg et al. (2011).
6 (Marine)	Detailed distribution of regolith in coastal areas with water depths between 3 and 6 m	Nyberg et al. (2011)
7 (Lakes in the central part of the model area)	Interpretation from corings in lakes,	Hedenström (2003, 2004a, b), Sohlenius and Hedenström (2009)
Area 8 (Lakes and shallow bays)	Interpreted from DEM and surrounding regolith	Interpreted from distribution of surrounding regolith (Hedenström and Sohlenius 2008)

To characterise the different regolith types, samples have been analysed for grain-size distribution and other chemical and physical properties. The methods for these analyses are described in Hedenström and Sohlenius (2008) and Sohlenius and Svensson (2022). More specific studies aiming at determining the mobility of elements by determining the Solid/liquid partition coefficients (K_d) in different regolith types (Shepard et al 2011) were done for input to the radionuclide models used in SKB´s safety assessment.

More recent studies of regolith properties were made on deposits from wetlands with high nature values (Sohlenius et al. 2020; Sohlenius and Svensson 2021). The aim was to conclude if the wetland deposits might become acidic if the deposits were exposed to oxygen due to a low groundwater table during the construction of SFK.

3.3 Summary of updated methodologies and model overview

The methodology used for geometric modelling of ground elevation and regolith distribution in the Forsmark area is described in Sohlenius and Svensson (2022). The report also elaborates the methods for determining properties of the most commonly occurring regolith types and suggests further development and improvement of the models. The models presented here reflect the baseline conditions in Forsmark, i.e., the state prior to the initiation of the construction of the repository for spent nuclear fuel and the extension of SFR. The method for modelling the ground elevation, the Digital elevation model (DEM), has earlier been reported by Petrone and Strömgren (2020) (see section 3.4.1), and the method for modelling the geometrical distribution of regolith, the Regolith depth model (RDM) has been reported by Petrone et al. (2020) (see section 3.5.1).

3.4 Digital Elevation Model, DEM

3.4.1 Updated methodology in Baseline Forsmark

Previous efforts for SFK and SFR yielded three digital elevation models (Brydsten and Strömgren, 2004; Strömgren and Brydsten, 2008, 2013). The main differences between the previous DEM and the Baseline DEM presented here are summarised in Table 3-3. Since the last DEM, new airborne laser scanning data, LiDAR (light detection and ranging), became accessible for the entire terrestrial region of Forsmark providing accurate elevation data at 1m spatial resolution. The quality of the bathymetry data was increased by additional depth soundings in the sea and lakes. However, the marine part of the Baseline DEM area is still based on a relatively low number of observations which decreases the confidence and the quality of the DEM (Petrone and Strömgren, 2020).

Table 3-3. Comparison between the previous and the current Baseline digital elevation models produced for the Forsmark site (from Petrone and Strömgren, 2020).

	Baseline DEM	**Previous DEM (Strömgren and Brydsten 2013)**
Model area	Smaller and further to the west and north	Larger and further to the east and south
Number of input data	154 075 561	2 348 588
Spatial resolution	1, 5, 10 and 20 m for the terrestrial area, 10 and 20 m for the marine area	20 m for the terrestrial and marine areas
Model projections (xy /z)	RT 90 2.5 gon V / RHB70; SWEREF 99 18 00 / RH 2000	RT 90 2.5 gon V / RHB70
Culverts	Adjustment layer for the culverts in all spatial resolutions	No adjustment layer for culverts
Sea shoreline	Partly adjusted from LiDAR data	No adjustment from LiDAR data
Lake bathymetry	Lake bathymetry digitised from depth maps and estimated depth of lakes not previously processed	No lake bathymetry digitised from depth maps and no estimated

	Baseline DEM	Previous DEM (Strömgren and Brydsten 2013)
		depths of lakes outside the site investigation area
Marine bathymetry	New interpolation and re-processing of previously used data. Additional data added from newer investigations (Petrone and Strömgren, 2020).	Available survey data collected until 2011 (Strömgren and Brydsten, 2013).
Kriging interpolation from points	Exact interpolation performed in both the marine and terrestrial areas	Exact interpolation performed in the terrestrial area and smooth interpolation performed in the marine area
Nuclear power plant inlet canal	Re-digitised and increased number of points	
Brook measurements	Significantly increased number of points. (Adding additional points from another source related to e.g. stream bed, see Petrone and Strömgren, 2020)	

3.4.2 Updated Baseline DEM

The airborne laser scanning data has largely replaced the data utilized in the previous DEM across most terrestrial regions. In the marine areas, the data from the earlier DEM has been reprocessed, incorporating additional data obtained from more recent studies (Petrone and Strömgren, 2020). The baseline dataset used for interpolation contains approximately 154 million elevation points, contrasting with the 2.35 million data points used in the preceding DEM (Figure 3-3). The Baseline DEM is produced with 1 and 5 m resolutions in models covering the terrestrial area only and with 10 and 20 m resolutions in models covering both the terrestrial and the marine areas (Petrone and Strömgren, 2020). The Baseline DEM is available in the coordinate systems RT 90 2.5 gon V and SWEREF 99 18 00 with the associated height systems RHB 70 and RH 2000, respectively.

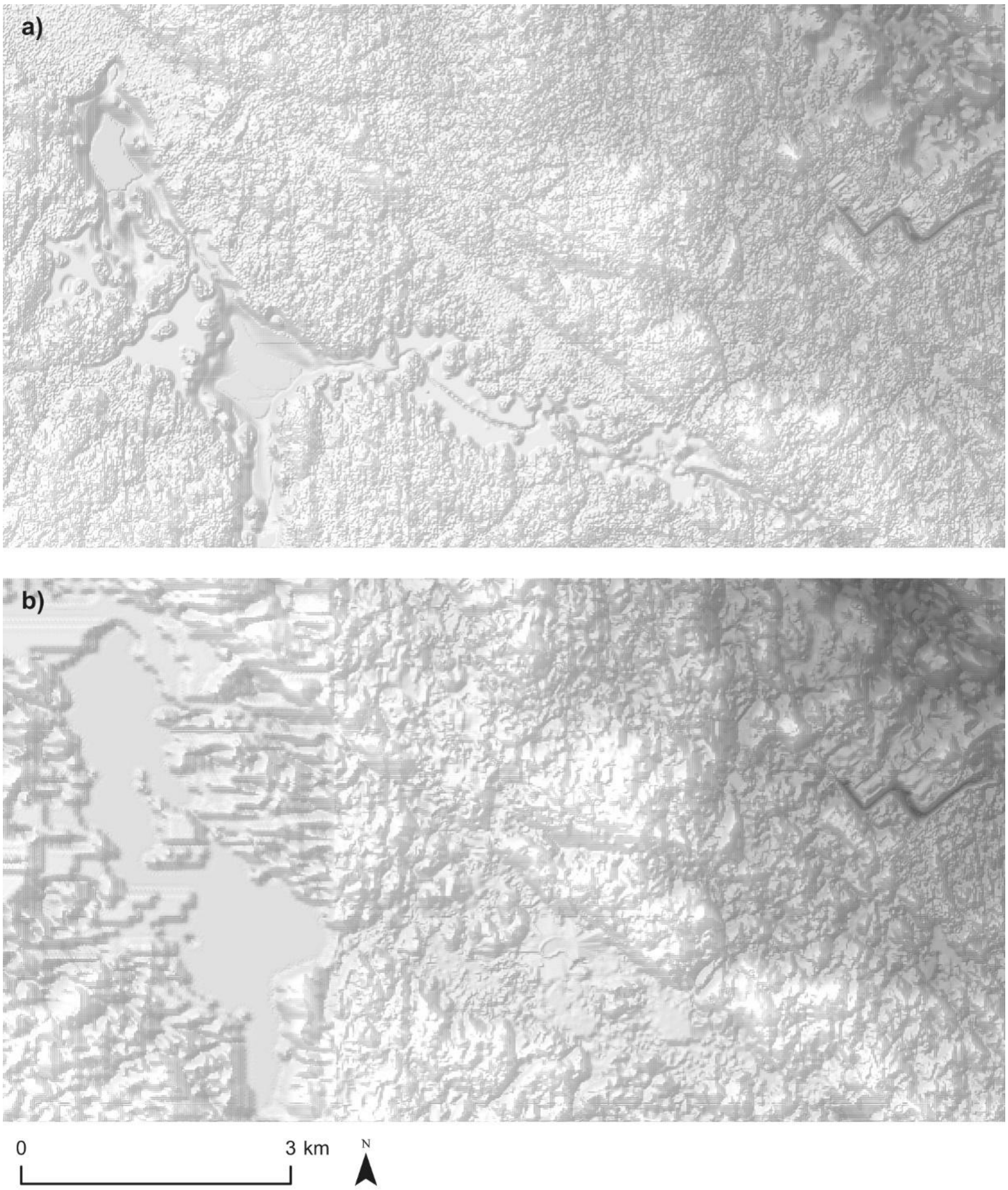

__Figure 3-3.__ Comparison of the same terrestrial area in the Baseline DEM (a) and the previous DEM (b) (from Strömgren and Brydsten, 2013). Both models are stretched and hillshade effect is used. The lighter parts represent high elevation areas and the darker parts represent low elevation areas. The terrestrial part of the current DEM has a finer structure than in the previous DEM. The resolution is 20 m in both models shown in the figure. (from Petrone and Strömgren, 2020).

3.5 Regolith Depth Model

3.5.1 Updated methodology in Baseline Forsmark

Data from the stratigraphical studies was used during the site investigation to construct a conceptual stratigraphical model for the area (Figure 3-4, Table 3-4). The model shows in what order the regolith layers are distributed in different environments. Data obtained after the site investigations have confirmed this stratigraphy (e.g. Sohlenius et al. 2019). However, at a certain site, e.g. a lake, some of the layers might be missing even though the layers always are distributed in the order shown in Figure 3-4.

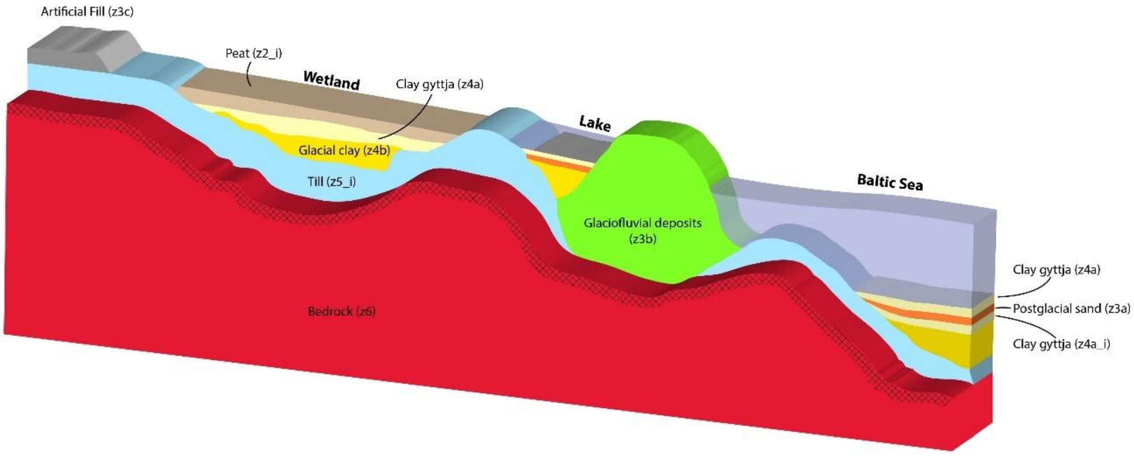

Figure 3-4. The general distribution of the regolith layers (Z-layers) used in the RDM (from Petrone et al 2020).

Table 3-4. General stratigraphical distribution of Quaternary deposits (i.e. the regolith) in the Forsmark area. The Z-layers associated with the different deposits are shown in the RDM produced by Petrone et al. (2020). Note that all these layers are not always present at the same location, i e an area covered by peat is not necessarily underlain by all the regolith layers shown in the table. Artificial fill (Z3c) is the youngest deposit but is not shown in the table.

Regolith type	Relative age	Layer in the RDM
Peat	Youngest	Z2_I
Gyttja	↓	Z4c
Clay gyttja		Z4a
Postglacial sand and gravel		Z3a
Clay gyttja		Z4a_I
Glacial clay	↓	Z4b
Glaciofluvial sediments		Z3b
Till	Oldest	Z5_I
Bedrock		Z6

The stratigraphical data, including the conceptual stratigraphical model (Figure 3-4), has been used together with the DEM and map of regolith to construct a regolith depth model (RDM), which shows the distribution and thickness of the nine most commonly occurring regolith types (Petrone et al. 2020). That model was made in a software (SubsurfaceViewer MX®) using specific interpretations along sections in combination with interpolations to estimate the thicknesses of the regolith layers. The RDM has a resolution of 20x20 m but a more detailed RDM with a 1x1 m resolution was made for the Söderviken area (Follin (ed) 2019). Data from the site investigations were used for earlier RDMs (Hedenström et al. 2008, Sohlenius et al. 2013). The present RDM used the same data but was in several aspects improved: 1) layers gyttja and postglacial sand was added, 2) A much more detailed DEM for especially the terrestrial areas was used, 3) additional geographical areas was added, 4) thin surficial regolith layers (less than 0.5 m) was added, 5) the use of manually drawn sections made it possible to produce regolith layers with a more realistic thicknesses and distribution which in turn made it possible to produce a mere realistic RDM.

3.5.2 Baseline regolith

The updated map of regolith shows the surficial distribution of the different regolith types at 0,5 meter below the ground surface (Figure 3-5).

The updated RDM (Figure 3-6) shows the depth and areal distribution of the nine most commonly occurring regolith types, as well as the elevation of the bedrock surface and the altitude of each regolith layer. The regolith layers are generally thinner in high topographical areas compared to depression, and on a large scale the regolith thickness is lower in the terrestrial areas compared to the deepest marine areas where the thickest regolith layers of the area are found. The present RDM differs from earlier versions in several aspects: 1) a smoother bedrock surface compared to the earlier model, which was characterized by very sharp unrealistic variations in regolith depth between e.g. outcrops and surrounding areas. 2) The average thickness of regolith is 2.5 m thinner in the present RDM (1.7 m when only comparing areas included in the previous RDM). The major discrepancies are likely from the inability of the previous model to account for variations in soil depth across areas with different soil types. One effect of that is unrealistically thick regolith depths close to areas with outcrops. This is particularly evident in regions at the sea floor where data between the surveyed lines is lacking. Additionally, the previous model exhibited sharp transitions in soil depth between land and sea. In contrast, the new model presents a smoother and more realistic depiction of the bedrock surface. 3) The present RDM includes two additional layers, gyttja and sand, that makes it more useful for transport modelling.

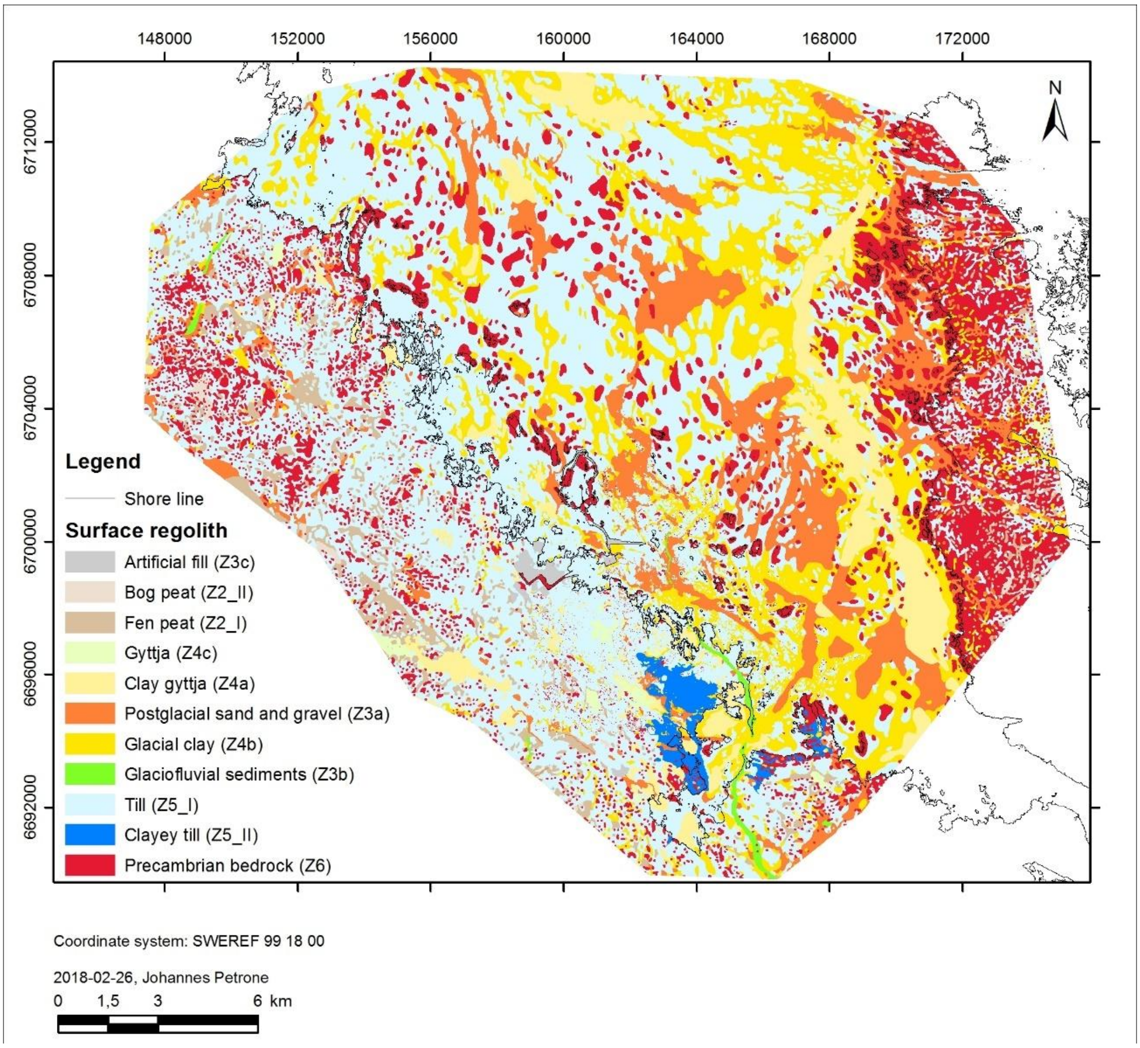

Figure 3-5. *The distribution of regolith 0.5 m below the ground surface (from Petrone et al. 2020). The map is a compilation of eight maps, originally presented in different scales (see Figure 3-2 and Table 3-2). The original maps show some additional regolith sub-types not shown here.*

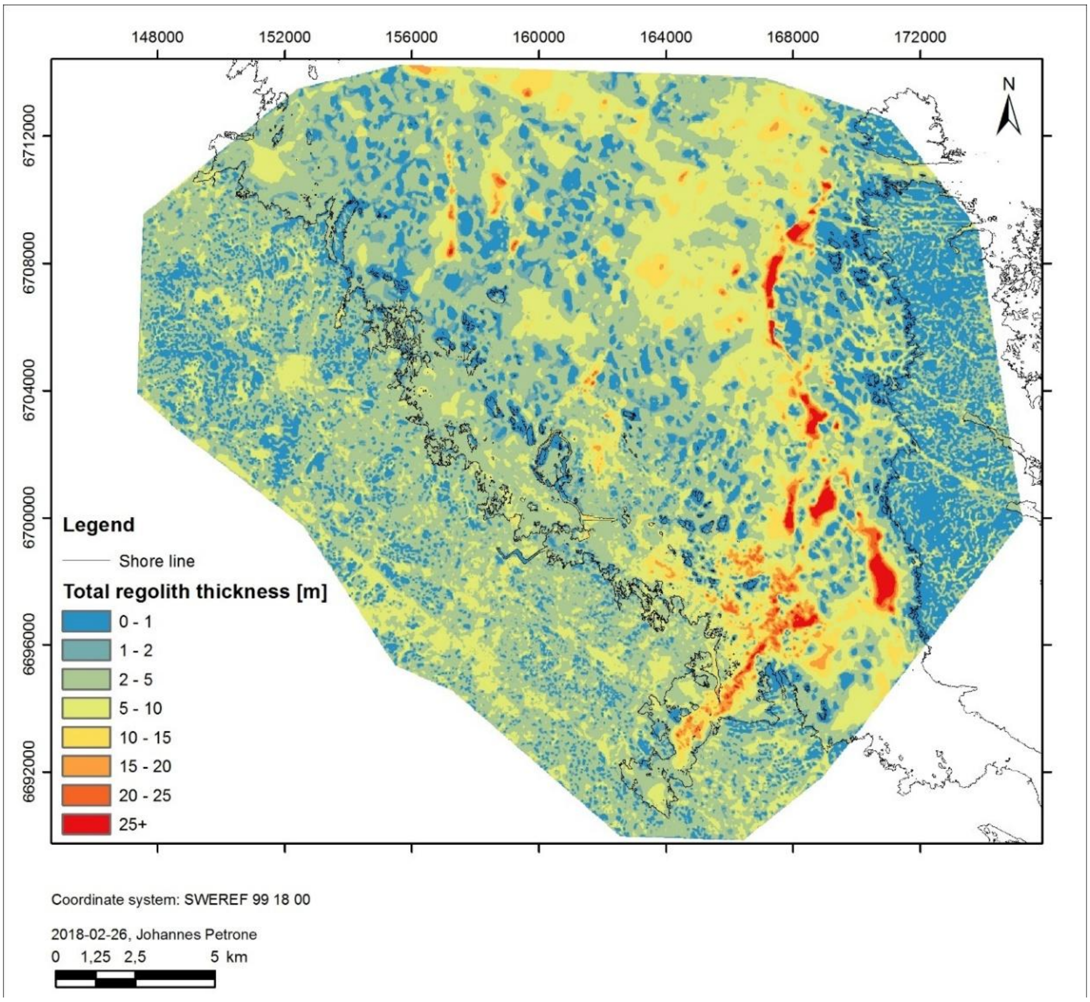

Figure 3-6. *Total modelled regolith depths (from Petrone et al. 2020).*

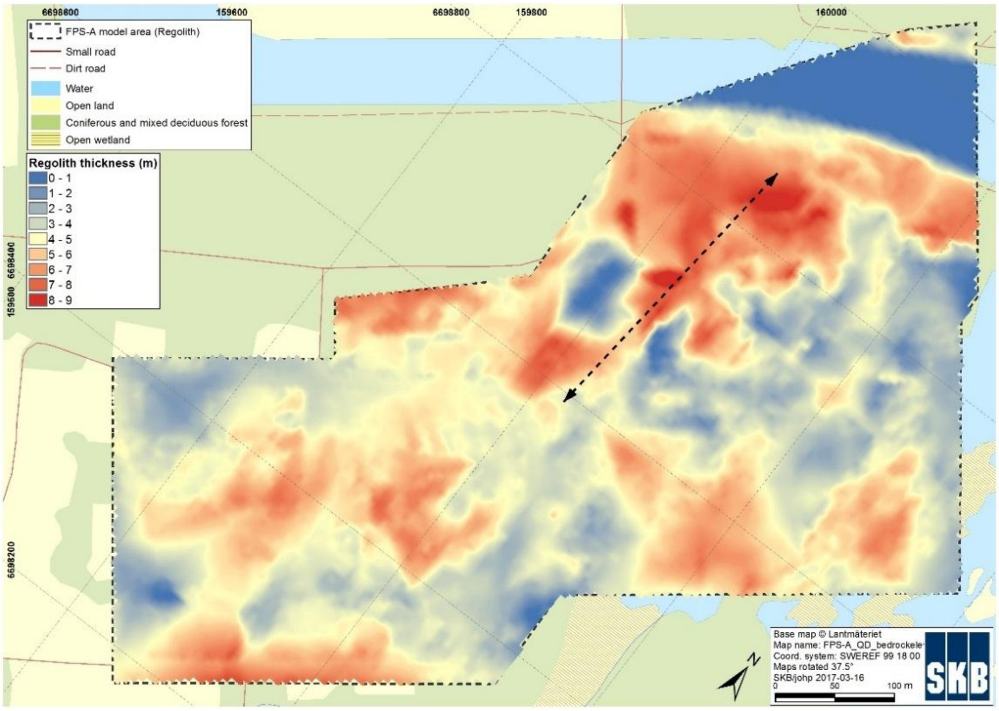

Figure 3-7. *Regolith thickness in the access area in Söderviken (from: Follin (ed) 2019). The thickest regolith layers occur in the bedrock depression marked with a dashed line.*

The RDM for the access area in Söderviken is characterised by relatively thin layers of regolith even though thicker layers are found in bedrock depressions (Figure 3-7). The result shows that the bedrock relief in general is more undulating than the topography of the ground surface. Most of the regolith volume constitute till which to a large part is overlaid by artificial fill.

3.5.3 Uncertainties in regolith models

The uncertainties of the regolith map vary since the geographical density of data points used to produce the model varies within the studied area (Figure 3-2The terrestrial area is mainly based on direct field observation whereas hydroacoustic and geophysical data with larger uncertainties was used in the marine areas. The central part of the area from which data was collected during SKB's site investigations (Figure 3-3) exhibits generally lower uncertainties in comparison to the surrounding peripheral areas, where data sourced from SGU's regular mapping program (lower field observation density, see figure 3-8) was utilized.

In the terrestrial Area 2 (Figure 3-3) the map was produced during SGU´s regular mapping program and the delineation between different regolith types can have errors of several tens of meters, and some features e.g. small outcrops have a too large extension on the map, whereas small areas of clay or peat are not shown at all. In Area 1, as part of SKB's investigation program, the accuracy in delineation between various regolith types are typically under 10 meters. Figure 3-8 presents a comparison between the previous map from SGU's mapping (SGU database) and a more detailed map derived from SKB's site investigation in Area 1 (Sohlenius et al. 2004).

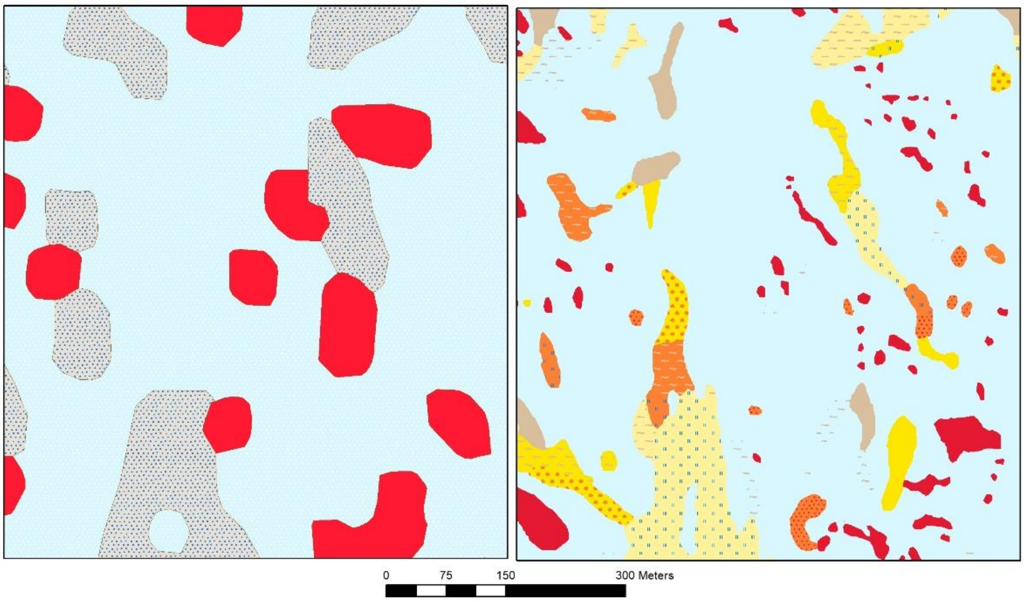

Figure 3-8. *A comparison between two maps from Area 1a (see Figure 3-3). The map from SGUs regular mapping program is shown to the left, and the map to the right was produced during SKBs site investigation (Sohlenius et al. 2004). The comparison shows that the classification of deposits varies between the two maps but also that the delineation between e,g bedrock (red) and till (blue) has been done in a much more detailed way when mapping Area 1.*

Geophysical and hydroacoustical investigations, which have been used in the marine area generally have a larger uncertainty than direct observations from drillings and excavations (Sohlenius and Svensson 2022). In the marine areas the quality and geographical density varies due to the quality and quantity of input data. In areas 4 and 6 regolith data were collected along survey lines with a 100 m spacing. It was, however, not possible to obtain data from the boat in the shallowest areas (Area 7 in Figure 3-3). In some marine areas there is a 1 km separation between these survey lines (Area 5 in Figure 3-3) and because of that it is likely that the areas between the lines have relatively large uncertainties.

The uncertainties from the regolith map are partly reflected in the uncertainties of the RDM. The RDM, however, is to a large part based on stratigraphical observations. Even though the geophysical investigations from the marine area have larger uncertainties than result from corings the number of stratigraphical observations is much larger in most marine areas compared to other parts of the study area. Especially in areas 4 and 6 the numbers of observations are large. Large parts of the terrestrial areas (Area 2), including many lakes, lack both stratigraphical data and regolith depth data. Even though area 1 has been mapped in detail the number of stratigraphical observations is rather few, especially observations showing the thickness of till. Therefore, the thicknesses of the regolith layers are generally more uncertain in the terrestrial areas due to lower data density, including lakes, compared to parts of the marine area. The interpreted thickness of the till is regarded more uncertain in the marine area, whereas the thickness of marine soft sediments is regarded as more confident. However, some of the marine clay sediments contain gas that makes it impossible to estimate the thickness of the regolith layers. The clay deposits at the sea floor around SFR interpreted during the marine geological survey (Nyberg et al. 2011) have been validated within a later study (Borgiel et al. 2022).

The number of analysed samples varies between regolith types, and some analyses have been difficult to perform. As an example, it has been difficult to take undisturbed samples of till to determine bulk density. It is consequently uncertain if all analysed regolith parameters are representative for each regolith type.

In Sohlenius and Svensson (2022) the uncertainties of the models are more thoroughly discussed.

3.6 Discussion

3.6.1 Baseline status

The baseline status for DEM and RDM prior the start of construction has been established and described in Petrone and Strömgren 2020, Petrone et al, 2020 and Sohlenius and Svensson 2022.

3.6.2 Remaining uncertainties

- In some marine areas the bathymetri was based on a lower data density in previous SDM.
- Stratigraphical findings obtained from drillings exhibit greater reliability compared to interpretations derived from geophysical measurements. Nevertheless, the density of geophysical data points in a large part of the marine area is significantly greater than corresponding data in terrestrial areas.

Large parts of the terrestrial areas in the RDM, including many lakes, lack both stratigraphical data and regolith depth data.

3.6.3 Implications for future SDM updates

New techniques, developed after the site investigations, have made it possible to obtain high resolution topographical data from both terrestrial and water covered areas. In the terrestrial areas, the baseline DEM would make it possible to improve the regolith map in Area 2 (Figure 3-3) and the use of new in techniques for determining seafloor bathymetry would make it possible to improve both the quality of the DEM and the regolith map.

There are now more data available that can be used for improving the present RDM (Petrone et al. 2020). That includes the map of regolith around Gunnarsboträsket (Area 1b in Figure 3-3,) as well as new stratigraphical investigations from studies in wetlands and installations of groundwater pipes (Johansson and Werner 2019). Also, in the access area in Söderfjärden more stratigraphical data is available which can be used to improve the detailed RDM (Follin (ed) 2019). Furthermore, the topography of the access area has changes due to construction work and there is therefore a need to update both the RDM and the DEM in that area.

The RDM could be improved by more thorough comparisons to measurements of the regolith. This could also enable a more thorough quantification of uncertainties. That could also include a better evaluation of uncertainties of all input data used for that model.

Regolith properties are used as input to several models and for some regolith types the relevant data has been scarce. One such parameter is K_d in deposits from wetland and lakes. Therefore, many samples for characterising K_d in different types of regolith from lakes and wetlands have recently been taken. The study includes sampling and analyses of samples during reduced (oxygen free) conditions which will give Kd values that more realistically demonstrates the natural conditions.

Earlier stratigraphical studies have shown that there are sites with an old till that might have formed during an earlier phase of the glaciation and that is characterised by specific physical properties (Sundh et al. 2004). That old till is currently investigated with the aim to obtain more information regarding the age and properties of that deposit.

4 Bedrock geology

A keystone in the description of the bedrock at the Forsmark site is a series of coordinated geological models, which includes three deterministic aspects: rock domains, structures (principally deformation zones) and fracture domains. In combination, these models provide the geometrical context for the descriptive modelling of other geoscientific disciplines, such as thermal properties, rock mechanics, hydrogeology, hydrogeochemistry and transport properties.

The deterministic geological models of Baseline Forsmark are basically inherited from SDM-Site and SDM-PSU, with subsequent updates by using data obtained after 2010. Although the models of Baseline Forsmark are based on the established structural concepts of the original site descriptive models and follow similar modelling methodologies, there has been a progressive refinement of both concepts and models to meet the needs of downstream users. For details regarding the development of previous model versions and related analyses of underlying data, the reader is referred to Stephens et al. (2007, 2008), Curits et al. (2011) and Stephens and Simeonov (2015).

4.1 State of knowledge

4.1.1 Structural concepts – short summary

The tectonic setting of the Forsmark site, inside a tectonic lens within a ductile high-strain belt, is summarised in Section 1.3. Field investigation data indicate that all deformation zones were formed within the same tectonic regime. Geometric relationships between different sets are consistent with their formation in a strike-slip tectonic regime (e.g. Stephens et al. 2007). Different sets of deformation zones have been reactivated repeatedly in response to changes in the stress situation during the subsequent tectonic evolution. Around and after c. 1.45 Ga, loading and unloading cycles related to the deposition and denudation, respectively, of sedimentary rocks or glacial material have provided a significant impact on the geodynamic evolution in the Forsmark area. These cycles particularly contributed to the reactivation of gently dipping structures and are believed to be the driving mechanisms behind the formation of sheet joints, which are commonly found at shallow depths in the bedrock. The proposed mechanism for sheet joint formation involves compression parallel to a convex bedrock surface (Twidale et al. 1996; Martel 2011, 2017); a situation that can occur due to elastic bending of the lithosphere during phases of isostatic rebound (see section 5.1.2 in Petersson et al. 2024 for additional details).

Regionally significant, WNW striking deformation zones (Forsmark, Singö and Örskär), along with their NW splays like the Eckarfjärden deformation zone, initially developed under amphibolite-grade conditions and further under decreasing temperature conditions. However, most of deformation zones in the Forsmark area exhibit only brittle deformation, with increased fracture frequencies in combination with variable wall-rock alteration commonly referred to as oxidation. Vertical and steeply dipping deformation zones are primarily defined by high frequency of sealed fractures, commonly in the form of a complex sealed fracture network, whereas gently dipping zones contain a higher frequency of open fractures and non-cohesive crushes, a feature with significant implications for the hydraulic modelling.

The distribution of horizontal to sub-horizontal sheet joints within the shallow part of the bedrock is highly variable, with increased spacing towards depth. Sheet joints occur throughout the Forsmark area, including the SFR volume, but are particularly concentrated inside the north-western part of the tectonic lens, where the formation conditions are more favourable; a more isotropic bedrock (i.e. higher degree of lithologic homogeneity and less intense ductile fabric) in combination with a history of significantly higher differential rock stresses (cf. Glamheden et al. 2007; SKB 2013). Current knowledge, along with the limited drilling outside the lens do not provide sufficient support for a deterministic extension of a shallow rock slab with frequent sheet joints beyond FFM02.

Further details of the structural concepts relative to the tectonic evolution in a regional perspective are provided by Stephens et al. (2007; 2015) and more specifically for the formation of sheet joints by Petersson et al. (2024).

4.1.2 Significance of geophysics

The geological conditions at the site significantly influence the choice and applicability of geophysical survey methods for identification of deformation zones and anomalous lithologies. The use of geophysics has developed successively during the site investigation work at Forsmark, with the following geometrical constraints on the occurrence of deformation zones:

- *The use of lineaments in the modelling of steeply dipping deformation zones.* The area's low topographic relief, which complicates the interpretation of digital topographic data, has led to the exclusive use of low magnetic lineaments, particularly in areas with highly resolved ground magnetic data. However, exceptions exist in areas with disturbed magnetic data.

- *The use of the surface reflection seismic data in the modelling of gently dipping zones.* Integration with geological, geophysical and hydrogeological borehole data have shown that the prominent, gently dipping reflectors in the central part of the tectonic lens represent hydraulically conductive, gently dipping fracture zones (cf. Juhlin and Stephens 2006).

- *Very limited correlation between low velocity anomalies (in seismic refraction data) and magnetic lineaments or deformation zones.* Non-matching anomalies are instead inferred to represent narrow depressions in the bedrock surface filled with Quaternary cover material or local variabilities in the vertical extent of the more intensely fractured layer of near-surface bedrock.

4.1.3 Key remaining issues

Increasing confidence and successively reducing uncertainties, alongside improvements in conceptual understanding, have been the main driving forces behind the surface-based investigations at Forsmark. Remaining uncertainties at completion of SDM-Site and SDM-PSU are summarised in SKB (2008a) and SKB (2013), respectively, with a more systematic, multi-disciplinary compilation for SDM-Site in SKB (2008b). Further notes on uncertainties in the Forsmark deformation model version 2.3 are presented by Stephens and Simeonov (2015).

Based on these reports, the key remaining issues and their handling in the geological model can be summarised as follows:

- **Size and spatial distribution of gently dipping deformation zones. The** estimated size of deterministically modelled zones is based on surface seismic reflection data and intersections along boreholes; information which is mainly limited to the north-western part of Forsmark tectonic lens. The absence of gently dipping zones in the other model volumes is coupled directly to an inherent data bias, with a lack of both borehole and reflection seismic data. The identified gently dipping zones are modelled using a conservative approach, to terminate against the nearest vertical or steeply dipping zone. Although there remain questions regarding the along-strike and down-dip truncation of these zones, it is judged that the uncertainty regarding their extent is sufficiently constrained.

- **The orientation and size of the possible deformation zones in the single-hole interpretations that have not been modelled deterministically.** It is judged that these structures either represent intersections with minor zones (se Stephens et al. 2007) or branches from already modelled deformation zones. From the absence of geophysical anomalies, it can be concluded that all these sections are less than 3 km in length, but it cannot be ruled out that some of them are longer than 1 km. These zones have been handled stochastically, with the assumption that they are minor zones.

- **The size and spatial distribution of horizontal to sub-horizontal fractures (i.e. sheet joints) in the upper part of the crystalline bedrock.** Some of these fractures are inferred to affect significantly the hydraulic conditions and rock mass stability. At the stage of SDM-Site, these uncertainties were handled and quantified by assigning the upper part of bedrock inside the tectonic lens to a separate fracture domain (FFM02), as a basis for the subsequent stochastic DFN modelling. Thereafter, SKB has completed several supplementary borehole investigations in the near-surface realm both in the SFK and the SFR areas (see section 2.4 and 2.5). Refined analysis of these data has yielded further insights in the phenomenon of sheet joints, with the development of a conceptual model for formation, local deterministic modelling (cf. section 4.4) and a subdivision of fracture domain FFM02 in two sub-domains (cf. section 4.6).
- **Size and spatial distribution of subordinate rock types, such as amphibolite, with anomalous thermal and mechanical properties.** Borehole information and lithological heterogeneity have not permitted a deterministic approach. The uncertainty has been handled by thermal simulation at the canister scale.
- **Size distribution and size-intensity models for fractures at repository depth of SFK. The** uncertainty results from the fact that the stochastic DFN approach was restricted to the use outcrop data to construct size models for fractures. This directly affects primarily hydrogeological and transport modelling, and consequently the repository design and the safety assessment. The uncertainty has been constrained by use of alternative models with their inherent quantified uncertainties (cf. Stephens et al. 2007).
- **The continuity and size of the small deformation zones in the SFR area, especially in the steeply dipping WNW to NW set.** A strongly disrupted magnetic field makes the identification of linear low-magnetic anomalies difficult. However, it is judged that all deformation zones exceeding 1 km in trace length along the ground surface have been detected (Curtis et al. 2011).

4.1.4 Summary of updated knowledge at baseline stage

The updated state of knowledge after the release of the original site descriptive models can be summarised as follows:

- Verification of established structural concepts, together with refined geometries and geological characterisation of previously modelled deformation zones in two areas: near the planned accesses and operational area of the repository for spent nuclear fuel, and within the volume of the planned extension of the SFR facility.
- Improved spatial understanding of sheet joints, enabling very localised deterministic modelling of individual sheet joints and further subdivision of the shallow fracture domain model of SDM-Site, based on a marked contrast in the occurrence of sheet joints with observable apertures.
- A reassessment of the previous lineament interpretation at the sea floor, northeast of the SFR facility, enabling revision of previously modelled zones of SDM-PSU and elimination of artificial blind ends.
- Increased understanding of the deformational conditions in the parts of the future sub-catchment area at Forsmark site, beyond the SDM-Site regional volume, based on complementary interpretation of lineaments (Isaksson and Johansson 2020) and geological field studies to examine the geological significance of inferred lineaments (Bakker 2021; Petersson et al. 2024).

4.2 Complementary geological and geophysical baseline data

The geological mapping and the supportive geophysical data from the boreholes completed after conclusion of the investigations for SDM-Site and SDM-PSU are key inputs to the geological modelling work of Baseline Forsmark. For certain aspects, such as the identification and modelling of sheet joints (see section 4.4.3), data from older boreholes have also been used after renewed evaluation.

Prior to modelling, the borehole data underwent a step of single-hole interpretation, essentially creating a 1D-model of a single borehole. A description of the procedures adopted during the various stages of the single-hole interpretation work is provided by for example Stephens et al. (2007) and Curtis et al. (2011). The method updates proposed by Hermanson and Petersson (2022) have not yet been applied in practice. The results of the interpretations for the boreholes completed after 2010 are presented in four separate data reports, one for each drilling campaign:

- KFM13–KFM23 and HFM39–HFM41 (Appendix C in SKB 2012)
- KFM24 (Dahlin and Maskenskaya, 2017)
- KFM25–KFM27 and HFM42–HFM47 (Rauséus and Petersson 2020)
- KFR117–KFR121 (Winell and Samuelsson 2022).

The primary significance of data acquired from single-hole interpretations of boreholes completed after 2010 has been a confirmation of previous concepts and existing geological models. New data that have led to revisions or additions to the geometries and characterizations of modelled deformation zones are limited to bedrock volumes in proximity of the planned accesses and operational area of the final repository and the volume of the planned extension of the SFR facility (see section 4.4).

Special studies concerned with the assembly of surface bedrock data after 2010 mainly support the current site understanding by verifying established concepts. Only a small portion of the data have contributed directly to the deterministic modelling and the characterisation of modelled features. None of the data have provided incentive to update the bedrock geological map at the scale 1:10,000 that covers the mainland and the archipelago area at the Forsmark site (Bedrock geological map, Forsmark, version 1.2); nor have they justified extending the map further to cover remaining parts of the future sub-catchment area. Additionally, the surface data do not alter the current knowledge regarding the potential for metallic mineralisations and industrial mineral deposits (cf. Lindroos et al. 2004).

4.3 Updated methodologies and model overview

4.3.1 Methodology for deterministic geological modelling of the bedrock

The methodology for deterministic geological modelling of the bedrock (Hermanson and Petersson 2022) describes the principles for identification and deterministic modelling of rock domains and tectonic structures that might influence the repository design and safety assessment during construction and operation of the repository. The aim is to continuously develop the geological knowledge of the target volumes of the two repositories (SFR and SFK) to support the modelling in other subject areas, the design of the repository, and future analyses of post closure safety.

The basic principles of the methodology are the same as those previously described in Munier et al. (2003) and Munier and Hermanson (2001). The approach was applied and improved in the development of conceptual understanding and three-dimensional geological models over a period of more than five years of site-descriptive modelling in both Forsmark and Laxemar (Stephens et al. 2007, Wahlgren et al. 2008).

The methodology is adapted for handling large amounts of data from both boreholes and tunnels to enable parallel work in different parts of the repositories. It also describes the analytical process of borehole and tunnel data carried out before initiating the 3D- modelling. In summary, the methodology for deterministic geological modelling of tectonic structures and rock volumes includes the following components:

- use of subsurface observations of geological features that are not necessarily outcropping at the ground surface,
- new guidelines for modelling deterministic objects regarding interpolation, extrapolation, variable thickness, naming and property assignment,
- identification of deformation zones and rock units with a higher degree of detail and confidence of existence than that in SDM-Site and SDM-PSU, and
- objective uncertainty assessment, both through conditioned stochastic simulation of the extent of identified objects and by determining the degree of confidence for deterministically interpreted objects and geological properties.

4.3.2 Model overview

To serve the needs of other modelling disciplines, repository design and post-closure safety assessment, the integrated geological understanding of the Forsmark site is represented by a series of deterministic models. Each model encompasses a specific volume filled with three-dimensional geometries of geological objects, along with descriptions of their geological characteristics. Object types and volumes of the deterministic geological models included in Baseline Forsmark are listed in Table 4-1 and their areal coverage is presented in Figure 4-1.

Table 4-1. Summary of all deterministic geological models included in Baseline Forsmark.

Model	Object types	Volume
DMS	Deformation zones + deterministically modelled sheet joints	Future sub-catchment area + SDM-site regional model volume/area
RFM reg	Rock domains	SDM-Site regional model volume/area
RFM loc	Rock domains	SDM-Site local model volume/area
RFR loc	Rock domains	SDM-PSU local model volume/area
FFM	Fracture domains	SDM-Site local model volume/area

The current Baseline models are largely derived from the site descriptive models of SDM-Site (SKB 2008a) and SDM-PSU (SKB 2013), which were developed in multiple stages between 2002 and 2011. The geological basis for SDM-Site was models of deformation zones, rock domains and fracture domains of the Forsmark stage 2.2 modelling (Olofsson et al. 2007, Stephens et al. 2007), whereas geological models of the project SDM-PSU included deformation zones and rock domains presented by Curtis et al. (2011). The Forsmark stage 2.2 deterministic models for deformation zones has subsequently been updated to model version 2.3 (Stephens and Simeonov 2015), after taking account of the SDM-PSU deformation zone model of regional extent. Model version 2.3 was later revised based on data from supplementary investigations conducted in shallow boreholes drilled in proximity of the planned accesses and operational area of the final repository (see Follin (ed) 2019). Geometrical geological models were developed for two different volumes, named regional and local, for each site descriptive model. The areal extent of these volumes is illustrated in Figure 4-1.

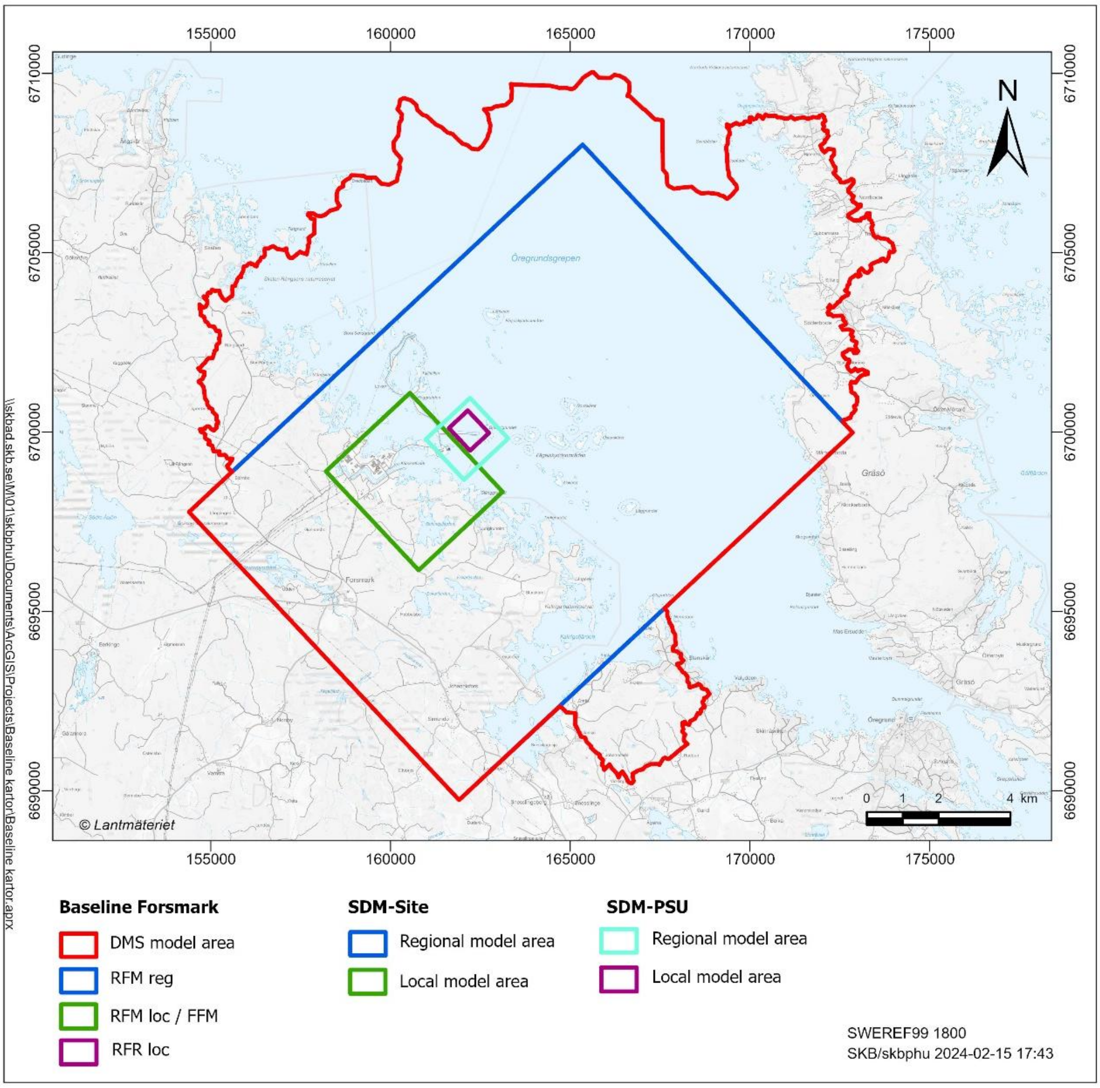

Figure 4-1. *The areal coverage of the deterministic geological models included in Baseline Forsmark relative to the models of SDM-Site and SDM-PSU (see Table 4-1 for further details).*

4.4 Deterministic model for structures (DMS)

A master version of the deformation zone model has been developed by merging the individual deformation models of SDM-Site (updated to model version 2.3) and SDM-PSU. This master version is named DMS (*Deterministically Modelled Structures*) and includes all deterministically modelled deformation zones in the Forsmark area, regardless of size. To ensure consistency in the basic geometrical modelling principles, the merging process required adjustments with regards to termination depth, extent, and thickness for some deformation zones, especially those from SDM-PSU. The most significant change up to the release of Baseline Forsmark is the extension and addition of regional deformation zones in the future sub-catchment area, outside the SDM-Site regional volume. Additionally, deterministically modelled sheet joints were added in shallow bedrock volumes based on data in closely spaced boreholes.

Before merging the individual deformation zone models of SDM-Site and SDM-PSU, the resolution of modelled deformation zones differed between the local and regional model volumes. Each volume included all modelled deformation zones down to a certain size, based on the measured lineament trace length on the ground surface. After merging, all modelled deformation zones are included in a single volume, regardless of size. However, the heterogeneity in data density prevents deterministic modelling of small-size zones and gently dipping zones throughout the new model volume. This has significant implications to modelling of hydraulic connectivity, solute transport and rock stresses. Such uncertainties in the deterministic heterogeneity is recommended to be addressed by alternative representations using stochastic DFN models (cf. Selroos et al. 2022; Hartley et al. 2024).

4.4.1 Updated baseline methodology

The methodology and assumptions for deterministic modelling of deformation zones in DMS Baseline Forsmark are summarised in section 5.3 of Petersson et al. (2024). The key changes and additions to the DMS, following the integration of the individual deformation zone models from SDM-Site and SDM-PSU, can be summarised as follows:

- Revision of deformation zone geometries based on borehole data acquired from the preparatory investigations conducted after 2010 in proximity of the planned accesses and operational area of the final repository and the volume of the planned extension of the SFR facility.
- Extension and addition of regional deformation zones beyond the SDM-Site regional volume to encompass the future sub-catchment area (see Figure 4-1).
- Reassessment of the truncation pattern of deformation zones northeast of the SFR facility to eliminate artificial blind ends of previously modelled zones.
- Introduction of confidence estimates for deformation zones following the proposed approach of Hermanson and Petersson (2022).

The criteria for identification of sheet joints with aperture in boreholes and the strategy for deterministic modelling are discussed by Petersson et al. (2024). The identification of sheet joints, developed by extensional failure, have been based on assessment of available borehole images, with support from geological mapping records. Sheet joints are considered less predictable than shear structures as the distance from observation points increases. Therefore, reasonable confidence in the validity of interpolation is only expected in rock volumes where observation points are closely situated. Consequently, rock volumes with few observation points to allow reliable deterministic modelling must be described using coupled stochastic simulations.

The deterministic modelling principles relies primarily on assumptions established by Hermanson and Petersson (2022) based om observations from the excavation for the inlet channel to the nuclear power plants (Carlsson 1979) and details in the literature on sheet joints. The primary criterion for individual representation is observations in three or more boreholes, separated by a horizontal distance of ≤ 100 m. Joints that fail to fulfil this criterion are not included in the deterministic representation regardless of their actual extent.

4.4.2 Baseline model for deformation zones

A total of 159 deformation zones have been deterministically modelled in the DMS Baseline Forsmark. After merging, 14 new zones have been added, 29 zones of the original models have been changed geometrically (orientation, trace length along the ground surface and/or thickness) and 116 have remained geometrically unchanged (Figure 4-2).

Based on orientation, the modelled zones can be divided into three main sets:

- Vertical and steeply dipping fracture zones with sub-sets referred to as ENE (NE) and NNE (72 zones).
- Vertical and steeply dipping deformation zones with sub-sets referred to as WNW and NW (47 zones).
- Gently dipping fracture zones with dips to the south and SE (24 zones).

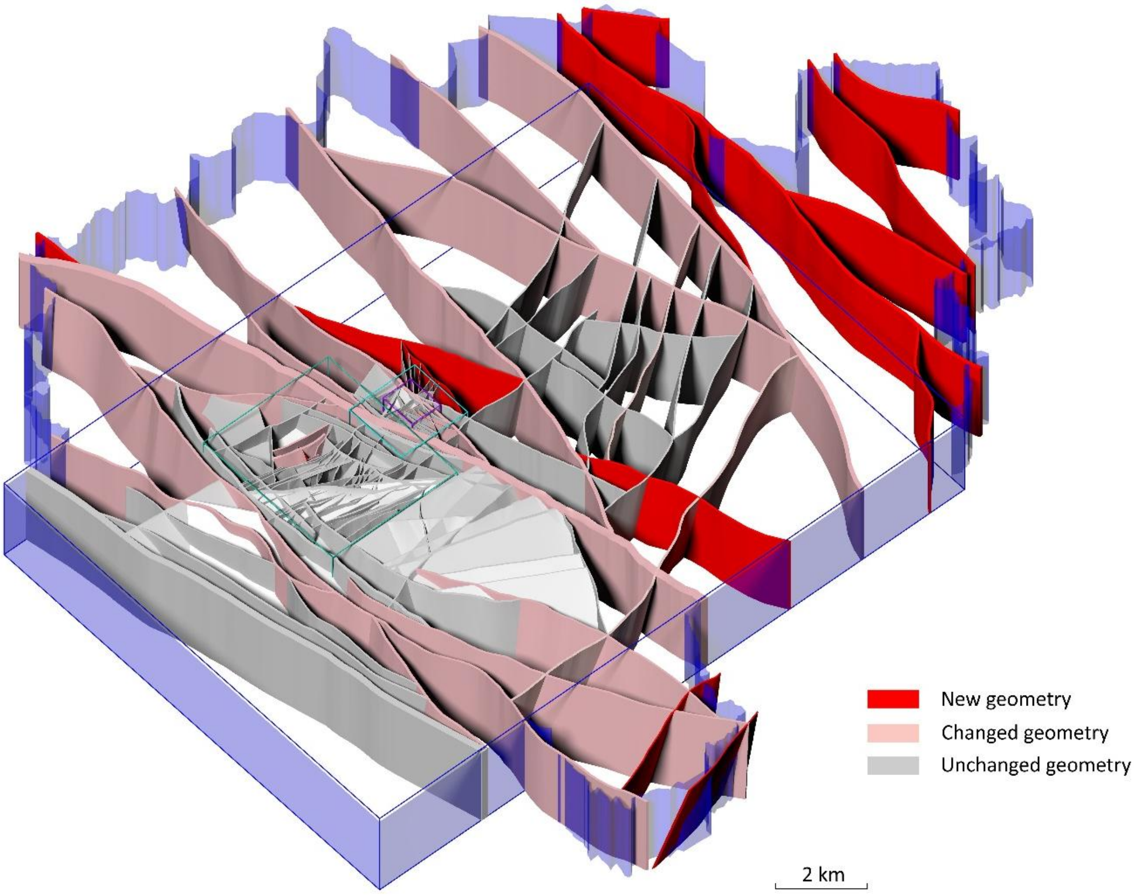

Figure 4-2. *The DMS Baseline Forsmark relative to the model volumes presented in Figure 4-1. Oblique view towards the north showing deformation zones that were added or geometrically changed after the merging of SDM-Site and SDM-PSU in red and pale red, respectively.*

Additionally, there are 16 vertical and steeply dipping deformation zones that belong to the sub-sets referred to as NNW and EW. The trace length along the ground surface of the different sub-sets is strongly related to the spatial distribution zones, and consequently to the tectonic anisotropy of the Forsmark area. According to the current understanding, vertical and steeply dipping zones of the WNW and NW sub-sets are largely restricted to the margins of and to the high-strain areas outside the Forsmark tectonic lens, whereas the fracture zones of the other sub-sets mainly have developed in volumes of less intense strain, as second order structures, in response to displacements along these more extensive zones.

The properties of deformation zones included in DMS Baseline Forsmark are compiled into property tables, presented in Appendix 7 of Petersson et al. (2024). These tables are largely based on previous compilations presented by Stephens et al. (2007), Curtis et al. (2011) and Stephens and Simeonov (2015). A summary of some key aspects of the dominant orientation sets of deformation zones at Forsmark is presented in Table 5-6 of Petersson et al. (2024), with further details in Stephens et al. (2007, 2015) and Curtis et al. (2011). Hydrothermal alteration along brittle deformation zones at Forsmark are described in more detail in Sandström et al. (2008) and Petersson et al. (2012), whereas kinematic data for the zones are presented in Saintot et al. (2011).

Following the methodology proposed by Hermanson and Petersson (2022), confidence estimates is assigned for each deformation zone in DMS Baseline Forsmark. The primary basis for these estimates is the relative impact of various data sources together with different modelling decisions related to object geometry. The approach includes four confidence categories, where each is divided in two subcategories. The total relative confidence for a zone is achieved by summing the confidence estimates for eight individual subcategories, each ranging from 1 to 3 (low, medium, high). Assigned confidence estimates are presented in the property tables of Petersson et al. (2024), with a visualisation of the assembled estimate for each zone by means of colour coding (Figure 4-3). The applicability of the surface-based approach to determine deformation zone confidence included in the DMS Baseline Forsmark needs to be evaluated by future sub-surface investigations.

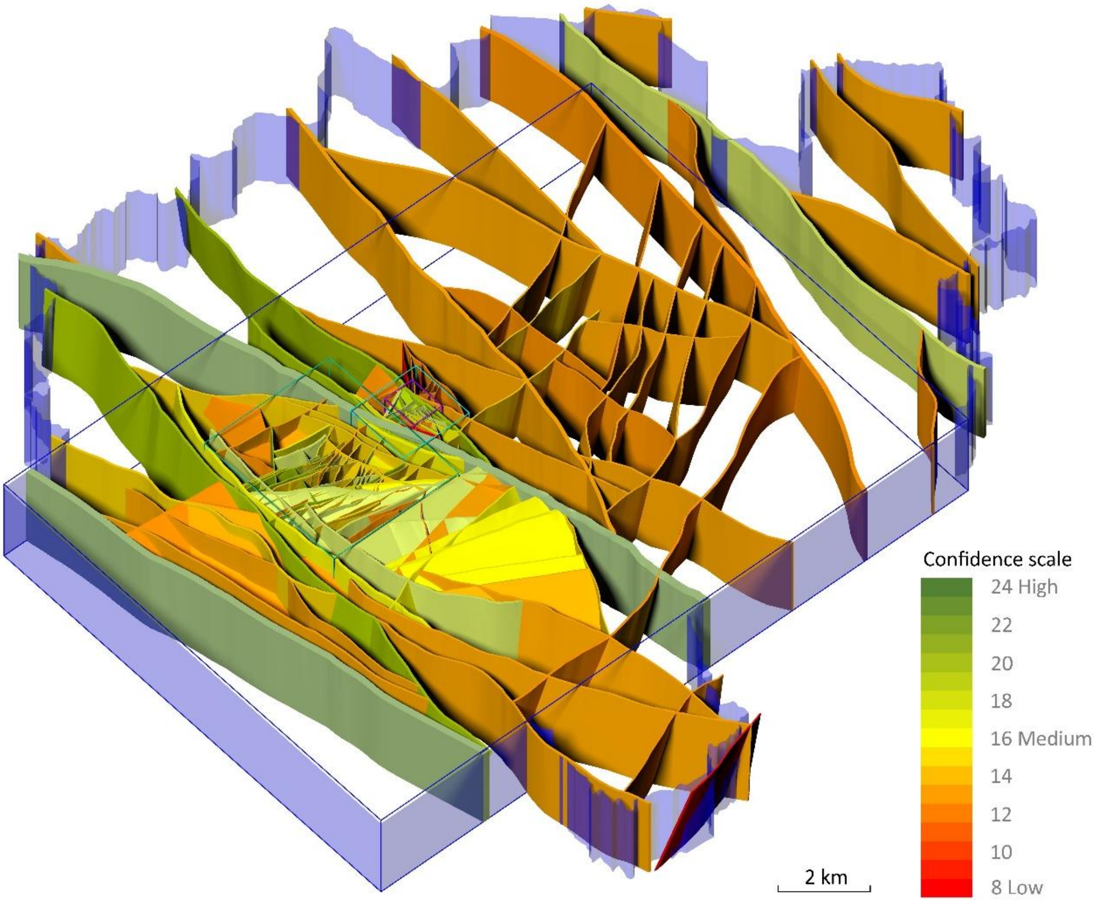

Figure 4-3. *The DMS Baseline Forsmark relative to the model volumes presented in Figure 4-1. The assembled confidence estimate for each zone are visualised by means of colour coding, with a confidence range from 8 (low) to 24 (high).*

4.4.3 Baseline model for sheet joints

The geometric representation of deterministically modelled sheet joints in DMS Baseline Forsmark includes the following two main components:

- Three-dimensional visualisations of sheet joints along the inlet channel to the nuclear power plants, based on mapping of joint traces made by Carlsson (1979).
- Geometries of individual sheet joints with distinctive aperture, modelled based on interpolation between observation points in boreholes.

In total eleven individual sheet joints with distinct aperture have been modelled deterministically, distributed among the three subareas illustrated in Figure 4-4.

Figure 4-4. Top view of the three subareas with deterministically modelled sheet joints (red) together with a visualization of the sheet joints documented by Carlsson (1979) along the inlet channel (green). Water is shaded and horizontal borehole projections marked by thin black lines.

4.5 Rock domain models

Baseline Forsmark includes all three rock domain models developed during SDM-Site and SDM-PSU (see Table 4-1). The rock domain models form a nestled system, where the local volumes (RFM and RFR) are sub-models within the volume of the RFM regional model. The distinction between the volumes lies in the division of some regionally defined domains into local volumes to support downstream users and repository design. The number of domains in each model volume and the division of some regionally defined domains in the local model volumes are listed in Table 4-2.

No new data acquired after the completion of SDM-Site and SDM-PSU has required a revision of the rock domain geometry from a geological perspective. However, slight geometrical adjustments have been made with the release of Baseline Forsmark to adapt to changes in the RVS modelling tool.

None of the new data acquired after 2010 have necessitated revision of the domain boundaries. However, the new borehole data set have resulted in minor adjustments to the quantitative estimates of rock types and alteration types of rock domains compared with the three models developed during SDM-Site and SDM-PSU (see Petersson et al. 2024). Property tables and information regarding the modelling procedure for the previously established model versions are provided by SKB (2005, 2006), Stephens et al. (2007) and Curtis et al. (2011). More detailed descriptions of the key domains in the target volumes for the planned repositories are presented by Stephens et al. (2007) and Curtis et al. (2011).

Table 4-2. The number of rock domains in each of the three model volumes included in Baseline Forsmark, along with information about the division of two regionally defined domains in the local models.

Model volume	Number of domains	Comments on division
RFM regional	38	–
RFM local	14	RFM029R of the regional volume divided into RFM029 and RFM045
RFR local	4	RFM021 divided into three sub-domains: RFR01–RFR03 RFM033 = RFR04

4.6 Fracture domain model

The basis for FFM Baseline Forsmark is the fracture domains of SDM-Site, developed during the modelling stage 2.2, which serve as the basis for the statistical DFN modelling. The major changes leading up to the release of Baseline Forsmark include representing deformation zones as single, infinitely thin surfaces instead of volumes, and dividing the relatively shallow fracture domain FFM02 into two subdomains. This division is based on a noticeable contrast in the occurrence of sub-horizontal fractures (i.e., sheet joints) with observable apertures.

As a prerequisite for the development of an updated model for discrete fracture networks (DFN), six separate fracture domains have been recognised within the RFM local volume during the work with the SDM-Site (Olofsson et al. 2007). However, borehole data that allow satisfactory characterisation are only available for four of the domains – FFM01, FFM02, FFM03 and FFM06 (Figure 4-5).

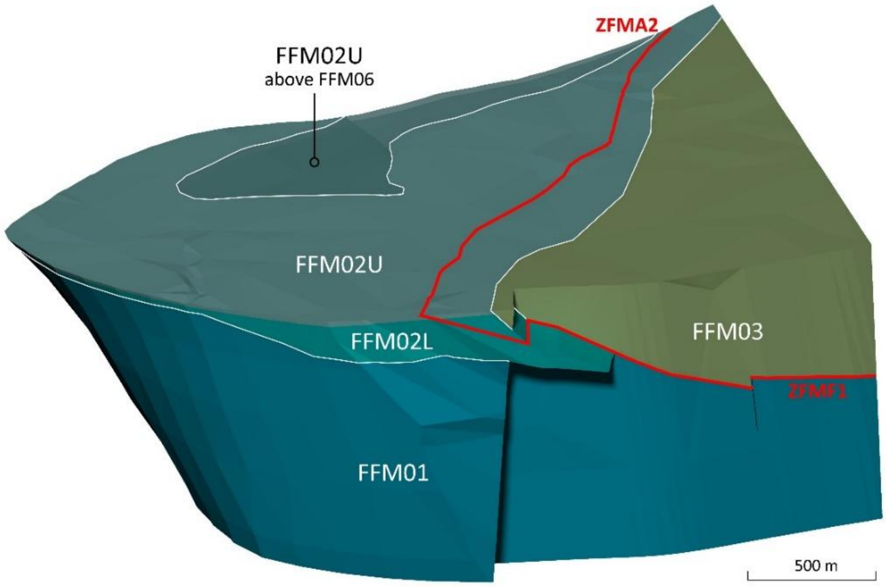

Figure 4-5. *Three-dimensional model for fracture domains FFM01, FFM02 and FFM03 viewed towards the ENE. FFM06 is enclosed by FFM01 and situated beneath FFM02 and is for this reason not visible. FFM02 is divided into two subdomains, FFM02U and FFM02L. Origin surfaces for the gently dipping zones ZFMA2 and ZFMF1 also shown in red.*

The bedrock has been divided into fracture domains based on the following geological features:

- A marked contrast in the fracture orientation and intensity distribution patterns with depth, particularly in the frequency of open and partly open fractures.
- Contrasts in fracture character linked to both the degree and character of the ductile strain and primarily compositional homogeneity.
- Differences in fracture pattern that can be ascribed to the large-scale occurrence of altered (albitised) granitic rock, with contrasting grain-size and composition.

The subdivision of the bedrock into fracture was further supported by feedback from the disciplines hydrogeology, hydrogeochemistry and rock mechanics.

Except for some slight modifications of fracture domain FFM02 after the conclusion of SDM-Site, the framework and overall concept of the fracture domain model remains unchanged. Details regarding the fracture character, modelling procedures and uncertainties for the previously established model version are provided by Olofsson et al. (2007), with summaries in Stephens et al. (2007) and SKB (2008a).

In the fracture domain model of SDM-Site, the volume of rock inside deformation zones were treated as separate domains. This has been changed in the FFM Baseline Forsmark, and each deformation zone is now represented by a single, infinitely thin surface – the origin surface, which generally corresponds to the centre of the zone. However, volumetric representations of deformation zones with contrasting fracture intensity, can be achieved by superimposing deformation zone boundary geometries in DMS Baseline Forsmark.

Based on the observation that the shallow rock mass in the north-western part of the tectonic lens (down to approximately 20–25 m depth) is sheeted by sub-horizontal fractures with distinct aperture, fracture domain FFM02 has been divided into two subdomains – FFM02U (upper) and FFM02L (lower), see Figure 4-5. Relative to the shallow rock mass of FFM02U, the subdomain FFM02L is characterised by an increasing spacing with depth between horizontal to sub-horizontal fractures with distinct aperture. The origin of these fractures at great depth can be different than at shallow depth, with a genetic relationship to the other fracture sets in the area. A high variability in the distribution of horizontal to sub-horizontal fractures within both subdomain FFM02U and FFM02L is notable.

Although sheet joints are relatively common throughout the Forsmark area, this depth-dependent contrast in the frequency of sub-horizontal fractures with distinct aperture is less pronounced outside fracture domain FFM02. Thus, the sparse drillings along and outside the margins of the tectonic lens do not provide sufficient support for a deterministic extension of a shallow rock slab with frequent sheet joints beyond FFM02.

The borehole data acquired after 2010, have also provided incitement for a local revision of the boundary between FFM02 and FFM01. By using the frequency distribution of open and partly open fractures, the boundary between FFM02 and FFM01 has been moved upward, closer to the ground surface, by about 5 m in the volume near the planned accesses and operational area of the repository for spent nuclear fuel.

4.7 Discussion

4.7.1 Baseline status

The deterministic geological models of Baseline Forsmark rely on a comprehensive site understanding, which has been the basis for well-founded modelling concepts, supported by the wealth and quality of available data and feedback from other disciplines. Generally, none of the new data acquired after 2010 from the Forsmark area impact the previously developed site descriptive models (SDM-Site and SDM-PSU) with any significance. Thus, the conceptual ideas originally adopted for the Forsmark area in the SDM-Site (e.g. Stephens et al. 2007, 2015) have proved to be valid for the more highly resolved models in the SFR area (cf. Curtis et al. 2011) and the structural framework of the future sub-catchment area outside the SDM-Site regional volume (cf. Petersson et al. 2024).

A central part of the model changes completed up to the release of Baseline Forsmark is the merging of all modelled deformation zones of SDM-Site and SDM-PSU into the DMS Forsmark, which now includes all deterministically modelled deformation zones regardless of size. Such a representation has an inherent deterministic heterogeneity and mixes sub-volumes of different data density within a single model boundary. This in turn can have major implications to the downstream users and the deterministic inconsistencies is recommended to be addressed by alternative representations using stochastic DFN models (cf. Hartley et al. 2024).

It, furthermore, is emphasized that the geological Baseline models are updates of the previous site descriptive models.

4.7.2 Remaining uncertainties

After the compilation and revision of the deterministic geological models covered by Baseline Forsmark version, there remains several more specific uncertainties; the majority of which were identified already at the completion of SDM-Site and SDM-PSU:

- Size of gently dipping deformation zones, especially their down-dip truncation, which are currently extended to the nearest steeply dipping zone.
- Lateral extent of vertical to steeply dipping deformation zones that are largely defined by magnetic minima connections (e.g. ZFMWNW0123).
- Truncation pattern of vertical to steeply dipping deformation zones outside areas of high-resolution magnetic measurements or in magnetically disrupted areas.
- Orientation and size of unresolved deformation zones identified in the single-hole interpretation.
- Existence and geological character of gently dipping zones beneath the planned repository for spent nuclear fuel.
- Presence of additional deformation zones not captured in the deterministic Baseline model, such as gently dipping zones in areas that lack reflection seismic surveying and drillings.
- Spatial variability and size of sheet joints in the upper part of the crystalline bedrock, as well as the spatial distribution of glacial sediments along the joints.
- Size and spatial distribution of subordinate rock types, especially for anomalously thick amphibolite bodies in domain RFM045.

4.7.3 Implications for future SDM updates

Some of the uncertainties listed in the preceding section are judged to be sufficiently bounded by the current model, especially where the significance for engineering design and post-closure safety assessment is considered to be limited. In some cases, it is also questionable whether the uncertainties could successfully be further reduced by additional surface-based investigations (SKB, 2008b). However, there are still several uncertainties with significant impact on the hydrogeological and rock mechanical modelling that warrant further examination. Recommendations to shed further light on these remaining uncertainties include the following activities:

A. A reassessment of the underlying data and the inferred lineaments, possibly in combination with surface-based drillings, to evaluate the geometric extent of deformation zone ZFMWNW0123.

B. A reassessment of existing seismic data and additional surface-based drillings in the northern to northwestern parts of rock domain RFM032 to investigate the nature of seismic reflector A1/A0, as well as the possible existence of additional deformation zones with gentle dips towards the southeast beneath the planned repository for spent nuclear fuel.

C. Further insight into the spatial variability and size of sheet joints towards depth by (1) analysis of the geological drawings for the outlet tunnels from the nuclear reactors and (2) studies of known occurrences in quarries and canyons with exposures that reach considerable depths.

D. Analysis and modelling of the growing amount of subsurface data from the construction of the two repositories to resolve further details on the extent and truncation patterns of deformation zones, as well as the spatial variability and size of sheet joints.

An essential task with the growing amount of subsurface data, is to test the validity of the deterministic geological models on a prediction-outcome basis. This includes correlations between data from pilot boreholes and associated tunnels, and will probably be made continuously during the underground construction of the repositories. The tunnel data acquired from the repositories do also allow for full application and testing of the updated methodology for deterministic geological modelling presented by Hermanson and Petersson (2022). Another aspect is the possibility of further evaluation of the extended confidence estimate for deformation zones introduced in the DMS Baseline Forsmark (see section 4.4.2).

In addition, feedback from the hydrogeological modelling team highlights a future need for alternative geometries of some deformation zones and analyses to support forthcoming DFN-modelling, by for example expansion of or complement to the existing fracture domain model. There is also an explicit request of a greater integration with both hydrogeological and rock mechanical modelling.

5 Bedrock thermal properties

The main objective of the thermal modelling is to provide a thermal site description adequate for the requirements of the repository design and the safety assessment, involving the estimate of the most suitable distance between deposition holes to satisfy the prescribed temperature requirement for the bentonite buffer surrounding the canisters. The thermal site description includes the characterization of the following thermal properties: thermal conductivity, thermal diffusivity, heat capacity, temperature and the coefficient of thermal expansion.

During the period following SDM-Site, the amount of thermal property investigations and subsequent modelling performed has been limited. Subsequently, a proper discipline specific Baseline report for Thermal properties has not been produced; however, the undertaken work at this stage is presented and described in Appendix 1 instead. This chapter summarizes the knowledge at SDM-Site stage, the new available information, the updated Baseline model and the new modelling methodology for the description of thermal properties.

5.1 Summary of knowledge at previous SDM

In SDM-Site thermal conductivity, thermal diffusivity and heat capacity were described for the most common rock types and, in particular, the spatial statistical description of the rock mass thermal conductivity was studied and modelled at different scales with focus on the rock domains at the repository area (RFM029 and RFM45; and in earlier stages also RMF12). In addition, the temperature increase with depth was well established and thermal expansion coefficients for the most common rock types were analysed and reported (SKB R-07-47; SKB R-08-65).

5.2 Key remaining issues after SDM-Site and SDM-PSU

Key remaining issues of SDM-Site and SDM-PSU can be summarised as follows:

- **Problem of capturing the wide span of scales** involved in the thermal modelling was identified. The measurements are performed in the cm-dm scale while the subordinate rocks with importance for the thermal modelling occur down to the dm-m scale, also, correlation lengths range from dm to 50 m or longer, and the domain properties may require simulation volumes of 50–100 m or more. This makes the description of the thermal properties of the rock mass challenging, and great care should be taken when the simulation scale and the simulation volume is decided.
- **The influence of the lithological heterogeneity, spatial variability and size distribution of the different rock types** on the rock mass thermal properties in the repository area should be investigated along with the future updates of the geological site description, as more information is obtained from investigations conducted during the execution of planned underground constructions at Forsmark.

5.3 Description of Baseline data

Since SDM-Site 35 Transient Plane Source (TPS) tests have been conducted on three different rock types (101057, 102017, and 108018) on cores from five different boreholes, KFM01A, KFM04A, KFM05A, KFM24 and KFM90B.

5.4 Summary of updated modelling methodology

The methodology for thermal modelling at the Forsmark site is presented in two reports, Part 1 and Part 2 (Back and Sundberg 2022; Back et al. 2022), and they include a compilation of the developments that have been made after the previous version (Back and Sundberg 2007) regarding the most important steps in the methodology, where different aspects of the simulation scale are discussed since the scale has been identified as a key remaining issue from SDM-Site. This new methodology is more focused on the description of thermal properties at the local scale, with especial attention to the thermal conductivity. The possibility to introduce anisotropy and conditioning to site data in the thermal modelling is also discussed; however, it has not been included in the current modelling stage, since the available data is very sparse. Finally, a new definition of thermal rock classes system (TRC) has been included for modelling the spatial statistical structure of the lithology that corresponds better to the geological rock classification.

5.5 Summary of Baseline model

The main objective for the Baseline version is to analyse the available new laboratory data on thermal properties regarding certain rock types, and to compare these results with the thermal parameters reported in previous SDM-Site models. An additional objective is to analyse the spatial data coverage and identify any potential parts of the repository rock volume where there is a lack of thermal properties data.

The Baseline thermal model is focused only on the single rock *type* level. On a larger scale, the rock mass in the rock domains consists of a certain mixture of rock type bodies of different sizes and shapes; however, no updated thermal modelling at the rock mass scale has been conducted at this stage and the previous SDM-site thermal properties of rock domains have been adopted here for the Baseline thermal model.

The models for thermal properties of the six main rock types considered relevant for this study and the two main rock domains for SFK are presented in Table 5-1. Most of the model parameter values are the same as in SDM-Site (Back et al. 2007; Sundberg et al. 2008) while a few are slightly modified based on new data and other arguments discussed in Appendix 1 for each rock type.

Table 5-1. Thermal property models for main rock types. The models apply for 20 °C.

Rock code	Model parameter	Mean	St Dev	Min	Max
101057	Thermal conductivity W/(m·K)	3.54	0.23	3.13	3.96
	Heat capacity MJ/(m^3 K)	2.11	0.18		
	Thermal expansion coefficient ×10^{-6} m/(m·K)	7.7	2.2	2.1	15
101057_104 or 101058_104	Thermal conductivity W/(m·K)	3.89	0.23	3.43	4.35
	Heat capacity MJ/(m^3 K)	2.12	0.11		
101058	Thermal conductivity W/(m·K)	3.81	0.13	3.55	4.01
	Heat capacity MJ/(m^3 K)	2.08	0.10		
	Thermal expansion coefficient ×10^{-6} m/(m·K)	7.5			
101061	Thermal conductivity W/(m·K)	3.33	0.20	2.93	3.73
	Heat capacity MJ/(m^3 K)	1.92	0.14		
101051	Thermal conductivity W/(m·K)	2.96	0.18	2.59	3.33
	Heat capacity MJ/(m^3·K)	2.21	0.11		
	Thermal expansion coefficient ×10^{-6} m/(m·K)	7.8			
102017	Thermal conductivity W/(m·K)	2.32	0.12	2.08	2.56
	Heat capacity MJ/(m^3 K)	2.35	0.21		

5.6 Implications for future SDMs

During the execution of the planned underground constructions at Forsmark more information will be available about the lithological heterogeneity, spatial variability and size distribution of the different rock types. Based on future updates of the geological description, the description of the thermal properties at the repository area must be updated and reinterpreted at different scales using the new methodology for thermal modelling. The focus must be on modelling the thermal properties, in particular the thermal conductivity, at a scale suitable for the accurate description of the deposition areas of the Forsmark site repository. Since the thermal modelling methodology relies on stochastic simulations for estimating thermal conductivities, thermal field data will be valuable for future thermal modelling. Additionally, future SDMs can consider working on modelling anisotropy with increasing data availability.

6 Rock mechanics

The main objective of the Rock mechanics modelling is to characterize the bedrock at the Forsmark site with focus on the planned repository areas, providing a thorough and detailed site description required for the safety assessment and repository design. Previous and newer data available from several sources are compiled, analysed and interpreted, consisting mainly in results from boreholes investigations, such as rock stress measurements and drill core samples for laboratory testing to determine intact rock and fracture properties. Results from the core mapping as well as the geological description are also an input to rock mechanics modelling.

The rock mechanics descriptive model comprises different parameters regarding the in- situ stress, intact rock, fractures and rock mass. The stress field is important for the repository design and basis for assessing the impact of the thermal loading phase, earthquake scenarios, glaciation cycles and the hydromechanically coupled groundwater flow. The intact rock parameters are used to evaluate the most suitable design of tunnels and excavations, deposition hole stability and other repository design concerns. Fracture parameters are relevant to estimate rock mass properties and safety issues such as co-seismic secondary fracture displacements. The fracture deformability parameters, normal and shear stiffnesses, are crucial for modelling the hydromechanical coupled behaviour of fractures important to estimate the groundwater flow and transport from the repository.

6.1 State of knowledge

6.1.1 Summary of previous SDM

In SDM-Site the rock mechanics properties were described for the most common rock types in the rock domains RFM029 and RFM045. Models were based on laboratory testing on intact rock drill cores samples including mainly uniaxial compressive testing, indirect tensile testing and triaxial testing (Glamheden et al. 2007). Small samples of natural open fractures were also tested using both tilt tests and direct normal and shear testing in the laboratory. These results constitute the basis for description of mechanical properties for single open fractures presented in (Glamheden et al. 2007). On the rock mass scale, the property parameters are estimated both based on numerical modelling and on empirical approaches.

A model for the in-situ stress field was presented where the magnitudes for principal components are given as functions of the depth, for the fracture domains FFM01/FFM02 and FFM03, respectively. The orientation for the major principal stress was modelled as constant (NW-SE) in the whole Forsmark volume. The stress model was based on a combination of direct and indirect data on the stress state in investigation boreholes (Glamheden et al. 2007). Some additional complementary investigations are presented in (Glamheden et al 2008), and all the SDM-Site rock mechanics models are summarized in (SKB 2008a; 2013).

6.1.2 Key remaining issues after SDM-Site and SDM-PSU

In SKB (2008a) the overall confidence in the SDM-Site models for SFK are discussed and presented. For rock mechanics the stress magnitude is identified as having the main uncertainty, while the orientation of the stress field was judged known within quite narrow bounds. Understanding in situ rock stresses was considered important for design of the repository in order to mitigate potential spalling and other stability problems and for the assessment of thermally induced spalling as a part of the safety assessment.

In Glamheden et al. (2007), which is the main underlying report for the rock mechanics discipline in SDM-Site, two main issues of remaining lower confidence were pointed out:

1) **The magnitude of the horizontal stress components.** The number of reliable measurement data at depth was limited and the results from overcoring and hydraulic stress measurements did not agree.

2) **The large-scale mechanical properties of fractures.** The fracture samples tested in laboratory are very small compared to the fractures of interest in the analyses. Further the representativity of the tested fractures to large major water bearing fractures is questionable. Further the stress dependency for fracture normal stiffness was not modelled in SDM-Site.

6.1.3 Summary of updated knowledge at Baseline stage

In Baseline some of the remaining issues from SDM-Site have been addresses. The main work has been the development of an **updated methodology** report (see Section 6.3).

A reliability ranking has been conducted on all the available overcoring stress measurements at Forsmark, where two different types of data sets in the overcoring data were successfully ranked (Sjöberg et al. 2024). Result from the new ranking and additional analysis of indirect stress indicators have resulted in a new **stress model** in Baseline (see further Section 6.4).

On drill core samples in the various rock types occurring at SFK and SFR, a limited number of new laboratory tests using both conventional and newer test methods for **intact rock** has been compiled and analysed together with previous data (see Section 6.5).

For **single fractur**e properties, sealed and open, several different research efforts have been performed in the period after SDM-Site. The results ae summarized and references given in Section 6.6.

6.2 Description of complementary Baseline data

The amount of intact rock samples in the Baseline dataset used for the intact rock model evaluation is compiled in Table 6-1. Roughly 24% is new analysis done post SDM-site and SDM-PSU, with 13 new uniaxial compressive tests and 72 additional indirect tensile tests. Based on that dataset, the uniaxial compressive strength, Young's modulus, Poisson's ratio as well as indirect tensile strength have been re-evaluated. One new parameter for intact rock has been introduced in Baseline: the fracture toughness of rock which is important for modelling of processes involving crack propagation. A total of 15 fracture toughness tests have been successfully conducted to determine the fracture toughness parameter.

Table 6-1. Amount of laboratory test for intact rock model evaluation in Baseline.

Rock Type ID	**101057** Granite to granodiorite, metamorphic No, or faint, albitization	**101057_104 or 101058_104** Medium to strong albitization	**101058*** Granite, metamorphic, aplitic No, or faint, albitization	**101061** Pegmatite, pegmatitic granite.	**101051** Granodiorite to tonalite, metamorphic, fine- to medium-grained	**102017** Amphibolite	**103076** Felsic to intermediate volcanic rock
Number of uniaxial compression tests	71	15	0	16	8	8	5
Number of indirect tensile tests	169	10	0	20	10	25	10
Number of fracture toughness tests	15	0	0	0	0	0	0

*Models based on results on 101057

The three different categories of fractures (sealed, open and PFL fractures) have had their mechanical properties estimated separately, resulting in an improved description in Baseline compared to previous site descriptive models. The mechanical properties are normal and shear stiffnesses, fracture shear strength also including dilation angle and sealed fracture tensile strength.

6.3 Updated methodology and model overview

Most of the rock mechanics parameters and models have been revisited in Baseline rock mechanics report (Hakami et al. 2025), and updated following the rock mechanics modelling methodology (RMMM) presented in Hakami et al. (2022).

In summary the RMMM presents:

- The strategy for stress modelling
- The characterization of intact rock, including the fracture toughness property parameter and scale effects
- Stress dependent deformability parameters of single open fractures
- Hydromechanical coupling strategy and scale effects on single fracture properties
- The description and geometrical classification of water-bearing fractures (PFL)
- Separate sealed fractures description
- The rock mass characterization following numerical and analytical DFN-based approaches, and the empirical approach

The in-situ stress model has been re-evaluated based on the results of a reliability ranking system recently applied to the overcoring stress measurement data. Specifically, the new data quality ranking system was applied to all available overcoring data to document and provide a way to classify these measurements in a traceable way. The ranked overcoring data together with indirect stress information was analysed to produce an update stress field model.

A new geometrical classification based on acoustic televiewer logging in intersecting borehole, has been presented for the PFL fractures in Hakami et al. (2024). Additionally, the fracture normal and shear stiffnesses consist now of a stress dependent function. This is described further in Section 6.6.

The following sections summarize the revisited and updated parameters and models covered in Hakami et al. (2025).

6.4 Stress field

A numerical model to demonstrate the potential influence of deformation zones on the stress field was performed by Hakala et al. (2019) and later updated by Valli et al. (2023) with new numerical simulations including the updated model of deterministic deformation zones.

A new reliability ranking system (Sjöberg et al. 2025) was applied to all the available overcoring data, where all data is classified into the two overarching categories A and B, where A corresponds to measurements with newer probes capable of recording transient strains during overcoring, and B are older results with no transient data available. The overall reliability of the overcoring data is estimated through the consideration of the reliability for the elastic modulus, transient strains and variability stress solution, respectively, and the selection of the worst case from any of these. Thus, the A class data allow to include the reliability of the transient strain response in the reliability assessment, which is not the case for the B class due to the lack of recorded transient strain data. Both the A and B classes are categorised further into data quality Poor, Moderate and Good. The Baseline model only have B-good data available at repository depth for SFK. The ranking results of the overcoring data for maximum and intermediate principal stresses vs vertical depth are shown in Figure 6-1.

The ranked overcoring measurement data was analysed together with the indirect stress information from core and ring disking and borehole breakout studies to propose an updated model for the stress field. The Baseline in situ stress field model (Figure 6-2) is accordingly modified compared to previous stress models (Hakami et al. 2025).

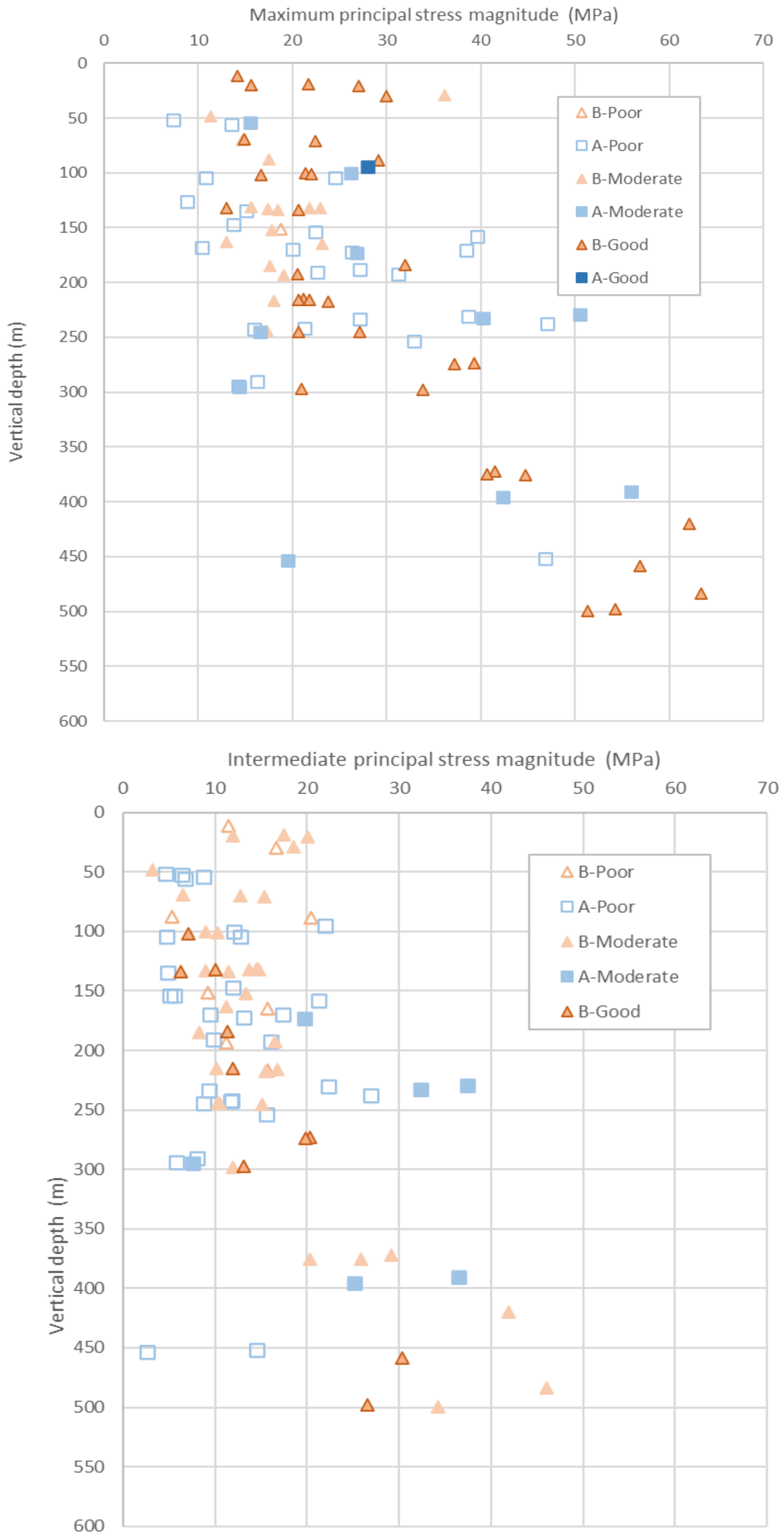

Figure 6-1. *The overcoring data for maximum (top) and intermediate (bottom) principal stress vs vertical depth, with different symbols corresponding to the reliability classification for the two data sets A and B, according to Sjöberg et al. (2025).*

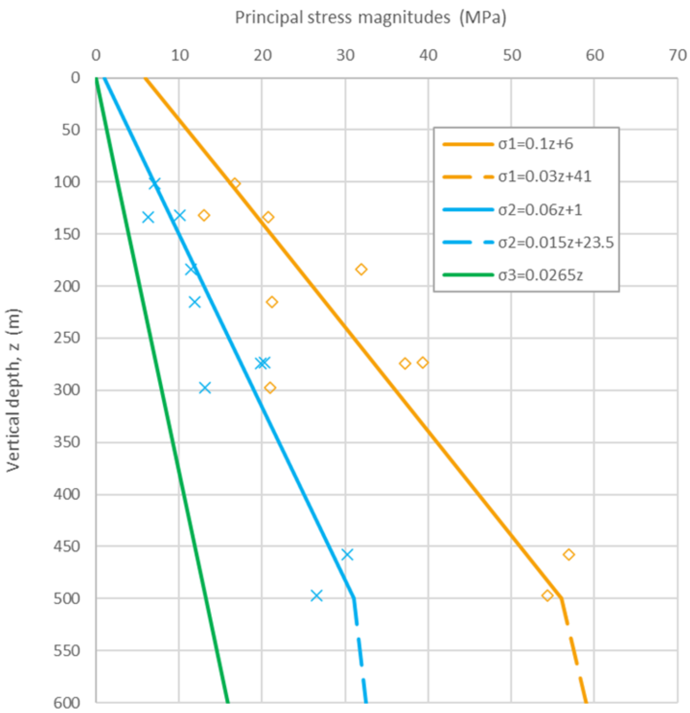

Figure 6-2. *The Baseline Forsmark stress model showing the mean of the principal in situ stress components described as linear functions of the vertical depth, z. The equations of the model for the vertical depth intervals 0-500 m and >500 m, respectively, are given in the legend. The marked stress measurement data points have both $\sigma 1$ and $\sigma 2$ with B-Good ranking (cf.* ***Figure 6-1****). The linear equations of the model are best fit to these datapoints. The vertical stress $\sigma 3$ is modelled as corresponding to the overburden.*

Overcoring tests without measurements were conducted at the lower part of cored borehole KFM24 to assess the suitability for conducting stress measurements (Hakami and Holmberg, 2021). That study was followed by incomplete rock stress measurement trials with new and traditional probes (Hakala 2023; Ask 2023).

A method description for stress measurement in excavated tunnel surfaces with a new LVDT technique, including a reliability ranking system for quality control, was written by Hakala (2022). The technique is based on the methodology tested at the Äspö Hard Rock Laboratory and proposed by Hakala et al. (2012); and further applied in the Onkalo underground investigation facility at the Olkiluoto site in Finland (Hakala et al. 2014).

To deal with the uncertainty of the spatial variability of the rock stress model, a new methodology is currently under development for the analytical quantification of the spatial variability of the stresses at Forsmark. This methodology is based on a tensorial probabilistic approach, capable of quantifying analytically the stress variability, identifying stress domains and generating stochastic stress tensors (Figueiredo et al. 2020, Javaid et al. 2022, Javaid et al. 2024). It will be used to update and improve future in situ stress models.

6.5 Intact rock

The intact rock mechanical properties are tested on drill core samples in the laboratory. The model parameters have been updated according to the additional laboratory testing performed after SDM-Site. A summary of the models for uniaxial and tensile strength as well as the deformation properties is given in Table 6-2 (extract from Hakami et al. 2025). Only the seven most frequently occurring rock types (>2% of volume occurrence at any rock domain of Forsmark) are considered relevant and enough for a suitable site description. The dominating rock type, granite to granodiorite 101057, has been divided and characterized separately based on the alteration degree of albitization, i.e. treated as separate rock types (Figure 6-3) (see Petersson et al. 2024). The difference in mechanical properties depending on albitization was less clear in SDM-Site, where the models were presented differently depending on domains instead. In Baseline, the models for the intact rock mechanical properties are the same for the whole Forsmark site.

From a comparison between SDM-Site and Table 6-2 it may be noted that the mean and standard deviation of uniaxial strength is almost the same (previously 226/28 MPa). The model for the aplitic granite 101058 (unaltered) is assumed the same as for 101057 (unaltered), since there are no laboratory tests data available for that rock type. The description now includes a model for amphibolite which is the weakest rock type, and the felsic to intermediate volcanic rock 103076 is included because this rock type occurs at the SFR site.

The dominating rock type has a varying degree of foliation. In Baseline, a closer study was made of the influence of clear foliation, which exist in some parts of the rock type 101057 (Figure 6-3). The study showed that the tensile strength is about 2 MPa lower in the direction perpendicular to foliation compared to the parallel direction or non-foliated rock.

Table 6-2. Summary table for deformation and strength properties from uniaxial and tensile strength tests on intact rock in Baseline Forsmark. Models are all truncated normal distributions.

Rock Type ID Parameters given as: Mean/Standard dev. Min–Max truncation	**101057** Granite to granodiorite, metamorphic No, or faint, albitization	**101057_104 or 101058_104** Medium strong albitization	**101058*** Granite, metamorphic, to aplitic No, or faint, albitization	**101061** Pegmatite, pegmatitic granite.	**101051** Granodiorite to tonalite, metamorphic, fine- to medium-grained	**102017** Amphibolite	**103076** Felsic to intermediate volcanic rock
Number of uniaxial compression tests	71	15	0*	16	8	8	5
Uniaxial compr. strength, UCS (MPa)	225/26 157–289	352/46 229–391	225/26 157–289	213/39 153–285	187/40 143–228	188/113 45-334	177/81 104-283
Young's modulus (GPa)	76/2.7 69–83	81/2.2 78–86	76/2.7 69–83	74/4 69–80	75 73–76	81/24.7 41/115	80/8.9 68-89
Poisson's ratio	0.24/0.036 0.14-0.3	0.28/0.021 0.25-31	0.24/0.036 0.14-0.3	0.30/0.041 0.19-0.35	0.29/0.025 0.25-0.34	0.38/0.062 0.29-0.50	0.29/0.035 0.24-0.33
Number of indirect tensile tests	169	10	0*	20	10	25	10
Indirect tensile strength, ITS (MPa)	13.3/1.8 8.1–17.9	14.8/1.3 12.8–16.6	13.3/1.8 8.1–17.9	11.4/2.9 6.6–16.7	16.0/1.1 14.4-17.5	11.0/6.1 1.2-21.4	18.8/1.3 16.9-20.7
Number of fracture toughness tests	15	0	0	0	0	0	0

Rock Type ID Parameters given as: Mean/Standard dev. Min–Max truncation	**101057** Granite to granodiorite, metamorphic No, or faint, albitization	**101057_104 or 101058_104** Medium to strong albitization	**101058*** Granite, metamorphic, aplitic No, or faint, albitization	**101061** Pegmatite, pegmatitic granite.	**101051** Granodiorite to tonalite, metamorphic, fine- to medium-grained	**102017** Amphibolite	**103076** Felsic to intermediate volcanic rock
Fracture toughness, K_{IC} (MPa $m^{1/2}$)	1.67/0.22 1.15–1.99	-	-	-	-	-	-

*Models based on results on 101057

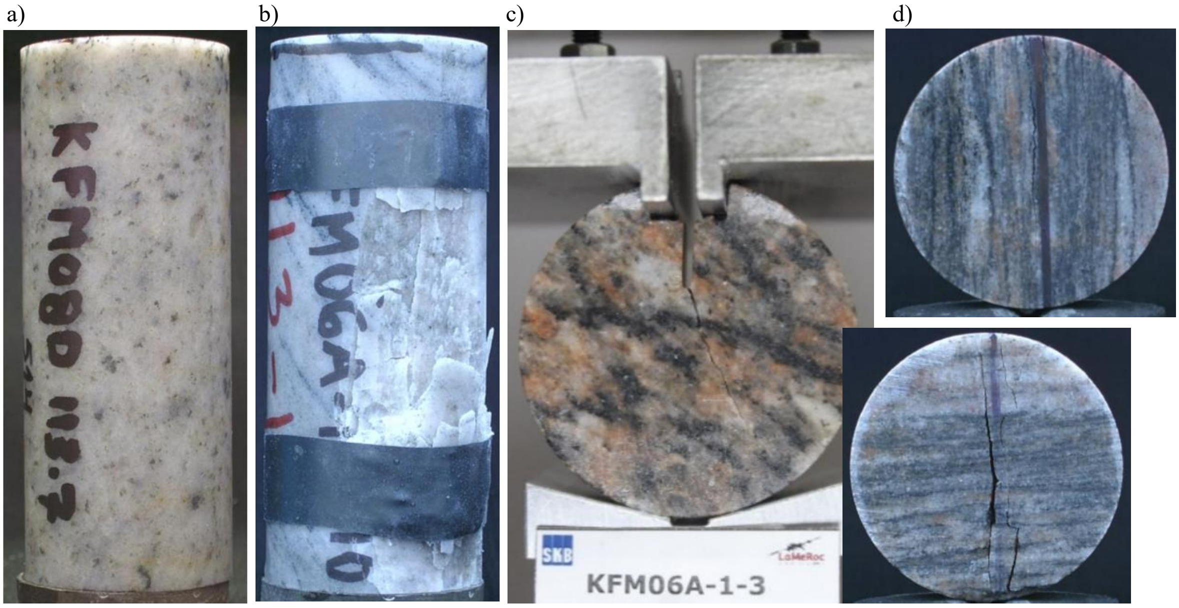

Figure 6-3. *a) The sample of 101057_104 having the highest UCS, 391 MPa. b) Example of typical failure mode in uniaxial test in the strongly albitized 101057_104. c) Example of samples after fracture toughness testing with pCT in a non-albitized 101057. d) Example of indirect tensile tests performed parallel and perpendicular to the foliation in non-albitized 101057.*

A new mechanical parameter added in Baseline is the fracture toughness of rock. This new description parameter will be useful for theoretical modelling of processes involving crack propagation, required for the safety assessment of the planned repository at Forsmark.

6.6 Fractures

The natural fractures in the rock mass have different geological history and show different characteristics. In the description of fractures at Forsmark the main characterization is performed during the core mapping. Following this methodology, the fractures are generally divided in sealed or open. Among the open fractures, some fractures have shown larger inflow into the borehole (denoted Posiva Flow Log (PFL) fractures, see e.g. section 7. and Hakami et al. 2022) compared to others. These PFL fractures have been recently studied more closely than in previous rock mechanics characterizations.

In the following, it will be summarized how the mechanical properties for these three categories of fractures (open, PFL, sealed) have been estimated, separately, resulting in an improvement in the Baseline description compared to previous site descriptive models.

In Hakami et al. (2024), a study of the most water bearing fractures, i.e. the PFL fractures, was performed with the aim of finding any support to suggest an alternative characterization of the mechanical properties of these fractures, which are significantly relevant for the hydromechanical modelling. Nine different boreholes were included in the study, where both flow logging and acoustic televiewer loggings had been carried out. The different AT image appearances were divided into geometrical classes, and their distribution was determined for each borehole. The distribution of geometrical classes corresponding to all boreholes is presented in Hakami et al. (2024). Several mapped parameters for PFL fractures were compared to the non-PFL open fractures; but no significant differences were found apart from the aperture.

Small open fractures were sampled from drill cores and studied mechanically in the laboratory during the SDM-site investigation. The laboratory results show that the normal stress increases rapidly with the increased closure of the fracture, which means that the fracture stiffness is strongly stress dependent. In previous fracture descriptions, the secant value of the curve (between 0.5 MPa and 10 MPa normal stress approximately) was used as the stiffness characterization. However, in Baseline, the description was improved to provide also information on the stress dependency, following the recommendations in the rock mechanics methodology (Hakami et al. 2022).

Direct measurements of all the different geometrical classes of PFL fractures on small scale samples in laboratory is in general not feasible, and the normal stiffness model has therefore been estimated at this stage based on literature studies, in combination with the results and observations from the study of geometrical properties and further comparisons between PFL fractures and non-PFL fractures. The starting point behind the estimation is that the PFL fractures are considered clearly unmated while the non-PFL are more mated. This means that the distance between contact points of the opposing fractures surfaces are much larger for PFL fractures and consequently may result in lower stiffnesses. The same strongly stress dependent model for the normal stiffness, determined for the open fractures (non-PFL), is assumed for the PFL fractures and the stiffness characteristic is expected to be roughly ten times more compliant than that of the ordinary open fractures. More details about the estimation of stiffnesses for the more water bearing fractures can be found in Hakami et al. (2025).

Analogous to the normal stiffness, the existing laboratory data regarding the shear stiffness was analysed. An updated model for the shear stiffness description was developed, consisting of a stress dependent function instead of the previous model with a single value (see Hakami et a 2025).

The new descriptions for the normal and shear stiffnesses have the advantage of dealing with models including different ranges of stress levels.

The fracture shear strength properties for open fractures have not been revisited within Baseline, and no new laboratory site specific test has been performed.

Sealed fractures were previously tested in the laboratory, with shear tests conducted on four samples under different normal stresses. The results are found in Table 4-9 in Glamheden et al. (2007). In Baseline, the studies of sealed fractures were continued by making indirect tensile tests with the point load apparatus (Hakami and Winell 2022). In this study the aim was to compare the result with point load tests on intact rock and to differentiate between the sealed fractures with different type of infilling minerals, since a significant difference could be expected between very thin, often old, sealed fractures and sealed fractures with thicker weaker infillings. The tests showed that fractures with weak main mineral such as chlorite, calcite and laumontite had a tensile strength that is clearly weaker than the tensile strength of intact rock. On the other hand, the sealed fractures with stronger infilling minerals, such as adularia, quartz or only oxidized walls, have a tensile strength similar to the intact rock.

6.7 Rock mass

The bedrock on a larger scale, including both the intact rock and fractures of different kinds is called "rock mass", and its mechanical properties are described with parameters for the larger volume as a continuum equivalent material. This type of description was part of SDM-Site model (Glamheden et al. 2007) and within Baseline no updates of the site-specific models have been made. However, some new approaches in the methodology developments for rock mass modelling are described in the methodology report (Hakami et al. 2022).

With the goal of improving the rock mass characterization, a methodology has been developed to determine analytically the rock mass effective elastic properties through a DFN-based rock mass model. This methodology is under further development to include the analytical estimation of the rock mass strength. Updates of the rock mass models, using both conventional, empirical and new and updated methodologies, are planned for future site descriptive models.

6.8 Discussion

6.8.1 Baseline status

At Baseline the methodologies for most rock mechanics parameters can be considered ready, while the implementations of the methodologies are not carried out for all properties or for all domains. The methodology is presented in (Hakami et al. 2024).

The stress model is not expected to reach closer to the final model until the excavation phases and measurements from excavations are carried out. The main improvement from Baseline is the improved reliability assessment procedures for different overcoring measurement methods (Section 6.4).

The Baseline update is more complete than the SDM-Site model in the sense that it now includes descriptions of components that were previously not described, the sealed fractures and the main waterbearing fractures (Section 6.6).

The remaining uncertainties in the models that will call for additional investigations in the future is listed in the next section.

6.8.2 Remaining uncertainties in rock mechanics models

After Baseline most of the key issues and uncertainties that prevailed after SDM-Site remains, although significant improvements of the rock mechanics SDM have been made as explained in Sections 6.3 to 6.7. The main remaining uncertainties, in order of importance, for safety assessment are:

A. Uncertainty in the model for in situ stress magnitudes

B. Uncertainty in the mechanical and hydromechanical models for fractures

C. Lack of laboratory data for some rock types

D. Uncertainties in the large-scale rock mass property modelling

6.8.3 Implications for future SDM updates

The implications of the main remaining uncertainties in rock mechanics models aforementioned, for forthcoming SDM updates can be summarized as follows:

Regarding A

- The reliability ranking of stress measurements performed showed that only “B-good” data are available at repository depth. Therefore, additional new A-data measurements are required and planned during the repository excavation operation, both at PSU and SFK.
- Tunnel convergence and overcoring stress measurement method designed for tunnel excavations, the LVDT stress measurement method (Hakala 2022), will be applied when tunnels are available.
- The new interpretation methodology based on a tensorial probabilistic approach, by (Javaid et al. 2024) will be used in future stress modelling.

Regarding B

- Despite the lack of new laboratory test data on fractures, research projects with the aim of increasing the general understanding of the mechanical behaviour have been carried out after previous site investigations (Pérez Rey at al. 2024). The results from these studies will, together with additional planned laboratory testing on Forsmark samples with focus on PFL fractures, constitute a basis to the updated SDM in the future.
- The difference on the surface hardness was also studied using a Leeb hardness tester (LHT). This tool was used and tested to evaluate its potential as a field tool for future characterization of both intact rock and fracture surfaces. The results indicated softer surfaces to a certain extent, for the PFL fractures compared to non-PFL surfaces; however, some unexpected limitations where found in the LHT tool performance during the study.

Regarding C

- Complementary uniaxial, indirect tensile testing and triaxial testing is planned for relevant rock types with few or no laboratory data (such as 101058) to reduce the uncertainty and complete the intact rock characterization for future site descriptive model.
- New fracture toughness tests are planned for the amphibolite (102017) and for the albitized granite to granodiorite (101057_104).

Regarding D

- Updates of the rock mass models, using new and updated methodologies, are planned for future site descriptive models.

7 Bedrock hydrogeology

The subject area of bedrock hydrogeology depends on other underlying data and models, particularly those related to bedrock geology (Chapter 4) and rock mechanics (Chapter 6). Table 7-1 presents the main reports related to bedrock hydrology, produced as part of the previous modelling and investigation stages (SDM-Site, SDM-PSU, and the SFK access area update), and those of the current Baseline Forsmark modelling stage. It is noted that the table only shows main reports; these are based on a large number of other reports regarding investigations and monitoring of bedrock hydrogeology.

Table 7-1 Main reports related to bedrock hydrogeology, produced as part of SDM-Site, SDM-PSU, the SFK access area update, and those of the current Baseline Forsmark modelling stage. SKB Reports are reference by their report number.

	SDM-Site	SDM-PSU	SFK access area	Baseline Forsmark
Data reports – properties	R-07-48	R-11-03	P-16-27, P-17-17	R-22-07
Data reports – state variables	R-08-10	-	P-17-19	R-24-03
Conceptual and quantitative groundwater flow modelling	R-07-49, R-08-23	R-11-10	-	R-23-06
Bedrock system synthesis	R-08-95	R-13-25	-	-
Main report	TR-08-05	TR-11-04	R-17-13	Current report

Section 7.1 focus on important hydrogeological findings and uncertainties for the bedrock systems investigated in SDM-Site (SKB 2008) and SDM-PSU (SKB 2013), respectively. Section 7.2 presents important findings in the complementary investigations performed posterior to the completion of SDM-Site and SDM-PSU. Section 7.3 describes two of the modelling methodologies shown in Table 1-1 developed posterior to the completion of SDM-Site and SDM-PSU and comments their applicability within site descriptive modelling, construction of final disposal facilities, and analysis of post closure safety.

7.1 Key findings and uncertainties in SDM-Site and SDM-PSU

In total, 25 cored (KFM) and 38 percussion boreholes (HFM) were investigated for SDM-Site (Figure 2-2), and seven cored (KFR) and three percussion boreholes (HFR) were investigated for SDM-PSU (Figure 2-4). The hydrogeological modelling was largely based on the measurements performed in the cored boreholes. First, the structural information provided by cored boreholes is superior for discrete fracture network (DFN) analysis and modelling in comparison with the structural information provided by percussion boreholes. Second, the spatial resolution of the hydraulic data acquired in cored boreholes with the Posiva Flow Log method (PFL) is 0.1m, which is superior in comparison with the spatial resolutions of the hydraulic information acquired with other hydraulic test methods, which is 5m or larger. Follin et al. (2007a) provides detailed information about different hydraulic test methods.

Twelve KFM boreholes and eight KFR boreholes were measured in total with the PFL method. Several of the KFM boreholes were kilometre-long and three of these reached a vertical depth of one kilometre. The two deepest KFR boreholes reached c. 350 m and c. 425 m vertical depth. The hydraulic properties deduced from the measurements are collated in Earon et al. (2025). It is noted that the equipment used to conduct PFL measurements in the KFM boreholes required a steel casing. This prohibited a good fracture characterisation of all types of fractures in the uppermost part of the bedrock down to the casing shoe at c. –90 m elevation (approximately 90 m vertical depth below the ground surface). The steel casings in the KFR boreholes were shorter, c. 30 m vertical depth below the sea bottom, which reduced the shortfall of data.

7.1.1 SDM-Site

Figure 7-1 shows two key findings from the hydraulic measurements performed in boreholes that cross modelled deformation zones located inside the local model domain in SDM-Site (cf. Figure 1-4 and Figure 4-3). First, evaluated in-plane transmissivities decrease several orders of magnitude with depth. Second, the in-plane transmissivities reveal substantial lateral heterogeneity at all depths, more than two orders of magnitude according to measurements at different locations in the same deformation zones. The observed heterogeneity in data is probably due to various factors, including aleatoric uncertainty, but possibly also due to epistemic uncertainty. For instance, the largest in-plane transmissivities are associated with gently dipping deformation zones. These are oriented at a high angle to the minimum principal stress in Forsmark (cf. Section 6.4), and motivates a hydromechanically coupled flow model (Follin and Stigsson, 2014).

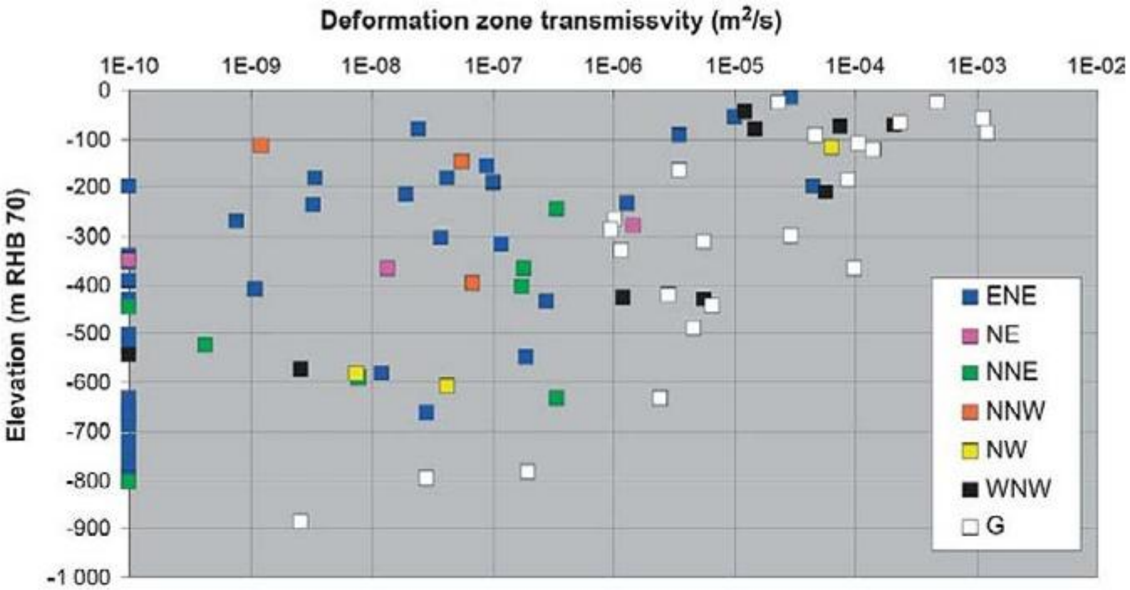

Figure 7-1. Evaluated in-plane transmissivities of investigated deformation zones modelled inside the local model domain in SDM-Site. The figure legend explains the strike of steeply dipping deformation zones, cf. Section 4.4. "G" denotes gently dipping deformation zones. From Follin (2008).

Figure 7-2 shows data from PFL measurements performed in eleven cored boreholes drilled through fracture domains FFM02, FFM01, and FFM06 (see Figure 4-5): KFM01A, -01D, -02A, -04A, -05A, -06A, 07A, -07C, -08A, -08C, and -08D. All boreholes reached elevations below −700 m, two of which reached −1,000 m elevation. Figure 7-2 reveal two key findings: strong contrast in PFL data frequency and PFL transmissivity above and below c. –200 m elevation, and no PFL data below c. –400 m elevation. The absence of flowing fractures below c. –400 m elevation was corroborated by complementary hydraulic measurements using double-packer injection tests, see Follin et al. (2007a) for details. Hence, the lack of PFL data below c. –400 m elevation is not a measurement deficit. (The lack of data above c. –90 m elevation is a shortfall caused by the steel casings.)

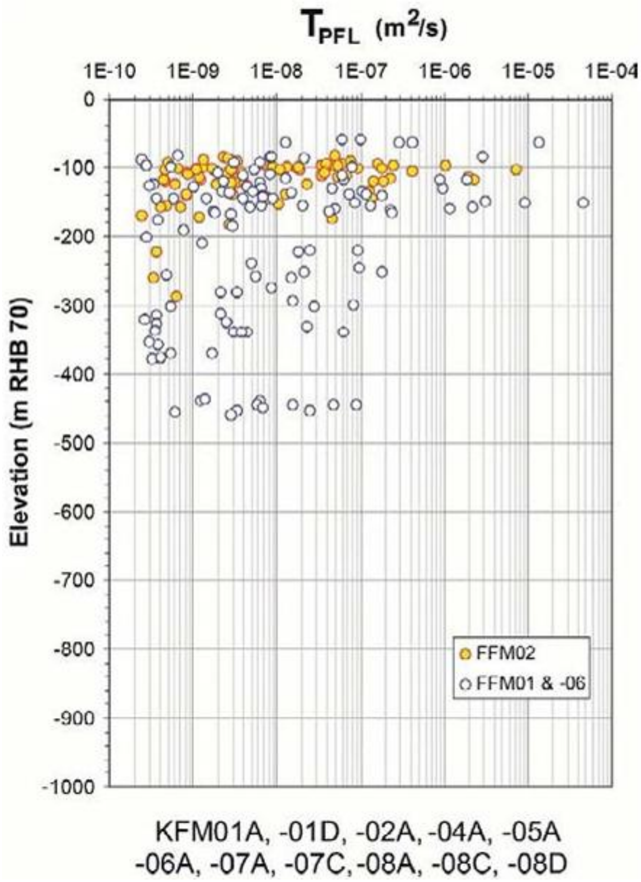

Figure 7-2. *Inferred PFL transmissivities of connected open fractures with depth in fracture domains, FFM02, FFM01 and FFM06. From Follin (ed) (2019).*

The observations of open fractures and flowing open fractures detected with the PFL method were divided into three elevation intervals in SDM-Site, see Figure 7-3 and Table 7-3. The lack of data above c. −90 m was not resolved prior to the completion of SDM-Site but has been resolved by the complementary surface-based boreholes and hydraulic measurements performed posterior to the completion of SDM-Site, see Section 7.2.

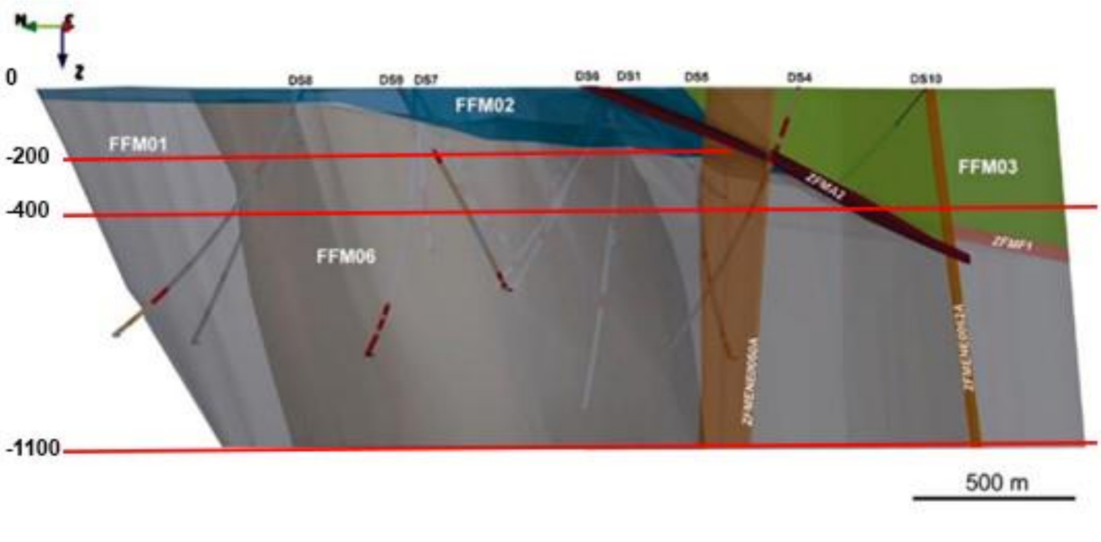

Figure 7-3. *Cross section striking NW – SE through the local model domain in SDM-Site shown in Figure 4-1. The cross section shows several borehole trajectories, four major deformation zones, for fracture domains, and three elevation intervals. Steel casings prohibited a good fracture characterisation of all types of fractures in the uppermost part of the bedrock, i.e., between the regolith depth and the casing shoe at c. –90m elevation. From Follin (2008).*

Table 7-2. Average linear fracture intensity of open fractures ($P_{10,o,corr}$) and flowing fractures detected with the PFL method ($P_{10,PFL,corr}$) for fracture domains FFM02 and FFM01/06. Maximum and minimum values of PFL fracture transmissivity (TPFL) in each fracture domain and elevation interval are also shown together with the geometric mean (<TPFL >). From Follin et al. (2014).

	FFM02	FFM01/06	FFM01/06	FFM01/06
z_{min} , z_{max}	–200 m , –90 m	–200 m , –90 m	–400 m , –200 m	–1100 m, –400 m
$P_{10,o,corr}$ (m^{-1})	3.17	1.13	1.02	0.535
$P_{10,pfl,corr}$ (m^{-1})	0.33	0.153	0.041	0.005
Max T_{pfl} (m^2/s)	$7.3 \cdot 10^{-6}$	$1.9 \cdot 10^{-7}$	$1.8 \cdot 10^{-7}$	$8.9 \cdot 10^{-8}$
Min T_{pfl} (m^2/s)	$2.4 \cdot 10^{-10}$	$2.5 \cdot 10^{10}$	$2.7 \cdot 10^{-10}$	$6.2 \cdot 10^{-10}$
$<T_{pfl}>$ (m^2/s)	$1.0 \cdot 10^{-8}$	$6.9 \cdot 10^{-9}$	$2.4 \cdot 10^{-9}$	$6.5 \cdot 10^{-9}$

7.1.2 SDM-PSU

The fracture intensity in the rock mass outside deformation zones is high across the area investigated in SDM-PSU due to the high-strain belt that forms the north-Eastern margin to the tectonic lens (Figure 1-5). The high fracture intensity did not motivate a division of the rock mass outside deformation zones into fracture domains or elevation intervals (Curtis et al. 2011, SKB 2013). Table 7-3 shows the observed variation in fracture intensity above and below –200 m elevation in SDM-PSU. Another key observation in SDM-PSU is that the most transmissive open fractures occur in the rock mass outside modelled deformation zones. Third, sub-horizontal fractures are generally the most transmissive, also within steeply dipping deformation zones. In the hydrogeological modelling, hydraulic responses observed in boreholes during drilling and pumping were geometrically linked to high-transmissive, single-hole PFL measurements. The term SBA structures ("Shallow Bedrock Aquifer") was introduced to motivate the created “structures” conceptually: “a discrete network of connected flowing fractures consisting of long, sub-horizontal fractures of high transmissivity and shorter, subvertical fractures of lower transmissivity”. In total, eight SBA structures were deterministically defined, see Figure 7-5.

Table 7-3. Linear intensity of open fractures, $P_{10,o,corr}$, above and below –200m elevation in SDM-Site and SDM-PSU. Data are divided into two main categories regarding dip. From SKB (2013).

	FFM02	SDM-PSU	FFM01/06	SDM-PSU
z_{min} , z_{max}	–200m , –90m	–200m , –30m	–400m , –200m	–400m , –200m
Steeply dipping	1.59	3.48	0.59	2.77
Subhorizontal	1.58 (50%)	2.29 (40%)	0.54 (48%)	2.24 (45%)
Total	**3.17**	**5.77**	**1.13**	**5.01**

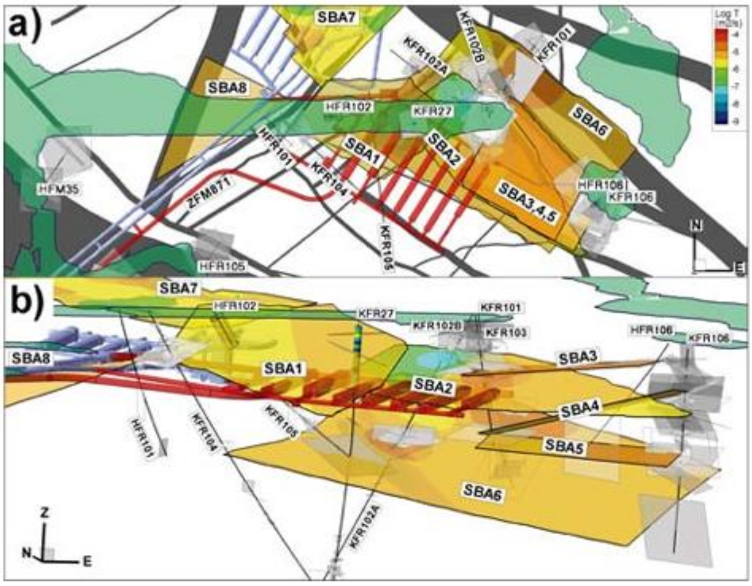

Figure 7-4. *Visualisation of modelled SBA structures in relation to SFR1 and a preliminary layout of SFR3. a) top view, b) oblique view looking towards northeast. The inferred SBA structures are coloured according to the PFL transmissivity data evaluated at borehole intercepts. From SKB (2013).*

7.2 Posterior hydrogeological investigations

This section summarises results from the complementary boreholes drilled and investigated posterior to the completion of SDM-Site and SDM-PSU. In total, 15 cored boreholes and five percussion boreholes have been drilled and investigated in the SFK area (Figure 2-5) and four new KFR boreholes in the SFR area (Figure 2-6). In addition, four new percussion boreholes have been drilled and investigated to study the hydraulic properties transverse the c. 180 m thick and steeply dipping Singö deformation zone that borders the tectonic lens and high-strain belt right between the repository areas in Forsmark, see Figure 1-5.

Figure 7-5 shows the extent and thickness of fracture domains FM02U and FFM02L defined in Section 4.6. (cf. Figure 4-5). The thickness of FFM02U is typically less than 30 m, whereas the thickness of FFM02L varies between zero and up to approximately 250 m. Fourteen of the fifteen complementary cored boreholes, KFM13-27, are c. 60 m long and one is c. 550 m long (KFM24). KFM13-23 and KFM25-27 have very short steel casings installed into the bedrock, a few metres of the order, and hence allow a detailed characterization of the bedrock above c. –90 m elevation (cf. Figure 7-2 and Figure 7-3).

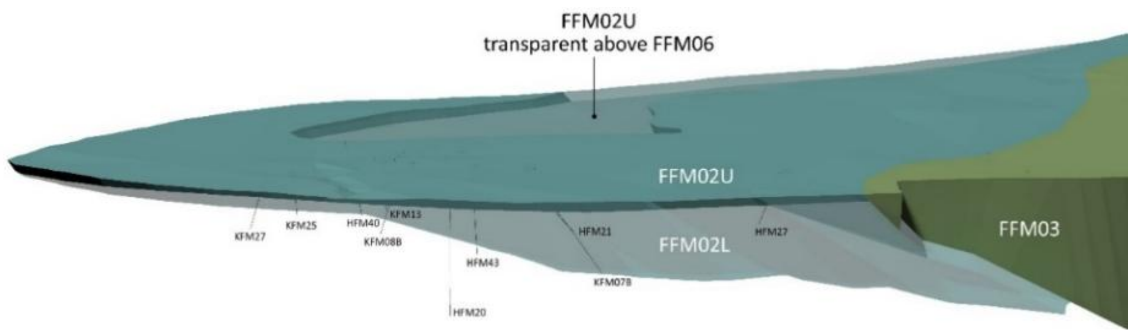

Figure 7-5. *Oblique view to northeast showing the relationship between FFM02U and FFM02L. FFM03 is shown for reference. FFM02U lies on top of FFM02L, which lies on top of FFM01/06. FFM02U is transparent above FFM02L to display the extent of FFM06 below FFM02L. Several of the boreholes used to define the boundary between FFM02U and FFM02L are not visible in this view. From Petersson et al. (2024).*

Table 7-4 shows calculated values of $P_{10,o,corr}$ for FFM02U, FFM02L, and FFM01/06 in KFM13-23 and KFM25-27 together with the values of linear fracture intensity of open fractures, $P_{10,o,corr}$, assumed for the uppermost 200 m of FFM02 and FFM01/06 in SDM-Site of (cf. Table 7-2 and Table 7-3). The values are plotted in Figure 7-6 and show that

- the values of $P_{10,o,corr}$ assumed for FFM02 and FFM01 above –90 m elevation in SDM-Site are significantly lower than the values evaluated from the data acquired in boreholes KFM13-23, 25-27, and
- the value of $P_{10,o,corr}$ evaluated for FFM02U matches the value of $P_{10,o,corr}$ derived in SDM-PSU for the rock mass above –200 m elevation.

Table 7-4. $P_{10,o,corr}$ in FFM01 and FFM02, FFM02U and FFM02L based on data acquired in the short, cored boreholes KFM13-23, 25-27, see Figure 7-5. The values used for hydrogeological DFN modelling in SDM-Site are also shown (cf. Table 7-2 and Table 7-3). Data are divided into two main categories regarding dip. From Follin et al. (2025).

	SDM-Site		Baseline		
	FFM01/06[#]	**FFM02[#]**	**FFM01/06***	**FFM02U***	**FFM02L***
z_{min}, z_{max}	–200m , –90m	–200m , –90m	–127m , –19m	–28m , –1m	–60m , –17m
Steeply dipping	0.59 (52%)	1.59 (50%)	1.19 (44%)	2.71 (47%)	1.09 (31%)
Subhorizontal	0.54 (48%)	1.58 (50%)	1.50 (56%)	3.11 (53%)	2.39 (69%)
Total	**1.13**	**3.17**	**2.69**	**5.82**	**3.48**

[#] KFM01A, -1D, -2A, -4A, -5A, -6A, -7A, -7C, -8A, -8C, -8D
* KFM13-23, 25-27, i.e., KFM24 excluded

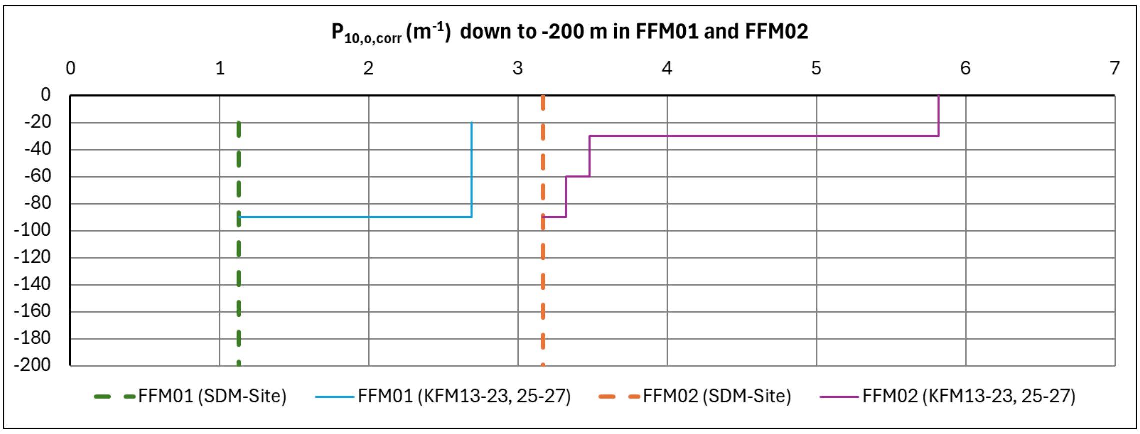

Figure 7-6. *Dashed lines show values of $P_{10,o,corr}$ used in SDM-Site for FFM01/06 and FFM02 above –200 m elevation. Solid lines show values of $P_{10,o,corr}$ for FFM01/06 and FFM02 above –90m elevation evaluated from the investigations in KFM13-23, 25-27. From Follin et al. (2025).*

Ten percent of the total intensity of open fractures in FFM02U and 13% in FFM02L are detected as flowing with the Posiva Flow Log. Figure 7-7 shows evaluated specific capacities, Q/Δh (so-called PFL fracture transmissivities, T_{PFL}) in terms of cumulative distribution functions (CDFs), three for FFM02U and three for FFM02L. "Steeply dipping" represents all flowing fractures that are not subhorizontal. However, subhorizontal flowing fractures are divided into two categories: "Sheet joints" and "Remaining Sub HZ". By definition, "Sheet joints" have distinct apertures, cf. Section 4.4. It is noted that

- in both FFM02U and FFM02L, all CDFs reveal significant variability in specific capacity Q/Δh (or T_{PFL}), roughly 2-3 orders of magnitude for "Steeply dipping" fractures and about 3-4 orders of magnitude for "Remaining Sub HZ" and "Sheet joints",
- in both FFM02U and FFM02L, "Steeply dipping" fractures have the lowest median T_{PFL} values and "Sheet joints" the highest, and
- the median T_{PFL} values are between 5-15 times higher in FFM02U than in FFM02L.

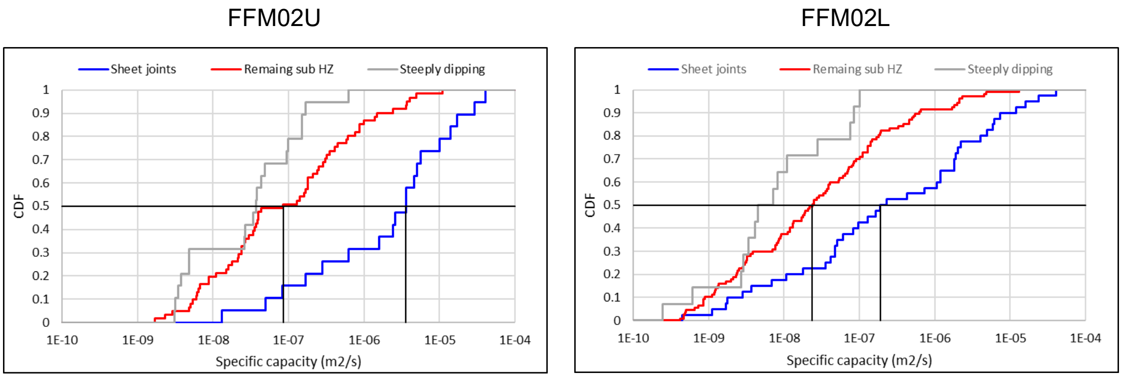

Figure 7-7. *Cumulative distribution functions of specific capacity, Q/Δh (T_{PFL}), for flowing fractures. Data are classified as "Sheet joints" (with distinct apertures), "Remaining Sub sub-HZ", and "Steeply dipping".*

No intervals with deformation zone type properties were identified in the geological interpretation of the 545 m deep (vertical depth), cored borehole KFM24 drilled in the access area for SFK (Figure 2-5). The number and elevations of flowing fractures detected with the PFL method in KFM24 were roughly the same as in other deep, cored boreholes drilled nearby for SDM-Site, see Table 7-5. The largest values of Q/Δh in KFM24 occurred at c. −190 m elevation and were mainly associated with subhorizontal fractures. No flowing fractures were detected with the PFL method below –415 m elevation, which is concordant with the results in the deep borehole drilled for SDM-Site, see Figure 7-2.

Table 7-5. Number of flowing fractures identified during flow logging with the PFL method in deep cored boreholes. KFM24 is a complementary borehole. The other boreholes were drilled during the site investigation for SDM-Site. From Follin (ed) (2019).

Borehole	KFM24	KFM01A	KFM01D	KFM08A	KFM08C	KFM08D	KFM07A	KFM07C
FFM02*	0	26	23	0	0	0	0	5
FFM01	34	6	11	32	5	17	1	8
FFM05	NA	NA	NA	NA	NA	NA	2	NA
FFM06	NA	NA	NA	NA	NA		NA	NA
PDZ	0	2	0	9	16	17	23	1
Total	34	34	34	41	21	34	26	14

* Data acquisition is biased by steel casings
NA = not applicable/available
PDZ = possible deformation zone

Though evaluated linear intensities of open fractures and measurements with the PFL method do not vary significantly with depth in the seven boreholes drilled for SDM-PSU, KFR101-106 (Figure 2-4), the SFR area was divided into three domains: “Shallow” (z ≥ −60 m), “Repository” (−200 m ≤ z < −60 m), and “Deep” (z ≤ −200 m). During the posterior investigations, five complementary cored boreholes were drilled, KFR117-121 (Figure 2-6). Two of the complementary boreholes (KFR119 and KFR121) were measured with the Posiva Flow Log. The results evaluated in the five complementary cored boreholes confirmed the results evaluated in the seven cored boreholes reported for SDM-PSU. There were no signs in KFR117-121 of new sub-horizontal, continuous, and water-bearing SBA structures (so-called SBA structures) within the area planned for SFR3. However, the results support the existing model for the deterministically modelled SBA6 (Figure 7-4), as well as the deterministically modelled sheet joint JFM16 (Figure 4-4).

Five interference pumping tests were carried out 2018 in the percussion boreholes HFM33 (***Figure 2-2***), HFM43 (Figure 2-5), and HFM44-46 (Figure 2-6). A total of 218 distinct hydraulic responses exceeding 0.1 m of drawdown were recorded in surrounding boreholes (Föhlinger et al. 2020). Most of these responses were found during the interference pumping test in HFM43 (Figure 2-5) followed by the interference pumping test in HFM33 (see Figure 2-2). During the test pumping of HFM44–46 (Figure 2-6) significantly fewer responses were detected. No responses were observed transverse the Singö deformation zone in any of the interference pumping tests. This result corroborates the results from the interference pumping test carried out 2007 in borehole HFM33 (Gokall-Norman and Ludvigson 2008).

7.3 Hydrological-hydrogeological modelling

7.3.1 Methodology for discrete fracture network modelling

Follin (2008) describes the methodology for *hydrogeological discrete fracture (DFN) network modelling* used in SDM-Site and SR-Site. The methodology is referred to as DFN-2008. Selroos et al. (2022) presents an interdisciplinary methodology suitable for *all kinds of DFN models* within site descriptive modelling, construction of final disposal facilities, and analysis of post closure safety. The interdisciplinary methodology integrates the basic DFN concepts developed in SDM-Site for geological DFN modelling (Fox et al. 2007) and DFN-2008 with new ones. Examples of such new concepts are hydromechanical coupling, genetic fracture generation including growing fractures, heterogeneous description of individual fracture planes, deformation zones consisting of multiple discrete fractures, and a framework for handling conceptual uncertainties at different stages. Below, the interdisciplinary methodology is referred to as DFN-2020. It is noted that DFN-2008 is integrated in DFN-2020.

The focus of DFN-2008 (Follin 2008) is on the linear intensity of open fractures modelled as regularly shaped planar surfaces (squares, disks etcetera) using statistically driven models with one set of generation parameters (‘model recipe’) for each fracture set and fracture domain. The generation of single, open fractures is assumed to follow a Poisson process and a power-law size-intensity model. Another key assumption is that the connectivity and transmissivity of open fractures can be mimicked by means of calibrated flow simulations using PFL data, see Figure 7-8. Finally, large deformation zones are modelled as undulating triangulated surfaces.

A key feature of DFN-2020 (Selroos et al. 2022) is growing planar objects of irregular shapes (non-symmetric polygons) using geologically driven DFN models, where structural elements from the deterministic geological model are used to constrain variations in fracture intensity and size, see Figure 7-9. A crucial part in hydrogeological applications of DFN-2020 is the hydro-mechanical determination of openness.

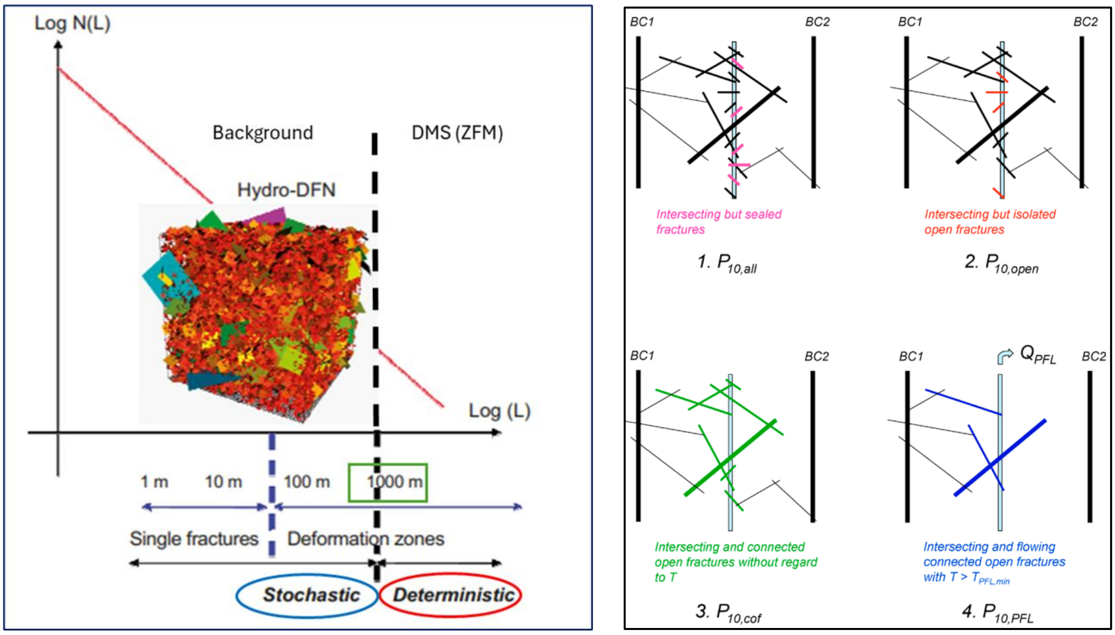

Figure 7-8. *Left: Illustration of the DFN-2008 concept showing a single power-law frequency model for open fractures on all scales ("tectonic continuum"). Right: Illustration of the relations between all, fractures, open fractures, connected open fractures, COF, and PFL data: P10,all ≥ P10,open ≥ P10,cof ≥ P10,pfl. From Follin (2008).*

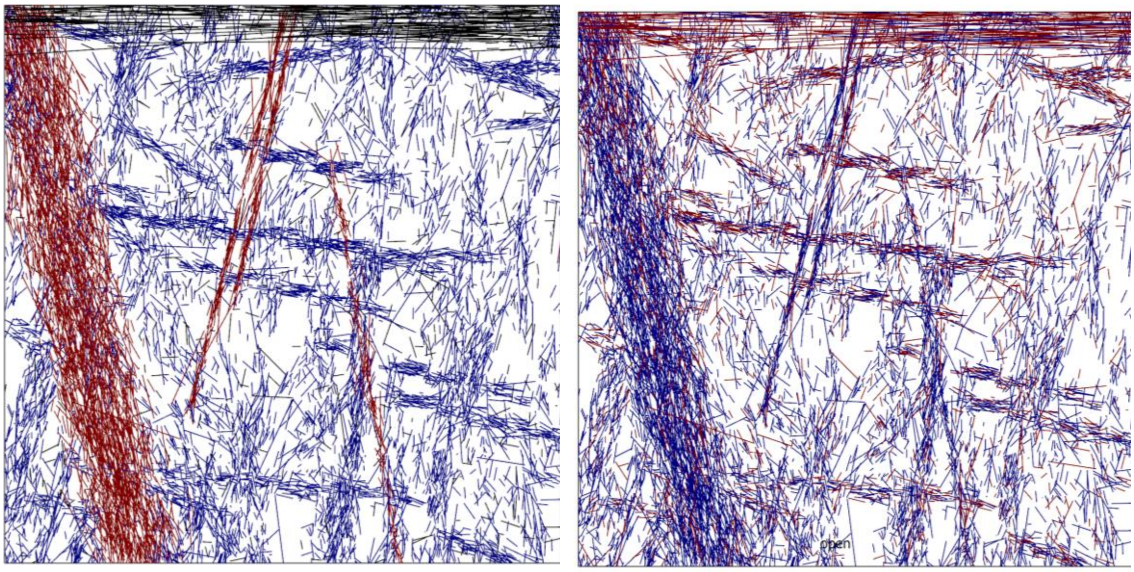

Red: Det. DZs as DFN swarms
Blue: Stoch. DZs as DFN swarms
Black: Background DFN and Sheet Joints

All = Red + Blue
Red: open (≈ 20-25% of All)
Blue: closed (≈ 75-80% of All)

Figure 7-9. *Illustration showing the geologically driven DFN-2020 concept. Note that deformation zones are also modelled as discrete fracture networks.*

7.3.2 Methodology for hydrological-hydrogeological modelling

The methodology for hydrological-hydrogeological modelling described in Odén et al. (2025) presents a protocol for hydrological-hydrogeological flow modelling of the Forsmark site. The protocol integrates discrete fracture network and porous media concepts, see Figure 7-10. The protocol starts with calibrated discrete fracture network (DFN) model realisations using, e.g., the DFN-2008 and/or DFN-2020 concepts described above. Second, the DFN model realisations are upscaled (transformed) to ECPM grid model realisations (Figure 7-11). Upscaled equivalent continuous porous medium (ECPM) models represent an alternative modelling approach that can be computationally less costly as multiple discrete fractures can be represented by a single ECPM cell.

However, this smears sub-cell-scale aspects of the DFN, such as directional connectivity and channelling. The current limits of computational power mean that for local- and regional-scale flow models, ECPM models can represent the only practical solution/approach. Two porous medium flow modelling tools have been in use in parallel since the start of the site investigations in Forsmark: one for the concepts describing hydrology and near-surface hydrogeology, MIKE SHE (DHI 2023), and another for the concepts describing groundwater flow and transport in heterogeneous and anisotropic rock, DarcyTools (Svensson 2010). Notably, the protocol is not code specific but stipulates that the two modelling tools used should render agreeable results regarding simulated magnitudes of vertical fluxes with depth and simulated particle exit locations.

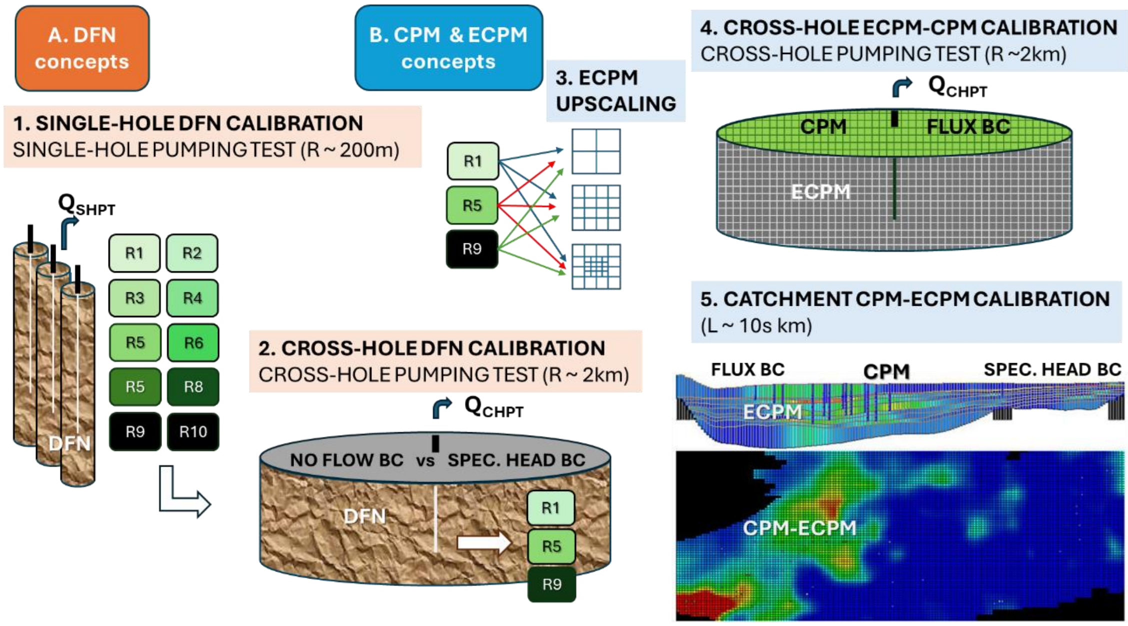

Figure 7-10. *Illustration showing the protocol for hydrological-hydrogeological flow modelling. The depicted workflow is divided into two stages, A and B. The flow modelling in Stage A is made with discrete media modelling tools and in Stage B with porous media modelling tools. The generation of fractures in Stage A requires a conceptual framework for fractures of different types and scales, e.g., one of the two structural DFN concepts briefly described in Section 7.3.1. The flow modelling in Stage B is made with ECPM grid models (see Figure 7-11) on two scales – cross-hole scale and catchment scale. From Oden et al. (2025).*

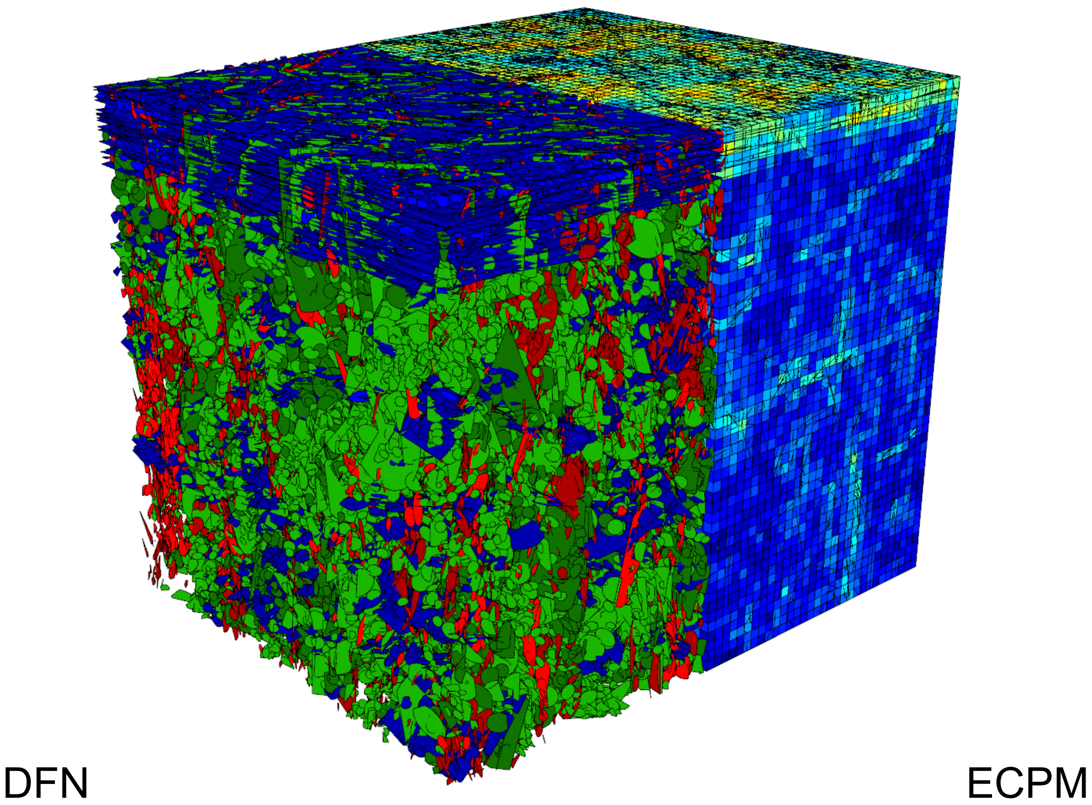

Figure 7-11. *Illustration showing the concept of upscaling from a discrete fracture network model realisation to an ECPM grid model realisation.*

To assess the reliability of the calibration process, the flow modelling tools used for modelling the Surface system and the Bedrock system on a kilometre-scale, respectively, are used to predict flow on a catchment scale using appropriate boundary condition. Two examples of applications are shown in Figure 7-12:

- upward and downward vertical groundwater fluxes between ground surface and repository depth, and
- particle exit locations.

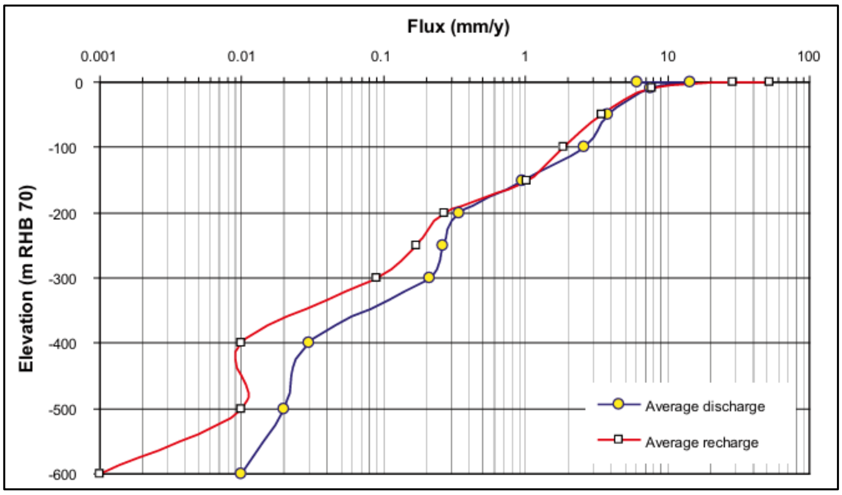

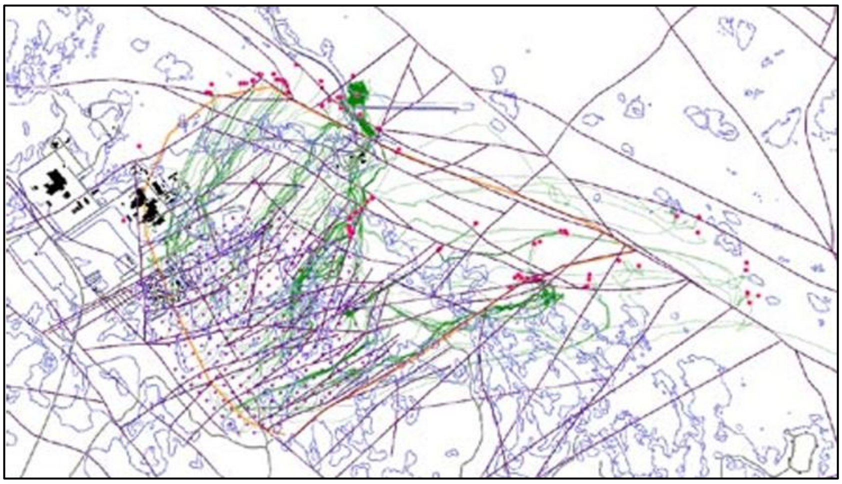

Figure 7-12. Top: Average values of simulated downward and upward vertical fluxes across a predefined horizontal area located at different depths below ground surface; Bottom: Flow paths (green trajectories) and exit locations at ground surface (red dots) of c. 300 particles released at 500 m vertical depth in a 100 m by 100 m mesh (purple dots). From Follin et al. (2007).

7.3.3 Protocol testing

ECPM models represent an alternative modelling approach that can be computationally less costly as multiple discrete fractures can be represented by a single ECPM cell, however, this smears sub-cell-scale aspects of the DFN, such as directional connectivity and channelling. The current limits of computational power mean that for local- and regional-scale models, ECPM models can represent the only practical solution/approach.

The applicability of the protocol for hydrological-hydrogeological modelling was tested in Follin et al. (2025). The testing compared vertical fluxes and particle exit locations for five groundwater flow models simulated with DarcyTools and MIKE SHE. The underpinning DFN models were created with FracMan (https://www.wsp.com/en-US/services/fracman). Three DFN model realisations were based on DFN-2020 concepts (Hartley et a. 2024) and two were based on DFN-2008 concepts (Follin et al. 2025). Section 8.5 comments the results. The main conclusion from the testing is that the protocol for hydrological-hydrogeological modelling works as intended. The two most important findings are

- Comparisons with field scale cross-hole interference pumping tests appear to be a feasible way for hydraulic parameter calibration of both DFN models and ECPM models. However, it is recommended to study the sensitivity of the calibration to the chosen size of model domain and applied boundary conditions. Moreover, if possible, it is recommended to calibrate all DFN model and ECPM model realisations against more than one cross-hole interference pumping test.

- The chosen resolution of the ECPM model grid is the single most important factor for achieving agreeable results between DFN model flow simulations and ECPM model flow simulations. The chosen resolution of the ECPM model grid is considered more important than the choice of upscaling method and choice of ECPM modelling code.

7.4 Recent developments and implications for SDM updates

The groundwater models developed for the bedrock in SDM-Site (Follin 2008) and in SDM-PSU (Öhman et al. 2012, 2013) met the objectives of groundwater modelling in SR-Site and SR-PSU. To support the continuing development of qualified groundwater models, complementary, surface-based boreholes have been drilled and investigated posterior to the completion of SDM-Site and SDM-PSU to unravel key data deficiencies and data uncertainties. The hydraulic data acquired in fifteen cored boreholes drilled in the SFK area (KFM13-27), five in the SFR area (KFR117-121), and five percussion boreholes drilled adjacent to the Singö deformation zone (HFM43-47) motivates a few conceptual considerations and technical modifications

- Regarding hydrogeological DFN modelling using the DFN-2008 concept, it is recommended that the DFN recipes shown in Appendix C in Follin (2008) for the uppermost 200 m of fracture domains FFM01/06 (Table 7-2) and FFM02 (Table 7-3) are updated using the calculated linear intensities of open fractures above c. −90 m elevation presented in Table 7-4 and Figure 7-6, see Follin et al. (2025) for details.
- Regarding hydrogeological DFN modelling of sheet joints using the DFN-2008 concept, it is recommended that the intensity of sheet joints in the uppermost c. 30 m of rock is calculated as a fraction of the intensity of the subhorizontal fracture set. Further, it is recommended that sheet joints are generated as perfectly horizontal fractures in the uppermost c. 30 m of rock across the Forsmark catchment using a positively skewed fracture size-intensity model, see Hartley et al. (2021) and Follin et al. (2025) for details. Sheet joints at larger depths are considered as being of tectonic origin as other deep fractures.
- Regarding future hydrogeological models using the SBA concept developed for the SFR area in SDM-PSU, it is noted that data in the deepest complementary borehole, KFM121, support the existing model for SBA6 (Figure 7-4), as well as the deterministically modelled sheet joint JFM16 (Figure 4-4). Regarding the other SBA structures, i.e., SBA1-5, SBA7 and SBA8 (Öhman et al. 2012), the information gathered in boreholes KFR117-121 is indefinite. It is noted that boreholes KFR117-120 may be too short (i.e. too shallow) to provide any valuable information.
- Regarding the hydrogeological DFN modelling using the DFN-2020 concept, it is recommended to revisit the geological terminology and concepts used for sheet joints at different depth and reassess the concepts used for hydromechanical modelling including the updated stress model described in Chapter 6. These aspects have not been factored into Baseline Forsmark.

8 Meteorology, hydrology and near-surface hydrogeology

This chapter gives an overview of data and models representing Baseline conditions at Forsmark in terms of meteorology, hydrology and near-surface hydrogeology abbreviated "hydrology" for convenience.

From a strictly hydrogeological viewpoint, the landscape can e.g. be divided in subareas in terms of groundwater recharge areas, groundwater discharge areas and "intermediate" (dominated by neither recharge nor discharge) areas. Furthermore, from a surface hydrological viewpoint the landscape is divided in hydrological "elements" such as wetlands, ponds, lakes, streams, and the sea.

Given the above divisions into subareas and elements, it is noted that the methodology for hydrological-hydrogeological modelling developed and tested as part of the Baseline Forsmark stage (Odén et al. 2025) is focused on hydrological-hydrogeological flow modelling on a regional scale. It is also noted that oceanography is usually defined as part of hydrology in SKB's work, but; oceanographic data and models are not part of Baseline Forsmark, except for sea level data used as boundary condition in the quantitative hydrological modelling.

8.1 Overview of baseline data

The subject area of hydrology depends on other underlying data and models, for instance those related to the physiographic setting in terms of various geometries (see Section 8.2). As shown in Chapter 2, the Baseline dataset comprises data from comprehensive investigations and long-term monitoring of hydrology at Forsmark. The maps and tables of Chapter 2 provide an overview of available installations and their current status, their relevance for hydrology, and at what modelling stages data become available.

Table 8-1 presents the main reports related to hydrology, produced as part of the previous modelling and investigation stages (SDM-Site, SDM-PSU, and the SFK access area update), and those of the current Baseline Forsmark modelling stage. It is noted that the table only shows main reports; these are based on a large number of other reports regarding investigations and monitoring of hydrology.

Table 8-1. Main reports related to hydrology, produced as part of SDM-Site, SDM-PSU, the SFK access area update, and those of the current Baseline Forsmark modelling stage. SKB Reports are reference by their report number.

	SDM-Site	SDM-PSU	SFK access area	Baseline Forsmark
Data reports – properties	R-08-08	R-13-19	P-17-19	R-22-07
Data reports – state variables	R-08-10	R-13-20	P-17-19	R-24-03
Conceptual and quantitative water flow modelling	R-08-09, R-08-10	R-13-19	-	R-23-06
Surface system synthesis	R-08-11	TR-14-06	-	-
Main report	TR-08-05	TR-11-04	R-17-13	Current report

In relation to the previous SDM-Site, SDM-PSU and SFK access area modelling stages (Table 8-1), updated hydrological datasets and modelling for Baseline Forsmark can be summarized as follows:

- Updates of underlying, geometrical models of topography, regolith depth and regolith stratigraphy (Chapter 4).
- Additional hydraulic properties data for the regolith, primarily based on single hole (slug) tests in groundwater monitoring wells.
- Prolonged state variables (monitoring) meteorological, hydrological and hydrogeological datasets, enabling interpretation of e.g. trends and variabilities on different time scales, and for detection and quantification of hydraulic responses to repository construction.

8.2 Overview of models

The current description of data and modelling related to hydrology is organized as follows:

- Physiographical data and models (Section 8.3), in terms of topography-controlled catchment area boundaries, and assignment of hydraulic properties of regolith and its interface with the bedrock.
- State variables data interpreted in terms of water balance components (Section 8.4), showing the impact of prolonged state variables datasets in relation to previous modelling stages.
- Conceptual and quantitative models (Section 8.5) of water-flow processes within surface and near surface parts of the hydrological cycle, including interactions with groundwater flow in the bedrock.
- Tests and documentation of an integrated, hydrology–bedrock hydrogeology modelling methodology (Section 8.5; SKB R-20-14 see also Table 1-1 and Chapter 7), including handling of multiple models of the hydrogeological properties of the bedrock in the hydrology modelling, e.g. model variants in terms of stochastic DFN realizations.

8.3 Modelling of catchment delineations

8.3.1 Updated methodology

The relatively flat Forsmark landscape with undulating, small-scale topography requires a high-resolution DEM (digital elevation model) for topography and bathymetry-controlled delineations of catchment area and marine basin boundaries, and identification of flow path directions and groundwater recharge and discharge areas. The quantitative hydrology (Section 8.5) and bedrock (Chapter 7) water flow modelling performed as part of Baseline Forsmark are based on the Baseline DEM (Section 3.4) with a horizontal resolution of 20 m. The Baseline DEM has an adjustment layer (“hydro-DEM”) that accounts for road culverts that are present in the area by adjusting (lowering) relevant pixel values. The boundaries for the Forsmark Catchment model area (Section 1.3) are delineated based on the corresponding 10 m DEM. For further details on the stream network, lake thresholds and other geometrical data used in the quantitative hydrological modelling of Baseline Forsmark, see Follin et al. 2025.

8.3.2 Implications of updated elevation model

As an illustration of the impact of the elevation model for hydrological modelling, Figure 8-1 shows catchment area boundaries for SKB’s four stream discharge gauging stations (cf. Section 2.6) delineated using the Baseline DEM (10 m resolution). The catchment delineations of Figure 8-1 demonstrate some differences to the corresponding delineations using the SDM-Site DEM (10 m resolution). Specifically, the largest catchment (station PFM005764; sum of the yellow, lilac and red boundary areas) has an area of 6.09 km^2 according to the present delineation, whereas the area is smaller (5.59 km^2) according to the SDM-Site DEM.

Moreover, the southernmost catchment (PFM002668; red boundary area) is somewhat smaller (2.02 km^2; 2.28 km^2 using the SDM-Site DEM). The downstream station (PFM002667) has a catchment area of 2.84 km^2 (3.01 km^2 according to the SDM-Site DEM), whereas the westernmost catchment (station PFM002669; blue boundary area) has an area of 2.84 km^2, which is almost equal (2.83 km^2) to the SDM-Site DEM.

It is noted that the Baseline DEM and associated catchment area delineations consider recent topographical alterations (e.g. due to contract works). However, the adjustment layer for road culverts was not used in the catchment delineations using the Baseline DEM, which may explain e.g. the different delineations along the western boundary of the PFM005764 catchment. Based on Figure 8-1, in the current Forsmark landscape it is necessary to take road culverts into account for delineations of catchment-area boundaries.

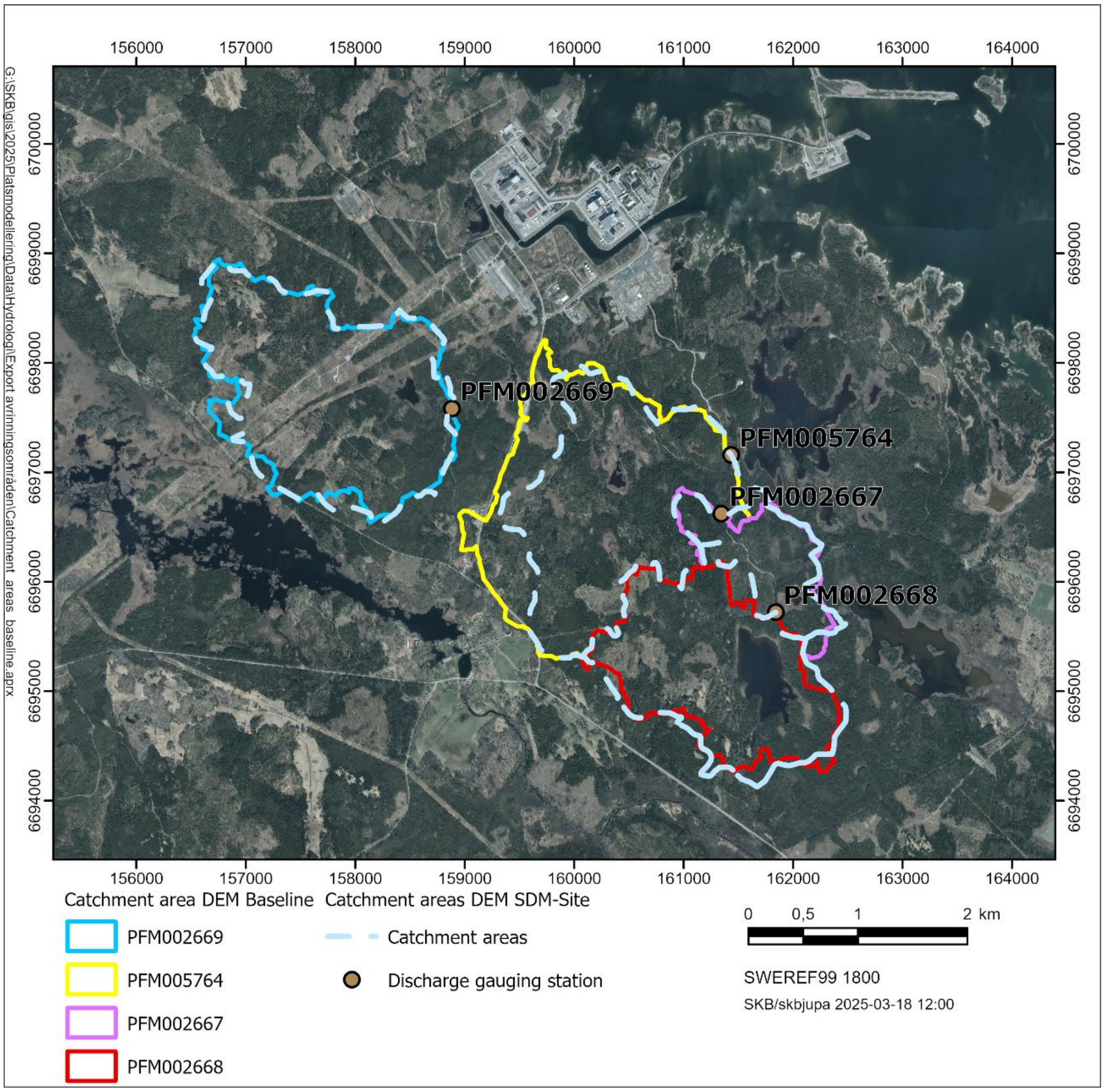

Figure 8-1. *Topography controlled catchment area boundaries for SKB's four stream discharge gauging stations in Forsmark based on the Baseline DEM (full coloured lines; 10 m resolution, and corresponding catchment areas based on the SDM-Site DEM, dashed light blue lines).*

8.4 Description of water balance components within catchments

The processes within and interactions between the water balance components within catchments) such as precipitation and stream discharge are important for describing and modelling the hydrological cycle. As an example, the long-term averages of water balance components are described in this section. The description can be used to show the impact of prolonged state variables datasets in relation to previous modelling stages named in Table 8-1. The datasets and joint data interpretation presented here exemplifies datasets and interpretations used for conceptual and quantitative water flow modelling as part of Baseline Forsmark.

For the hydrological years October 1, 2005–September 30, 2019, Figure 8-2 shows annual sums of R (runoff), P (precipitation; cf. Figure 8-5) and ET (actual evapotranspiration), estimated as ET = P – R. R is represented by the average specific discharge for SKB's four discharge gauging stations (Section 2.6) and associated catchment areas; missing data are completed using ***multiple linear regression.*** As can be seen in the plot, the annual runoff (R) is in the interval 63 to 332 mm during the considered period 2005–2019, and the average of all years is 196 mm. There is a large fraction of missing stream discharge data (and hence many data completions) during the period 2016–2017; excluding the R value from this period, which is the lowest R value in the dataset, the average of the remaining years is R = 206 mm.

This average R value is higher than the average runoff reported in SDM-Site (R = 150–160 mm), which, however, was based on much shorter P and R time series. The annual average P for the period October 1, 2005–September 30, 2019 (excluding the 2016–2017 hydrological year) is approximately 640 mm, which is above the SDM-Site average of 560 mm). In contrast, there is less difference between the SDM-Site (400–410 mm) and the current (ca. 430 mm) evaluation of annual average actual ET; the ratio ET/P ≈ 0.7 in both cases. Thus, it seems likely that the difference in average specific runoff is due to differences in precipitation during the investigated periods.

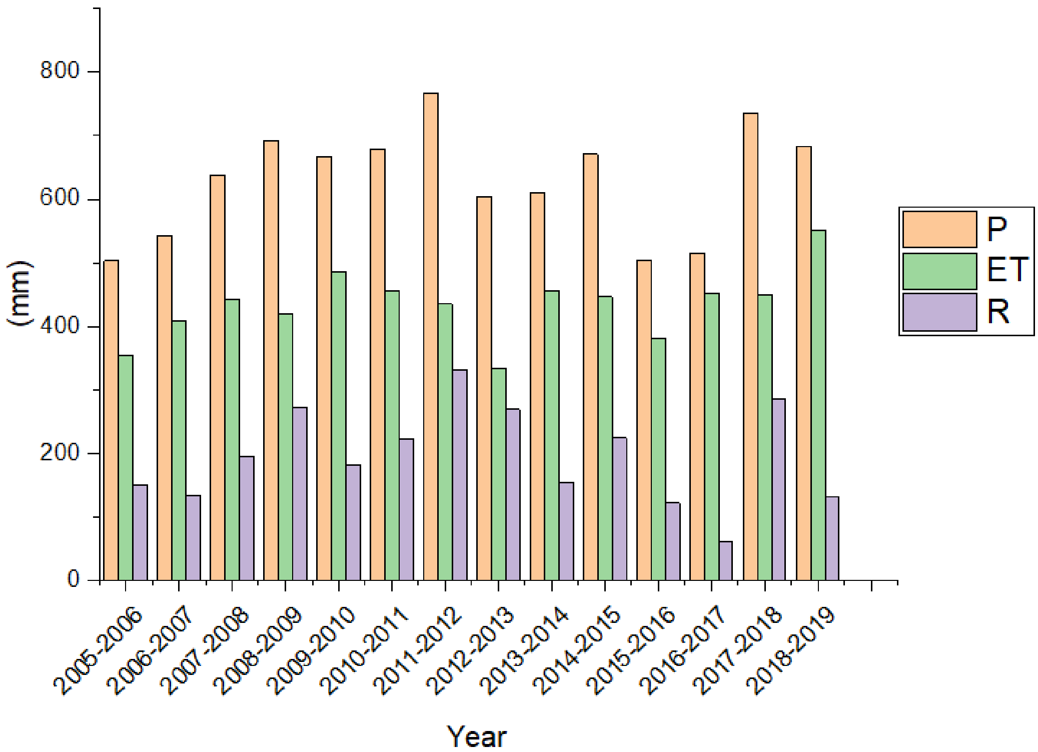

Figure 8-2. *Annual sums of R (runoff), P (precipitation; cf. Figure 8-5) and ET (actual evapotranspiration, calculated as ET = P – R) for hydrological years (October–September) during the period 2005–2019. R is represented by the average specific discharge for SKB's four discharge gauging stations (Section 2.4) and associated catchment areas; missing data are completed using multiple linear regression.*

8.5 Quantitative water flow modelling

As described in Section 7.3.2, tests and documentation of an integrated, hydrology–bedrock hydrogeology modelling methodology is an important contribution from the Baseline Forsmark modelling stage, as background for forthcoming Forsmark SDM modelling stages. This section gives an overview of the performance and examples of modelling results from the methodology tests, which have been performed using the water flow modelling tools MIKE SHE (this chapter) and DarcyTools (Chapter 7) in parallel. For further details, see the modelling methodology report (SKB R-20-14, Table 1-1) and the Baseline Forsmark report on conceptual and quantitative water flow modelling (SKB R-23-06, Table 8-1).

8.5.1 Model boundary conditions

Figure 8-3 shows the horizontal extent of the model area for the Baseline quantitative hydrological and near-surface hydrogeological modelling methodology tests of Baseline Forsmark, along with the extent of the Baseline Forsmark model area (Forsmark Catchment; Chapter 1). Moreover, the figure also shows the boundaries of a specific "water balance area" for the methodology tests. In principle, the hydrological model area boundaries follow catchment area boundaries in the terrestrial parts (based on the Baseline DEM). In the marine parts, the extent is based on previous assessments of the hydraulic influence area for the groundwater diversion from the existing SFR facility.

***Figure 8-3.** Overview map of the model area for the Baseline hydrological and near-surface hydrogeological modelling (abbreviated "HNSH model" in the figure), the Forsmark Catchment and the 2×2 km² "water balance area" for the flow modelling methodology tests of Baseline Forsmark.*

In the hydrological modelling, a no flow boundary condition is applied to the lateral boundaries in the terrestrial parts, also in the bedrock. In the marine parts, a prescribed pressure boundary condition is defined according to transient sea level data. Apart from this function as a boundary condition for the quantitative water flow modelling, sea level variations and trends are of importance for the layout of surface constructions and accesses to underground constructions in order to avoid flooding, and also in terms of the frequency of sea water intrusion into near coastal lakes and wetlands.

Figure 8-4 shows a time series plot and the corresponding linear trendline of daily average sea level (RH 2000) at the SKB sea level gauge (PFM010038) during the period May 22, 2003–December 31, 2021, used as upper and lateral model boundary condition in the marine parts of the hydrological modelling. Missing data are completed with data from SMHI's gauge id 2179 (SKB id PFM010039). As can be seen in the plot, the maximum daily average sea level at the SKB gauge is 1.18 m (January 2007), whereas the average sea level is 0.12 m during the considered period.

The interface between surface system models and those of the bedrock can generally be taken as the bottom boundary of the RDM (regolith depth and stratigraphy model; Section 3.5). However, the quantitative hydrological modelling includes bedrock down to an assumed no flow bottom boundary at -1,100 m, thereby capturing interactions between the surface and bedrock systems.

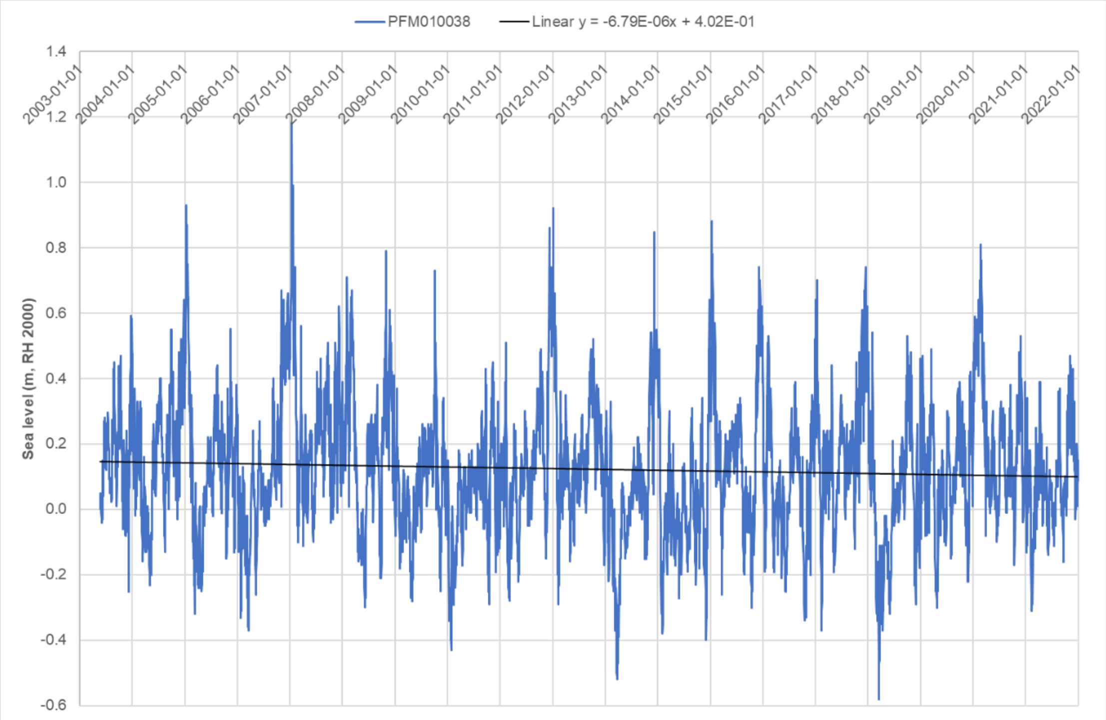

Figure 8-4. *Time series plot of daily average sea level (RH 2000) at the SKB gauge (PFM010038) during the period May 22, 2003–December 31, 2021, used as upper and lateral model boundary condition in the marine parts of the hydrological modelling (Section 9.5). Missing data are completed with data from SMHI's gauge id 2179 (SKB id PFM010039). The linear trendline (with year 1900 as time 0) gives an apparent sea level drawdown of approximately -2.5 mm/y.*

Meteorological data to represent the upper boundary condition for the hydrological modelling of the terrestrial parts comprise P (precipitation), AT (air temperature) and PET (potential evapotranspiration). The meteorological dataset of Baseline Forsmark, comprises data from the Storskäret, Högmasten and Labbomasten stations; compared to previous modelling, the Baseline dataset comprises prolonged time series from the Högmasten and Labbomasten stations. Moreover, a prolonged dataset for modelling of accumulation and release of water in the form of snow is available for three locations in Forsmark. TDR (time domain reflectometry) data, including water content data for assessment of e.g. infiltration and groundwater recharge, are also available but are not used in the Baseline modelling.

As an example of upper boundary condition data, Figure 8-5 shows annual P sums corrected for wind drift and other measurement errors, for hydrological years (October to September) during the period October 1, 2003–September 30, 2021. The dataset shown is put together using data from SKB's three meteorological stations (Storskäret, Högmasten and Labbomasten); missing data are completed with data from SMHI's station at Söderby-Karlsäng (SKB id PFM010818). As can be seen in the plot, the annual (hydrological years) P sum demonstrates large variability and is in the interval 503–821 mm during the considered period. Data from the period October 1, 2014–September 2017 (2014–2015 to 2016–2017 in Figure 8-5 are considered representative in a long term, average sense, and are used as upper boundary condition in the quantitative hydrological modelling of Baseline Forsmark.

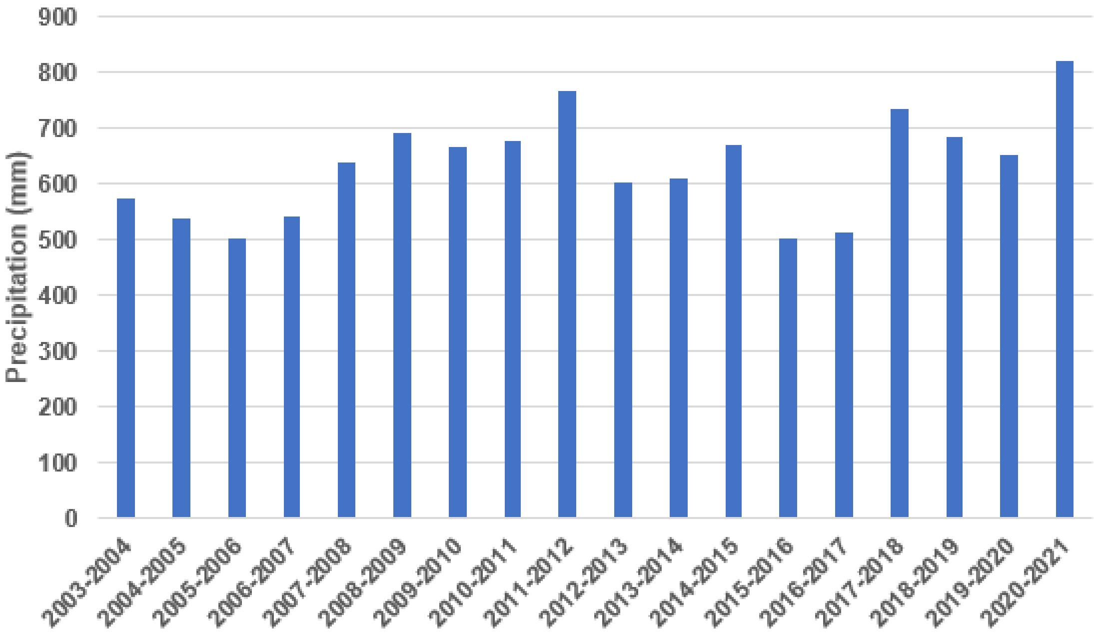

Figure 8-5. *Annual sums of corrected P (precipitation) for hydrological years (October–September) during the period 2003–2021. The dataset is put together using data from SKB's three meteorological stations; missing data are completed with data from SMHI's station at Söderby-Karlsäng.*

8.5.2 Hydraulic parameterization of regolith

The hydrogeological characterization of the regolith and the regolith/bedrock interface is based on hydraulic parameterization of a (deterministic) model for the horizontal and vertical distribution of regolith. The hydraulic parameterization of the Baseline RDM (Section 3.5) is based on the properties dataset available for Baseline Forsmark and results from previous Forsmark hydrological modelling studies (Table 8-1).

The quantitative water flow modelling methodology tests of Baseline Forsmark are based on the hydraulic parameter setup of SDM-PSU (Wermer et al. 2013), with some modifications to adapt to the regolith types incorporated in the Baseline RDM (for details, see Follin et al. 2025). Specifically, the following can be noted regarding the use of the parameterization of SDM-PSU (which used the SDM-PSU version of the Forsmark RDM) in the Baseline RDM:

- The Baseline RDM does not define a specific surface layer (Z1); such a layer is defined as part of the quantitative water flow modelling and parameterized according to the SDM-PSU modelling.
- The horizontal distribution of areas with "fine till" and coarse till" in layer Z5 follows that of the SDM-Site modelling.
- Based on results from the SDM-Site and SDM-PSU modelling, the horizontal hydraulic conductivity K_h is doubled in the layers Z1 (not defined in the RDM but as part of the quantitative water flow modelling) and Z5 specifically in the Lake Eckarfjärden catchment area.

- The Baseline RDM does not specify the thickness of layer Z6 ("uppermost" bedrock); the thickness of this layer is defined as part of the quantitative water flow modelling.
- A separate gyttja layer (Z4c) is defined in the Baseline RDM but not in previous RDM versions. This layer is in the Baseline modelling parameterized similarly as layer Z4a (gyttja/clay gyttja).

8.5.3 Summary of modelling methodology tests

In summary, the methodology tests of Baseline Forsmark comprise the following overall steps (see also Section 7.3.2 and Follin et al. 2025):

1. **Pre-study:** Investigation of the importance of the choice of methodology for upscaling of DFN (discrete fracture network) models to ECPM (equivalent continuous porous media models), and of the importance of the associated ECPM grid resolution. The pre-study is done using both MIKE SHE and DarcyTools for a simplified, cylinder shaped, model volume (bottom elevation at -500 m), and utilizes data from a hydraulic interference test in 2006 using borehole HFM14 as pumping well.
2. **Selection of DFN realizations:** Among a set of nine stochastic DFN realizations (denoted R1–R9) a subset (R4–R6) is selected to pursue for the Baseline methodology tests.
3. **Upscaling and ECPM water flow modelling:** Upscaling of the three selected DFN realizations R4–R6 to ECPM models, and parallel MIKE SHE/DarcyTools water flow modelling of the HFM14 interference test. As for the pre-study step, this step is done for a cylinder shaped (not shown here), but somewhat deeper (bottom elevation -1,100 m) model volume.
4. **Tuning of model setup:** "Global" (valid for all calculation cases considered) model setup adjustments prior to simulations of a series of calculation cases (see below). Specifically, the adjustments involve the representation of PET (potential evapotranspiration) data for calculation of upper boundary conditions, the degree day constant for snow melt calculations, and hydraulic parameterization of the "upper" bedrock layer (Z6) of the Baseline RDM. The tuning simulations were done for DFN realization denoted R5 and the HFM14 interference test, using a similar (not shown here), cylinder-shaped model volume as in the steps described above, but with lateral boundary conditions exported from the SDM-Site modelling stage.
5. **Calculation case simulations:** Simulations of a series of calculation cases (below denoted "BF", Sw. short for "beräkningsfall"), addressing a set of issues related to both the modelling methodology and some characteristics of importance for the hydrogeological site understanding (see list below). The simulations were done for the "HNSH model" area shown in Figure 8-3 (bottom elevation at -1,100 m) and for a chosen period of three consecutive hydrological years (October 1, 2014–September 30, 2017).

In the last step above, totally 11 calculation cases ("BF") were simulated using MIKE SHE (and also in DarcyTools) to address the following issues:

6. Comparison of DFN realizations produced with a DFN concept labelled "DFN-2020" (BF1–3; realizations R4–R6 described above), and comparison with DFN realizations produced with a DFN concept labelled "DFN-2008" (BF4–5); see Chapter 7. BF4–5 also investigate the importance of the representation of deterministic and stochastic deformation zones (homogeneous or heterogeneous).
7. Comparison of different hydrogeological representations of the Singö deformation zone, in terms of its hydraulic properties (BF4a–c); BF4b–c are variants of BF4a, with the Singö deformation zone parameterized as a flow barrier, with crossing conductive sheet joints above level -30 m in BF4c.

8. Investigation of the influence of "global" reductions of ECPM properties to handle potential upscaling artefacts (BF6–8), as well as the parameterization of the "upper" bedrock layer (Z6) at the regolith/bedrock interface (BF7 versus BF7b).

8.5.4 Evaluation of modelling results

For the calculation cases mentioned above, a range of MIKE SHE modelling results are available and compared to monitoring data for the simulated period (October 1, 2014–September 30, 2017), such as water balances for the "water balance area" of Figure 8-3, groundwater levels in regolith and bedrock, surface water levels in lakes and ponds, stream discharges, and inflow to the existing SFR facility (Follin et al. 2025). The figures below show some examples of modelling results, for which results are also available from the DarcyTools modelling (op. cit.).

Figure 8-6a through Figure 8-6f show depth dependent up- and downward vertical fluxes (mm/y) for the "Water balance area" shown in Figure 8-3. Figure 8-6 compares the following:

1. DFN-2020 BF1: a) MIKE SHE, b) DarcyTools.
2. DFN-2020 b) BF1, c) BF2, and d) BF3.
3. DFN-2020: b) BF1, c) BF2, d) BF3, and DFN-2008: e) BF4.
4. DFN-2008: e) BF4 (homogeneous properties) and f) BF5 (heterogeneous properties).

1) suggests that MIKE SHE and DarcyTools yield quite similar results in terms of vertical fluxes using a DFN realisation generated with DFN-2020, and 2) suggests that the variability between the three DFN realizations representing DFN-2020 is small. 3) suggests that the choice of DFN concept is noticeable, whereas 4) suggests that homogeneous hydraulic properties result in somewhat higher fluxes at depth compared to heterogenous properties.

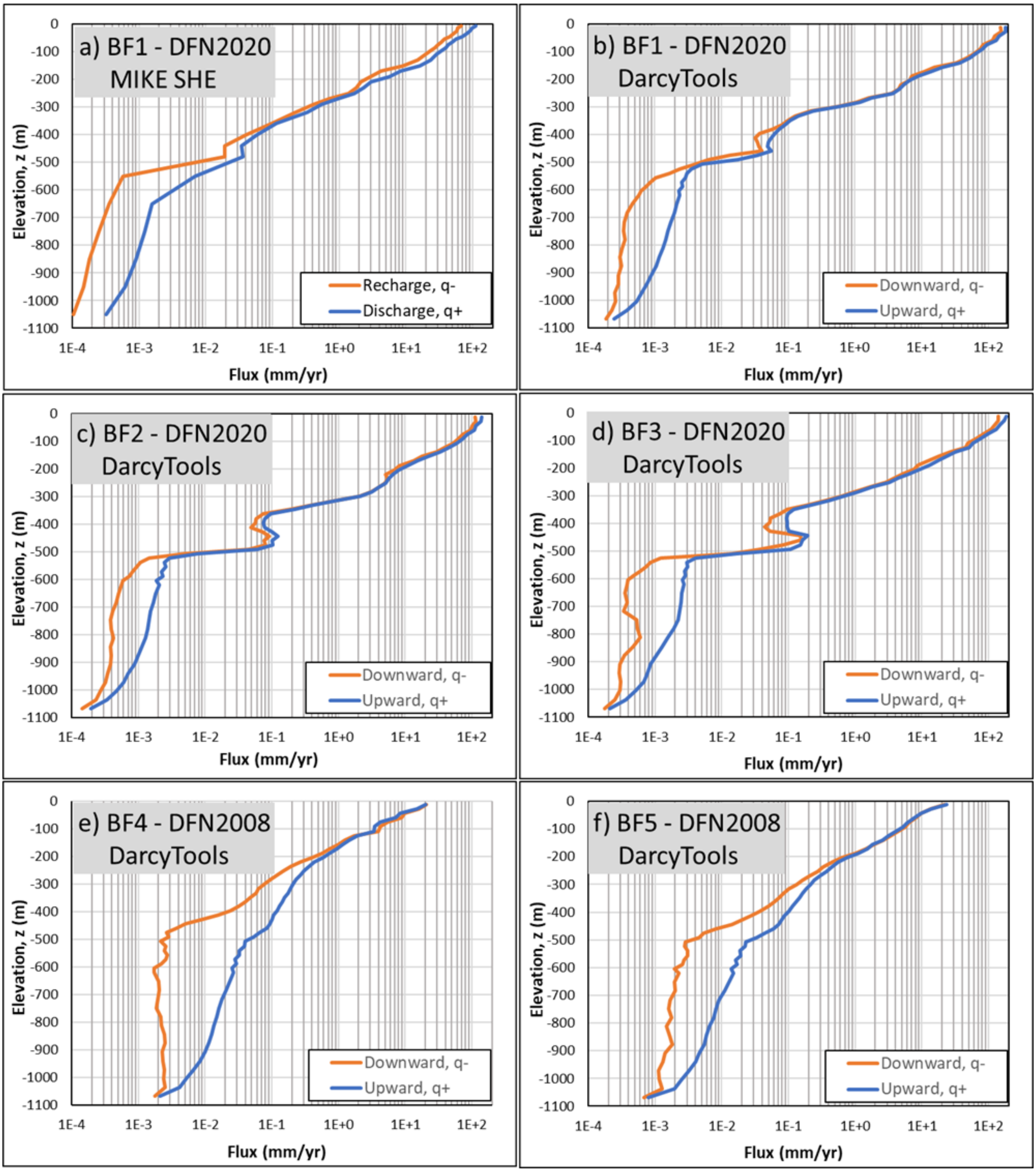

Figure 8-6. *Examples of depth dependent upward ("discharge") and downward ("recharge") vertical fluxes (mm/y) for the "water balance area" (Figure 8-3), shown for a) BF1 (MIKE SHE) and b)–f) DarcyTools).*

Figure 8-7 shows results of particle tracking in terms of densities (particles/m^2) of particle exit locations at the bedrock/regolith interface for BF4a (MIKE SHE) and for BF4a–c (DarcyTools; also showing particle trajectories), hence comparing results from the codes and addressing the influence of the hydrogeological representation of the Singö deformation zone. The particle tracking starts at repository depth. In terms of particle trajectories and their exit locations, MIKE SHE and DarcyTools yield quite similar results; trajectories are primarily concentrated to deformation zones (for clarity, not all deformation zones are shown). As shown in the bottom part of Figure 8-7 (% represents the fraction of released particles reaching the SFR factility, northeast of the Singö deformation zone), the hydrogeological properties of the Singö deformation zone have dramatic effects on particle passages across the zone. It should be noted that an underlying steady state groundwater flow field is used to produce the DarcyTools particle tracking results. The MIKE SHE particle tracking results shown in Figure 8-7 are based on a temporally averaged groundwater flow field, specifically for the period October 1, 2016–September 30, 2017.

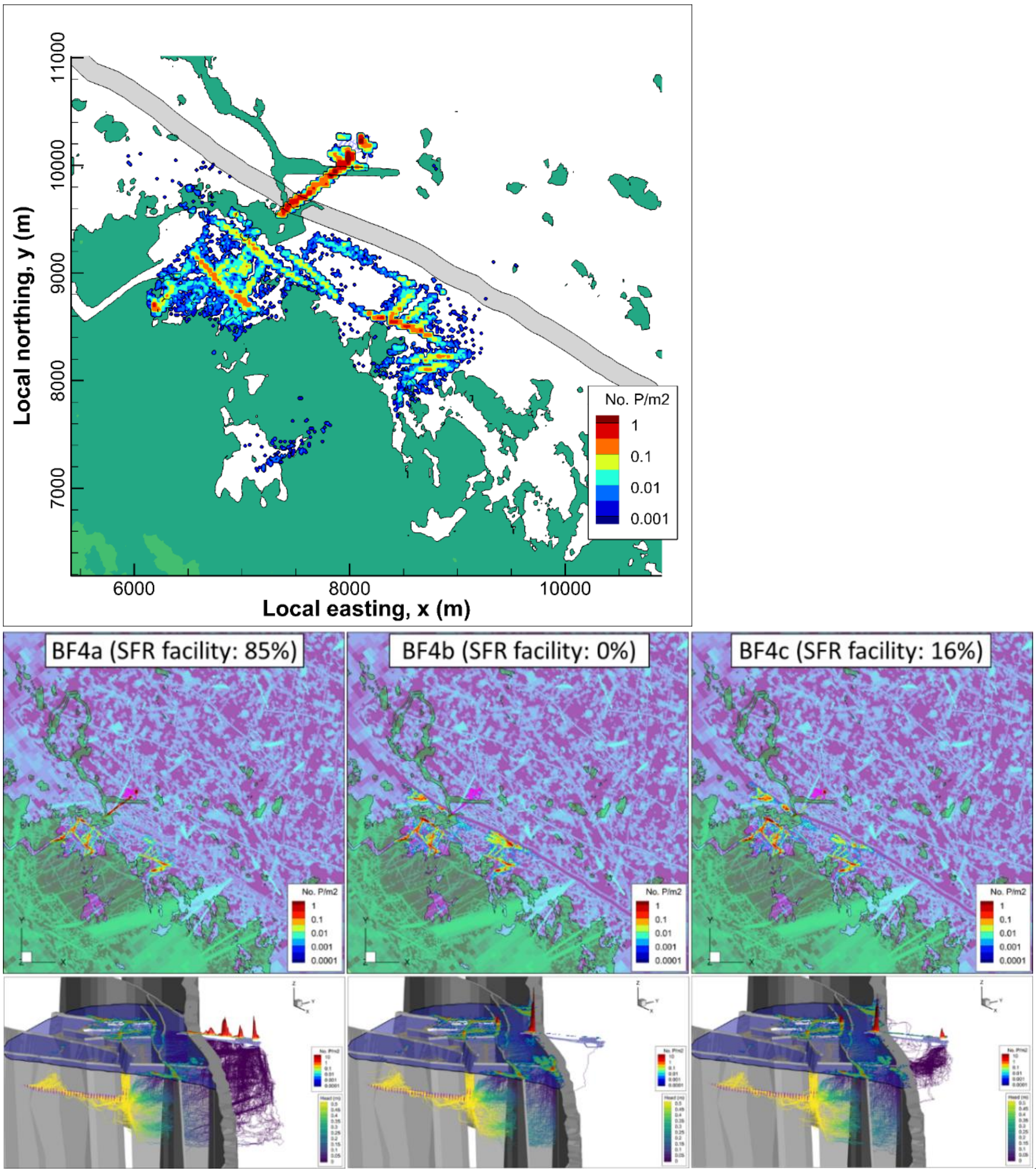

Figure 8-7. Densities (particles/m^2) of particle exit locations at the bedrock/regolith interface for BF4a (MIKE SHE; upper image), and exit locations and particle trajectories for BF4a–c (DarcyTools; lower images). The underlying groundwater flow field is steady state in DarcyTools, whereas the MIKE SHE particle tracking is based on a temporally averaged groundwater flow field for the period October 1, 2016–September 30, 2017. In the MIKE SHE image, land = green, sea = white and grey = Singö deformation zone. In the DarcyTools images, light blue = conductive fractures, dark blue = few or no fractures and grey = deterministic deformation zones; particle tracks are contoured by hydraulic head to indicate direction of flow. The area of the DarcyTools maps is 8 km by 8 km. The particle tracking starts at repository depth.

In summary, the developed and tested methodology for integrated, hydrology–bedrock hydrogeology modelling focuses on the role of the hydrologic cycle and structural-hydraulic uncertainties when assessing locations of discharge points on a regional scale. This methodology is an important contribution from the Baseline Forsmark modelling stage. Main findings from the methodology tests related to bedrock hydrogeology are summarized in Section 7.3.3.

As outlined above, the hydrological modelling of the integrated methodology incorporates handling of multiple DFN realizations and associated ECPM models. It is deemed feasible to use data from field scale interference pumping tests for choice of DFN model realizations for propagation to ECPM grid modelling of the hydrologic cycle.

However, it is noted that the calibration using cross-hole tests spans the drawdowns where they occur, i.e. within the postulated radii of influence around the modelled cross-hole pumping test borehole. Surface and subsurface flows outside the assumed radii of influence are not part of the calibration process, and could hence lead to inconsistent results on a catchment scale.

The methodology tests also indicate that in the hydrologic-cycle modelling step the RDM parameterization and other hydrological and near-surface hydrogeological features and properties may require specific adaption and/or calibration for each chosen ECPM model; it is even possible that some of the chosen model(s) cannot be realistically adapted or calibrated (cf. above).

For further details regarding findings from the modelling methodology tests of Baseline Forsmark, see Follin et al. (2025).

8.6 Recent developments and implications for SDM updates

Post SDM-Site/SDM-PSU developments and their implications for forthcoming SDM updates can be summarized as follows:

- Available updates of underlying, geometrical models of topography, regolith depth and regolith stratigraphy have been used in the Baseline modelling stage and incorporated in the quantitative hydrological modelling. Possible future updates of such physiographical models, e.g. based on additional data and/or physical alterations due to contract works, can be used as input to future SDM updates.
- Compared to SDM-Site/SDM-PSU, prolonged meteorological, hydrological and hydrogeological state variable datasets (the longest are almost 20 years) on meteorological, hydrological and hydrogeological state variables are available and used as input in the Baseline Forsmark modelling stage. As part of future SDM updates, these and further prolonged monitoring datasets enable interpretation of e.g. trends and variabilities on different time scales, and for detection and quantification of hydraulic responses to repository construction.
- An integrated, hydrology–bedrock hydrogeology modelling methodology is an important contribution from the Baseline Forsmark modelling stage. The findings from the modelling methodology tests, the methodology and the associated modelling protocol (guide) enable further development, fine-tuning and documentation for applications in future SDM updates.
- Some of the conceptual issues from SDM-Site/SDM-PSU, e.g. regarding the heterogeneity and cross-flow properties of the Singö deformation zone, are addressed as part of the Baseline Forsmark modelling stage. Further issues can be addressed in forthcoming SDM updates, also considering further prolonged state variable datasets on e.g. lake-groundwater-atmosphere interactions and cross-discipline interpretations of additional surface-system data.

- In relation to SDM-Site, SDM-PSU and the Baseline modelling stage, forthcoming SDM updates will handle large quantities of data emanating from detailed site investigations, performed as part of construction of surface and subsurface facilities. Moreover, SDM updates must also handle state variable data gathered in a dynamical hydrological and hydrogeological system, in response to the dynamics of construction works. These circumstances imply that prediction/outcome analyses, in terms of geometries, properties and state variable responses, will be important contributions to SDM updates.

9 Hydrogeochemistry

Hydrogeochemistry refers to the geochemical characteristics of groundwater, including its chemical composition and spatial distribution. It involves analysing the concentration of various elements and compounds in groundwater samples to understand their origin, transport, and in turn to understand future development of the site. Specifically, the hydrogeochemical model provides valuable information on the subsurface geology, ground water characteristics and hydraulic properties of the site.

9.1 State of knowledge

9.1.1 Summary of previous SDM

Previous site descriptive models concluded that the complex groundwater evolution and spatial pattern at the Forsmark site are a result of several different factors such as a) the present-day topography and proximity to the Baltic Sea, b) past changes in hydrogeology related to glaciation/deglaciation, land uplift and repeated marine/lake water regression/transgression, and c) alteration of the groundwater composition caused by water/rock interactions and/or microbial processes. The sampled groundwaters reflected to various degrees processes relating to modern, ongoing or ancient water/rock interactions and mixing.

Previous site descriptive models presented a conceptual hydrogeochemical model based on explorative analysis of chemical and isotopic composition of fracture and pore waters, dissolved gases, colloids and organic material and fracture filling minerals. The hydrogeochemical model presented a conceptual paleohydrochemical model, origin and residence times of different waters, rock matrix pore water information, redox conditions and water-rock interactions, pH and Eh-buffer capacities as well as ground water composition and mixing proportions.

Table 9-1 presents the main reports related to hydrogeochemistry, produced as part of the previous modelling and investigation stages (SDM-Site and SDM-PSU), and those of the current Baseline Forsmark modelling stage. It is noted that the table only shows main reports; these are based on many other reports regarding investigations and monitoring of hydrogeochemistry.

Table 9-1. Main reports related to hydrogeochemistry, produced as part of SDM-Site, SDM-PSU, and those of the current Baseline Forsmark modelling stage. SKB Reports are reference by their report number.

	SDM-Site	SDM-PSU	Baseline Forsmark
Bedrock system	R-08-47	R-11-06	R-25-06
Surface system	R-08-11	TR-14-06	R-25-06
Main report	TR-08-05	TR-11-04	Current report

9.1.2 Key remaining issues

In SKB (2008a) the overall confidence in the SDM-Site models for SFK are discussed and presented and is further detailed in the hydrochemical SDM reports (Laaksuharju et al. 2008, Section 7.2.7 and Nilsson et al. 2011, Chapter 7). The confidence assessment report details the reported uncertainties from SDM-Site (SKB 2008b, Section 3.5 and Section 6.2.5). The reported key issues are summarised below:

The depth and origin of dilute glacial meltwaters. A conceptual model for the succession of waters was presented in previous SDMs, but there was little to no evidence or discussion regarding the residence times of glacial meltwaters.

High sulphide concentrations. Sulphide concentrations reported were relatively high in SDM-site and SDM-PSU, and it was hypothesised that this might be due to disturbances during drilling.

Residence times of the deeper groundwaters. Residence times of the deeper groundwaters were reported as being a key remaining uncertainty. This was mostly attributed to a lack of analytical methods for measuring residence times.

Redox and alkalinity buffering capacity of flow paths. One key remaining issue where the uncertainties concerning the evaluation of the redox and alkalinity buffering capacity of flow paths in the rock in the target volume.

Rock matrix pore waters. The composition of rock matrix pore waters and how this relates to fracture waters were uncertain.

The sources, production rate and transport mechanisms of geogenic gases. Potential geogas of importance, such as hydrogen, were reported as a remaining uncertainty. This was mostly due to difficulties measuring gases using surface boreholes.

9.1.3 Summary of updated knowledge at Baseline stage

A revision of the paleo-hydrogeochemical model has been published with noticeable differences compared to earlier SDM:s (Gimeno et al, 2023). There are new water types that include information from the SFK (Tröjbom et al. 2008, Chapter 4) and the SFR (Nilsson et al. 2011, Section 3.3) sites into one model (Section 9.4). A new numerical method has been developed for estimating water types with incomplete data using a neural network type model .

All surface system water and groundwater samples have been revisited and statistically modelled for distribution analysis, and long-term trends have been analysed (Mercier 2026). Additionally, the mixing model has been revised with a new calculation scheme that incorporates uncertainties in the individual samples as well as in the proposed end-members (Nilsson et al, 2024). The new M3 model also uses a geochemical equilibrium with the Forsmark bedrock to estimate deep saline waters, giving a geochemical explanation for its composition.

Within Baseline new sulphide concentration data has been collected. The data has been analysed using the new Baseline modelling methodologies (SKB R-20-15), which makes it possible to further assess the observed high sulphide concentrations.

9.2 Description of Baseline data

The hydrogeochemical baseline data freeze was set at 2023. In this context, it is important to acknowledge that the SFR water chemistry data does not represent undisturbed natural conditions due to the existing repository (Section 1.4). Consequently, when interpreting the baseline hydrogeochemical conditions, it is important to keep in mind that baseline refers to conditions at the site prior to construction of SFR3 and SFK.

Since the previous SDM's (SKB 2008a, Lindborg 2008 and SKB 2013) the monitoring programme has been revised twice. Samples taken before 2010 used five section volumes for circulation with samples taken at the first, third and fifth circulation for analysis. During 2010 the same strategy was used, but a total of five samples were taken, one per section volume circulation. Post 2011 plug flow volumes were used for volumetric circulation instead of section volumes, with samples taken at 1, 3, and 5 plug flow volumes respectively. The description of plug flow volumes is detailed in Nilsson et al., 2020.

Since SDM PSU there have been 29 new boreholes drilled, see Section 2.4 and 2.5. There have also been five new complete chemical characterisations in boreholes KFM01D, KFM07A, KFM08D, KFM09A, and KFM24.

All samples collected are categorised into five different sample quality categories based on various parameters from the sampling such as number of water conduction fractures in the section, charge balance, availability of time series, and artificial disturbances. The methodology of sample quality categorisation has been updated, and the full methodology is available in Nilsson et al., 2020 as well as in Mercier et al. 2026.

Table 9-2 shows an overview of the baseline dataset from the hydrogeochemical monitoring programme. The monitoring data set is post 2010 and from fixed installations in the boreholes. The parameters analysed within the scope of Baseline Forsmark are pH, Conductivity, Na, K, Ca, Mg, HCO_3, Cl, SO_4, Br, F, DOC NH4, NO3, Fe, δ^2H, $\delta^{18}O$, Si, Mn, Sr, S^{-2}, TOC, ^3H, $\delta^{13}C_{inorg}$.

Table 9-2. Overview of monitoring data in the Baseline dataset. Q1-3 refers to sample quality 1 through 3, and 4-5 refers to sample quality 4 and 5, respectively. A higher sample quality number means lower sample quality.

	Percussion boreholes	SFK Cored boreholes	SFR Cored boreholes	Sum
Number boreholes	11	14	19	44
Number of sections	11	23	38	72
Samples	379	884	385	1648
Samples Q1-3	213	355	183	751
Samples Q4-5	166	529	202	897

Table 9-3 shows an overview for the complete chemical characterisation (CCC) data in the baseline dataset. The CCC data is generally the most reliable and representative samples and are obtained with other equipment compared to the monitoring sections (Nilsson et al., 2020).

Table 9-3. Overview of the CCC data in the Baseline dataset. Q1-3 refers to sample quality 1 through 3, and 4-5 refers to sample quality 4 and 5, respectively. A higher sample quality number means lower sample quality.

	SFK Cored boreholes	SFR Cored boreholes	Sum
Number of boreholes	12	5	17
Number of sections	30	8	38
Number of campaigns	34	8	42
Samples	212	34	246
Samples Q1-3	140	15	155
Samples Q4-5	72	19	91

Table 9-4 shows an overview of the surface system hydrochemical data baseline set. During the site investigations many locations were sampled on a monthly basis and have since been adjusted to only be sampled once per season.

Table 9-4. Surface system baseline dataset. Q1-3 refers to sample quality 1 through 3, and 4-5 refers to sample quality 4 and 5, respectively. A higher sample quality number means lower sample quality.

	Lake	Stream	Near surface GW	Precipitation	Sea
Sampling locations	30	10	93	4	19
Jan-Mar samples	341	295	240	35	136
Apr-Jun samples	371	365	230	30	312
Jul-Sep Samples	308	162	197	27	226
Oct-Dec Samples	266	260	204	32	165
Samples Q1-3	1174	1051	842	5	839
Samples Q4-5	112	31	29	119	0

9.3 Updated modelling methodology and model overview

The models provided for the hydrogeochemical site descriptive model are the paleo-hydrochemical model, mineralogical equilibrium models as well as the general description of major, minor and isotope systems in groundwater, surface water and near surface ground waters. The hydrogeochemical site descriptive model primarily contributes to the site descriptive model by setting constraints on the paleo-climatological model with analytical data and interpretation of residence times of the ground water. Another model is the description of the sulphide concentration, processes and historical evidence of changes in sulphur speciation and the reason for it.

The methodology for hydrogeochemical modelling is described in Mercier et al. 2026. The report describes the process of data management and analysis, that is, the procedure for the collection of primary data for the compilation of a quality-assured data table. The latter is based on the experience and knowledge SKB has accumulated in the subject area over time. The report further describes the methods that will be applied in the analysis of new data as it becomes available, for example data quality standards, evaluation of water types, mixing and speciation calculations, determination of redox conditions and evaluation of water residence times. The report goes through uncertainties and how they are handled.

In general, the hydrogeochemical model can be described in three major categories:

- Paleo-hydrochemical model
- Explorative analysis
- Geochemical description of major and trace elements as well as isotopic values

The paleo-hydrochemical model is a presentation of the geochemical signatures that is used to reconstruct the paleoclimatological history, for instance the penetration depth of glacial meltwaters in the geosphere. These models rely on two sub-models; the water types and the mixing model that are described in section 9.4 and 9.5, respectively.

Explorative analysis refers to investigating various correlations between processes in the system, for instance calcite equilibrium calculations in the surface system, pH verification in deep groundwater samples, or S^{2-} verification of samples with FeS equilibrium. Major element concentration in deep saline waters are also calculated, via a bedrock equilibrium model using common Forsmark granite.

Finally, the geochemical model describes major and trace elements as well as isotope measurements in terms of long-term trends and distributions.

9.4 Water types

Based on palaeo-hydrogeological considerations a subdivision into different water types is used in order to understand the groundwater system through a clear description and interpretation of their composition. The criteria used to define the water types are based on chemical and isotopic compositions (Cl, $\delta^{18}O$ and Mg), and the definitions have been set to distinguish groups of samples with similar characteristics.

9.4.1 Updated methodology

The present water type classification, shown in Table 9-5, is valid for the SFK and SFR areas and is different from the site-specific classifications used during the SDM studies (Laaksoharju et al., 2008, 2009; Nilsson et al., 2011). A detailed description of the water types and a thorough review is available in Gimeno et al., 2023.

Table 9-5. Water types that is used for the entire Forsmark area, its origin and rough estimate on residence times.

Groundwater Type	Origin	Residence time
Meteoric	Meteoric recharge	Modern water from the last 60 years
BrMet	Met. Recharge and water rock interaction	Modern water from the last 60 years
BrMarBal	Modern Baltic infiltration	Modern water from the last 60 years
BrMixed	**SFR**: Mixture of Marine (old and new) and glacial **Fors. Inland**: Mixture of Littorina, glacial and/or meteoric	Components of modern water from the last 60 years
BrMarLitt	Littorina sea infiltration, reaction with marine sediments and mixture with the previous waters	From present to 5,000-10,000 y (Holocene)
BrGlacial	Glacial meltwater from different deglaciation periods	Some of them are from the last glaciation-deglaciation (11,000 to 20,000 y), others are possibly from older glaciations
BrTrans	Mixture of marine and non-marine waters.	Somewhere between marine and non-marine waters.
BrNonMar	Old non-marine waters including components of old meteoric waters (from warm and cold climates) and even older non-marine groundwaters.	Older than the last deglaciation (>15,000 y). Residence times in the order of > 100,000 y
Saline	The oldest and more saline non-marine groundwaters.	Older than the last deglaciation (>15,000 y). Residence times in the order of > 100,000 y

The water types can be determined using concentration criteria for Mg, Cl and $\delta^{18}O$. For a number of samples $\delta^{18}O$ has, however, not been analysed, meaning that these samples cannot be determined according to these criteria. It is also possible to determine the water type on any samples using the SAMPLE model which is described in Mercier et al. 2026.

9.4.2 Resulting model

The new water type classification system merges the previous two different approaches used in SDM-Site and SDM-PSU into one unified classification for all Forsmark groundwaters. The new system has been checked and evaluated against the two older models and reproduces in most cases the older models. When the new model yielded a differing result, this was often judged to be more reasonable.

9.5 Mixing model

9.5.1 Updated methodology

The M3 mixing model has been updated with a new calculation scheme based on Bayesian inferencing as well as Markov chain Monte Carlo methods (MCMC) to generate posterior distributions.

The traditional way of calculating mixing proportions using the M3 methodology is summarised in (Laaksoharju et al., 2009). The methodology is based on transformation of the major constituents of the water samples into PCA space using standard covariance-eigenvalue decomposition transform with normalised data (z-scaling). The loadings calculated are on the complete Forsmark data set, and the variability explained on the principal components are hence the variability explained in the Forsmark data set.

The new methodology is very similar to the old but uses a new methodology for the end-member for deep saline waters. Instead of using a highly saline sample taken from the site investigation program, it is now calculated via bedrock equilibrium using a Phreeeqc model. The chemical composition of the old deep groundwater in crystalline bedrock aquifers is assumed to primarily be determined by the reactivity and mineral composition of the bedrock. This methodology was presented by Michard (1987). Similar models have previously been applied to SKB data by Grimaud et al., 1990 and Trotignon et al., 1999 and to data from other deep boreholes. The bedrock equilibrium model shows that it is the anion concentration that controls the resulting equilibrium concentration of the major constituents. The processes controlling the anion concentration is unknown for Forsmark, but there was a source of, for instance, Cl a very long time ago. To mitigate this the resulting chemical equilibrium was calculated for a range of Cl concentration. The equilibrium range was linearized and used with an uninformed uniform priori distribution as the end-member for deep saline waters. The mineralogical composition of the bedrock model was taken from SKB code 101057 (SKB 2008a) and the thermodynamic database used was WATEQ4F (Ball et al., 2001), with the modifications reported in Auque et al., 2006.

9.5.2 Resulting model

The results from the new methodology for the M3 model shows on average deeper penetration of glacial meltwaters, similar to what was reported in SKB R-17-13, with a lower amount of meteoric dilution. Table 9-6 shows some key differences in the results between the two model versions. There is on average a variance reduction even though there is a significant increase in degrees of freedom in the calculation due to the introduction of a largely unknown deep saline end-member. The reduction in variance is due to the Bayesian inferencing method.

Table 9-6. Changes in average fractions and variances when moving from the old model to the new.

	Average	Variance
Deep Saline	71%	-2%
Glacial	24%	-22%
Littorina	-12%	-50%
Meteoric	-19%	-35%

9.6 Paleo-hydrochemical model

With new data and the new water type categorisation there have been some revisions on the paleo-hydrochemical conceptual model, shown in Figure 9-1. The major factor for Forsmark waters is still explained via mixing of major paleo-hydrochemical events such as deglaciation, the salinity evolution of the Littorina and Baltic sea, and postglacial upheaval.

The presence of saline groundwaters (Cl values higher than 10,000 mg/L) in the deeper parts of the area seems to reflect the groundwater conditions before the last deglaciation. The behaviour of Cl, Mg and $\delta^{18}O$ reflects the mixing and dilution of a deeper, older and more saline groundwater, with other less saline and younger groundwaters from shallower depths. That is, prior to the last deglaciation, dilute waters must have entered the bedrock during warm and cold periods and mixed with the already present old and saline non-marine groundwaters producing a hydrochemical transition from brackish to saline groundwaters towards depth.

This general trend is, however, inhomogeneously distributed in the bedrock system supporting the compartimentalisation of the fractured bedrock and the presence of isolated pockets of older waters at shallower depths than expected. At present, the Saline water type has only been sampled at depths below 600m, but the BrNonMar waters have been found as shallow as 200 m and down to depths of 950 m.

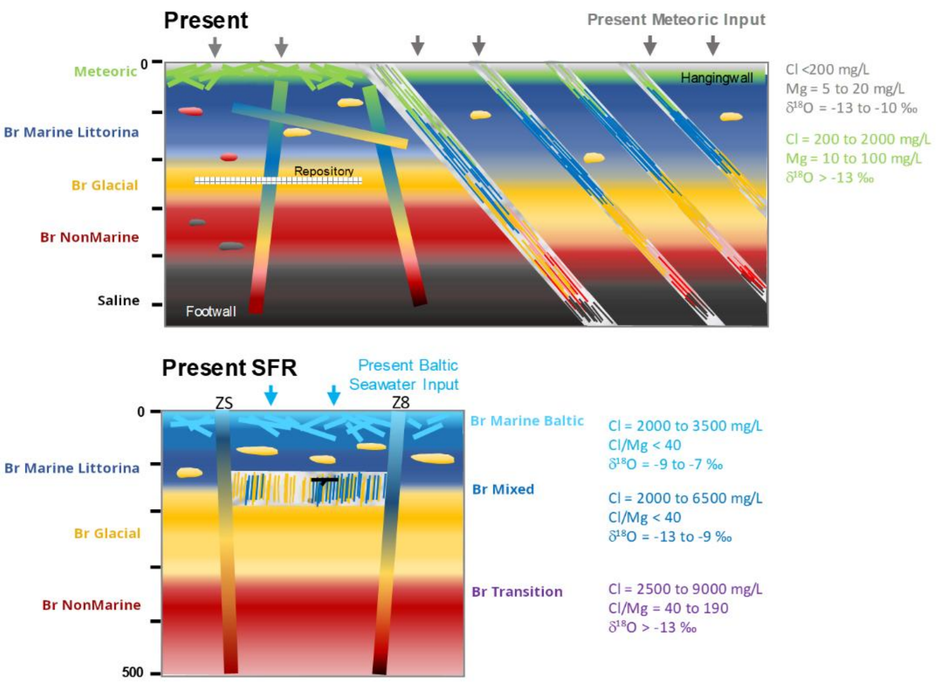

Figure 9-1. *The current paleohydrochemical conceptual model for the SFK area and SFR.*

9.7 Statistical modelling of primary data

The models used for analysing baseline conditions are mostly based on statistical modelling. There are a number of different models and data are treated substantially differently compared to previous site descriptive models due to the large amount of data available compared to previous site descriptions. During the development of SDM-Site and SDM-PSU a few samples were chosen as representative for each sampling location based on expert evaluation and was further used for modelling, with the total number of samples amounting to less than a hundred. The baseline models evaluate all available data, several thousands of samples.

In general, the baseline models attempt to establish distribution analysis based on general hierarchical structures, such as average concentration distributions for lakes in Forsmark which should be similar between samples, or samples taken in series in the groundwater which could be different from each other. Below follows a list of common types of results from the baseline models:

- Distribution analysis per sampling location
    - Most credible distribution
    - Long term trends with credible distribution for the trend
- Correlation between sampled parameters within each sampling point
- Visualisation of the different distributions compared between different sampling locations
- Anomaly identification such as outlier identification

9.7.1 Bedrock groundwater

There are new methodologies for evaluating borehole section data, time series and sampling strategy which have been used on all monitoring data for Forsmark. The new statistical models for borehole section data and surface system data quantifies;

- Effect on purge pumping before samples are taken
- Variance introduced in between sampling campaigns
- Long-term trends and deviations from trends for all major constituents and isotope systems
- Correlation between major constituents calculated per borehole section
- Stable or unstable baseline distributions for all major elements and isotope systems for every borehole section

Generally, the effects of the new sampling strategy in the monitoring borehole sections shows more stable concentrations over time with less variance between sampling campaigns. The concentration of some water constituents is also significantly different with the new sampling strategy.

There are some observable long-term trends in the monitoring data. Figure 9-2 shows a principal component analysis (PCA) on all major constituents as well as $\delta^{18}O$ and $\delta^{2}H$ on all monitoring sections. The calculated baseline distributions are visualized with the black ovals. All distributions are calculated per element basis and projected onto the PCA plot. The arrows show a 10-year trend, indicating which direction in the PCA figure the borehole section are moving on average. For instance, HFM27:2 is classified as brackish marine Baltic water, but shows trends on moving more towards a meteoric classification. All non-marine signatures are moving towards more deep-saline waters.

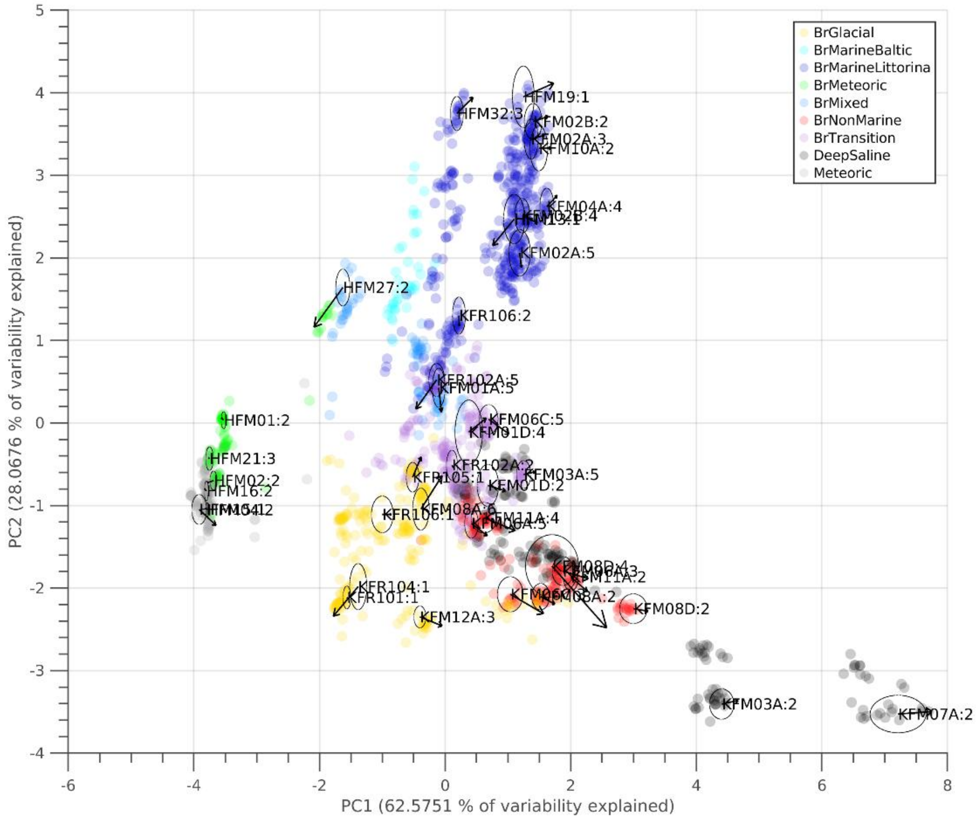

Figure 9-2. PCA figure for all borehole data based on Na, K, Ca, Mg, HCO3, Cl, SO4, Br, δ2H, δ18O. The scatter points are all individual sample occasion colour coded based on the water types. The circles are calculated based on the baseline distributions for the concentrations and the arrows shows a 10-year significant trend.

9.7.2 Surface and near surface waters

New methodologies have been developed for the evaluation of surface system data, time series and time distributed data (SKB R-20-15) and has been used on the entire monitoring data set (Mercier 2026). The new models for the surface sampling points quantify:

- Time distributed hydrochemical data for the surface system
- Long term trends and deviations from trend in time distributed hydrochemical surface system data
- Stable or unstable baseline concentration distributions for all major elements and isotope system for every surface monitoring point.

Since the site investigations the monitoring programme has undergone a few revisions, most notable the frequency of samples taken from the surface system is now once per season instead of monthly. The baseline models are still able to model monthly concentration distributions due to the large amount of previous data from the surface system (Mercier 2026).

9.8 Discussion

9.8.1 Baseline status

Baseline status before start of construction has been established for the majority of the sampling locations and elements and isotopes. The baseline data set have significant long-term trends in the monitoring sampling, and as such the baseline conditions are described as most credible distributions as well as their respective long-term trend. The baseline dataset also identified statistical anomalies in primary data such as systematic deviations in $\delta^{18}O$ during 2014 compared to data from other years.

9.8.2 Uncertainties

When determining the hydrogeochemical baseline dataset a number of uncertainties in the primary data was identified, such as obvious outliers indicating analytical errors or more systematic anomalies such as elevated pH concentrations during certain years or slightly heavier $\delta^{18}O$. More statistically anomalous data will most likely be discovered through further data analysis and will be handled systematically.

In the baseline dataset mostly major components were analysed and modelled as well as a few isotope systems. Erroneous data potentially encountered during further analyses will be recorded.

There are also limitations in the spatial availability of hydrogeochemical data. Currently SKB have detailed information from a few sections in the bedrock which is the underlying data for the conceptual model for the site. There are observations of older water above younger marine waters, such as glacial waters relatively near the surface at SFR. This is explained with isolated fracture networks that were closed during glaciations. Currently there is no information or model assessing how common this is.

The current model for mixing contains large uncertainties. By using the current end-member approach there is quite a small difference between meteoric waters and glacial waters, both are indicated in the model by a dilution factor in comparison to the relatively saline end-members Littorina and Deep Saline. The big difference between the two are the lower $\delta^{18}O$ in glacial waters. This leads to high uncertainty in the mixing fractions, especially between glacial and meteoric waters. A new methodology could focus on combining these two end-members and use a separate model in a second step to differentiate between glacial and meteoric dilution. Another update to the mixing methodology could be to introduce more marine indicators for older waters, such as REEs. There are also uncertainties in the deep saline end-member, although with the new methodology for estimating the concentrations, the model was validated with highly saline samples from Laxemar.

There are still uncertainties in the residence times, especially for the older non-marine waters. Currently, only ^{36}Cl dating method has been used to determine the residence times of deeper and older groundwaters, which contains inherent uncertainties. The glacial meltwaters also appear to originate from different deglaciations based on the few He data available.

9.8.3 Implications for future SDM updates

Future measurements in the monitoring programme can be compared to the values in the Baseline dataset. Differences are expected due to the drawdown when constructing SFK which will likely be marine infiltration in the tunnel with subsequent recharge of meteoric and modern Baltic sea waters in the upper parts of the geosphere.

Many new investigations are planned during the construction phase. Emerging data is expected to yield a spatially larger dataset for the hydrochemical status in the bedrock.

SKB plans to describe historic reconstruction of sulphide concentrations and sulphur processes in glacial cycles.

Residence times are generally estimates in the model currently, especially in the waters older than Littorina, with planned updates using actual measurements on residence times, using for instance ^{81}Kr as a residence times tracer.

10 Bedrock transport properties

The site-descriptive modelling of bedrock transport properties is focused on the parameters that characterise the retardation (or retention) properties of geologic materials. Specifically, this part of the site description consists of parameters that quantify the diffusion and sorption properties of intact (fresh) and altered rock, fracture coatings and fracture-filling materials. In the SDM these parameters are described within the framework of the 3D geometric models that are devised primarily by Geology and the associated materials (e.g. rock types) and structures (fractures and deformation zones).

Based on data from site investigations, the Transport SDM presents the site-specific information in terms of a retardation model (e.g. Byegård et al. 2008), which contains identified site-typical materials (including rock types) and structures with estimated parameters. The main parameters are the matrix porosity, diffusivity (D_e) and sorption distribution coefficients (K_d). In the safety assessment, the site-specific information is analysed and complemented by other data to cover all input data needs of the scenarios to be considered in the radionuclide transport modelling (e.g. Crawford 2010, 2013). For the development of the retardation model, Transport is dependent on inputs from other disciplines, primarily regarding the geological characterisation of rock mass and fractures, including fracture mineralogy, properties of flowing fractures and hydrochemical conditions (water types).

10.1 State of knowledge

10.1.1 Summary of previous SDM for SFK

Extensive bedrock and surface system investigations were performed at the Forsmark site in support of the analyses of the planned spent fuel repository (SFK). These investigations included borehole investigations in connection with and after drilling, execution of laboratory programmes, such as the long-running programmes for measurements of sorption and diffusion parameters, and long-term monitoring (still on-going, e.g. groundwater flow measurements).

Data sources for site-descriptive modelling of bedrock transport properties in SDM-Site can be summarised as follows:

- Laboratory porosity, diffusion and sorption measurements, including different types of diffusion measurement and measurements of BET (specific surface area) and CEC (cation exchange capacity) data supporting the analysis of sorption.
- *In-situ* data on diffusion properties obtained from interpretation of electrical resistivity logging of boreholes.
- Groundwater flow measurements by tracer dilution methods in permanent borehole installations (part of the monitoring programme).
- Single-well injection-withdrawal tests (SWIW) and multi-well tracer tests with sorbing and non-sorbing tracers.
- Supporting geological, hydrogeological and hydrogeochemical data, including fracture mineralogy and porewater characterisation.

Most of the laboratory measurements and the resulting data on transport properties are reported in Selnert et al. (2008). A complete list of data sources is provided in the SDM-Site main report (SKB 2008a, Table 6 in Appendix 3). Input data to the site-descriptive modelling are described in Byegård et al. (2008, Chapter 2) and summarised in Crawford (2008, Chapter 4).

Focusing on the laboratory and *in-situ* investigations providing the main retardation/retention parameters, i.e. those quantifying diffusion and sorption, some additional information on measurements and data handling is given below.

- The porosity of the rock matrix, in this context often referred to as diffusion available porosity, is primarily measured by a water saturation method within the laboratory programme. In addition, the spatial distribution of pores in the matrix has been studied using the PMMA impregnation method.
- Diffusion in the rock matrix has been measured both in the laboratory and by interpretation of borehole measurements. In the laboratory, the *effective diffusivity* D_e was measured in through-diffusion experiments on rock samples with HTO (uncharged) as tracer and by interpretation of "formation factors" from electrical resistivity measurements. Diffusivity data were also obtained from interpretation of *in-situ* formation factors from borehole resistivity logs. Qualitative confirmation of the existence of matrix diffusion and/or quantitative information has been obtained from *in-situ* tracer tests, primarily single-hole tests (SWIW).
- Sorption in the rock matrix has been measured in laboratory batch experiments using different fractions of crushed rock and fracture-filling materials, and in connection with diffusion experiments on a few larger pieces of rock (referred to as "monoliths"), and quantified/interpreted in terms of the *distribution coefficient* K_d. The sorption data interpretation is supported by site data on two standard parameters: BET surface area and cation exchange capacity (CEC). Similar to matrix diffusion, sorption has also been confirmed and/or quantified in *in-situ* tracer experiments, primarily the SWIW tracer tests.

The understanding of the site-specific retardation properties of the bedrock at Forsmark that resulted from the joint analysis of transport data and inputs from other disciplines was formulated in terms of a bedrock retardation model (Byegård et al. 2008). This model presented retardation parameter values in the context of qualitative and quantitative descriptions of a set of geological materials and structures identified as typical for the site or otherwise important for site understanding and transport modelling.

Specifically, the site descriptive modelling of transport properties was focused upon the rock domains RFM029 and RFM045, and the resulting retardation model contained data and descriptions of three types of geological materials and structural units: (1) the main rock types within these rock domains, (2) eight basic fracture types, and (3) four structural elements identified as characteristic of deformation zones. The eight fracture types are defined and illustrated in Figure 10-1. As indicated in the figure, the definition of the fracture types is based on fracture mineralogy and rock alteration.

In the retardation model, representative, "best estimate" transport parameters were presented for rock types where statistically significant data sets existed, i.e. for rock types with SKB codes 101051, 101057, 101058, 101061 and 102017. The sorption parameters (K_d values) for the main rock types in the retardation model represented rock types 101051 and 101057 (non-DZ only); the dataset included K_d for three (101051) or seven (101057) elements, and for four different groundwater types (see summary in SKB 2008, Table 10-4 through Table 10-7).

A potentially important consideration for the transport modelling is whether retardation parameters show differences between different rock types that would motivate the use of different parameter values in radionuclide transport models. In the SDM-Site work (Crawford 2008, SKB 2008), it was found that there were generally no significant differences in the retardation properties between the main rock types present in the rock domains RFM029 and RFM045. However, it was also emphasised that this observation was based on limited data.

Another factor of potential significance is that rock samples used in laboratory investigations are subject to stress release, which introduces uncertainties in parameter values due to differences between laboratory data and the *in-situ* conditions they are intended to represent. Based on the analyses in SDM-Site, where diffusion parameters were obtained from both laboratory and *in-situ* measurements, it was found that the rock matrix porosity and effective diffusivity parameters recommended for use in the SR-Site radionuclide transport modelling were well constrained.

The uncertainty in sorption parameters was considered only semi-quantitatively established in SDM-Site and was large for many species and water compositions. (It was further analysed in detail in SR-Site, see Crawford 2010.) Regarding sorption and K_d values, it should be noted that the measured site data presented in the retardation model covered only a few of the elements for which the safety assessment needed input data. This was in line with the strategy established before the site investigations (Widestrand et al. 2003), which stated that the laboratory programme should be focused on a limited set of elements representing different groups in terms of dominant sorption processes and other relevant characteristics.

Figure 10-1. *Typical fracture surfaces of Forsmark drill core samples illustrating identified fracture types. Mineral abbreviations: chlorite (Chl), calcite (Ca), epidote (Ep), hematite (Hm), laumontite (Lau), prehnite (Pr), pyrite (Py), quartz (Qz). Figure taken from Crawford and Löfgren (2019).*

10.1.2 Key remaining issues

Internal assessments and formal external reviews of SR-Site, SR-PSU and associated reporting of data and models have resulted in questions, comments and requests for complementary information regarding the different types of parameters handled by the Transport programme (see Section 10.1.1). Whereas most issues related to diffusion parameters have been resolved during the SFK/SR-Site review process, there are some remaining issues concerning sorption parameters that need to be dealt with in forthcoming investigations and modelling activities.

These sorption-related issues concern the use of analogues to represent elements for which there are no site data, needs for additional sorption data on specific elements, and the methodology employed to interpret and extrapolate site data to application conditions. The remaining issues have been addressed in the development of the programme for complementary laboratory and in-situ investigations, and in the updated modelling methodology outlined in Section 10.3. Furthermore, heterogeneity in bedrock transport properties and its simplified representation in the radionuclide transport modelling have been discussed by reviewers. These issues have been addressed through complementary modelling (Section 10.4) and in the modelling methodology development.

10.2 Description of complementary data

Almost all currently available site data on transport properties originate from the site investigations for SFK that were performed during the period 2002–2008 and reported in the SDM-Site main report (SKB 2008), where Chapter 10 summarises the modelling of transport properties based on the underlying discipline-specific reports by Byegård et al. (2008) and Crawford (2008). Thereafter, few new data on transport properties have been collected at the Forsmark site (see Section 10.5). Bedrock transport properties were not included in the site investigations and site-descriptive modelling for the SFR extension (SDM-PSU), although some site data were acquired in the following safety assessment stage (Löfgren 2014).

10.3 Updated methodology and model overview

The transport modelling methodology is presented in Berglund et al. (2025). This methodology report covers transport modelling performed during both site investigations, resulting in a site-descriptive model for transport properties, and safety assessments, where simulations of radionuclide transport and associated doses is the central component. An important part of the methodology is the description of how the site-specific parameters measured within the bedrock transport properties investigation programme are interpreted, evaluated and further developed into recommended input parameters for the radionuclide transport modelling in the safety assessment. The site-specific understanding of geologic materials and flow-bearing structures in the transport context is presented in the retardation model, which is a basic component of the transport SDM. The parameterisation of bedrock/geosphere models for safety assessment transport calculations is another important part of the methodology presented in the report.

The main task of the Transport (or Bedrock transport properties) discipline in the site-descriptive modelling is to provide the site-specific input to the development of retardation parameters for radionuclide transport simulations in the analysis of post-closure safety. This includes presentation and delivery of interpreted parameter values, as well as site information that could serve to support further analysis of parameters and representation of processes in radionuclide transport models. In addition, Transport should provide parameters and supporting information for modelling of transport processes within other disciplines, primarily Hydrogeology and Hydrogeochemistry.

Concerning transport parameters, it should be noted that the site-specific information is not the only input utilised when producing parameters for radionuclide transport simulations. As part of the safety assessment, the site-specific database is extended in various ways to obtain data also representing radionuclides, materials and conditions not included in the site investigations. There is no clear demarcation between site-descriptive modelling and safety assessment when it comes to the processing of site data. The retardation model (cf. below) is a central delivery from the site-descriptive modelling. This model summarises the site understanding and is intended to serve as a starting point for further analyses in the safety assessment.

In addition to the retardation parameters, flow-related transport parameters are used in the parameterisation of radionuclide transport models. These parameters are obtained from groundwater flow simulations performed by Hydrogeology. However, supporting analysis of advective transport and flow-related parameters may need to be carried out by or in cooperation with Transport to address issues related to, for instance, heterogeneity and upscaling. Depending on needs and who is performing the analyses, studies of this kind may or may not be reported in future Transport SDMs. The remainder of this chapter is focused on the retardation parameters.

10.4 Complementary analysis and updated retardation model

The multilayer fracture types in the SDM-Site retardation model were not used in the SR-Site radionuclide transport modelling. In SR-Site, the rock surrounding all flowpaths was assumed to be homogeneous, and the assigned transport parameter values were mainly based on the site-specific data for undisturbed rock matrix that were studied extensively in SDM-Site (e.g. Crawford 2008).

This simplified representation of the bedrock in the radionuclide transport calculations was one of the topics considered in the requests for complementary information that SSM submitted to SKB during the SR-Site review process. SKB responded to these comments and later organised a more extensive modelling effort reported in Crawford and Löfgren (2019). That study, from which the contents of the present section are taken, involves several important aspects of the site-descriptive modelling of transport properties, including what could be viewed as an update of the Forsmark retardation model. This update makes use of quantitative data on fracture mineralogy that were not available in the SDM-Site modelling (Eklund and Mattsson 2009, Löfgren and Sidborn 2010).

While partly a continuation of the earlier work associated with responses to SSM, the Crawford and Löfgren (2019) report describes calculations that were made in support of PSAR SFK, investigating the impact of more complex representations of the rock matrix and their consequences for far-field radiotoxicity flux. The impact of material property heterogeneity was studied by considering a multilayer rock matrix conceptualisation and several "fracture classes" (corresponding to the fracture types in the SDM-Site model) representing different rock matrix microstructural properties distributed in a realistic fashion along migration flow-paths from the repository to the surface.

Crawford and Löfgren (2019) aimed to investigate the radiological consequences of the presumption that the surrounding rock is not homogeneous but layered. Similar to the SDM-Site model, the layers considered are 1) fracture coatings, 2) an alteration rim of limited depth in the rock matrix, and 3) undisturbed (i.e. unaltered/fresh) rock. This is achieved by using a layered rock matrix model where all layers have individualised, although uniform, retardation properties. It is also assumed that the same layered structure does not persist along the entire flow-path, but that the flow-path encounters rock volumes featuring differing retardation properties.

In setting up the retardation model, a few important observations and criteria related to site understanding were honoured as described in the following.

- The host rock has been divided into two principal rock volumes. The first corresponds to the rock immediately surrounding the canister deposition holes and tunnels and was labelled the immediate far-field in Crawford (2008). In this rock volume, the flow-paths are assumed to be predominately hosted in discrete stochastic fractures. As the flow-paths leave the immediate far-field, they enter what was called the distant far-field. In this rock volume, flow-paths may be hosted in larger deformation zones.
- There is good evidence from the site investigations and supporting research that some percentages of the open fractures (or fracture planes) are covered by fracture minerals that are relatively porous. Therefore, the fracture classes should include at least one class with a relatively porous fracture coating.
- There are good indications from the site investigations at Forsmark that a percentage of the sampled fractures are characterised by fresh wall rock that is not coated by any fracture minerals. Accordingly, at least one class should feature uncoated wall rock.
- For the Forsmark site, there are no dedicated observations that either support or reject the possibility of a coating or layer of reduced pore connectivity. However, there are general observations of both fracture minerals and, for example, mylonitised rock at fracture surfaces having low or poorly connected porosity. Even though such fracture coatings are not likely to be widely distributed, they are conceptually important for safety assessment considerations, as they may hinder radionuclide retention in part of the underlying rock matrix.

In recognition of the above observations and heuristic assumptions, four different fracture classes are used in the layered rock model. These fracture classes are mostly defined based on the nature of the fracture coating, or absence of it. Fracture classes F1:1, F1:2 and F1:3 are assigned to the immediate far-field, whereas the fourth class (fracture class F2:1) is assigned to the distant far-field. Their main characteristics are described as follows:

Fracture class F1:1 features a fracture coating of relatively high porosity and effective diffusivity. It is assumed that the coating consists of a mixture of the commonly occurring fracture minerals chlorite and clay minerals, based on Byegård et al. (2008 Section 2.2.1) and Löfgren and Sidborn (2010).

Fracture class F1:2 features no fracture coating, which is consistent with observations of fresh fracture surfaces found when mapping the drill cores in the site investigations. A weak alteration rim is assumed to overlay the undisturbed rock.

Fracture class F1:3 features a fracture coating, or a polished fault surface, of low or poorly connected porosity. Evaluating the consequences of such a layer is in line with the request for complementary information by SSM.

Fracture class F2:1 is assigned to represent flow-paths in water conducting zones in the distant far-field, often coinciding with deterministically identified deformation zones. Such zones may provide fast routes for advective radionuclide transport through the geosphere. The fracture surface is coated by a relatively thick and porous layer of fracture coatings and there exists a strong alteration rim of significant thickness. Underneath the alteration rim, the rock matrix may have been subjected to large-scale ductile or brittle deformation.

Figure 10-2 shows the retardation model and the central calculation case parameterisation for fracture classes. The chosen parameter values, including the surface coverage fraction of each fracture class, are discussed in Crawford and Löfgren (2019).

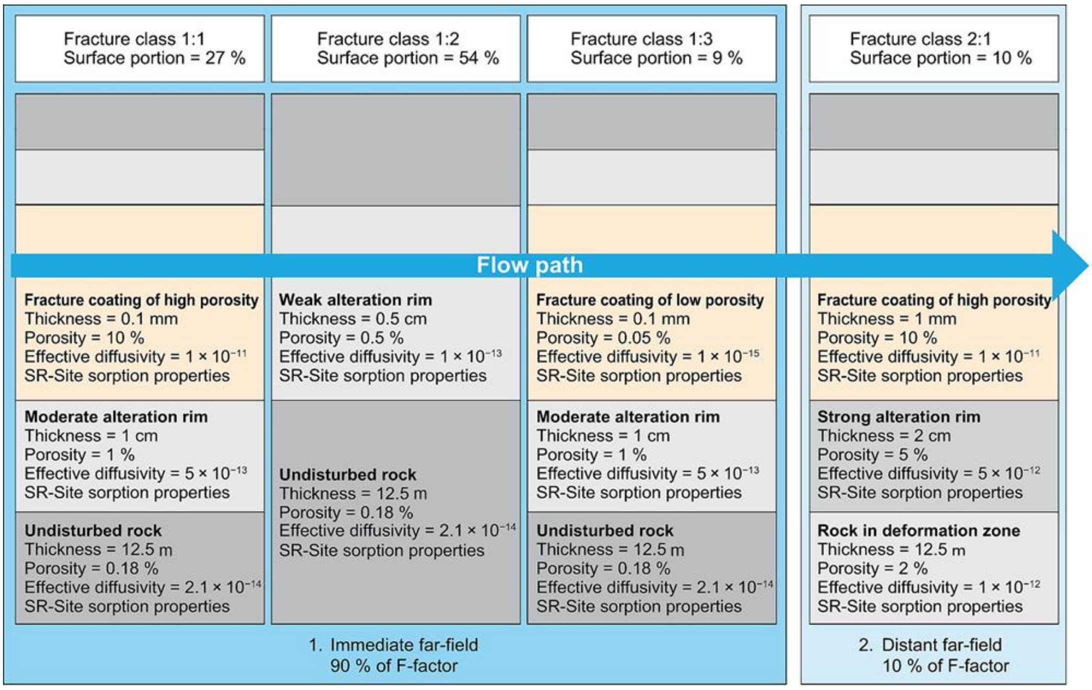

***Figure 10-2.** Parameterisation of fracture classes and layers in the updated retardation model. The upper fracture surface is assumed to be a mirror image of the lower surface. Figure from Crawford and Löfgren (2019).*

The numerical modelling results obtained using the multilayer model developed in Crawford and Löfgren (2019) suggest that the simplified, homogeneous rock matrix representation based on material properties of unaltered rock used in SR-Site is cautious and mostly results in overestimation of radiological risks. The results indicated that fracture coatings have limited effects on diffusive exchange and retardation, whereas the properties of the altered rock could be of importance for the retardation effect. This motivates an increased focus on the alteration rim in forthcoming complementary site investigations.

10.5 Recent developments and implications for SDM updates

As noted above, few site data on bedrock transport properties have become available after the conclusion of the site investigations that provided the basis for SDM-Site. Consequently, no data evaluation or descriptive modelling activities have been carried out by Transport in the present baseline stage. However, some investigations producing site data on transport properties have been performed; these data sources are summarised as follows:

- Diffusion and sorption data from measurements on “monolithic” Forsmark samples that were evaluated and reported in connection with the LTDE-SD experiments (Widestrand et al. 2010).
- Radium sorption measurements on Forsmark samples and associated modelling performed within research study reported in Fabritius et al. (2024).
- Porosity and diffusion data measured in connection with complementary porewater characterisation studies in the access area (Waber and Smellie 2012) and at SFR (Eichinger and Iannotta, 2024).
- Resistivity data from new boreholes, as reported in borehole geophysics data presentations, that can be interpreted in terms of matrix diffusion parameters (*in-situ* formation factor).

In addition, there are on-going (December 2025) measurements of porosity, pore size distribution, diffusivity and sorption of Mo. The various datasets listed above have not been evaluated and incorporated into the present baseline description. A detailed evaluation and presentation of these data will be made in the forthcoming SDM work. It may be noted that the usefulness of the new resistivity logs for estimating formation factors depends on the specific method and frequency used and whether supporting hydrochemical data are available.

In a broader perspective, progress has been made in several areas of importance for site understanding and preconditions for the modelling to be performed in forthcoming SDMs. These developments are summarised in the following paragraphs.

Complementary modelling and other activities have been carried out to support the on-going licensing processes for SFK and the SFR extension, i.e. in response to comments, questions and requirements from authorities and other reviewers on submitted applications and associated documents (SSM 2018, 2019). The main contribution from activities initiated by review comments is probably the modelling described in Section 10.4. The fracture types/classes presented in SDM-Site and by Crawford and Löfgren (2019) constitute important inputs to the continued development of retardation models in forthcoming SDM work. This work will involve a statistical analysis initiated to further support and develop earlier retardation models, possibly resulting in new and/or modified fracture types.

Significant advances have been made in the field of modelling tools during the last 10–15 years, especially tools for coupled modelling of groundwater flow and reactive transport (i.e. transport combined with hydrogeochemical reactions) in fractured rock. Although probably not used in the site-descriptive transport modelling, they could be used to support future analyses of sorption parameters. Furthermore, it may be noted that also the tools used in the modelling of radionuclide transport have been further developed. This concerns both codes used in the geosphere transport modelling (MARFA, FARFCOMP) and the overall organisation of the model chain used in the safety assessment modelling. These developments could have implications for future data deliveries, since they may allow additional processes and conditions to be represented in the transport simulations.

Development of methodology for interpretation of site investigation data and further “extrapolation” of data to fulfil all data needs for safety assessment modelling has been going on for much of the last 5–10 years. This work is reported in the transport modelling methodology report (Berglund et al. 2025). Whereas the methodology as such is not of major interest here, some of the knowledge gathered in the process fits well in the baseline context. Concerning modelling methodology, it should also be noted that the general role and methodology of the DFN modelling have been further developed with the aim that the DFN models to larger extent should serve as a basis for the modelling within other disciplines. For Transport, one such common basis could be that fracture types to larger extent are developed in cooperation with other modelling disciplines.

After the conclusion of the SFK and SFR/PSU site investigations, site data for other disciplines have been produced in a series of projects motivated by the data needs for inputs to repository design (especially the location and design of accesses to the SFK repository) and for complementary information on specific issues or geological objects. Results from these investigations and the continuous data collection within the monitoring programme are presented in the baseline reporting and will be available for further analyses in forthcoming Transport SDMs.

Advances within scientific research in solute/radionuclide transport and related fields have been made through research activities performed/financed by SKB and others. Of particular significance for Transport has been the research carried out at or related to the Äspö Hard Rock Laboratory and associated activities within the framework of the international SKB Task Force on Modelling of Groundwater Flow and Transport of Solutes, especially the recently completed Task 9. In Task 9, data from in-situ diffusion and sorption experiments within the LTDE-SD (at Äspö) and REPRO (at Olkiluoto, Finland) programmes were evaluated (Soler et al. 2019, Soler et al. 2021). The results provide important inputs to the development of forthcoming in-situ transport experiments at Forsmark.

Data from the groundwater flow measurements can be used in both transport and hydrogeological modelling. These data are produced continuously within the framework of the Forsmark site monitoring programme. The groundwater flow measurements were evaluated in 2018–19 (Andersson et al. 2019) and the programme was updated based on this evaluation.

11 Ecology and land use

Within Baseline Forsmark Ecology and land use comprise detailed investigations and descriptions of flora and fauna in the terrestrial, limnic and marine ecosystems. This information, in combination with the regolith models (Section 3.5), is the basis for the vegetation and land use map. Ecological data are also the basis for the quantification of important pools/fluxes in the radionuclide dose models within the safety assessments, and as baseline for identification of disturbances due to the construction works and natural long-term changes.

11.1 State of knowledge

Three previous publications describe the marine (Aquilonius 2010), limnic (Andersson 2010) and terrestrial (Löfgren 2010) ecosystems in Forsmark and further description can be found in sections 3.7 to 3.10 in Lindborg (2008). A comprehensive overview of the ecological monitoring within Forsmark can be found in Berglund (2017) section 7, including details on e.g. chlorophyll measurements in ponds, streams, lakes, and the sea, as well as finished investigations regarding stream fish migration, sea plant/fish/invertebrate communities, and vegetation within forests, wetlands and lakes.

11.1.1 Summary of knowledge from previous SDM

The vegetation map shown in Figure 11-1 shows a high-resolution picture of land use and terrestrial vegetation types in the Forsmark area.

Wetlands occur frequently in the Forsmark, cover 10–20% of the area, and are mainly coniferous forest swamps and fens. Most fens show indications of terrestrialization, which is partly driven by the dominance of dense stands of common reed (Phragmites australis). Other important wetland types are the freshwater shores (wet meadows or marshes) and riparian deciduous forest swamps along streams that are inundated at least once a year by the stream.

The large amount of calcareous material in the till in the Forsmark area favours calciphilous plants, such as brown mosses (e.g. Scorpidium scorpioides) in addition to the typical Sphagnum species. Also, a number of orchids regularly occur in mires and coniferous forest swamps and a number of red-listed species have been found in the fens (e.g. Carex pulicaris, Phragmites australis, Liparis loeslii (Hamrén & Collinder 2010; Löfgren 2010).

Around 73% (~500 hectares) of the Forsmark land area is covered by forests dominated by Scots pine (Pinus sylvestris, sv: Tall) and Norway spruce (Picea abies, sv: Gran). The area has a long history of forestry, as seen by a fairly high frequency of younger and older clear-cuts in different successional stages. The largest arable land unit in Forsmark is found on clayey till and is located in the south eastern part (Storskäret).

A large part of the Forsmark marine area is open sea which is surrounded by the steeply sloping island of Gräsö and the gently sloping mainland to the south-west. The coastal area has many different habitats, including shallow and narrow bays with slow water turnover and deeper basins with faster water turnover. The vegetation in the photic zone is dominated by brown filamentous algae (e.g. Spacelaria arctica) and red algae (e.g. Polysiphonia nigrescens) and the macro algae Fucus vesiculosus. The first investigations were performed 1998, a survey of the phytobenthic plants and macrofauna, and continued with e.g. several transect, a video camera sea bottom survey, and randomly selected sites in previously unvisited marine areas. A full overview can be found in (Berglund 2017).

The lake biomass in Forsmark is concentrated to the benthic habitat dominated by macroalgae Chara sp. and thick microbial mat consisting of heterotrophic bacteria and microphytobenthos. The biomass of pelagic microbiota (phytoplankton, bacterioplankton) and zooplankton is low and the fish biomass varies between close to and half of the regional average.

The streams in Forsmark cannot sustain a stationary fish population but function as feeding areas and/or migration paths. In 2004 a survey, covering around seven kilometres of total stream length in the Forsmark area, revealed that streams in Forsmark are small, that about 30 % of the surveyed stream length is periodically dry, and that around 80 % of the stream length has been excavated. The survey noted 56 species of macrophytes. A further study in 2008 measured Chlorophyll a, a measure of phytoplankton biomass, in eight streams. No further biological studies covering the bottom substrate and vegetation have been covered since. Further descriptions, including the original investigations, can be found in Berglund (2017) and Andersson (2010).

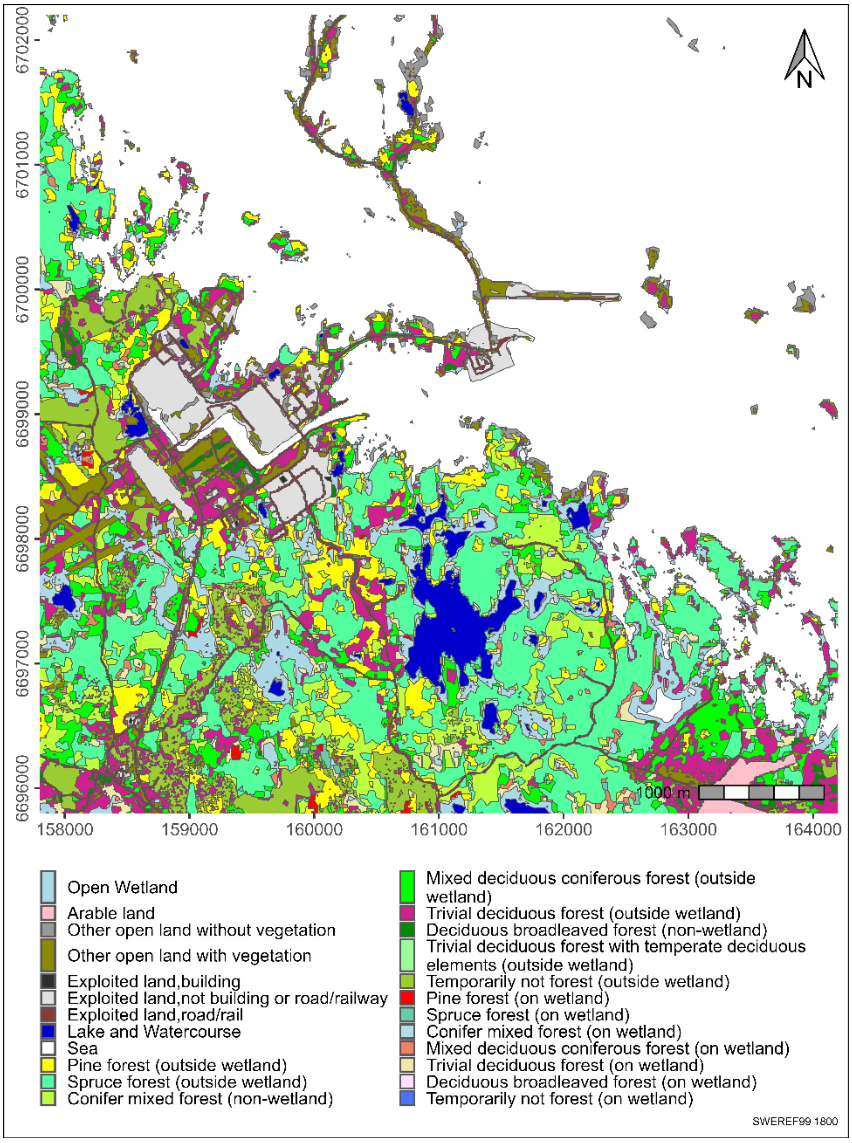

Figure 11-1. *High-resolution map of land use and terrestrial vegetation types in the Forsmark area. (Naturvårdsverket; Nationella marktäckedata 2018 basskikt: Produktbeskrivning (Utgåva 2.3, 2023-05-10).*

11.2 Description of complementary Baseline data

While extensive descriptions can be found within Aquilonius (2010), Andersson (2010) and Löfgren (2010) the focus in Baseline is on the new data that has been collected since the site investigations. Hence in the following sections focus on the ongoing monitoring programs within the ecosystems and targeted monitoring prior to the construction start in Forsmark. Monitoring data has been collected for wetlands, forest and agricultural land, marine and limnic ecosystems. The largest spatial scale addressed in this report is the regional scale, however, some data collection extending this scale is used for reference purposes.

During the last decade biological monitoring mainly has aimed to establish a baseline for wild life population changes. The data from the monitoring programme can be used to disentangle future natural biological variation from effects caused by the construction of the deep geological repository. Hence, before-after control-impact (BACI) designs using data collected before and after construction can be performed.

Furthermore, as the planned construction begin, environmental impact assessments that are needed before certain activities in the area can start will provide further data on the distribution of species and ecological structures. Such standardized investigations, following the Swedish standard (SIS 2023), regarding natural values have been performed in delimited areas at the location of a landfill that will be used for piling of unwashed rock masses from the repository excavation (Ekologigruppen AB 2024d, 2024a, 2024b). Investigations have also been carried out for a temporal road and a pressurized water line (Ekologigruppen AB 2024c).

11.2.1 New data and recent investigations in wetlands

Within wetlands three red-listed species are monitored yearly: the fen orchid (Liparis loeslii, sv: Gulyxne), the pool frog (Pelophylax lessonae, sv: Gölgroda), and the Northern crested newt (Triturus cristatus, sv: Större vattensalamander).

The fen orchid has been inventoried since 2012 and yearly reports show the population development over time, e.g. Holmgren and Lundkvist (2023). The population size shows large temporal and spatial variation. The environmental variables that affect the population sizes may vary on a regional (e.g. potential evapotranspiration in June) or local (e.g. low coverage of reed and shrubs) scale. Many variables are linked to the hydrological conditions that affect the population development (Jacobson 2022). In addition to the inventoring in the Forsmark area, SKB has started to monitor populations outside Forsmark to be used as referencesand inventoried other wetlands like Bruksdammen. Analysing the results it shows that populations within and outside Forsmark are rather stable and that the population within Forsmark area shows a more positive development over time than the population outside the area (Stephan 2024).

How different types of marshland management affect the plant communities is investigated in an experiment in wetland 48 (located in the south eastern part of the area shown Figure 11-2) that started 2015 (Eriksson and Collinder 2023). Besides fen orchid the species marsh lousewort (Pedicularis palustris, sv: Kärrspira), grass-of-Parnassus (Parnassia palustris, sv: Slåtterblomma), marsh helleborine (Epipactis palustris, sv: Kärrknipprot), flea sedge (Carex pulicaris, sv: Loppstarr), and early marsh-orchid (Dactylorhiza incarnata, sv: Ängsnycklar) are monitored. Yearly reports and several analyses indicate that the fen orchid population size increase over time and haying benefits this development (Eriksson et al. 2018; Jacobson 2022).

The pool frog has been inventoried since 2011and the northern crested newt and the smooth newt (Lissotriton vulgaris, sv: Mindre Vattensalamander) since 2012. While the populations of the pool frog have increased in size since 2011, the crested newt show no major changes (Holmberg andWzdulski 2023). To benefit amphibian populations one frog hotel (a gravel pile), and six ponds have been created. In 2023 and 2024 a number of species were translocated from wetland 12 (in the northern part of the area shown in Figure 11-2) to other wetlands in Forsmark as wetland 12 will be filled (Johansson 2023). The translocated species include the pool frog, northern crested newt, the smooth newt, the moor frog (Rana arvalis, sv: Åkergroda), the common toad (Bufo bufo, sv: Vanlig Padda), and the common frog (Rana temporaria, sv: Vanlig groda).

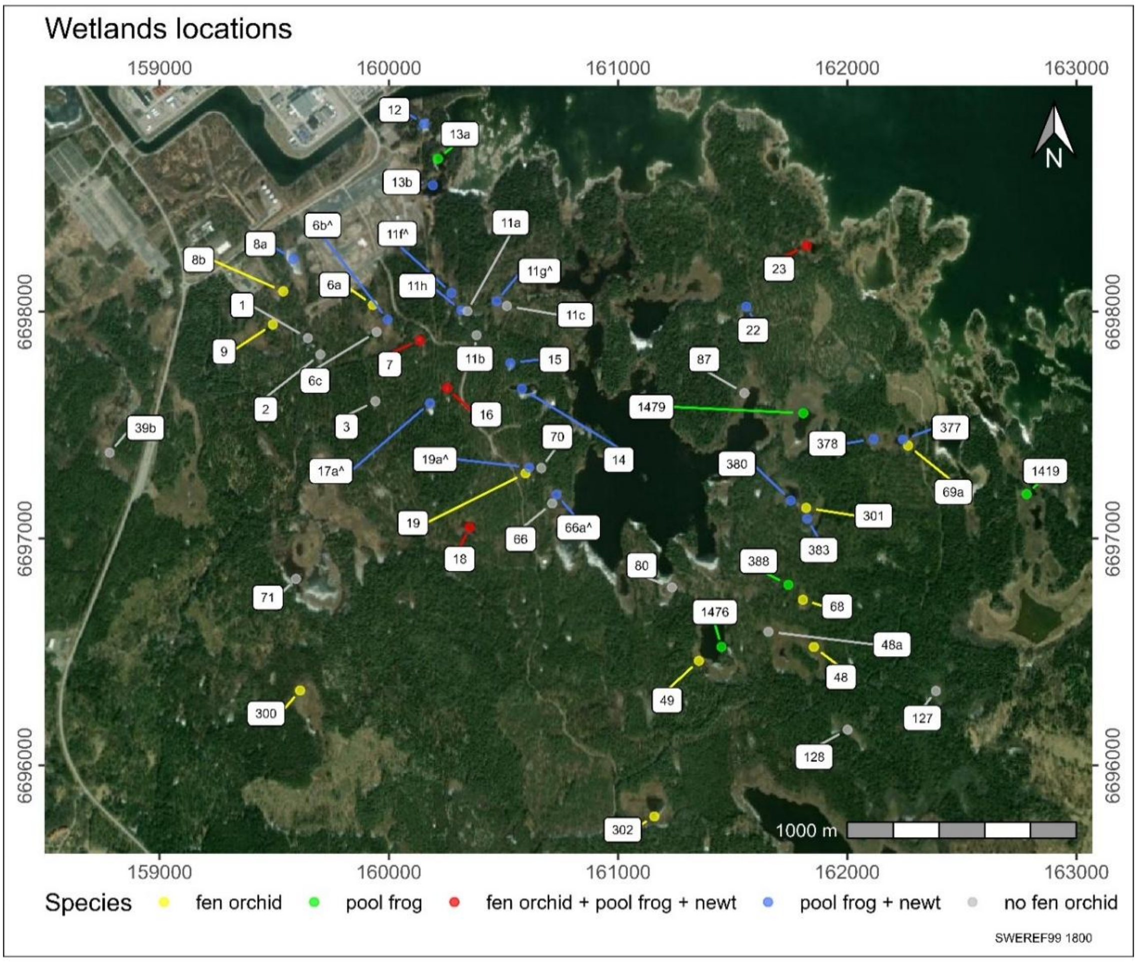

Figure 11-2. Wetlands within the Forsmark area that have been inventoried for fen orchids, pool frog and northern crested newt. The colours indicate if the respective species has been found at least once in any year since 2011/2012 within the wetland. "no fen orchid" indicates that SKB has surveyed but not found the fen orchid.

11.2.2 New data and recent investigations in forest and agricultural land

Monitoring of species in forests and agricultural land include birds and large mammals on a yearly basis and bats every five years. In 2024 a biotope-mapping (sv: Biotopkarteringen) was performed in connection to the formulation of a new forest plan (Ekologigruppen AB and Silva Strategi AB 2024).

Since 2002 SKB monitors bird species using different methods such as line transects and point counts (Green 2024). The same methodology is used by the Swedish Bird Survey. SKB performed these complete bird fauna surveys in 2002-2003, 2007, 2013, 2018, and 2023., Comparisons of the bird fauna in Forsmark to east Svealand and the whole of Sweden are presented in the reports for 2018 and 2023.

Since 2004 SKB monitors 13 selected red listed bird species that are breeding in Forsmark and their reproductive success is analysed. Birds in Forsmark are throughout reported to do well on a general level, e.g. shown by the stable or increasing abundance of 79 species between 2002 and 2023 (Figure 11-3).

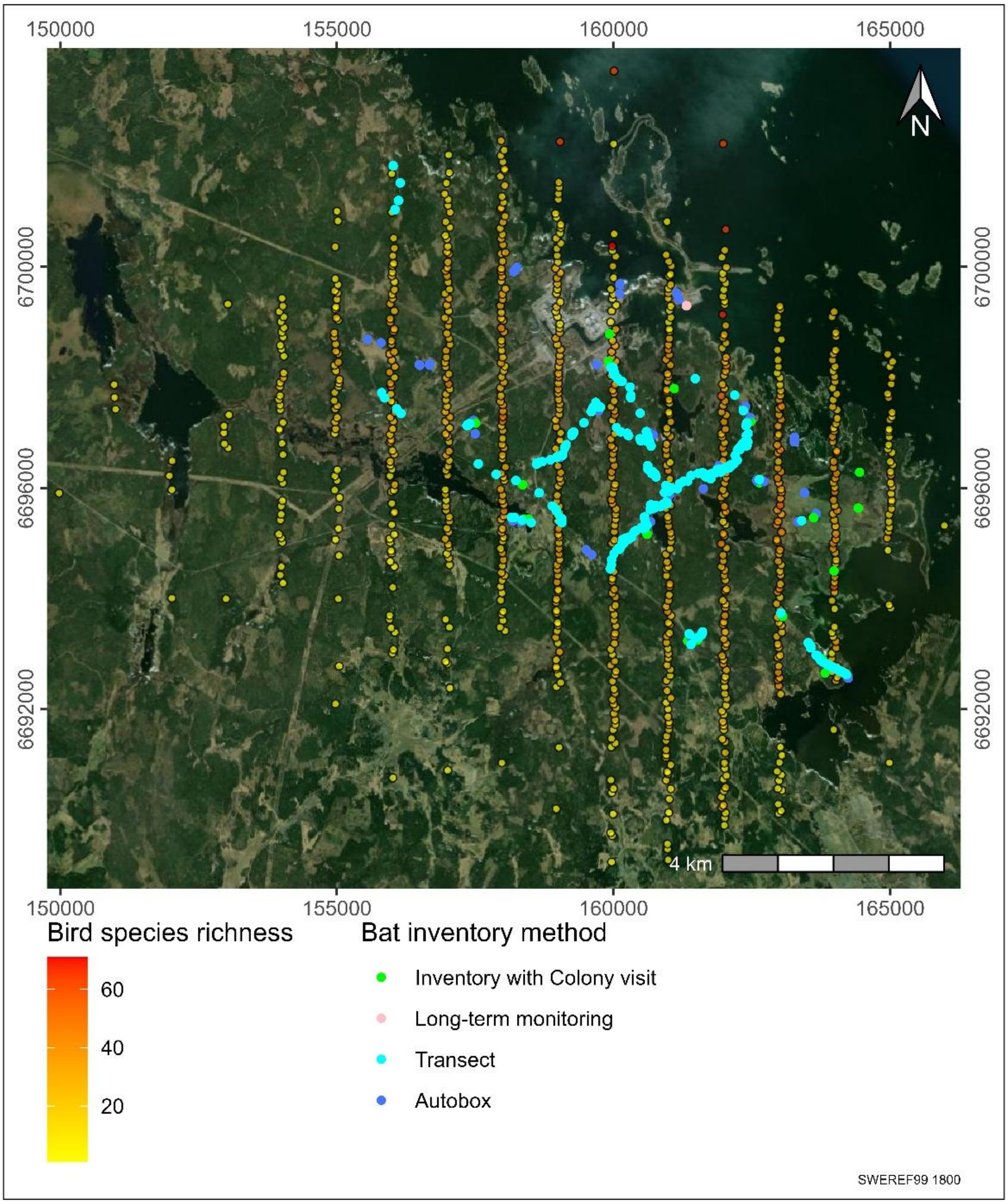

Figure 11-3. Bird species richness and inventory locations of bats in Forsmark. Spatial extend of the bird survey is illustrated by bird species richness, calculated on a 0.1 km² scale using all bird species from the complete bird fauna, the selected listed species, and the surveys of archipelago birds between 2018 and 2023. Locations of the bat inventory with respective method is shown using the locations of the recordings from all three surveys.

Bat surveys were first performed in 2004 and then in 2016 and 2021 more extensive surveys were performed using ultrasound detectors, trapping, and transects (Brüsin 2021) and Figure 11-3). The last survey found eight species and there are no indications that the populations have changed over time.

The red-listed Northern bat (Eptesicus nilssonii, sv: Nnordfladdermus, Near Threatened (NT)), the Common pipistrelle (Pipistrellus pygmaeus, sv: Dvärgpipistrell), the Daubenton's bat (Myotis daubentoniid, sv: Vattenfladdermus), as well as the Brandt's bat (Myotis brandtii, Tajgafladdermus) probably have established populations in the Forsmark area, but none of them are in the vicinity of SFR or Söderviken.

Terrestrial mammal monitoring in the Forsmark area started in 2001 (Broman and Truvé 2023). In the monitoring in 2001, 2003, 2007, and 2012 different techniques were tried. This included hunting statistics, aerial surveys, small mammal trapping, as well as different layouts of the searched area. Since 2016 a consistent monitoring is performed using snow tracking along water, snow tracking along transects, and faecal pellet counts.

Wild boar population in 2023 was estimated to be five times as large as in 2016. Otters are fairly widespread, and beavers were detected the first time in 2023. Special attention is payed to the red listed species common otter (Lutra lutra, sv: utter) and lynx (Lynx lynx, sv: lo) listed as NT and vulnerable (VU), respectively.

Additionally, a population of Lady's slipper orchid (Cypripedium calceolus, sv: Guckusko) is monitored yearly. In 2020 it was red listed (NT) in 2020, but now it is listed as least concern (LC).

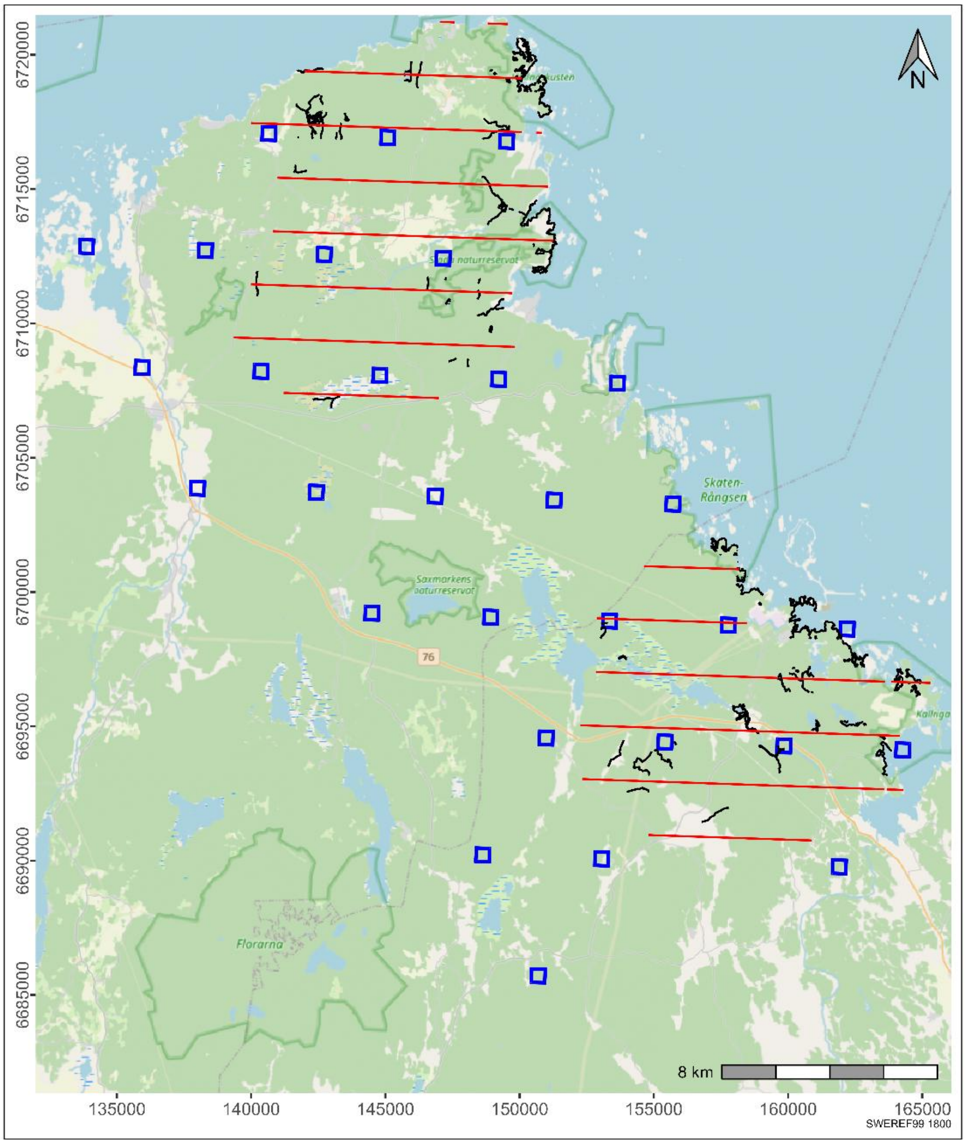

***Figure 11-4.** Terrestrial mammal monitoring showing snow tracking along water (black), snow tracking along transects between 2002 and 2012 (red), and faecal pellet counts as well as snow tracking since 2013 (blue).*

11.2.3 New data and recent investigations in the marine and limnic ecosystems

Within recent years the shallow marine areas around the SFR and Söderviken areas have been inventoried again with the aim to register valuable habitats and/or protected species (Qvarfordt and Borgiel 2022, Qvarfordt et al. 2020). In parts of the areas, large species such as seaweed and vascular plants occur in high densities, which implies high natural values as they create important habitats for animal life in the sea. No red-listed or particularly protection-worthy species were observed.

In addition to the bird survey on the terrestrial area special surveys of archipelago birds in the Forsmark area were performed in 2001, 2011, and 2016. Since 2019 this coastal survey is done yearly and the total number of recorded birds of selected species in the archipelago in 2023 was 9 014 individuals, with the bird numbers continued to be high over the years (Green 2024). Additionally, the coastal birds are also inventoried regularly by the Swedish University of Agricultural Sciences on assignment of the Forsmark Nuclear Power Plant (Adill et al. 2024). These data are also made available for SKB annually.

Studies within the lakes in Forsmark have focused on the biomass of primary producers and consumers and up to eight fish species have been found (Andersson 2010). In recent years no new ecological investigations have been performed in the lakes in Forsmark.

11.3 Discussion

Besides the evaluation of ecological structures in the nature value inventories, the recent biological observations consist of species observations. As any sampling the described estimations of species abundances are affected by many factors, like the observation errors arising from sampling limitations, the conditions, skills of the observer, or the specific whether conditions that day.

The published reports until now mostly describe the original data and the challenge in the future will be to separate natural population fluctuation from possible effects caused by SKB's constructions. This can be performed using appropriate statistical models. The ability to understand and characterize how abiotic conditions and biotic interactions influence species population dynamics has brought many different statistical approaches to life that differently deal with uncertainties in predicting the true population sizes. All these approaches have two sources of uncertainty: parameter uncertainty (statistical uncertainty in the relationships between population parameters and abiotic variables) and process variance (unexplained temporal variation in population parameters beyond that explained by variables in the model).

12 Summary of model updates

Baseline Forsmark is a multidisciplinary description of prevailing geological, geomechanical, hydrogeological, hydrogeochemical, hydrological, and ecological conditions prior to the start of constructions and hence represents a standard (reference or baseline) against which future geoscientific and ecological conditions can be compared. This gives a basis for assessing if future changes are due to natural causes, the repository construction or other anthropogenic causes. Most of the prevailing conditions in Forsmark are previously described in the site-descriptive models SDM-Site and SDM-PSU, which were established at the completion of the surface-based site investigations conducted between 200 and 2008 and between 2009 and 2010, respectively. Besides revisiting SDM-Site and SDM-PSU, Baseline Forsmark also describes complementary data and interpretations acquired from surface-based investigations performed up to 2022-10-31. The complementary investigations prolong the time series of monitored state variables and can be used to improve the analysis in comparison to SDM-Site and SDM-PSU.

Baseline data can be divided into two overarching categories based on the requirements for the data gathering, properties and state variables. Properties data relate to static characteristics which may be described using models that compile the information available for the system before start of construction. It can result in a best estimate from the information available. The state variables are used to describe the current state of a transient system.

An example of data in the properties category is the digital elevation model, a static description of elevation and bathymetry of the Forsmark area. Another example of data classified in the properties category are the deterministically modelled deformation zones (DMS). There are a number of deformation zones characterised by their location, orientation and size which are modelled based on borehole, surface, and SFR tunnel investigations. The DMS can be viewed as the present interpretation of the deformations zones in Forsmark, that will be updated or confirmed when new underground data is collected during the construction of SFK and the SFR extension.

An example of a state variable is the chemical composition of the groundwater. The Baseline models represent values for all major elements and isotopes in the monitoring sections by statistical distributions. In some cases, significant trends in water composition during the last 10 years reveal the transient character of the system. The state is as such both the current significant distribution of measured values as well as the direction of long-term trends. Future data collection will therefore show values differing from the baseline distributions, and future evaluations must take the transient state of the system into account.

Within Baseline Forsmark a new series of methodology reports have been developed between 2020 and 2024 to support the continuing development of qualified discipline-specific models. Some of the new modelling methodologies, or parts of them, have been tested in Baseline Forsmark to gain experience and provide feedback for improvements.

12.1 Summary of updated data and knowledge

Within Baseline Forsmark new data has been gathered and within some disciplines the acquisition methods have been updated. Given the new methods and longer monitoring time series, old data acquired prior to the completion of SDM-Site and SDM-PSU have been revisited in some disciplines. Thereby the quality of old data has been assessed, and quality issues and limitations have been addressed. Below, the improved knowledge compared to the state after the release of the original site descriptive models is summarised for each discipline.

12.1.1 Topography and regolith geology

New high-resolution data have been collected and have subsequently been used to update the DEM to a higher resolution than the previous SDM.

The new DEM and updated modelling methodologies have resulted in a more detailed RDM with additional regolith types. A few new areas in connection to construction work around the Söderviken area were mapped in detail. These results are included in the baseline models.

12.1.2 Bedrock geology

The established structural concepts, refined geometries, and geological characterisation of previously modelled deformation zones have been verified in two areas. The first is near the planned accesses for SFK, and the second is in connection to the planned extension of the SFR facility.

The spatial understanding of sheet joints has improved, based on a marked contrast in the occurrence of sheet joints with observable apertures. This enables very localised deterministic modelling of individual sheet joints and further subdivision of the shallow fracture domain model of SDM-Site.

The previous lineament interpretation at the sea floor northeast of the SFR facility has been reassessed, enabling revision of previously modelled zones of SDM-PSU and elimination of artificial blind ends.

The understanding of the deformational conditions has increased, based on a complementary interpretation of lineaments and geological field studies to examine the geological significance of inferred lineaments. This relates to the parts of the future sub-catchment area at the Forsmark site that lie beyond the SDM-Site regional volume.

12.1.3 Bedrock thermal properties

Since SDM-Site a new thermal modelling methodology has been presented and published (Back and Sundberg 2022). The main objective for Baseline has been to analyse the available new laboratory data on thermal properties regarding certain rock types, and to compare these results with the thermal parameters reported in previous SDM-Site models (Appendix 1).

The Baseline thermal model is focused only on the single rock *type* level. On a larger scale, the rock mass in the rock domains consists of a certain mixture of rock type bodies of different sizes and shapes; however, no updated thermal modelling at the rock mass scale has been conducted at this stage and the previous SDM-site thermal properties of rock domains have been adopted here for the Baseline thermal model.

12.1.4 Rock mechanics

A reliability ranking has been conducted on all the available overcoring stress measurements at Forsmark, where two different types of data sets in the overcoring data were successfully ranked. Result from the new ranking and additional analysis of indirect stress indicators have resulted in a new stress model in Baseline (see further Section 6.4).

On drill core samples in the various rock types occurring at SFK and SFR, a limited number of new laboratory tests using both conventional and newer test methods for intact rock has been compiled and analysed together with previous data (see Section 6.5).

For single fracture properties, sealed and open, several different research efforts have been performed in the period after SDM-Site. The results are summarized and references given in Section 6.6.

12.1.5 Bedrock hydrogeology

The new hydraulic data acquired in Baseline compared to SDM Site include fifteen cored boreholes drilled in the SFK area (KFM13-27), five in the SFR area (KFR117-121), and five percussion boreholes drilled adjacent to the Singö deformation zone (HFM43-47). The new data motivates a few conceptual considerations and technical modifications as described in the following.

- Regarding hydrogeological DFN modelling using the DFN-2008 concept, it is recommended that the DFN recipes used in SDM-Site for the uppermost 200 m of fracture domains FFM01/06 and FFM02 are updated using the calculated linear intensities of open fractures above c. −90 m elevation presented in Table 7-3 and Figure 7-6.

- Regarding hydrogeological DFN modelling of sheet joints using the DFN-2008 concept, it is recommended that the intensity of sheet joints in the uppermost c. 30 m of rock is calculated as a fraction of the intensity of the subhorizontal fracture set. Further, it is recommended that sheet joints are generated as perfectly horizontal fractures in the uppermost c. 30 m of rock across the Forsmark catchment using a positively skewed fracture size-intensity model. In contrast, sheet joints at larger depths are considered to be of tectonic origin in the same way as other deep fractures.
- It is recommended that three different hydraulic scenarios are considered for the Singö deformation zone in the groundwater modelling for future safety assessments: a zone that is permeable in all directions (isotropic), a zone that is permeable in the longitudinal direction but impermeable in the transverse direction (anisotropic), a zone that is impermeable in all directions (isotropic) except for the uppermost 30 m where it is permeable in the transverse direction due to sheet joints.
- Regarding future hydrogeological models using the SBA concept developed for the SFR area in SDM-PSU, it is noted that data from the deepest complementary borehole, KFR121, supports the existing model for SBA6 (Figure 7-4), as well as the deterministically modelled sheet joint JFM16 (Figure 4-4). Regarding the other SBA structures, i.e., SBA1-5, SBA7 and SBA8, the information gathered in boreholes KFR117-121 is not conclusive. It is noted that boreholes KFR117-120 may be too short (i.e. too shallow) to provide any valuable information in this regard.
- Regarding the hydrogeological DFN modelling using the DFN-2020 concept, it is recommended to revisit the geological terminology and concepts used for sheet joints at different depth and reassess the concepts used for hydromechanical modelling including the updated stress model described in Chapter 6. These aspects have not been factored into Baseline Forsmark.

12.1.6 Meteorology, hydrology and near-surface hydrogeology

Post SDM-Site and SDM-PSU developments and their implications for forthcoming SDM updates regarding meteorology, hydrology and near-surface hydrogeology can be summarized as follows

- Available updates of geometrical models of topography, regolith depth and regolith stratigraphy have been used in the Baseline modelling stage and incorporated in the quantitative hydrological modelling. Future updates of such physiographical models, e.g. based on additional data and/or physical alterations due to contract works, can be used and incorporated in future SDM updates.
- Compared to SDM-Site and SDM-PSU, prolonged meteorological, hydrological and hydrogeological state variable datasets (the longest are almost 20 years) are available and used in the Baseline Forsmark modelling stage. As part of future SDM updates, these and further prolonged monitoring datasets enable interpretation of e.g. trends and variability on different time scales, and for detection and quantification of hydraulic responses to repository construction.
- The integrated, hydrology–bedrock hydrogeology modelling methodology is an important contribution from the Baseline Forsmark modelling stage. Based on the findings from the modelling methodology tests, the methodology and the associated modelling protocol (guide) can be further developed, fine-tuned and documented for applications in future SDM updates.
- Some of the conceptual issues from SDM-Site and SDM-PSU, e.g., regarding the heterogeneity and cross-flow properties of the Singö deformation zone, are addressed as part of the Baseline Forsmark modelling stage. Further issues can be addressed in forthcoming SDM updates, also considering further prolonged state variable datasets on e.g. lake-groundwater-atmosphere interactions and cross-discipline interpretations of additional surface-system data.

- In relation to SDM-Site, SDM-PSU and the Baseline modelling stage, forthcoming SDM updates will handle large quantities of data emanating from detailed site investigations, performed as part of construction of surface and subsurface facilities. The methodologies developed in Baseline Forsmark are an important input to handling of these data.

12.1.7 Hydrogeochemistry

A revision of the paleo-hydrogeochemical model has been published with some noticeable differences compared to earlier SDM's. There are new water types that include information and merges the approaches previously used for both the earlier sites (Section 9.4). A new numerical method has been developed for estimating water types with incomplete data using a neural network type model.

All surface system water and groundwater samples have been revisited and statistically modelled, and long-term trends have been analysed. Additionally, the mixing model has been revised with a new calculation scheme that incorporates uncertainties in the individual samples as well as in the proposed end-members. The new M3 model also uses a geochemical equilibrium with Forsmark bedrock to estimate deep saline waters, which gives a geochemical explanation for the composition.

Within Baseline, new sulphide concentration data has been collected. The data has been analysed using the new Baseline modelling methodologies, which makes it possible to further assess the high sulphide concentrations observed in previous SDMs.

12.1.8 Bedrock transport properties

Some new site data on bedrock transport properties have become available after SDM-Site. The new data did not necessitate further evaluation or descriptive modelling activities regarding transport properties with Baseline. The investigations carried out within Baseline are summarised as follows:

- Diffusion and sorption data from measurements on "monolithic" Forsmark samples were evaluated and reported in connection with the LTDE-SD experiments.
- Radium sorption measurements on Forsmark samples and associated modelling has been carried out.
- Porosity and diffusion data have been measured in connection with complementary porewater characterisation studies in the SFK access area and at SFR.
- Resistivity data from new boreholes, as reported in borehole geophysics data presentations, has been gathered. The data can be interpreted in terms of matrix diffusion parameters (*in-situ* formation factor).

In addition, there are on-going measurements of porosity, pore size distribution, diffusivity and sorption of Mo. It may be noted that the usefulness of the new resistivity logs for estimating formation factors depends on the specific method and frequency used and whether supporting hydrochemical data are available.

12.1.9 Ecology and land use

The ongoing monitoring program mainly aims to establish a baseline that can be used to relate different kinds of disturbances to wildlife population changes. This can be used in the future to disentangle natural biological variation from effects caused by the SKB's construction work in Forsmark. The focus of the targeted monitoring in Forsmark prior constructions concerns wetlands, forest and agricultural land, marine and limnic ecosystems.

12.2 Implications for upcoming SDMs

Updates of the site descriptive models are planned as SKB gradually collects more information during the detailed investigations during construction. Baseline Forsmark is a compilation and description of data collected since the previous SDM as well as methodology tests for newly developed modelling methodologies. Still remaining uncertainties are described in the discipline specific chapters. However, one of the major points of an SDM is integrated modelling which as noted in Section 1.1 has not been done in Baseline Forsmark.

13 References

SKB's (Svensk Kärnbränslehantering AB) publications can be found at http://www.skb.com/publications.

SKBdoc documents will be submitted upon request to document@skb.se.

Adill A, Eiler SM, Holliland PB, Wallin Kihlberg, I, Åkerund C, 2024. Biologisk recipientkontroll vid Forsmarks kärnkraftverk : årsrapport för 2023 Department of Aquatic Resources, Swedish University of Agricultural Sciences.

Adl-Zarrabi B, 2005a. Drill hole KFM06A. Thermal properties: heat conductivity and heat capacity determined using the TPS method. Forsmark site investigation. SKB P-05-123, Svensk Kärnbränslehantering AB

Adl-Zarrabi B, 2005b. Borehole KFM07A. Thermal conductivity and thermal diffusivity determined using the TPS method. Forsmark site investigation. SKB P-05-214, Svensk Kärnbränslehantering AB

Adl-Zarrabi B, 2006a. Borehole KFM08A Thermal conductivity and thermal diffusivity determined using the TPS method. Forsmark site investigation. SKB P-05-219, Svensk Kärnbränslehantering AB

Adl-Zarrabi B, 2006b. Borehole KFM01A, KFM01C, KFM01D, KFM04A, KFM05A, KFM06A and KFM09A. Thermal properties of rocks using calorimeter and TPS method, and mineralogical composition by modal analysis. Forsmark site investigation. Updated 2024-09 SKB P-06-233, Svensk Kärnbränslehantering AB

Albrecht, J, 2005. Forsmark site investigation - Study of Quaternary sediments in connection with investigations of bedrock lineaments. SKB-P-05-138, Svensk Kärnbränslehantering AB.

Andersson E, 2010. The limnic ecosystems at Forsmark and Laxemar-Simpevarp. SKB TR-10-02, Svensk Kärnbränslehantering AB.

Andersson P, Gustafsson E, Wass E, 2019. Analysis and evaluation of groundwater flow measurements in permanently installed boreholes at Forsmark 2005–2017. SKB TR-18-16, Svensk Kärnbränslehantering AB.

Aquilonius K (ed), 2010. The marine ecosystems at Forsmark and Laxemar-Simpevarp, SR-Site Biosphere. SKB TR-10-03, Svensk Kärnbränslehantering AB.

Ask D, 2023. Measurement attempts with Borre Probe III in borehole KFM24, Forsmark. SKBdoc 2023670, Svensk Kärnbränslehantering AB.

Auqué LF, Gimeno M J, Gómez J, Puigdomènech I, Smellie J, Tullborg E-L, 2006. Groundwater Chemistry around a Repository for Spent Nuclear Fuel over a Glacial Cycle Evaluation for SR-Can; SKB Technical Report TR-06-31; Svensk Kärnbränslehantering AB: Stockholm, Sweden, Available online: http://www.skb.se.

Back P-E, Wrafter J, Sundberg J, Rosén L, 2007. Thermal properties. Site descriptive modelling Forsmark – Stage 2.2. Comparison of thermal properties measured by different methods. SKB R-07-47, Svensk Kärnbränslehantering AB.

Back P-E, Sundberg J, 2022. Methodology for modelling of thermal properties of the Forsmark site. Part 1 - Recommended data and interpretation methods. SKB R-20-18, Svensk Kärnbränslehantering AB.

Back P-E, Sundberg J, Wrafter J, Rosén L, 2022. Methodology for modelling of thermal properties of the Forsmark site. Part 2 – Background and methodology development. SKB R-20-19, Svensk Kärnbränslehantering AB.

Bakker A, 2021. Geological characterisation of geophysical lineaments as part of the expanded site descriptive model around the planned repository site for high-level nuclear waste, Forsmark, Sweden. Dissertations in geology at Lund University, No. 623, 48 pp.

Ball J W, Nordstrom D K, 2001. User's Manual for WATEQ4F, with Revised Thermodynamic Data Base and Test Cases for Calculating Speciation of Major, Trace, and Redox Elements in Natural Waters; Open File Report; U.S. Geological Survey: Reston, VA, USA, pp. 91–183.

Berglund S, 2017. Monitoring Forsmark – evaluation and recommendations for programme update. SKB TR-15-01, Svensk Kärnbränslehantering AB.

Berglund S, Jakobsson A-M, Selroos J-O, Crawford J, Trinchero P, 2025. Methodology for site descriptive and safety assessment transport modelling of the bedrock at Forsmark. SKB R-20-17, Svensk Kärnbränslehantering AB.

Borgiel M, Sohlenius G, Kristofferson Å, Grolander S, 2022. Dykundersökning av område 157_2 och provtagning av regolitens kemiska och fysikaliska egenskaper. SKB P-22-15, Svensk Kärnbränslehantering AB. (In Swedish.)

Bosson E., Gustafsson, L-G, Sassner M, 2008. Numerical modelling of surface hydrology and near-surface hydrogeology at Forsmark. Site descriptive modelling SDM-Site Forsmark. R-08-09, Svensk Kärnbränslehantering AB

Broman E, Truvé J, 2023 Övervakning av däggdjursfaunan i Forsmark -Inventeringsresultat 2023. SKB P-23-13, Svensk Kärnbränslehantering AB.

Brunberg A-K, Blomqvist P, 1998. Vatten i Uppsala län 1977. Beskrivning, utvärdering, åtgärdsförslag. Rapport nr 8/1998. Upplandsstiftelsen.

Brunberg K, Carlsson T, Blomqvist P, Brydsten L, Strömgren M, 2004. Forsmark site investigation. Identification of catchments, lake-related drainage parameters and lake habitats. SKB P-04-25. Svensk Kärnbränslehantering AB.

Brydsten L, Strömgren M, 2004. Digital elevation models for site investigation programme in Forsmark. SKB R-04-70, Svensk Kärnbränslehantering AB.

Brüsin M, 2021. Fladdermusinventering vid Forsmark 2021 – Uppföljningsinventering. SKB P-21-19, Svensk Kärnbränslehantering AB.

Byegård J, Selnert E, Tullborg E-L, 2008. Bedrock transport properties. Data evaluation and retardation model. Site descriptive modelling, SDM-Site Forsmark. SKB R-08-98, Svensk Kärnbränslehantering AB. https://www.skb.se/publikation/1935906

Carlsson A, 1979. Characteristic features of a superficial rock mass in Southern central Sweden. Horizontal and sub-horizontal fractures and filling material. Striae 11.

Crawford J, 2008. Bedrock transport properties Forsmark. Site descriptive modelling. SDM-Site Forsmark. SKB R-08-48, Svensk Kärnbränslehantering AB. https://skb.se/publikation/1906886

Crawford J, 2010. Bedrock Kd data and uncertainty assessment for application in SR-Site geosphere transport calculations. Updated 2011-10. SKB R-10-48, Svensk Kärnbränslehantering AB. https://www.skb.se/publikation/2192981

Crawford J, 2013. Quantification of rock matrix Kd data and uncertainties for SR-PSU. SKB R-13-38, Svensk Kärnbränslehantering AB. https://www.skb.se/publikation/2479870

Crawford J, Löfgren M, 2019. Modelling of radionuclide retention by matrix diffusion in a layered rock model. SKB R-17-22, Svensk Kärnbränslehantering AB. https://skb.se/publikation/2494829

Curtis P, Markström I, Petersson J, Triumf C-A, Isaksson H, Mattsson H, 2011. Site investigation SFR. Bedrock geology. SKB R-10-49, Svensk Kärnbränslehantering AB.

Dahlin P, Maskenskaya O, 2017. Boremap mapping of core drilled borehole KFM24. SKB P-16-28, Svensk Kärnbränslehantering AB.

DHI (2023). MIKE SHE User Guide and Reference Manual. https://manuals.mikepoweredbydhi.help/2023/Water_Resources/MIKE_SHE_Print.pdf

Earon R., Rasul, H., Werner, K., 2025. Baseline Forsmark – Compilation of hydraulic properties of bedrock and regolith based on interpretation of single hole hydraulic tests, regolith samples and permeameter tests, SKB-R-22-07, Svensk Kärnbränslehantering AB. (in prep)

Eichinger F, Iannotta J, 2024. Characterisation of porewater of core samples from borehole KFR121. Chemical composition in out-diffusion experiment solutions and stable isotopes. SKB R-21-21, Svensk Kärnbränslehantering AB.

Eklund S, Mattsson K-J, 2009. Forsmark site investigation. Quantitative mapping of fracture minerals in Forsmark. SKB P-08-47, Svensk Kärnbränslehantering AB. https://skb.se/publikation/1991080

Ekologigruppen AB, 2024a. Upplagsplats, Forsmark Naturvärdesinventering enligt SIS-standard 199000:2023, samt inventering av groddjur och fladdermöss i två områden inför planerad deponi i Forsmark. SKBdoc 2058735, v 3.0, Svensk Kärnbränslehantering AB.

Ekologigruppen AB, 2024b. Groddjur vid Forsmark - Inventering av lekande groddjur och groddjurshabitat inom fastigheterna Östhammar Ön 1:1 och Östhammar Berkinge 9:1, Östhammar kommun. SKBdoc 2058736, v 1.0, Svensk Kärnbränslehantering AB.

Ekologigruppen AB, 2024c. Naturvärdesinventering för nytt vägförslag till reningsvåtmark i Forsmark, Östhammar - Naturvärdesinventering enligt SIS 199000:2014, med tillägg naturvärdesklass 4. SKBdoc 2053409, v 1.0, Svensk Kärnbränslehantering AB.

Ekologigruppen AB, 2024d. Naturvärdesinventering i Forsmark, Östhammar Naturvärdesinventering enligt SIS 199000:2014, med tillägg naturvärdesklass 4. SKBdoc 2033992, v 1.0, Svensk Kärnbränslehantering AB.

Ekologigruppen AB, Silva Strategi AB, 2024. Skogsplan Forsmark - plan för Naturnära hyggesfritt skogsbruk och naturvårdsskötsel för SKB:s skog vid Forsmark, fastigheterna Östhammar Forsmark 6:20 och Östhammar Forsmark 3:32. SKBdoc 2067945, v 1.0, Svensk Kärnbränslehantering AB.

Elhammer A, Sandkvist Å, 2005. Forsmark site investigation. Detailed marine geological survey of the sea bottom outside Forsmark. SKB P-03-101, Svensk Kärnbränslehantering AB.

Eriksson Å, P Collinder, 2023. Uppföljning av skötselåtgärder i rikkärr och dess påverkan på gulyxne, Forsmark 2023. SKB P-23-16, Svensk Kärnbränslehantering AB.

Eriksson Å, Schnoor T, Jakobsson S, Collinder P, 2018. Uppföljning av skötselåtgärder i rikkärr och dess påverkan på gulyxne, Forsmark 2017. SKB P-18-01, Svensk Kärnbränslehantering AB.

Fabritius O, Fabritius A, Hellings M, Sorokina T, Sojakka T, Jakobsson A-M, Li X, Sammaljärvi J, Siitari-Kauppi M, 2024. Radium sorption on crystalline rock; spatial distribution and sorption modeling study. Applied Geochemistry 162, 105930.

Figueiredo B, Sjöberg J, Mas Ivars D, 2020. Use of a fully tensorial approach to characterize the stress variability at Forsmark. 5th International Itasca Symposium – 2020 – Billaux, Hazzard, Nelson & Schöpfer (eds.) Paper: 12-08 ©2020 Itasca International, Inc., Minneapolis, ISBN 978-0-9767577-5-7in Vienna, Austria.

Follin S, Levén J, Hartley L, Jackson P, Joyce S, Roberts D, Swift B, 2007a. Hydrogeological characterisation and modelling of deformation zones and fracture domains, Forsmark modelling stage 2.2. Updated 2024-11, Forsmark modelling stage 2.2. SKB-R-07-48, Svensk Kärnbränslehantering AB.

Follin S, Johansson P-O, Hartley L, Jackson P, Marsic N, 2007. Hydrogeological conceptual model development and numerical modelling using CONNECTFLOW, Forsmark modelling stage 2.2. SKB-R-07-49, Svensk Kärnbränslehantering AB.

Follin S, Hartley L, Jackson P, Roberts D, Marsic N, 2008. Hydrogeological conceptual model development and numerical modelling using CONNECTFLOW, Forsmark modelling stage 2.3. SKB-R-08-23, Svensk Kärnbränslehantering AB.

Follin S, 2008. Bedrock hydrogeology Forsmark; Site descriptive modelling, SDM-Site Forsmark. SKB-R-08-95, Svensk Kärnbränslehantering AB.

Follin S, Hartley L, Rhén I, Jackson P, Joyce S, Roberts D, Swift B, 2014. A methodology to constrain the parameters of a hydrogeological discrete fracture network model for sparsely fractured crystalline rock, exemplified by data from the proposed high-level nuclear waste repository site at Forsmark, Sweden. Hydrogeology Journal.

Follin S, Stigsson M, 2014. A transmissivity model for deformation zones in fractured crystalline rock and its possible correlation to in situ stress at the proposed high-level nuclear waste repository site at Forsmark, Sweden. Hydrogeology Journal. 22. 10.1007/s10040-013-1078-9.

Follin S (ed), 2019. Multidisciplinary description of the access area of the planned spent nuclear fuel repository in Forsmark prior to construction. SKB R-17-13, Svensk Kärnbränslehantering AB.

Follin S, Werner K, Lindmark J, Rasul H, Stigsson M, Sassner M, Lampinen A, Öhman J, Bym T, 2025. Baseline Forsmark – Hydrological and hydrogeological modelling using FracMan, DarcyTools, and MIKE SHE. SKB R-23-06, Svensk Kärnbränslehantering AB.

Fox A, La Pointe P, Hermanson J, Öhman J, 2007. Statistical geological discrete fracture network model. Forsmark modelling stage 2.2. Updated 2008-12. SKB-R-07-46, Svensk Kärnbränslehantering AB.

Föhlinger S, Koehler B, Harrström J, 2020. Hydraulic interference tests in HFM33 and HFM43-46, SKB-P-19-11, Svensk Kärnbränslehantering AB.

Gimeno M, Tullborg E-L, Nilsson A-C, Auqué L Nilsson L, **2023**. Hydrogeochemical characterisation of the groundwater in the crystalline basement of Forsmark, the selected area for the geological nuclear repositories in Sweden. J. Hydrol. 624, 129818.

Glamheden R, Fredriksson A, Röshoff K, Karlsson J, Hakami H, Christiansson R, 2007. Rock mechanics Forsmark, Site descriptive modelling Forsmark stage 2.2. SKB R-07-31, Svensk Kärnbränslehantering AB.

Glamheden R, Lanaro F, Karlsson J, Lindberg U, Wrafter J, Hakami H, Johansson M, 2008. Rock mechanics Forsmark. Modelling stage 2.3. Complementary analysis and verification of the rock mechanics model. SKB R-08-66, Svensk Kärnbränslehantering AB.

Gokall-Normal K, Ludvigson J-E, 2008. Forsmark site investigation; Hydraulic interference test with borehole HFM33 used as pumping borehole, SKB-P-07-229, Svensk Kärnbränslehantering AB.

Green M, 2024. Fågelövervakning i Forsmark 2023. SKB R-24-05, Svensk Kärnbränslehantering AB.

Grimaud D, Beaucaire C, Michard G, 1990. Modelling of the evolution of ground waters in a granite system at low temperature: the Stripa ground waters, Sweden. Appl. Geochem. 5, 515–525.

Hakala M, Kemppainen K, Siren T, Heine J, Christiansson R, Martin D, Koskinen T, 2012. Experience with a new LVDT-Cell to measure in-situ stress from an existing tunnel. Paper presented at the ISRM International Symposium - EUROCK 2012, Stockholm, Sweden, May 2012.

Hakala M, Siren T, Kemppainen K, Christiansson R, Martin D, 2014. In situ stress measurement with LVDT-cell – method description and verification. POSIVA 2012-43 (ISBN 978-951-652-223-7). Posiva Oy, Eurajoki.

Hakala M, Ström J, Valli J, Juvani J, 2019. Structural control on stress variability at Forsmark. SKB R-19-23, Svensk Kärnbränslehantering AB.

Hakala M, 2022. SKB MD 181.0021 - Method description for LVDT rock stress measurement method. SKBDoc 1981591. Svensk Kärnbränslehantering AB.

Hakala M, 2023. Rock stress measurement in KFM24 – Stress Measurement Company (SMCOY) experiences. Internal PM. SKBDoc 2023195, Svensk Kärnbränslehantering AB.

Hakami E, Holmberg J, 2021. Overcoring of pilot hole in KFM224. Evaluation of the required conditions for future overcoring stress measurements. SKB P-21-12, Svensk Kärnbränslehantering AB.

Hakami E, Sánchez Juncal A, Mas Ivars D, 2025. Baseline Rock Mechanics. SKB R-23-05. Svensk Kärnbränslehantering AB.

Hakami E, Winell S, 2022. Point load testing of intact rock and of samples with sealed fractures. SKB P-22-01, Svensk Kärnbränslehantering AB.

Hakami E, Winell S, Sánchez Juncal A, 2024. Geometry and mechanical properties of water bearing fractures. SKB P-22-27, Svensk Kärnbränslehantering AB.

Hamrén U, P Collinder, 2010 Vattenverksamhet i Forsmark – Ekologisk fältinventering och naturvärdes-klassificering samt beskrivning av skogsproduktionsmark (R-10-16).

Harrström J, Sjöberg O, Öhman J, 2018. Evaluation of Hydraulic Interference Tests in Forsmark with KFM24 as pumping borehole. SKB P-17-17. Svensk Kärnbränslehantering AB.

Hartley L, Baxter S, Carty J, Libby S, 2021. Exploratory integration of discrete fracture network models and 1D stress models with data from hydraulic tests for the shallow bedrock at the Forsmark site. R-21-13, Svensk Kärnbränslehantering AB.

Hartley, L, Libby S, Bym T, Carty J, Cottrell M, Mosley K, 2024. Baseline Forsmark - A discrete fracture network (DFN) model applying grown fractures and hydromechanical (HM) coupling. SKB-P-23-01, Svensk Kärnbränslehantering AB.

Hedenström A, 2003. Forsmark site investigation. Investigation of marine and lacustrine sediments in lakes. SKB P-03-24, Svensk Kärnbränslehantering AB.

Hedenström A, 2004a. Forsmark site investigation. Investigation of marine and lacustrine sediments in lakes. Stratigraphical and analytical data. SKB P-04-86, Svensk Kärnbränslehantering AB.

Hedenström A, 2004b. Forsmark site investigation. Stratigraphical and analytical data of Quaternary deposits. SKB P-04-148, Svensk Kärnbränslehantering AB.

Hedenström A, Sohlenius G, 2008. Description of the regolith at Forsmark. Site descriptive modelling, SDM-Site Forsmark. SKB R-08-04, Svensk Kärnbränslehantering AB.

Hermanson J, Petersson J, 2022. Methodology for deterministic geological modelling of the Forsmark site. Application to the development of the final repository for spent nuclear fuel. SKB R-20-10, Svensk Kärnbränslehantering AB.

Holmberg E, Wzdulski M, 2023. Inventering av gölgroda och större vattensalamander i Forsmarksområdet 2023. SKB P-23-17, Svensk Kärnbränslehantering AB.

Holmgren A, Lundkvist S, 2023. Inventering av gulyxne i Forsmark 2023. SKB P-23-18, Svensk Kärnbränslehantering AB.

Hurmerinta E, 2017. Forsmark site investigations. Difference flow logging in borehole KFM24. SKB P-16-27, Svensk kärnbränslehantering AB.

Hökmark H, Lönnqvist M, Kristersson O, Sundberg J, Hellström G, 2009. Strategy for thermal dimensioning of the final repository for spent nuclear fuel. SKB R-09-04. Svensk Kärnbränslehantering AB.

Isaksson H, Johansson L, 2020. Complementary lineament interpretation in the SDM-SAR drainage area at Forsmark. SKB P-20-14, Svensk Kärnbränslehantering AB.

Ising J, 2005. Forsmark site investigation. Forsmark site investigation. Mapping of Quaternary deposits on the bottom of shallow bays outside Forsmark. SKB P-06-88, Svensk Kärnbränslehantering AB.

Jacobson P, 2022. Populationsutveckling för gulyxne i Forsmark 2012 2021. Sammanställning och utvärdering av SKB:s inventeringar av gulyxne och skötselåtgärder i Forsmarksområdet. SKB R-22-01, Svensk Kärnbränslehantering AB.

Jacobsson L, Sjöström J, 2019. Forsmark - Laboratory tests for investigation of the influence of rock type, oxidation, and other factors in borehole breakouts. Boreholes KFM01A, KFM04A, KFM05A and KFM24. Thermal properties by TPS method and uniaxial compression and indirect tensile strength tests of intact rock. Updated 2020-10. SKB P-18-08. Svensk Kärnbränslehantering AB.

Jakobsson A-M, Selroos J-O, Berglund S, 2025. Methodology for site descriptive and safety assessment transport modelling of the Forsmark site. SKB R-20-17, Svensk Kärnbränslehantering AB. (In preparation.)

Javaid MA, Harrison JP, Mas Ivars D, Kasani HA, 2022. A Bayesian regression analysis of in situ stress using overcoring data. Published in the proceedings of Eurock 2022,12-15 September 2022, Helsinki, Finland.

Javaid MA, Harrison JP, Mas Ivars D, Kasani HA, 2024. A method for quantifying uncertainty in stress domain boundaries. Eurock 2024, July 2024, Alicante, Spain.

Johansson M, 2023. Hur påverkas gölgrodan (Pelophylax lessonae) av translokering? Uundersökningar av hemvändarbeteende och kroppskondition. Sveriges lantbruksuniversitet, Uppsala.

Johansson P-O, 2008. Description of surface hydrology and near-surface hydrogeology at Forsmark. Site descriptive modelling SDM-Site Forsmark. R-08-08, Svensk Kärnbränslehantering AB

Johansson P-O, Werner K, 2019. Surface-water levels and groundwater levels in regolith at the Forsmark site. Monitoring programme updates prior to start of repository construction. SKB P-18-10, Svensk Kärnbränslehantering AB.

Johansson P-O, Öhman J, 2008. Presentation of meteorological, hydrological, and hydrogeological monitoring data from Forsamrk. Site descriptive modelling SDM-Site Forsmark. SKB R-08-10, Svensk Kärnbränslehantering AB.

Juhlin C, Stephens M B, 2006. Gently dipping fracture zones in Paleoproterozoic metagranite, Sweden: Evidence from reflection seismic and cored borehole data and implications for the disposal of nuclear waste. Journal of Geophysical Research 111, B09302, 19 pp.

Laaksoharju M, Skårman E, Gómez JB, Gurban I, 2009. M3 version 3: user's manual. SKB TR-09-09, Stockholm, Sweden: Svensk Kärnbränslehantering AB.

Laaksoharju M, Smellie J, Tullborg E-L, Gimeno M, Hallbeck L, Molinero J, Waber N, 2008. Bedrock hydrochemistry Forsmark. Site descriptive modelling SDM-Site Forsmark. R-08-47, Svensk Kärnbränslehantering AB.

Lindborg T, 2008. Surface system Forsmark – Site descriptive modelling – SDM-Site Forsmark. SKB R-08-11, Svensk Kärnbränslehantering AB.

Lindroos H, Isaksson H, Thunehed H, 2004. The potential for ore and industrial minerals in the Forsmark area. SKB R-04-18, Svensk Kärnbränslehantering AB.

Löfgren A, 2010. The terrestrial ecosystems at Forsmark and Laxemar-Simpevarp, SR-Site Biosphere. SKB TR-10-01, Svensk Kärnbränslehantering AB.

Löfgren M, 2014. Recommendation of rock matrix effective diffusivities for SR-PSU. Based on formation factor logging in situ by electrical methods in KFR102B and KFR105. SKB R-13-39, Svensk Kärnbränslehantering AB.

Löfgren M, Sidborn M, 2010. Statistical analysis of results from the quantitative mapping of fracture minerals in Forsmark. Site descriptive modelling – complementary studies. SKB R-09-30, Svensk Kärnbränslehantering AB.

Martel S J, 2011. Mechanics of curved surfaces, with application to surface-parallel cracks. Geophysical Research Letters, vol 38, L20303.

Martel S J, 2017. Progress in understanding sheeting joints over the past two centuries. Journal of Structural Geology, vol 94, pp 68–86.

Mercier L, Pontér S, Nilsson A-C, Gimeno M-J, Tullborg E-L, 2025. Methodology for hydrochemical modelling of the Forsmark site, SKB R-20-15 Svensk Kärnbränslehantering AB. *IN PREP*.

Mercier L, 2026. Baseline Forsmark – Hydrogeochemistry, SKB R-25-06, Svensk Kärnbränslehantering AB. *IN PREP.*

Michard G, 1987. Controls of the chemical composition of geothermal waters. In Chemical Transport in Metasomatic Processes; Helgeson, H.C., Ed.; NATO Advanced Study Institute Series C 218; D. Reidel Publ. Co.: Springer, Dordrecht, Netherlands; pp. 323–353.

Munier R, Hermanson J, 2001. Metodik för geometrisk modellering. Presentation och administration av platsbeskrivande modeller. SKB R-01-15, Svensk Kärnbränslehantering AB.

Munier R, Stenberg L, Stanfors R, Milnes A G, Hermanson J, Triumf C-A, 2003. Geological Site Descriptive Model. A strategy for the model development during site investigations. SKB R-03-07, Svensk Kärnbränslehantering AB.

Nilsson A-C, Gimeno M-J, Tullborg E-L, Smellie J, Jönsson S, Puigdomenech I, Berg C, 2020. Methodology for Hydrogeochemical Sampling to Characterise Groundwaters in Crystalline Bedrock: Developments Made within the Swedish Radwaste Programme. Geofluids, 8749482.

Nilsson L, Pontér S, Gimeno MJ, 2024. A Bayesian Approach to End-Member Mixing Estimations in a Geological Nuclear Waste Repository in Sweden. Minerals.14(4):357.

Nilsson A-C, Tullborg E-L, Smellie J, Gimeno M, Gómez J, Auqué L, Sandström B, Pedersen K, 2011. SFR site investigation. Bedrock Hydrogeochemistry. R-11-06, Svenska kärnbränslehantering AB.

Nyberg J, Elhammer A, Sohlenius G, Kjellin B, Nordgren P, 2011. Results from marine geological investigations outside Forsmark. SKB P-11-39, Svensk Kärnbränslehantering AB.

Odén M, Follin S, Öhman J, Vidstrand P, 2014. SR-PSU Bedrock hydrogeology. Groundwater flow modelling methodology, setup and results. SKB R-13-25, Svensk Kärnbränslehantering AB.

Odén M, Follin S, Öhman J, Werner K, 2025. Methodology for hydrological and hydrogeological modelling of the Forsmark site. SKB R-20-14, Svensk Kärnbränslehantering AB.

Olofsson I, Simeonov A, Stigsson M, Stephens M, Follin S, Nilsson A-C, Röshoff K, Lindberg U, Lanaro F, Fredriksson A, Persson L, 2007. Site descriptive modelling Forsmark, stage 2.2. A fracture domain concept as a basis for the statistical modelling of fractures and minor deformation zones, and interdisciplinary coordination. SKB R-07-15, Svensk Kärnbränslehantering AB.

Pérez Rey I, Johansson F, Mas Ivars D, Kasani H, Larsson J, Jacobsson L, Flansbjer M, 2024. Fracture parametrisation for repository design and post-closure analysis (Post), phase 2, 3 and 4 – Final Report. SKB R-24-XX, Svensk Kärnbränslehantering AB, Stockholm.

Persson C, 1985. Jordartskarta 12I Östhammar NO med beskrivning. Geological survey of Sweden Ae 73. (In Swedish with English summary.)

Persson C, 1997. Jordartskartan Norrtälje NV med beskrivning. Geological survey of Sweden Ae 122. (In Swedish with English summary.)

Petersson J, Stephens M B, Mattsson H, Möller C, 2012. Albitization and quartz dissolution in Paleoproterozoic metagranite, central Sweden – Implications for the disposal of spent nuclear fuel in a deep geological repository. Lithos, v. 148, pp. 10–26.

Petersson J, Hultgren P, Hermanson J, Isaksson H, Sarlus Z, Stigsson M, Markström I, 2024. Baseline Forsmark – Geology. Updating of existing site descriptive models. SKB R-24-07, Svensk Kärnbränslehantering AB.

Petrone J, Sohlenius G, Ising J, 2020. Baseline Forsmark – Depth and stratigraphy of regolith. SKB R-17-07, Svensk Kärnbränslehantering AB.

Petrone J, Strömgren M, 2020. Baseline Forsmark – Digital elevation model. SKB-R-17-06, Svensk Kärnbränslehantering AB.

Qvarfordt S, Borgiel M, 2022. Bottenkartering i Forsmarks hamn. SKBDoc 1997773, Svensk Kärnbränslehantering AB.

Qvarfordt S, Borgiel M, Wallin A, 2020. Bottenkartering utanför Vegakontoret samt i kylvattenkanalen. SKBDoc 1898143, Svensk Kärnbränslehantering AB.

Rauséus G, Petersson J, 2020. Geological single-hole interpretation of HFM42–HFM47 and KFM25–KFM27. SKB P-20-13, Svensk Kärnbränslehantering AB.

Saintot A, Stephens M B, Viola G, Nordgulen Ø, 2011. Brittle tectonic evolution and paleostress reconstruction in the southwestern part of the Fennoscandian Shield, Forsmark, Sweden. Tectonics, v. 30, pp. 1–36.

Sandström B, Tullborg E-L, Smellie J, MacKenzie A B, Suksi J, 2008. Fracture mineralogy of the Forsmark site. SDM-Site Forsmark. SKB R-08-102, Svensk Kärnbränslehantering AB.

Selnert E, Byegård J, Widestrand H, 2008. Forsmark site investigation. Laboratory measurements within the site investigation programme for the transport properties of the rock. Final report. SKB P-07-139, Svensk Kärnbränslehantering AB.

Selroos J-O, Mas Ivars D, Munier R, Hartley L, Libby S, Davy P, Darcel C, Trinchero P, 2022. Methodology for discrete fracture network modelling of the Forsmark site. Part 1 – concepts, data and interpretation methods. SKB R-20-11, Svensk Kärnbränslehantering AB.

Sheppard S, Sohlenius G, Omberg L-G, Borgiel M, Grolander S, Nordén S, 2011. Solid/liquid partition coefficients (Kd) and plant/soil concentration ratios (CR) for selected soils, tills and sediments at Forsmark. SKB R-11-24. Svensk Kärnbränslehantering AB.

Sjöberg J, Figueiredo B, Hakala M, 2024. Reliability ranking of overcoring stress measurements at Forsmark. SKB R-21-08, Svensk Kärnbränslehantering AB.

SKB, 2005. Preliminary site description Forsmark area – version 1.2. SKB R-05-18, Svensk Kärnbränslehantering AB.

SKB, 2006. Site descriptive modelling Forsmark stage 2.1. Feedback for completion of the site investigation including input from safety assessment and repository engineering. SKB R-06-38, Svensk Kärnbränslehantering AB.

SKB, 2008a. Site description of Forsmark at completion of the site investigation phase. SDM-Site Forsmark. SKB TR-08-05, Svensk Kärnbränslehantering AB.

SKB, 2008b. Confidence assessment. Site descriptive modelling SDM-Site Forsmark. SKB R-08-82, Svensk Kärnbränslehantering AB.

SKB, 2013. Site description of the SFR area at Forsmark at completion of the site investigation phase. SDM-PSU Forsmark. SKB TR-11-04, Svensk Kärnbränslehantering AB.

SKB, 2014. Biosphere synthesis report for the safety assessment SR-PSU. SKB TR-14-06, Svensk Kärnbränslehantering AB.

Sohlenius G, Hedenström A, Rudmark L, 2004. Forsmark site investigation. Mapping of unconsolidated Quaternary deposits 2002–2003. Map description. SKB R-04-39, Svensk Kärnbränslehantering AB.

Sohlenius G, Hedenström A, 2009. Platsundersökning Forsmark. Stratigrafiska undersökningar i våtmarksobjekt. SKB P-09-18, Svensk Kärnbränslehantering AB. (In Swedish.)

Sohlenius G, Strömgren M, Hartz F, 2013. Depth and stratigraphy of regolith at Forsmark. SR-PSU Biosphere. SKB R-13-22, Svensk Kärnbränslehantering AB.

Sohlenius G, Wilin L, Hedenström A, Karlsson C, 2019. Quaternary deposits in the drainage area of Gunnarsboträsket in Forsmark. Stratigraphical and surficial distribution of Quaternary deposits. SKB P-12-03, Svensk Kärnbränslehantering AB.

Sohlenius G, Becher M, Boman A, 2020. Regolith in wetlands with high nature values Physical and chemical properties. SKB P-20-11, Svensk Kärnbränslehantering AB

Sohlenius G, Svensson M, 2021. Regolith in wetlands with high nature values. Additional studies. P-21-09, Svensk Kärnbränslehantering AB.

Sohlenius G, Svensson M, 2022. Methodology for elevation and regolith modelling of the Forsmark site. SKB R-20-16, Svensk Kärnbränslehantering AB.

Soler J, Neretnieks I, Moreno L, Liu L, Meng S, Svensson U, Trinchero P, Iraola A, Ebrahimi H, Molinero J, Vidstrand P, Deissmann G, Ríha J, Hokr M, Vetešník A, Vopálka D, Gvoždík L, Polák M, Trpkošová D, Havlová V, Park D-K, Ji S-H, Tachi Y, Ito T, 2019. Evaluation and modelling report of Task 9A based on comparisons and analyses of predictive modelling results for the REPRO WPDE experiments. Task 9 of SKB Task Force GWFTS – Increasing the realism in solute transport modelling based on the field experiments REPRO and LTDE-SD. SKB R-17-10, Svensk Kärnbränslehantering AB.

Soler J M, Meng S, Moreno L, Neretnieks I, Liu L, Kekäläinen P, Hokr M, Říha J, Vetešník A, Reimitz D, Višňák J, Vopálka D, Kröhn K P, Tachi Y, Ito T, Svensson U, Iraola A, Trinchero P, Voutilainen M, Deissmann G, Bosbach D, Park D K, Ji S-H, Gvoždík L, Milický M, Polák M, Makedonska N, Kuluris S, Karra S, Viswanathan H, Gylling B, Lanyon G W, 2021. Evaluation report of Task 9B based on comparisons and analyses of modelling results for the Äspö HRL LTDE SD experiments. Task 9 of SKB Task Force GWFTS – Increasing the realism in solute transport modelling based on the field experiments REPRO and LTDE-SD. SKB TR-20-17, Svensk Kärnbränslehantering AB.

SIS, 2023. SS 199000:2023, SS 199000:2023, Naturvärdesinventering (NVI) - Kartläggning och värdering av biologisk mångfald - Krav och vägledning. Swedish Institute for Standards.

SSM, 2018. Strålsäkerhet efter slutförvarets förslutning. SSM 2018:07, Strålsäkerhetsmyndigheten. (In Swedish.)

SSM, 2019. Granskningsrapport – Utbyggnad och fortsatt drift av SFR. SSM 2019:18, Strålsäkerhetsmyndigheten. (In Swedish.)

Stephan J, 2024. Comparison of fen orchid (Liparis loeselii) populations inside and outside Forsmark. SKB R-23-11, Svensk Kärnbränslehantering AB.

Stephens M B, Simeonov A, 2015. Description of deformation zone model version 2.3, Forsmark. SKB R-14-28, Svensk Kärnbränslehantering AB.

Stephens MB, Fox A, Pointe PL, Simeonov A, Isaksson H, Hermanson J, Öhman J, 2007. Geology Forsmark; Site descriptive modelling Forsmark stage 2.2. SKB-R-07-45, Svensk Kärnbränslehantering AB.

Stephens M B, Simeonov A, Isaksson H, 2008. Bedrock geology Forsmark. Modelling stage 2.3. Implications for and verification of the deterministic geological models based on complementary data. SKB R-08-64, Svensk Kärnbränslehantering AB.

Stephens M B, Follin S, Petersson J, Isaksson H, Juhlin C, Simeonov A, 2015. Review of the deterministic modelling of deformation zones and fracture domains at the site proposed for a spent nuclear fuel repository, Sweden, and consequences of structural anisotropy. Tectonophysics, v. 653, pp. 68–94.

Strömberg B, 1989. Late Weichselian deglaciation and clay varve chronology in East-Central Sweden. Sveriges Geologiska Undersökning, Ca 73.

Strömgren M, Brytsten L, 2008. Digital elevation models of Forsmark. Site descriptive modelling SDM-Site Forsmark. SKB R-08-62, Svensk Kärnbränslehantering AB.

Strömgren M, Brydsten L, 2013. Digital elevation model of Forsmark. Site-descriptive modelling, SR-PSU biosphere. SKB R-12-03, Svensk Kärnbränslehantering AB.

Sundberg J, Ländell M, 2002. Determination of linear thermal expansion. Samples from borehole KA2599G01. Äspö HRL. SKB IPR-02-63. Svensk Kärnbränslehantering AB.

Sundberg J, Back P-E, Bengtsson A, Ländell M, 2005. Thermal modelling. Preliminary site description Forsmark subarea – version 1.2. SKB R-05-31. Svensk Kärnbränslehantering AB.

Sundberg J, Wrafter J, Back P-E, Ländell M, 2006. Thermal modelling. Preliminary site description Laxemar subarea – version 1.2. SKB R-06-13. Svensk Kärnbränslehantering AB.

Sundberg J, Wrafter J, Sundberg A, 2007. Forsmark site investigation. Anisotropy of thermal properties in granite at Forsmark. Large-scale field measurements and comparison with small-scale field measurements and laboratory measurements. SKB P-07-194, Svensk Kärnbränslehantering AB.

Sundberg J, Wrafter J, Ländell M, Back P-E, Rosén L, 2008. Thermal properties Forsmark Modelling stage 2.3. Complementary analysis and verification of the thermal bedrock model, stage 2.2. SKB R-08-65, Svensk Kärnbränslehantering AB.

Sundh M, Sohlenius G, Hedenström A, 2004. Forsmark site investigation. Stratigraphical investigation of till in machine cut trenches. SKB P-04-34, Svensk Kärnbränslehantering AB.

Svensson U, 2010. Darcy Tools version 3.4 Verification, validation and demonstration. SKB R-10-71, Svensk Kärnbränslehantering AB.

Trotignon L, Beaucaire C, Louvat D, Aranyossy J-F, 1999. Equilibrium geochemical modelling of Äspö groundwaters: a sensitivity study of thermodynamic equilibrium constants. Appl. Geochem. 14, 907–916.

Tröjbom M, Söderbäck B, Kalinowski B, 2008. Hydrochemistry of surface water and shallow groundwater. Site descriptive modelling SDM-Site Laxemar. SKB R-08-46, Svensk Kärnbränslehantering AB.

Twidale C R, Vidal Romani J R, Champell E M, Centeno J D, 1996. Sheet fractures: response to erosional offloading or to tectonic stress? Zeitschrift für Geomorphologie Supplementband, vol 106, pp 1–24.

Valli J, Hakala M, Mattila J, Winderholler R, 2023. Control of deterministically modeller structures on the stress variability at Forsmark. SKB R-23-04, Svensk Kärnbränslehantering AB.

Waber H N, Smellie J A T, 2012. Forsmark site characterisation. Borehole KFM22 and KFM23: Derivation of porewater data by diffusion experiments. SKB P-12-18, Svensk Kärnbränslehantering AB.

Wahlgren C-H, Curtis P, Hermanson J, Forssberg O, Öhman J, Fox A, La Pointe P, Drake H, Triumf C-A, Mattsson H, Thunehed H, Juhlin C, 2008. Geology Laxemar. Site descriptive modelling SDM-Site Laxemar. SKB R-08-54, Svensk Kärnbränslehantering AB.

Werner K, Sassner M, Johansson E, 2013. Hydrology and near-surface hydrogeology at Forsmark - synthesis for the SR-PSU project. SR-PSU Biosphere. R-13-19, Svensk Kärnbränslehantering AB

Werner K, Norville J, Öhman J, 2014. Meteorological, hydrolopgical and hydrogeological monitoring data from Forsmark - compulation and analysis for the SR-PSU project. SR-PSU Biosphere. R-13-20, Svensk Kärnbränslehantering AB.

Werner K, 2018. Data compilation and analysis for the description of the access area of the planned spent fuel repository in Forsmark - meteorology, hydrology and near-surface hydrogeology. SKB P-17-19, Svensk Kärnbränslehantering AB.

Rasul H, Werner K, 2025. Baseline Forsmark – Compilation of meteorological, hydrological and hydrogeological state variables data. SKB R-24-03, Svensk Kärnbränslehantering AB.

Widestrand H, Byegård J, Ohlsson Y, Tullborg E-L, 2003. Strategy for the use of laboratory methods in the site investigations programme for the transport properties of the rock. SKB R-03-20, Svensk Kärnbränslehantering AB.

Widestrand H, Byegård J, Selnert E, Skålberg M, Höglund S, Gustafsson E, 2010. Long Term Sorption Diffusion Experiment (LTDE-SD). Supporting laboratory program – Sorption diffusion experiments and rock material characterisation. With supplement of adsorption studies on intact rock samples from the Forsmark and Laxemar site investigations. SKB R-10-66, Svensk Kärnbränslehantering AB.

Winell S, Samuelsson E, 2022. Geological single-hole interpretation of KFR117–KFR121. SKB P-21-25, Svensk Kärnbränslehantering AB.

Öhman J, Follin S, Odén M, 2013. Bedrock Hydrogeology - Groundwater flow modelling. Site investigation SFR. SKB-R-11-10, Svensk Kärnbränslehantering AB.

Öhman J, Bockgård N, Follin S, 2012. Site investigation SFR. Bedrock hydrogeology. SKB-R-11-03, Svensk Kärnbränslehantering AB.

A Appendix 1. Bedrock thermal properties

A1 Objective and scope for thermal models in Baseline

During the period following the SDM-Site models, the amount of thermal property investigations and subsequent modelling performed has been limited. Nevertheless, a new thermal modelling methodology has been presented and published (Back and Sundberg 2022). These recommended modelling procedures are foreseen to be applied in future updates of the site characterization, in particular when data become available from the deposition area of the final storage of spent nuclear fuel.

The main objective for the Baseline version is to analyse the available new laboratory data on thermal properties regarding certain rock types, and to compare these results with the thermal parameters reported in previous SDM-Site models. An additional objective is to analyse the spatial data coverage and identify any potential parts of the repository rock volume where there is a lack of thermal properties data.

The scope of Baseline thermal model update is focused only on the single rock *type* level. On a larger scale, the rock mass in the rock domains consists of a certain mixture of rock type bodies of different sizes and shapes; however, the thermal modelling at the rock *mass* scale has not been considered as part of the scope for the Baseline thermal model.

A2 Available data

A2.1 Number and location of TPS tests

The SDM-Site model for thermal properties was based on a mixture of input data, consisting of direct laboratory measurements of thermal properties, lithological data from core mapping, mineral composition data, density data and a few field measurements. The available data at SDM-Site stage is reported in detail in (Back et al. 2007). The amount of the available laboratory data (measured by the Transient Plane Source method, TPS) in Baseline stage is presented in Table A-1.

The thermal conductivity, heat capacity and thermal diffusivity results from the TPS tests are found in the Sicada property table "thermal properties" for each sample identified by borehole ID and borehole depth. The rock type code for each sample is collected from Sicada tables "p_rock" (for sections longer than 1 m borehole length) and in table "p_rock_occurrence" (for sections of 1 m or shorter borehole length). The results may also be found in the P-report for the performed laboratory test, listed in Table A-1 together with the number of available *samples* in each borehole of a certain rock type. The P-reports are particularly useful in the way that photos of each sample are presented, such that the mineralogy and potential differences in characteristics can be studied.

The total number of TPS *test* results reported in Sicada is sometimes higher than the number of *samples* given in Table A-1, since some samples have been tested several times in order to get their thermal properties at different temperatures (See Section A5). The numbers of tests in Table A-1 are tests at 20-23 °C.

Table A-1. Available laboratory TPS data on thermal conductivity.

Rock type code	Rock type name	RFM 029 %	RFM 045 %	No. of TPS	Sampling boreholes	Laborator y SKB Report	No. of new TPS	Points (>2m dist.)
101057	Granite to granodiorite	76	19	**98**			**23**	**47**
				(26)	KFM01A	P-04-159		(10)
				(2)	KFM01A	P-06-233		
				(4)	KFM01A	P-18-08	(4)	
				(1)	KFM01C	P-06-233		(1)
				(1)	KFM01D	P-06-233		(1)
				(15)	KFM02A	P-04-161		(6)
				(6)	KFM03A	P-04-162		(2)
				(10)	KFM04A	P-04-199		(2)
				(2)	KFM05A	P-18-08	(2)	(1)
				(5)	KFM07A	P-05-214		(5)
				(7)	KFM08A	P-05-219		(7)
				(6)	KFM90B	P-07-194	(6)	(4)
				(2)	KFM24	P-18-08	(2)	(8)
				(9)	KFM24	P-21-07	(9)	
				(1)	PFM001157	P-03-08		
				(1)	PFM001162	P-03-08		
101057_104 and/or 101058_104	With medium to strong albitization.	1	29	**6**	KFM06A	P-05-123	0	**2**
101058	Granite, aplitic (***not*** albitized)	1	17	**6**			0	**6**
				(3)	KFM06A	P-06-233		(3)
				(3)	KFM08A	P-05-219		(3)
101061	Pegmatite, pegmatitic granite	12	14	**4**			0	**2**
				(2)	KFM07A	P-05-214		(1)
				(2)	KFM08A	P-05-219		(1)
101051	Granite, granodiorite and tonalite	4	10	**13**			0	**8**
				(4)	KFM01C	P-06-66		(2)
				(3)	KFM03A	P-04-162		(1)
				(3)	KFM05A	P-06-233		(3)
				(2)	KFM06A	P-06-233		(2)
				(1)	KFM08A	P-05-219		(1)

Rock type code	**Rock type name**	**RFM 029 %**	**RFM 045 %**	**No. of TPS**	**Sampling boreholes**	**Laboratory SKB Report**	**No. of new TPS**	**Points (>2m dist.)**
102017	Amphibolite	4	5	**22** (2) (2) (4) (1) (6) (1) (1) (2) (2) (1)	 KFM01A KFM01A KFM01C KFM01D KFM04A KFM05A KFM05A KFM07A KFM08A KFM24	 P-06-233 P-18-08 P-06-66 P-06-233 P-18-08 P-06-233 P-18-08 P-05-214 P-05-219 P-18-08	**10** (2) (6) (1) (1)	**13** (1) (1) (1) (1) (3) (1) (1) (1) (2) (1)
111058	Granite	1	2	**3** (1) (1) (1)	 KFM04A KFM05A KFM06A	 P-06-233 P-06-233 P-06-233	0	3
101033	Diorite, quartz diorite and gabbro	<1	2	**1**	PFM001158	P-03-08	0	1
103076	Felsic to intermediate volcanic rock	<1	1	**2** (1) (1)	 KFM01C KFM08A	 P-06-233 P-05-219	0	2
101056	Granodiorite	<1	<1	**5**	KFM04A	P-04-199	0	1
108018	Scarn	<1	<1	**2**	KFM01A	P-18-08	2	1
101054	Tonalite to granodiorite	<1	<1	**5** (3) (1) (1)	 KFM03A PFM001157 PFM001162	 P-04-162 P-03-08 P-03-08	0	1

Rock types below bold line have expected occurrence below 2% and will not be included in Baseline model.

The estimated volume of occurrence in the main rock domains are given in percentage in Table A-1, based on Petersson et al. (2024). The last column gives the number of separate “points” defined as sampling locations with one or more nearby tested samples, where those locations are separated more than 2 m from each other. This is intended to facilitate the judgment of the sampling coverage at the site.

A3 Results from laboratory tests

The resulting thermal conductivities determined from the available TPS tests at the Baseline stage are summarized in Table A-2. The statistical parameters derived from those tests are given for all the rock types that have more than 2 % expected occurrence in the rock domains (see Table A-1). The rock types with lower occurrence are considered of less importance for the description, and the thermal conductivity results for the few tests performed can be found in (Back et al. 2007).

The mean value, standard deviation, minimum and maximum values are given in Table A-2 for different subgroups of the available data specified in the "Comment" column. In the case of "Points within SFK", the mean value of neighbouring samples at the tested point is used, i.e., one value included per point. Also, the test results from samples taken from boreholes lying outside the area planned for the final storage (SFK) are excluded as well as the surface samples. Additionally, some alternative statistical analyses are presented for the main expected rock type (101057) for comparison, since it has a greater number of tests performed.

The italic row in Table A-2 gives the statistics for all available TPS tests at Baseline stage (with the number of tests in parenthesis), without any subdivision attempt. The model presented in SDM-Site stage (Back et al. 2007) is finally given for all rock types, for comparison. Not all rock types have new data in Baseline (refer also to Table A-1).

Table A-2. Statistics of measured thermal conductivity using the TPS method.

Rock code	Rock name	Comment	Mean W/(m·K)	St Dev	Min	Max
101057	Granite to granodiorite, metamorphic, medium grained	Points within SFK (37)* Points within SFK (37)** Points within SFK (37)*** All tests within SFK (65) *All tests (98)* (SDM-Site) (74)	3.54 3.49 3.58 3.58 *3.61* (3.68)	0.18 0.22 0.21 0.23 *0.22* (0.17)	3.13 2.70 3.13 2.70 *2.70* (3.25)	3.96 3.96 4.00 4.00 *4.01* (4.01)
101057_104 or 101058_104	Granite to granodiorite or granite, metamorphic, aplitic. When albitization is medium to strong.	Points within SFK (2)* *No new* (SDM-Site) (6)	3.89 (3.89)	- (0.13)	3.78 (3.70)	3.99 (4.06)
101058	Granite, metamorphic, aplitic (*Not* albitized/altered)	Points within SFK (6) *No new tests but 2 more sorted as not albitized* (SDM-Site) (4)	3.81 (3.77)	0.13 (0.12)	3.68 (3.68)	3.98 (3.95)
101061	Pegmatite, pegmatitic granite	Points within SFK (2)* *No new* (SDM-Site) (4)	3.33 (3.33)	- (0.20)	3.18 (3.07)	3.48 (3.50)
101051	Granite, granodiorite and tonalite, metamorphic, fine- to medium grained	Points within SFK (8)* *All tests (13)* (SDM-Site) (12)	2.96 *2.88* (2.85)	0.16 *0.26* (0.26)	2.81 *2.46* (2.46)	3.30 *3.38* (3.39)
102017	Amphibolite	Points within SFK (10) All test within SFK (16)* *All tests (22)* (SDM-Site) (12)	2.32 2.32 *2.51* (2.33)	0.10 0.12 *0.40* (0.10)	2.22 2.19 *2.19* (2.21)	2.48 2.60 *3.48* (2.48)

* The mean value of the tests at each point is used
** The lowest value of the tests at each point is used
*** The maximum value of the tests at each point is used

A4 Analysis of data coverage for main rock types

This Section presents an effort to analyse the representativity of the TPS test data and the corresponding uncertainty in property models. The TPS test has in some case been performed on several samples cut from the same short core section, and thus from rock types with analogous mineral composition. Hence, the term measurement "point" has been introduced here in the Baseline analysis. A sample location is considered a separate "point" if the distance to another closest sample is more than two metres. This is to be able to distinguish between samples taken next to each other and samples spread out in the borehole, such that the spatial coverage is more easily understood and evaluated.

During the site investigation phase sampling were mostly performed at three different levels of the cored boreholes (300, 500 and 700 m). But after the first investigated boreholes the focus moved from the most common rock type to the subordinate rock types. This resulted in a large variation in number and spatial distribution of samples from different rock types. Also, the great difference in expected occurrence explains this disparity in sampling and testing performed (cf. Table A-1).

In the following sections the test results (Table A-1 and Table A-2) will be commented on for each of the expected main rock types, with focus on the data representativity for the rock volume of the planned spent nuclear fuel storage (SFK).

A4.1 101057 – Granite to granodiorite

The most common rock type in Forsmark is clearly the granite to granodiorite with rock code 101057, which is expected to form about 75% of the largest domain RFM029. It has therefore been tested for thermal properties much more than the other rock types.

The spatial distribution for TPS samples in rock type 101057 is presented in the maps shown in Figure A-1 and Figure A-2. The first map in Figure A-1 provides data from the total number of tested samples at each drill site (in some cases several different boreholes are drilled from the same drill site, e.g., KFM01A, KFM01C and KFM01D are from BP1). The total number of tests from the drill site is given in parenthesis.

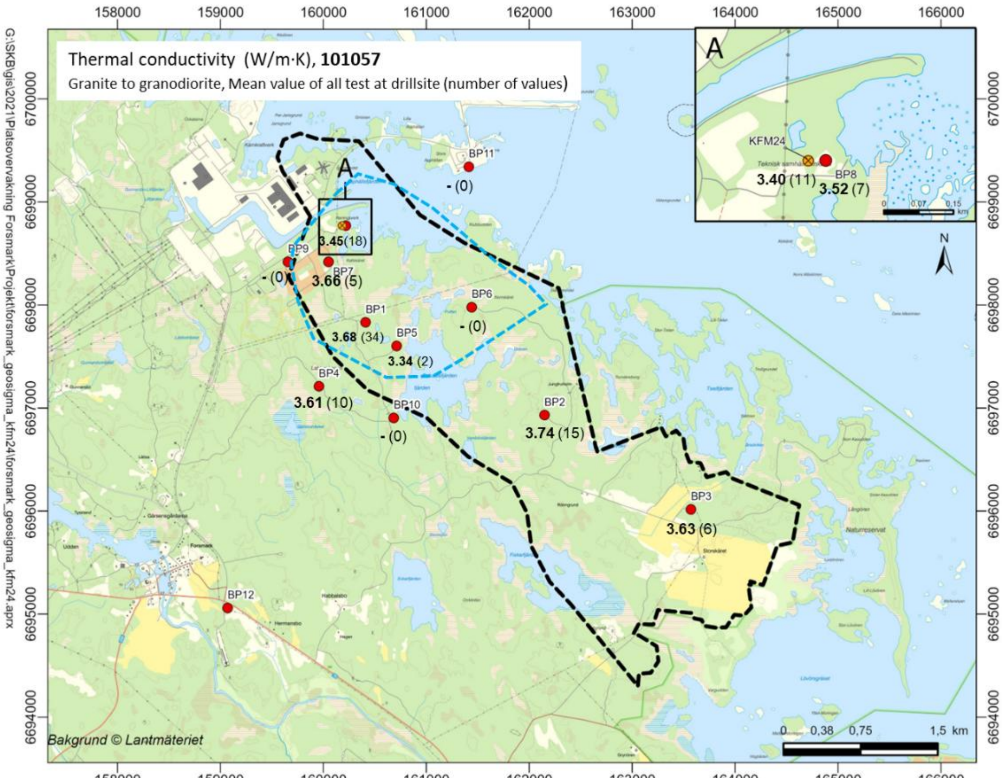

Figure A-1. Results from all TPS test of thermal conductivity in granite to granodiorite (101057) at the different drill sites. The mean is given with the number of tests in parenthesis.

The second map in Figure A-2 gives results from separate sample "points" at each drill site (in each point one thermal conductivity value is determined as the mean from tests at this point). The map presents the mean thermal conductivity at each drill site, with the number of points from the drill site given in parenthesis. From these two maps it may be noted that there is no major difference between the drill sites, the mean varies between 3.34 and 3.68 W/(m·K). There may be a slight trend towards lower thermal conductivity in the north where data shows a mean of 3.45 W/(m·K), which is mainly due to results in the more recent KFM24.

The main aim for the thermal Baseline is to establish a base for prediction for the SFK, and therefore it is of particular interest to study the data from this rock volume. It may be noted that all data are from the west half side of the planned SFK area (blue-marked in Figure A-2). The lowest thermal conductivity is found in the bottom of KFM05A which is the easternmost tested point for 101057 (borehole KFM05A is drilled towards north-east and sampled in only one point at 891 m borehole depth). This gives a higher uncertainty of the thermal conductivity for 101057 in the eastern half of the volume compared to the western side. Within the domain RFM045 (see Section 4.5) there has not been any thermal testing of 101057, but the occurrence of this unaltered variant is lower in this rock domain.

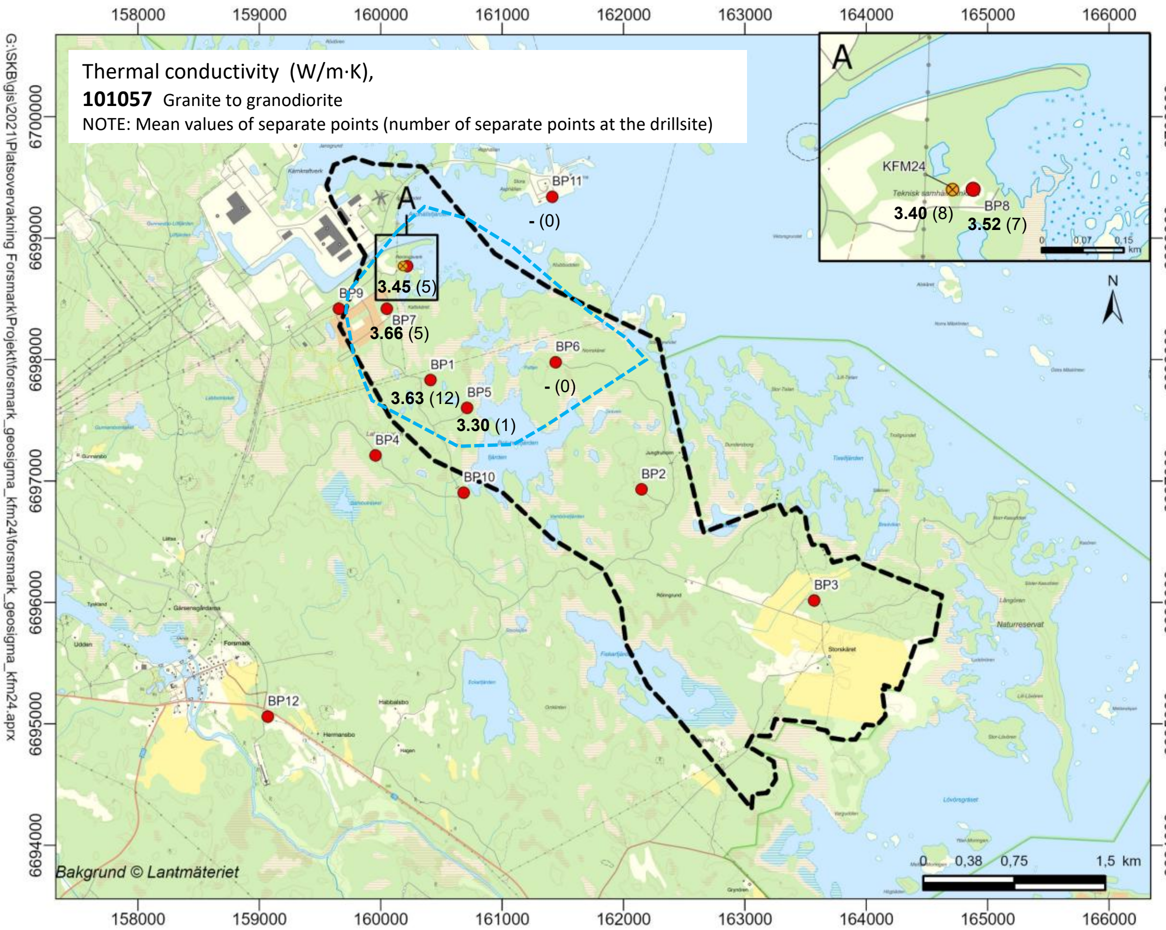

Figure A-2. The results from TPS tests of thermal conductivity in 101057 at separate sampling points in drill sites within the repository (SFK) area (blue-dashed line). The mean is given with the number of "points" in parenthesis. The mean value at each point is used in this calculation.

There could exist a spatial variation of thermal properties also with depth, but the depth of the investigated repository volume is much less than the horizontal borehole distances at the Forsmark site. The distance between the boreholes KFM05A and KFM06A is for example about 1 km, and the repository depth is planned to 470 m. Presentation of TPS results towards the sample depth can be found in (Back et al 2007). No indication for depth dependence has been observed.

In Table A-2 the statistics for different subgroups of the TPS data is presented and it may be noted that the thermal conductivity is slightly lower, compared to the model presented in SDM-Site stage, when considering only the SFK area and with the subdivision of the data. A lower thermal conductivity is unfavourable for the repository design, consequently a more conservative choice for the Baseline model may therefore be an adjustment to 3.54 W/(m·K) as the mean value for the rock type 101057. The model spread of the thermal conductivity distribution should be based on the data without any averaging at points, leading to the standard deviation of 0.23 obtained from the 64 tests on all the samples within SFK. Since the number of test is quite high for this rock type, the span from "points" within SFK (3.13–3.96 W/(m·K)) is chosen as Min-Max truncation values for the model.

A4.2 101057 or 101058 with medium to strong albitization

The albitization of rock is frequent in the rock domain RFM045, where it is expected to form a large part of the rock volume in this domain (see Section 4.5). When the albitization is of medium to strong intensity, the rock shows a strongly changed appearance with a much whiter colour than the unaltered 101057 or 101058. Figure 1-3 exemplifies how TPS samples from 101057, 101058 and 101058_104 (104 denotes the albitized variant) typically look like. Rock with only weak or faint albitization, which is also quite common, are here counted as non-albitized. The similar look of albitized 101057_104 and albitized 101058_104 makes the visual differentiation of these two rock types difficult to make during core mapping. Therefore, these two rock types, with a medium to strong albitization, are grouped together in the Baseline description for properties.

However, at this stage there are only six samples, from one borehole (KFM06A), tested with TPS in the albitized group. These 101058_104 samples are further all taken from a short deep interval of the core (823–829 m borehole length), which means that there is no test data basis for a study of spatial variability. The available tested samples have a mean thermal conductivity of 3.89 W/(m·K). The albitized rock types thus seem to have slightly higher thermal conductivity than the non-altered rock. The low standard deviation (0.13 W/(m·K)) observed from these six samples could be a result of the small spatial spread of the samples. Considering the large amount of this rock type expected in domain RFM045, some complementary testing in points spread out in the repository volume is anticipated to reduce the model uncertainty in the future.

Figure A-3. *Examples of TPS samples: (left) Un-altered 101057 (Adl-Zarrabi 2006a); (middle) Un-altered 101058 (Adl-Zarrabi 2006b); (right) Strongly albitized 101058_104 (Adl-Zarrabi 2005a).*

The model choice for 101057_104 and/or 101058_104 is to use the mean thermal conductivity, 3.89 W/(m·K), from the six available samples. Since the tested points are only two it is not realistic to use the observed values as the expected total spread and potential truncation Min-Max values for a model. Therefore, the choice for the model is to use plus-minus two standard deviation instead (3.43–4.35 W/(m·K)). The standard deviation is selected to be 0.23 adopted from the unaltered 101057 and this span (of four standard deviations in total) is roughly corresponding to the actually observed Min-Max span for the more extensively tested unaltered 101057.

A4.3 101058 – Granite, metamorfic aplitic

The unaltered granite (metamorphic, aplitic) 101058 is less common than the altered rock with albitization, but still not unusual in rock domain RFM045. Six samples have been tested in this rock type, which were taken at different "points" but within a limited depth span, three samples in borehole KFM06A (641–660 m borehole depth) and three in KFM08A (784–813 m). The mean thermal conductivity for the model in Baseline is 3.81 W/(m·K) and the standard deviation 0.13 is also chosen based on the six separated tests, although this could be an underestimation since the spatial spread of test samples is limited. The truncation span using plus-minus two standard deviations becomes 3.55–4.01 W/(m·K), which is only slightly wider than the observed test result span for 101058.

A4.4 101061 – Pegmatite and pegmatitic granite

Pegmatite, or pegmatitic granite, is expected to make up roughly 13% of the rock mass in both RFM029 and RFM045. The occurrence of pegmatite is mainly as dyke rocks, where the thickness of these dykes can vary from centimetre to metre scale. Pegmatitic granite are typically coarse-grained and individual grains can locally reach the same size order as the drill core samples or even larger. This makes the judgement of the representativeness of thermal properties based on these small scale TPS tests difficult, and a spread in the results should be expected. From Forsmark site only four samples (with grain sizes around 5 mm) have been tested, two at about 679 m depth in KFM07A (Adl-Zarrabi 2005b) and two at 669 m depth in KFM08A (Adl-Zarrabi 2006a). These tests show a mean of 3.33 W/(m·K), which is thus slightly lower than the main rock types 101057/101058. The standard deviation from these few tests (0.20 W/(m·K)) is in similar order as seen for other rock types. No new testing has been performed since SDM-Site and the model will only be modified to have a truncation span corresponding to four standard deviations, as for the other rock types with few tested samples.

A4.5 101051 – Granite, granodiorite and tonalite

The granite, granodiorite and tonalite (metamorphic, fine- to medium-grained101051 is a rock type that deserves some attention in the modelling because the thermal conductivity is among the lowest at the site. The occurrence is expected to be about 10% in RFM045 but less in RFM029. The results from the 13 TPS test available at Baseline is plotted on the site map in Figure A-4 in the same manner as for other rock types. It can be noted that the lowest values are found in samples from KFM03 in the south which makes the mean for points only within SFK volume slightly higher than the mean for all tests (Table A-2).

The mean thermal conductivity counted for the seven "points" is 2.91 W/(m·K), with a value span from 2.81 to 3.07 W/(m·K). Out of these samples there are only two close points tested in the eastern half of the site (KFM06A), and only a single test in the north (KFM08A). These borehole tests show the lowest conductivities. This increases the uncertainty in the model for prediction in the eastern and northern part of the site, which is the side where the main occurrence of this rock type is expected (in RFM045). Some complementary testing could remedy this uncertainty in the future when more drill cores are available. The spread in the thermal conductivity of this rock type seems to be in the same order as for other rock types. No new tests on 101051 have been performed after SDM-Site (one sample was removed from this rock type after re-examination). The choice for modelling this subgroup is to use the mean from points inside SFK (2.96) and the standard deviation from all ten tests inside SFK (0.18) and the truncation span as the plus-minus two standard deviations 2.59–3.33 W/(m·K).

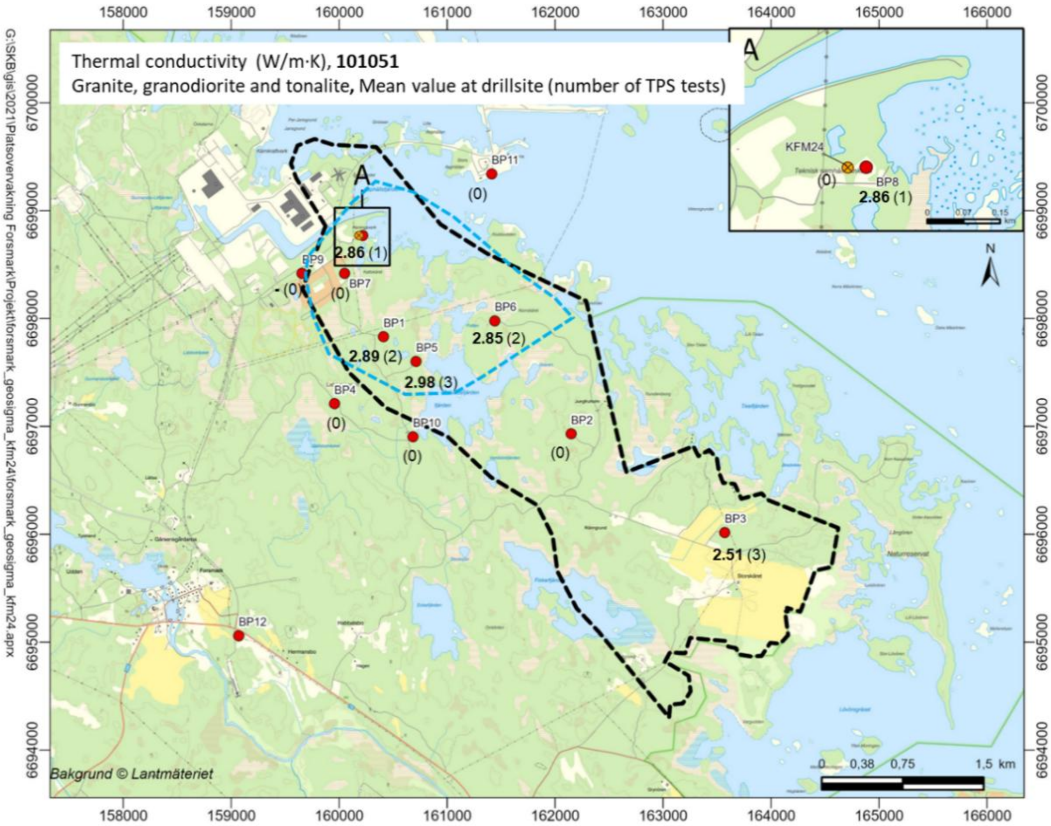

Figure A-4. Results from all TPS test of thermal conductivity in granite, granodiorite and tonalite (101051) at the different drill sites (marked BP). The mean is given with the number of tests in parenthesis.

A4.6 102017 – Amphibolite

The rock type with the lowest thermal conductivity in Forsmark is amphibolite (102017). It occurs mainly as dykes with thickness of a decimetre to a meter but could also appear as larger bodies (Back and Sundberg 2022). The amphibolite is occurring more frequently in rock domain RFM045 which is a more heterogeneous rock domain in general. Two investigation cored boreholes (KFM06A and KFM08C) are intersecting this domain. Based on these two boreholes the amphibolite occurrence is estimated to 5 % in the RFM045. In RFM029 the amphibolite is expected to form 4 % of the domain volume.

In Figure A-5 the results from TPS tests at different drill sites are presented in the same way as for the previous rock types. New additional TPS tests have been performed in amphibolite after the SDM-Site. These new tests show results generally in agreement with the previous findings. Amphibolite has a larger spread in the composition and thermal properties, compared to other rock types. There are a couple of amphibolite samples from KFM04A that clearly resulted in a higher thermal conductivity than the mean value. These samples are not included in the statistics of points only "within SFK", explaining the lower value for this case (Table A-2). The standard deviation of all tests in Baseline is also higher compared to SDM-Site because of the larger spread in properties seen in the samples.

As illustrated in Figure A-6 it is not easy to determine differences in amphibolite characteristics directly with the naked eye. The variation in rock composition and features may be compared to the large variation also seen in tensile strength obtained on the same samples used for TPS tests. The KFM04 amphibolite sample with the highest measured thermal conductivity has a low tensile strength, while the KFM24 sample with very low thermal conductivity has an exceptionally high tensile strength for amphibolite. However, no direct simple correlation can be observed and determined between these parameters.

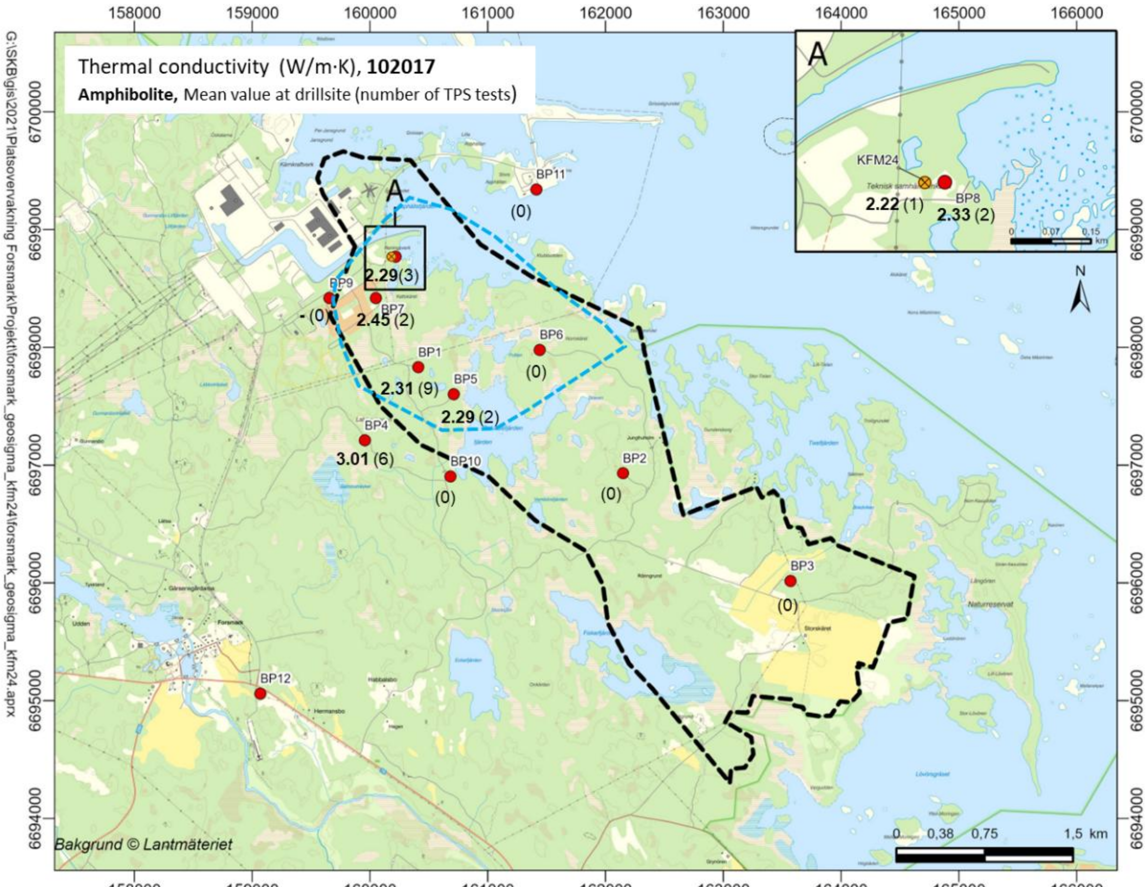

Figure A-5. *Results from all TPS test of thermal conductivity in amphibolite (102017) at the different drill sites. The mean is given with the number of tests in parenthesis.*

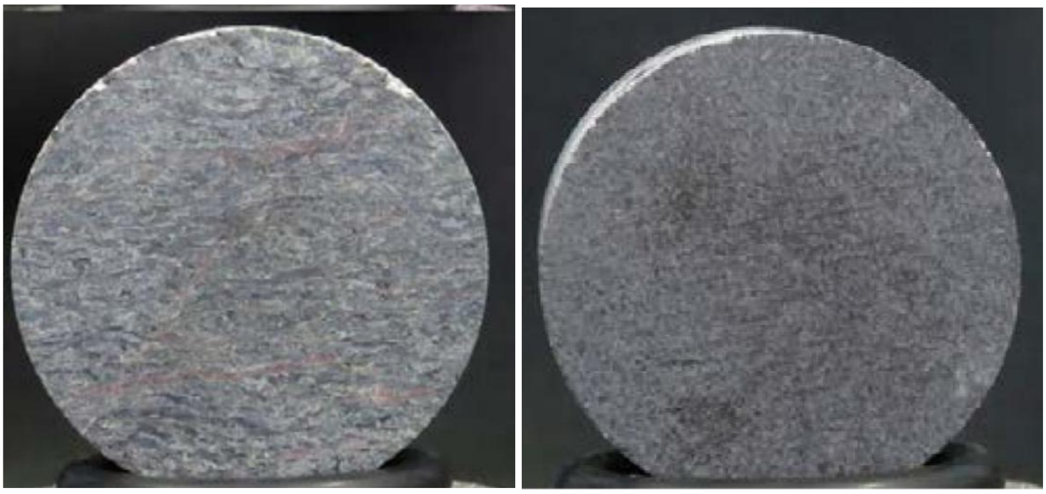

Figure A-6. *Examples of two different core samples in amphibolite (102017). Left: Sample from KFM04 at 309 m borehole depth with thermal conductivity k=3.48 W/(m K) and indirect tensile strength ITS =2.16 MPa. Right: KFM24 at 517 m with k=2.20 W/(m·K) and ITS = 16 MPa. From (Jacobsson and Sjöström 2019).*

No significant general spatial trend can be observed in the amphibolite TPS results even if the spread is large. The reason is probably that the amphibolite generally occurs as a younger intruding rock in the form of dyke-like tabular bodies and irregular inclusions that are elongated parallel to the mineral stretching lineation. These amphibolite bodies and inclusions are affected by pervasive ductile deformation under different degrees and conditions of metamorphism, showing a wide range of mineralogical compositions and textural variability (Stephen et al. 2007) regardless of the geographic location. Depending on how large the total occurrence of amphibolite will be defined in future SDMs for the repository volume, additional thermal laboratory testing of the actual amphibolite at the deposition level might be necessary, to decrease the uncertainty that arises from the currently observed variation.

For the Baseline model the choice is to use the mean from the points within SFK (2.32), the standard deviation from all ten tests inside SFK (0.12) and the truncation span as the plus-minus two standard deviations 2.08–2.56 W/(m·K).

A5 Temperature influence on the thermal conductivity

During the storage period in SFK the temperatures will increase in the repository due to the heat generated from the spent fuel in the deposited canisters. Therefore, the thermal properties at the site should be described also for temperatures other than room temperature, which has been the regular TPS laboratory test condition. The temperature dependence has been studied based on TPS performed also at elevated temperatures. This dependence has been reported by (Sundberg et al. 2008), where the following linear models (Equation 2 1 and Equation 2 2.) for temperature dependence are provided:

$\lambda_1=\lambda_0(1+\alpha_\lambda(T_1-T_0))$ Equation A-1

$C_1=C_0(1+ \alpha_C(T_1-T_0))$ Equation A-2

were

λ_0 Thermal conductivity at 20 °C, T_0, W/(m·K).

λ_1 Thermal conductivity at elevated temperature T_1, W/(m·K).

C_0 Heat Capacity at room temperature T_0, MJ/(m^3 K).

C_1 Heat Capacity at elevated temperature T_1, MJ/(m^3 K).

α_λ Temperature coefficient for thermal conductivity, 1/°C.

α_C Temperature coefficient for heat capacity, 1/°C.

The temperature coefficient αλ for the rock types in Forsmark varies between -0.5×10−3 and -1.1×10−3 where the most common rock type 101057 has the value of -1.0×10−3. This means, for example, that for a temperature increase of 100 °C the thermal conductivity will decrease 10% in rock type 101057. In addition, assuming that the mean thermal conductivity is 3.54 W/(m·K) at 20 °C (Table A-2), the mean at 90 °C would be 3.33 W/(m·K) according to the above linear model.

A6 Anisotropy influence on the thermal conductivity

The anisotropic structural features present in the rock types (lineation and foliation) will also induce anisotropy in the thermal properties. In Forsmark, the main rock type 101057 has been studied in this respect. Thermal anisotropy has been investigated in a large-scale field experiment (Sundberg et al. 2007), combined with laboratory and field testing at smaller scale. The mean factor of anisotropy $\lambda_{pa}/\lambda_{pe}$ (defined as the relationship between the thermal conductivities parallel and perpendicular to the foliation) was found to be 1.40 in the centimetre scale and 1.15 in the decimetre to metre scale.

An accurate determination of anisotropy requires extensive and costly investigations. Therefore, the methodology for thermal modelling (Back and Sundberg 2022; Back et al. 2022) recommends that, until sufficient laboratory or field data are available, the potential anisotropy in rock types is handled by the end users of the thermal model in a comprehensive manner, e.g. in the thermal dimensioning.

A7 Baseline thermal property models

In the following sections the models for thermal properties of the six main rock types considered relevant for this study and the two main rock domains for SFK are presented. Most of the model parameter values are the same as in SDM-Site (Back et al. 2007; Sundberg et al. 2008) while a few are slightly modified based on new data and arguments presented in previous sections for each rock type.

A7.1 Thermal property models for main single rock types

Table A-4 gives the Baseline models for thermal properties of the main rock types occurring at Forsmark site. The geological description corresponding to each rock code is found in Table A-1. The models should be regarded as the best property predictions to be used at this Baseline stage. Note that parameter *models* are not identical to a pure data presentation (such as in Table A-2), because of the limitations in coverage and number of tested samples. The certainty in the models for different rock types may further not be the same or have the same significance for safety assessment, because they have different occurrence (Table A-1).

To provide a more complete model presentation, several thermal property parameters are presented, also including parameters not discussed above (heat capacity and thermal expansion coefficient). The basis for these models is found in the reports of SDM-Site stage. For the two rock type cases where new TPS tests have been performed (Table A-1) the heat capacity models are adjusted. The mean and standard deviation for all heat capacity values available at present from TPS tests are used for the Baseline models of Table A-3.

The thermal expansion coefficient is not measured on all rock types, but more extensively for 101057 (56 samples). Therefore, only a complete model distribution for this rock type is provided. It may be noted that the mean values, for the few samples tested in other rock types, are close to the mean in 101057, around 7.7 10^{-6} m/(m·K). A truncation of two standard deviation is a realistic choice for modelling. Furthermore, this is also supported by the previous measurements made at Äspö HRL (Sundberg and Ländell 2002, Sundberg et al. 2005, 2006), where no significant variation due to rock type was found.

Table A-3. Thermal property models for main rock types. All models are truncated normal distributions at the given Min and Max values. The models apply for 20 °C.

Rock code	Model parameter	Mean	St Dev	Min	Max
101057	Thermal conductivity W/(m·K)	3.54	0.23	3.13	3.96
	Heat capacity MJ/(m^3 K)	2.11	0.18		
	Thermal expansion coefficient ×10^{-6} m/(m·K)	7.7	2.2	2.1	15
101057_104 or 101058_104	Thermal conductivity W/(m·K)	3.89	0.23	3.43	4.35
	Heat capacity MJ/(m^3 K)	2.12	0.11		
101058	Thermal conductivity W/(m·K)	3.81	0.13	3.55	4.01
	Heat capacity MJ/(m^3 K)	2.08	0.10		
	Thermal expansion coefficient ×10^{-6} m/(m·K)	7.5			
101061	Thermal conductivity W/(m·K)	3.33	0.20	2.93	3.73
	Heat capacity MJ/(m^3 K)	1.92	0.14		
101051	Thermal conductivity W/(m·K)	2.96	0.18	2.59	3.33
	Heat capacity MJ/(m^3·K)	2.21	0.11		
	Thermal expansion coefficient ×10^{-6} m/(m·K)	7.8			
102017	Thermal conductivity W/(m·K)	2.32	0.12	2.08	2.56
	Heat capacity MJ/(m^3 K)	2.35	0.21		

A7.2 Thermal property models for rock domains

The thermal model at rock mass scale has not been analysed within Baseline. The last update was presented in (Sundberg et al. 2008). A summary of results from simulated thermal conductivity in the mixture of rock types in the two domains is presented in Table A-4. It may be noted that the higher heterogeneity in rock domain RFM045 causes a larger standard deviation for the thermal conductivity. The fewer underlying laboratory data from this domain, as discussed in Section A4, gives an additional higher uncertainty in the models of this domain. Details and discussion may be found in (Sundberg et al. 2008).

Table A-4. Summary of rock domain thermal conductivities in rock domains, based on (Sundberg et al. 2008) and (Back et al. 2007).

Statistical parameter for thermal conductivity. Simulations at 1 m scale. Valid at 20 °C	Rock Domain RFM029 W/(m·K)	Rock Domain RFM 045 W/(m·K)
Mean	3.58	3.57
Standard deviation	0.29	0.42
0.1 percentile	2.30	2..24

The heat capacity has been considered less critical in the safety assessment compared to the thermal conductivity according to Hökmark et al. (2009), and no further analysis of heat capacity has been performed within the Baseline stage. Previously, statistics of heat capacity, based on simulation at the rock mass scale were presented by (Sundberg et al. 2008). The mean value for RFM029 was 2.06 MJ/(m^3 K), and 2.12 MJ/(m^3 K) for RFM045. The standard deviation of heat capacity in the rock domain simulations was 0.10 and 0.15, for RFM029 and RFM045 respectively.

A8 In situ temperature model

Within Baseline no new analysis of the bedrock in situ temperature has been performed. The measurements of temperature in boreholes at the Forsmark site within SDM-Site stage were presented in (Sundberg et al. 2008). The mean in situ temperature, from measurements in the different investigation boreholes, was determined for 400, 500 and 600 m depth to 10.5, 11.6 and 12.8 °C, respectively. Also, the calculated gradients showed a trend of increasing gradient with depth, from about 0.01°C/m at 300 m to about 0.013°C/m at 700 m.